

# **REMOVAL OF CRYSTALLINE CONFECTIONERY MATERIAL FROM HARD SURFACES**

by

**NURUL ZAIZULIANA ROIS ANWAR**

A thesis submitted to  
The University of Birmingham  
for the degree of  
DOCTOR OF PHILOSOPHY

School of Chemical Engineering  
University of Birmingham  
December 2015

UNIVERSITY OF  
BIRMINGHAM

**University of Birmingham Research Archive**

**e-theses repository**

This unpublished thesis/dissertation is copyright of the author and/or third parties. The intellectual property rights of the author or third parties in respect of this work are as defined by The Copyright Designs and Patents Act 1988 or as modified by any successor legislation.

Any use made of information contained in this thesis/dissertation must be in accordance with that legislation and must be properly acknowledged. Further distribution or reproduction in any format is prohibited without the permission of the copyright holder.

# ABSTRACT

Cleaning of surfaces in contact with chocolate is necessary in chocolate manufacturing to ensure high production quality. This research was carried out to study the removal behaviour of solid dark chocolate from three surface materials; stainless steel 316, polycarbonate and polytetrafluoroethylene (PTFE). In order to understand the crystallization behaviour and its relationship with the chocolate rheology, a differential scanning calorimeter (DSC) was used to characterize the polymorphs, while a rheometer was used to study the rheological behaviour of chocolate. The polymorphism was found to be influenced by the tempering and cooling processes, with no dependency on the surface material if cooling is properly controlled. Crystallisation can also be studied from the rheological data. Micromanipulation technique and texture analyser were then used to determine the ease of removal of a solid chocolate layer from the surfaces. Finally, both removal behaviour and time to clean were identified using a flow cell cleaning rig with respect to a number of parameters. It was found that surface roughness of the three materials, crystallization and cleaning conditions affect the removal behaviour of solid chocolate layer from those surfaces. Water alone did not produce a clean surface for all the materials used, thus chemical was added. The results from cleaning work and micromanipulation measurements were found to be comparable.

# ACKNOWLEDGEMENTS

Alhamdulillah, thanks to Allah for giving me such a wonderful experience during completing my PhD in the University of Birmingham. I would like to acknowledge the Ministry of Education, Malaysia and Universiti Sultan Zainal Abidin for the financial support throughout my PhD study.

A massive thank you to my supervisors, Professor Peter Jonathan Fryer and Dr Serafim Bakalis for their supervisions, valuable guidance and support which always made me feel confident to keep going. Special thanks to Dr James Bowen and Ibrahim Palabiyik for their time to help me in completing my experimental work. Without their help, this study would not have been completed on time.

Finally, I would like to thank my beloved husband, Maizul-Azlan Umar, beautiful girl, Zara Maleeha Azzalea and handsome boy, Zarif Muqri for always be with me during good and hard times. This success could not be achieved without their endless love, patience, support and understanding. To my family and friends, thank you so much for your prayers and friendship.

# TABLE OF CONTENTS

<b>1</b>	<b>INTRODUCTION.....</b>	<b>1</b>
1.1	Chocolate history and development.....	1
1.2	Chocolate manufacturing.....	3
1.3	Research background.....	6
1.4	Objectives of study.....	9
1.5	Thesis outline.....	9
<b>2</b>	<b>LITERATURE REVIEW.....</b>	<b>11</b>
2.1	Introduction.....	11
2.2	Chocolate Ingredients.....	11
2.3	Cocoa butter crystallisation.....	12
2.3.1	Basics of crystallisation.....	14
2.3.2	Polymorphism.....	15
2.3.3	Crystal arrangement.....	16
2.3.4	Factors affecting the crystals formation.....	18
2.3.5	Tempering process.....	19
2.3.6	Blooming.....	23
2.3.7	Cooling process.....	26
2.3.8	Methods to characterise the polymorphs.....	29
2.4	Chocolate-mould interaction.....	31
2.4.1	Factors contributing to the adherence of chocolate to the mould.....	31
2.4.2	Micromanipulation.....	33
2.4.3	Texture analyser.....	35

2.5	Chocolate rheology.....	36
2.6	Cleaning of Formulated Food Products Deposits.....	39
2.7	Conclusions.....	41
<b>3</b>	<b>MATERIALS AND METHODOLOGY.....</b>	<b>42</b>
3.1	Introduction.....	42
3.2	Surface characterisation.....	43
3.2.1	Contact angle measurement.....	43
3.2.2	Surface roughness measurement.....	44
3.3	Chocolate crystallisation.....	44
3.3.1	Materials.....	44
3.3.1.1	Preparation of untempered dark chocolate.....	44
3.3.1.2	Preparation of tempered dark chocolate.....	45
3.3.2	Differential scanning calorimetry (DSC).....	46
3.3.3	Solidification using a Peltier stage .....	47
3.4	Rheological characterisation.....	49
3.4.1	Steady flow study.....	49
3.4.2	Dynamic oscillatory test.....	50
3.5	Force measurement using micromanipulation technique.....	50
3.5.1	Micromanipulation rig.....	50
3.5.2	Force transducer.....	52
3.5.3	Calibration of force transducer.....	53
3.5.4	Micromanipulation measurement.....	56
3.5.5	Data analysis of micromanipulation.....	57
3.6	Force measurement using texture analyser.....	58

3.7	Cleaning rig.....	62
3.7.1	Water rinsing.....	65
3.7.2	Chemical cleaning.....	65
3.7.3	Image analysis.....	65
3.7.4	Film characterisation.....	66
3.8	Conclusions.....	67
<b>4</b>	<b>CRYSTALLISATION AND RHEOLOGICAL STUDY.....</b>	<b>68</b>
4.1	Introduction.....	68
4.2	Crystallisation study using the DSC measurements.....	69
4.2.1	Checking the effectiveness of the lab scale tempering process.....	69
4.2.2	Characterisation of the polymorphism after cooling by using the Peltier stage.....	71
4.2.2.1	Effect of tempering and cooling rate on the crystallisation.....	72
4.2.2.2	Effect of material variations on the crystallisation.....	75
4.3	Rheological study of dark chocolate.....	78
4.3.1	Steady flow behaviour of the molten dark chocolate.....	79
4.3.2	Effect of cooling on the viscosity evolution of dark chocolate.....	81
4.3.3	Effect of shearing whilst cooling on the viscosity evolution of dark chocolate.....	84
4.3.4	Effect of pre-crystallisation on the viscosity evolution of dark chocolate.....	88
4.3.5	Dynamic measurements.....	90
4.3.5.1	Influence of temperature on the modulus evolution.....	90

4.3.5.2	Influence of chocolate type on the modulus evolution.....	93
4.4	Conclusions.....	95
<b>5</b>	<b>FORCE MEASUREMENT USING MICROMANIPULATION TECHNIQUE AND TEXTURE ANALYSER .....</b>	<b>96</b>
5.1	Introduction.....	96
5.2	Surface characterisation.....	97
5.3	Measurement of removal force using micromanipulation technique.....	100
5.3.1	Typical behaviour of scraping process.....	101
5.3.2	Effect of chemical usage, soaking time and temperature on the pulling energy and removal.....	103
5.3.3	Effect of probe speed on the pulling energy and removal.....	116
5.3.4	Effect of surface material on the pulling energy and removal.....	118
5.3.5	Effect of tempering and cooling on the pulling energy and removal.....	121
5.4	Separation force measurement using texture analyser.....	127
5.4.1	Effect of the distance between the probe and the chocolate surface on the separation force.....	128
5.4.2	Effect of the chocolate-probe contact time on the separation force.....	129
5.4.3	Effect of the tempering and surface material on the separation force.....	131
5.5	Conclusions.....	137



<b>6</b>	<b>REMOVAL BEHAVIOUR OF SOLID CHOCOLATE LAYER USING FLOW CELL CLEANING RIG.....</b>	<b>138</b>
6.1	Introduction.....	138
6.2	Image analysis.....	140
6.2.1	Determination of cleaning time from image analysis.....	142
6.2.2	Disadvantages of image analysis.....	142
6.3	Determination of clean state.....	144
6.4	Repeatability of the experimental results.....	144
6.5	Water circulation.....	146
6.5.1	Effect of water temperature and velocity.....	146
6.5.2	Effect of surface materials.....	151
6.6	Chemical circulation.....	155
6.6.1	Effect of temperature and velocity.....	157
6.6.2	Effect of surface materials and chemical usage.....	169
6.6.3	Effect of tempering and cooling.....	174
6.7	Comparison with micromanipulation and texture analyser measurement.....	182
6.8	Conclusions.....	184
<b>7</b>	<b>CONCLUSIONS AND RECOMMENDATIONS.....</b>	<b>185</b>
7.1	Conclusions.....	185
7.1.1	Crystallisation and rheological study.....	185
7.1.2	Force measurement using micromanipulation technique and texture analyser.....	187
7.1.3	Removal behaviour of solid chocolate layer using flow cell cleaning rig.....	189
7.2	Recommendations.....	190

# LIST OF FIGURES

- Figure 1.1: Process flow of chocolate making.
- Figure 2.1: Structure of triglyceride and the fatty acids.
- Figure 2.2: Packing arrangements of (a) double chain and (b) triple chain of TAG.
- Figure 2.3: (a) DSC cooling curves of tempered chocolate at different cooling rates. (b) DSC remelting curves of tempered chocolate at 5°C/min for different cooling rates. (c) DSC cooling curves of untempered chocolate at different cooling rates. (d) DSC remelting curves of tempered chocolate at 5°C/min for different cooling rates (Stapley *et al.*, 1999).
- Figure 2.4: The well tempered chocolate on top with glossy surface, but the untempered chocolate will experience a bad demoulding process (Le Reverend *et al.*, 2008).
- Figure 2.5: Chocolate that has blooming problem due to (A) storage, fat migration, (C) heat hit, (D) over-tempering, (E) non tempering (Lonchampt and Hartel, 2004).
- Figure 2.6: (a) 2-D and (b) 3-D AFM scans of dark chocolate surface with blooming problem (Hodge and Rousseau, 2002).
- Figure 2.7: Polarized light micrographs of cooled rapidly (A) and slowly (B), and lard cooled rapidly (C) and slowly (D) (Campos *et al.*, 2002).
- Figure 2.8: The insertion of a frozen plunger into the chocolate during FrozenCone process (Baichoo, 2007).
- Figure 2.9: Example of XRD scan of cocoa butter cooled rapidly and heated slowly (Le Reverend, 2009).
- Figure 2.10: Example of the cooling and melting DSC curves for tempered chocolate cooled at 1°C/min to -30°C and rewarmed at 10°C/min (Baichoo, 2007).
- Figure 2.11: SEM images of egg albumin deposits (a) before and (b) after contacting with 0.5% NaOH solution for 60 min at 20°C (Liu *et al.*, 2007).
- Figure 2.12: Apparent viscosity of palm oil under different shear rates (De Graef *et al.*, 2008).
- Figure 2.13: Cleaning map which consider the type of cleaning chemical and soil complexity to classify the cleaning problems (Fryer & Asteriadou, 2009).
- Figure 3.1: Contact angle measurement apparatus..

- Figure 3.2: Temperer Revolution 2.
- Figure 3.3: Temperature history for DSC.
- Figure 3.4: Cooling rig.
- Figure 3.5: Schematic view of the cooling rig.
- Figure 3.6: Micromanipulation rig.
- Figure 3.7: Schematic diagram of the micromanipulation rig.
- Figure 3.8: T-shaped probe.
- Figure 3.9: BG-1000 force transducer.
- Figure 3.10: Weights and weight hanger.
- Figure 3.11: Schematic diagram of weights and weight hanger.
- Figure 3.12: Example of the output voltage when 700g weights were hung at the T-shaped probe.
- Figure 3.13: Calibration curve for 1000g transducer.
- Figure 3.14: The chocolate layer was pulled away leaving a thin layer on the coupon.
- Figure 3.15: Typical curve obtained when pulling a chocolate layer from a surface (the voltage has been converted to force for Y-axis).
- Figure 3.16: TA-XTplus Texture Analyser.
- Figure 3.17: Schematic diagram of the pulling test; (a) liquid dark chocolate in the sample holder, (b) the chocolate-probe interface was created and (c) the probe was pulled off from the chocolate surface.
- Figure 3.18: Cleaning rig.
- Figure 3.19: Schematic diagram of the cleaning rig (Goode *et al.*, 2010) with some modifications.
- Figure 3.20: Test section with fouled coupon attached to it.
- Figure 3.19: Area considered for the calculation.
- Figure 4.1: DSC curves for tempered chocolate cooled at 1°C/min and 10°C/min and remelted at 5°C/min.
- Figure 4.2: DSC melting curves for tempered and untempered chocolate cooled at 1°C/min and 10°C/min.
- Figure 4.3: DSC melting curves for tempered and untempered chocolate left at room temperature for 1 hour.
- Figure 4.4: DSC melting curves for tempered chocolate on different surfaces cooled to 10°C at 1°C/min (a), 10°C/min (b) and left at room temperature for 1 hour (c).

- Figure 4.5: Apparent viscosity of liquid dark chocolate sheared from 0 to  $100\text{s}^{-1}$  at different temperatures.
- Figure 4.6: Square root of the shear stress vs square root of the shear rate for different temperatures.
- Figure 4.7: Viscosity evolution of untempered dark chocolate cooled from  $50$  to  $10^{\circ}\text{C}$  at different cooling rates whilst sheared at  $15\text{s}^{-1}$ . Zones A and B are corresponding to the different states of cocoa butter and described in the text.
- Figure 4.8: Rate of change in apparent viscosity and the temperature at which sudden change occurs subjected to cooling rates.
- Figure 4.9: Viscosity of untempered dark chocolate cooled from  $50$  to  $10^{\circ}\text{C}$  at  $1^{\circ}\text{C}/\text{min}$  (a),  $5^{\circ}\text{C}/\text{min}$  (b) and  $10^{\circ}\text{C}/\text{min}$  (c) whilst sheared at  $15$  and  $50\text{s}^{-1}$ .
- Figure 4.10: Viscosity of tempered dark chocolate cooled from  $31$  to  $20^{\circ}\text{C}$  at  $0.5$  and  $1^{\circ}\text{C}/\text{min}$  whilst sheared at  $15\text{s}^{-1}$ .
- Figure 4.11: Viscosity of untempered dark chocolate cooled from  $50$  to  $20^{\circ}\text{C}$  at  $0.5$  and  $1^{\circ}\text{C}/\text{min}$  whilst sheared at  $15\text{s}^{-1}$ .
- Figure 4.12: Complex modulus as a function of oscillation stress for dark chocolate at  $35^{\circ}\text{C}$  (a),  $40^{\circ}\text{C}$  (b) and  $70^{\circ}\text{C}$  (c) (average of three measurements).
- Figure 4.13: Complex modulus as a function of oscillation stress for untempered dark (blue) and milk (yellow) chocolates at  $35^{\circ}\text{C}$  (average of three measurements).
- Figure 5.1: Images from video contact angle device; (a) stainless steel, (b) polycarbonate, (c) PTFE.
- Figure 5.2: Surface topography images of (a) stainless steel, (b) polycarbonate and (c) PTFE scanned by using interferometer.
- Figure 5.3: Typical curve of force versus sampling time for scraping a chocolate layer from a surface.
- Figure 5.4: Schematic diagram of scraping process by the T-shaped probe.
- Figure 5.5: Pulling energy as a function of water temperature when the sample was submerged in water for 10 minutes prior to the measurement. Data are average of three repeats with the pulling speed of  $1.1\text{mm/s}$ .

- Figure 5.6: Pulling energy as a function of soaking time when the sample was submerged in water at 30°C prior to the measurement. Data are average of three repeats with the pulling speed of 1.1mm/s.
- Figure 5.7: Removal percentage as a function of soaking time for different water temperature.
- Figure 5.8: Typical curve showing force versus sampling time for pulling a chocolate layer from coupon surface under two conditions: after submerging in water and that after submerging in 0.1% NaOH. Data are average of three repeats with the pulling speed of 1.1mm/s.
- Figure 5.9: Pulling energy and removal percentage as a function of solution temperature (the sample was submerged in a 0.1% NaOH solution for 10 minutes prior to the measurement). Data are average of three repeats with the pulling speed of 1.1mm/s.
- Figure 5.10: Dissolution occurred when soaking in 0.1% NaOH for 10 minutes. (a) Soak in water at 40°C, (b) Soak in 0.1% NaOH at 25°C, (c) Soak in 0.1% NaOH at 30°C and (d) Soak in 0.1% NaOH at 40°C.
- Figure 5.11: Pulling energy as a function of sample mass. Data are average of three repeats with the pulling speed of 1.1mm/s.
- Figure 5.12: The amount of energy per unit gram as a function of temperature.
- Figure 5.13: Pulling energy as a function of soaking time when the sample was soaked in 0.1% NaOH solution at 30°C prior to the measurement. Data are average of three repeats with the pulling speed of 1.1mm/s.
- Figure 5.14: Removal percentage as a function of soaking time when the sample was submerged in a 0.1% NaOH solution at 30°C prior to the measurement. Data are average of three repeats with the pulling speed of 1.1mm/s.
- Figure 5.15: Pulling energy and removal percentage as a function of soaking time when the sample was submerged in a 0.12% commercial cleaning solution at 30°C prior to the measurement.
- Figure 5.16: Amount of energy per unit gram as a function of soaking time for removal of chocolate soaked in 0.1% NaOH and 0.12% commercial cleaning solution.

- Figure 5.17: Pulling energy and removal percentage as a function of probe speed (the sample was submerged in a 0.1% NaOH solution at 30°C for 10 minutes prior to the measurement). Data are average of three repeats.
- Figure 5.18: Pulling energy for removal from different material surfaces (the sample was submerged in a 0.1% NaOH solution at 30°C for 10 minutes prior to the measurement). Data are average of three repeats.
- Figure 5.19: Removal percentage for different material used (the sample was submerged in a 0.1% NaOH solution at 30°C for 10 minutes prior to the measurement). Data are average of three repeats with the pulling speed of 1.1mm/s.
- Figure 5.20: The amount of pulling energy per unit gram for different material.
- Figure 5.21: Chocolate residue on (a) stainless steel, (b) polycarbonate and (c) PTFE surfaces.
- Figure 5.22: Pulling energy for tempered and untempered chocolate (the sample was submerged in a 0.1% NaOH solution at 30°C for 10 minutes prior to the measurement). Data are average of three repeats with the pulling speed of 1.1mm/s.
- Figure 5.23: Removal percentage for tempered and untempered chocolate (the sample was submerged in a 0.1% NaOH solution at 30°C for 10 minutes prior to the measurement)
- Figure 5.24: The amount of energy per unit gram for the tempered and untempered chocolate.
- Figure 5.25: Effect of cooling on the pulling energy and removal percentage of tempered chocolate (the sample was submerged in a 0.1% NaOH solution at 30°C for 10 minutes prior to the measurement).
- Figure 5.26: The amount of energy per unit gram for different cooling condition.
- Figure 5.27: Force per unit area for separation of solid tempered chocolate from polycarbonate surface with respect to distance between the probe and the chocolate surface. Data are the average of three repeats.

- Figure 5.28: Force per unit area for separation of solid tempered chocolate from polycarbonate surface with respect to contact time. Data are the average of three repeats.
- Figure 5.29: Typical plot of force versus time for separation of probe surface from the (a) untempered and (b) tempered chocolate.
- Figure 5.30: Schematic diagram showing the (a) expansion of the untempered chocolate and (b) contraction of the tempered chocolate.
- Figure 5.31: Force per unit area for the separation of solidified (a) untempered and (b) tempered chocolate from different surface material. Data are the average of three repeats.
- Figure 6.1: Example of the (a) original cropped image and (b) the same image which has undergone the threshold setting in Image J software.
- Figure 6.2: Example of the area reduction profile for the circulation of 0.1% NaOH solution at  $0.5\text{ms}^{-1}$  and  $55^{\circ}\text{C}$ .
- Figure 6.3: Example of the images termed as (a) 'clean' and (b) 'not clean'.
- Figure 6.4: PTFE surface covered with a thin film resulted from the water circulation at  $25^{\circ}\text{C}$ .
- Figure 6.5: Comparison of the area reduction profiles between two experiments carried out at  $0.5\text{ms}^{-1}$  and  $70^{\circ}\text{C}$  demonstrating the repeatability.
- Figure 6.6: Images taken during water circulation at  $0.25\text{ms}^{-1}$  at  $50^{\circ}\text{C}$ .
- Figure 6.7: Images taken during water circulation at  $0.25\text{ms}^{-1}$  at  $70^{\circ}\text{C}$ .
- Figure 6.8: Images taken during water circulation at  $0.5\text{ms}^{-1}$  at  $70^{\circ}\text{C}$ .
- Figure 6.9: Area reduction profiles of chocolate at three different conditions showing different removal mechanism.
- Figure 6.10: Images taken during water circulation to remove chocolate layer from stainless steel surface at  $0.5\text{ms}^{-1}$  and  $70^{\circ}\text{C}$ .
- Figure 6.11: Images taken during water circulation to remove chocolate layer from PTFE surface at  $0.5\text{ms}^{-1}$  and  $70^{\circ}\text{C}$ .
- Figure 6.12: Area reduction profiles of chocolate for three different surface materials
- Figure 6.13: Images taken during circulation of 0.1% NaOH solution to remove chocolate layer from polycarbonate surface at  $0.5\text{ms}^{-1}$  and  $70^{\circ}\text{C}$ .

- Figure 6.14: Area reduction profiles of chocolate using chemical circulation.
- Figure 6.15: The dependence of cleaning time of solid chocolate on the flow temperature at  $0.5 \text{ ms}^{-1}$ . Each data is averaged from two experiments and the standard deviation plotted as error bars.
- Figure 6.16: Images taken during circulation of 0.1% NaOH solution to remove chocolate layer from polycarbonate surface at  $0.5 \text{ ms}^{-1}$  and  $25^\circ\text{C}$ .
- Figure 6.17: Raman spectra for cocoa butter (blue) as a reference and the film (red).
- Figure 6.18: Images taken during circulation of 0.1% NaOH solution to remove chocolate layer from polycarbonate surface at  $0.5 \text{ ms}^{-1}$  and  $40^\circ\text{C}$ .
- Figure 6.19: Images taken during circulation of 0.1% NaOH solution to remove chocolate layer from polycarbonate surface at  $0.5 \text{ ms}^{-1}$  and  $55^\circ\text{C}$ .
- Figure 6.20: Area reduction profiles of chocolate using chemical circulation at different flow temperatures.
- Figure 6.21: The dependence of cleaning time of solid chocolate on the flow velocity at  $70^\circ\text{C}$ . Each data is averaged from three experiments and the standard deviation plotted as error bars.
- Figure 6.22: Images taken during circulation of 0.1% NaOH solution to remove chocolate layer from polycarbonate surface at  $0.25 \text{ ms}^{-1}$  and  $70^\circ\text{C}$ .
- Figure 6.23: Images taken during circulation of 0.1% NaOH solution to remove chocolate layer from polycarbonate surface at  $0.37 \text{ ms}^{-1}$  and  $70^\circ\text{C}$ .
- Figure 6.24: Area reduction profiles of chocolate using chemical circulation at different flow velocities.
- Figure 6.25: Cleaning time as a function of surface material for water and chemical circulations at  $0.5 \text{ ms}^{-1}$  and  $70^\circ\text{C}$ . Each data is averaged from three experiments and the standard deviation plotted as error bars.
- Figure 6.26: Images taken during circulation of 0.1% NaOH solution to remove chocolate layer from stainless steel surface at  $0.5 \text{ ms}^{-1}$  and  $70^\circ\text{C}$ .
- Figure 6.27: Images taken during circulation of 0.1% NaOH solution to remove chocolate layer from PTFE surface at  $0.5 \text{ ms}^{-1}$  and  $70^\circ\text{C}$ .
- Figure 6.28: Area reduction profiles of chocolate using chemical circulation for removal from different surface materials.
- Figure 6.29: Cleaning time for tempered and untempered chocolates cooled at different cooling conditions underwent chemical circulation at  $0.5 \text{ ms}^{-1}$  and  $70^\circ\text{C}$ .



Each data is averaged from three experiments and the standard deviation plotted as error bars.

- Figure 6.30: Images taken during circulation of 0.1% NaOH solution at  $0.5\text{ms}^{-1}$  and  $70^{\circ}\text{C}$  to remove the untempered chocolate layer cooled on the Peltier stage at  $10^{\circ}\text{C}/\text{min}$ .
- Figure 6.31: Area reduction profiles for the removal of tempered and untempered chocolate cooled on the Peltier stage at  $1^{\circ}\text{C}/\text{min}$ .
- Figure 6.32: Images taken during circulation of 0.1% NaOH solution at  $0.5\text{ms}^{-1}$  and  $70^{\circ}\text{C}$  to remove the tempered chocolate layer cooled at  $10^{\circ}\text{C}/\text{min}$  on the Peltier stage.
- Figure 6.33: Images taken during circulation of 0.1% NaOH solution at  $0.5\text{ms}^{-1}$  and  $70^{\circ}\text{C}$  to remove the tempered chocolate layer cooled at room temperature for 60 minutes.
- Figure 6.34: Images taken during circulation of 0.1% NaOH solution at  $0.5\text{ms}^{-1}$  and  $70^{\circ}\text{C}$  to remove the tempered chocolate layer cooled in the refrigerator for 60 minutes.
- Figure 6.35: Area reduction profiles of chocolate using chemical circulation for removal from different surface materials.

# LIST OF TABLES

- Table 2.1: Nomenclature and melting points of cocoa butter polymorphs reported by previous researchers.
- Table 4.1: Rheological parameters of the Casson Model for untempered dark chocolate.
- Table 4.2: LVR and yield value of dark chocolate at different temperatures.
- Table 5.1: Water contact angle,  $\theta_w$  ( $^\circ$ ) and average surface roughness,  $S_a$  (nm) of the surfaces. The errors represent the standard error of the mean from 6 replicates (water contact angle) and 3 replicates (average surface roughness).
- Table 6.1: The experimental conditions investigated for the removal of solid chocolate layer using the circulation of 0.1% NaOH solution. Each condition was repeated at least twice.

# LIST OF SYMBOLS AND ABBREVIATIONS

W	Work
F	Force
L	Length
$\sigma$	Apparent adhesive strength/shear stress
A	Surface area
t	Time
$E_a$	Force per unit area
$\sigma_0$	Yield stress
$K_1$	Casson viscosity
$\gamma$	Shear rate
DSC	Differential scanning calorimeter
TAG	Triacylglycerols
AFM	Atomic force microscopy
XRD	X-ray diffraction
CCD	Charge-coupled device
PTFE	Polytetrafluorethylene
LVR	Linear viscoelasticity region
NaOH	Sodium hydroxide
$G'$	Storage modulus
$G''$	Loss modulus
SCM	Sweet condensed milk
SEM	Scanning electron microscopy

# **1 INTRODUCTION**

Chocolate which is derived from the seed of cocoa tree is a popular food type recently. The main producers of cocoa are Cote d'Ivoire, Ghana, Nigeria, Brazil, Ecuador, Malaysia and Indonesia (World Cocoa Foundation, 2012). The flavour of cocoa beans is dependent on the variety, soil, temperature, sunshine and rainfall which makes chocolate tasting much more interesting.

Chocolate is an emulsion containing a dispersed phase (mainly sugar and cocoa solids) and a continuous phase rich in cocoa butter, milk fat and other vegetable fats depending on the type of chocolate. Common types of chocolate found in the market are milk chocolate, white chocolate and dark chocolate. An interesting characteristic of chocolate is that, it exists in a solid form at room temperature and only melts in the mouth. This characteristic is contributed by the existence of the cocoa butter, the main fat involved in chocolate making. The complication of the chocolate processing is due to the complex and lengthy process before final product can be obtained.

## **1.1 Chocolate history and development**

The history of chocolate has begun since 600 AD when the Maya established the first cocoa plantations in Mexico. Cocoa trees were cultivated by the Aztecs of Mexico and the Incas of Peru when the European discovered America (Beckett, 2008). At that time, cocoa beans were prized so highly and used as a currency. The cocoa seeds were mixed with various seasonings to make a spicy, frothy drink which called as 'Chocolatl' which had a

different taste to the chocolate consumed today. It was only prepared for special occasions among the upper classes due to its value.

It is believed that the first cocoa beans were brought to Europe by Christopher Columbus, but no one knew what to do with them until Don Cartes found the commercial value as a drink (Minifie, 1989). The drink was introduced to Spain in the 1520s and sugar was added to produce a sweeter drink because the Spanish did not like the bitter flavour of chocolate. The popularity of chocolate drink only spread to Italy and France in 1600s (Beckett, 2008). The first chocolate factory in the United Kingdom (Joseph Fry & Sons) was built in Bristol and started the production in 1728. Solid chocolate was only made after the invention of cocoa press by the Dutchman Van Houten in 1828 which can produce cocoa butter. It was then mixed with sugar and cocoa powder to produce a gritty dark chocolate. Initially only a plain block of chocolate was produced and the chocolate bars were only made in 1847. Later in 1880, Rodolphe Lindt invented the conching machine which can reduce the particle size of chocolate resulting in a tasty chocolate with smoother texture.

The invention of the first milk chocolate was made by Daniel Peters in Switzerland in 1875 with the help of Henri Nestle who invented the condensed milk formula. Further development has been made in the early twentieth century with the use of milk crumb as an intermediate ingredient obtained by dehydrating the mixture of sugar, milk and cocoa mass which can produce a good flavour of milk chocolate (Beckett, 2008). In early 1900s, Cadbury's Dairy Milk bar has been produced and known worldwide. Since that, more products have been developed by Cadbury, one of the most popular chocolate manufacturers in the UK including countline products which is chocolate covering

different centres such as Crunchie, Twirl and Double Decker, Cadbury Creme Eggs and many other products. Research is also being carried out for future product development.

## **1.2 Chocolate manufacturing**

Manufacturing of chocolate is a complicated process which involves several stages starting with the preparation of the ingredients, mainly cocoa butter. Figure 1.1 illustrates the typical process of chocolate making. Chocolate manufacturing starts when the cocoa beans are fermented to allow the development of the colour and flavour of the beans. The wet mass is then dried for ease of transportation from the growing area to the chocolate production area. It is then sorted and cleaned. The process continues with winnowing to separate the shell from the nibs which then are roasted to give a good aroma of chocolate. The roasted nibs are ground to reduce the particle size generally smaller than 40  $\mu\text{m}$  which can improve the texture and flow properties of the chocolate (Beckett, 2009). The cocoa mass are further pressed to extract the cocoa butter. The cake produced is powderized into cocoa powder which can be used as a beverage or in cooking.

Dark chocolate (represented by red arrow in Figure 1.1) is produced by mixing of the cocoa mass with cocoa butter and sugar. The mixture is then ground and conched. Conching is a process of kneading to refine the taste and texture of chocolate while agitating the molten chocolate continuously. At the same time, the evaporation of the moisture content takes place whereby the moisture removal will take with it the bitter and acid flavours of the cocoa beans (Beckett, 2008; Afoakwa, 2011). So conching is extremely important in developing a unique, rich flavour and reducing the viscosity and particle size. The chocolate is then needs to undergo the tempering process which is very

crucial to ensure the correct polymorph to form (Form V) with high melting temperature as it is the most preferable to the consumers. Other polymorphic forms will cause chocolate bloom due to the migration of the fat to the chocolate surface resulting in a formation of white spots or the transformation of solid-solid phase during storage (Becket, 2001). The tempering process consists of heating and cooling to a certain temperature under continuous shear to produce a large number of seed crystals to initiate crystallisation into a correct form. The surface of the tempered chocolate will be smooth and glossy which is attractive to the consumers. The importance of tempering process has been widely discussed. It determines the chocolate microstructure, mechanical properties and appearance (Afoakwa *et al.*, 2008a). This will be discussed more deeply in Chapter 2.

For the production of milk chocolate (represented by yellow arrow), the cocoa mass will be mixed with sugar and condensed milk. The mixture will be dried to produce chocolate crumb. The main purpose of introducing the chocolate crumb in milk production is to remove water from milk that causes the development of mold (Wells, 2009). This will help to extend the shelf life as well as provide a unique flavour to the chocolate. The crumb is then ground and mixed with cocoa butter. As for dark chocolate, milk chocolate also needs to be conched and tempered for further processed. The process flow of white chocolate is similar to the milk chocolate production but without the cocoa mass (represented by purple arrow).

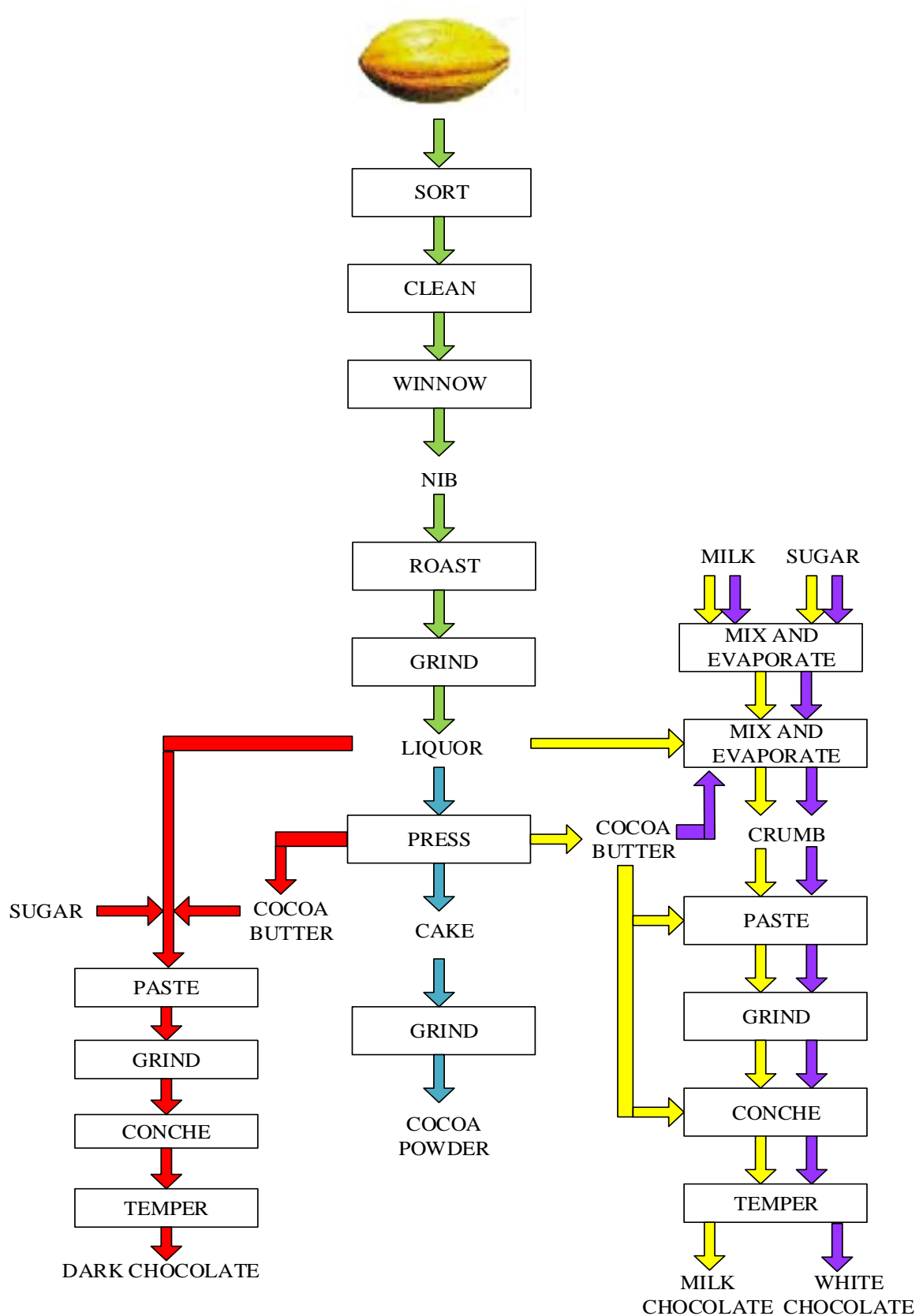


Figure 1.1: Process flow of chocolate making (Pinschower, 2003) with some modifications.



After completing the tempering stage, the liquid chocolate is now ready to be poured into moulds and undergo cooling process. Pinschower (2003) described the steps of the moulding process which begins with deposition of the tempered chocolate into the moulds followed by the vibration of the moulds to ensure an even level of the chocolate. The mould temperature needs to be controlled to be at approximately the same temperature as the tempered chocolate as it will cause some problems if it is too warm or too cold (Gray, 2009). The process will continue with cooling at specified rates. The selection of cooling conditions is dependent on the type of product. Combination of all three heat transfer mechanisms – conduction through the solid chocolate, mould and conveyor belt, convection to the cooling air flow and radiation to water-cooled absorber plates is used in the cooling tunnels (Tewkesbury *et al.*, 2000). Finally, it will be demoulded by inversion and is ready to be packed. The moulded chocolate will be easily come out of the mould if it is properly tempered (Whetstone, 1996). Well tempered chocolate is reported to contract more than under-tempered or untempered chocolates which do not break away from the mould (Pinschower, 2003).

### **1.3 Research background**

In chocolate production, the moulding process is a way to make the liquid chocolate turns into a desired shape. Moulding varies depending on the type of chocolate to be produced. For example, in production of solid bars, the liquid chocolate is poured into mould which is vibrated to spread the chocolate evenly. This is followed by the cooling process to solidify the chocolate. In production of filled bars, after the vibration took place, the mould is then turned over and the liquid chocolate will flow out leaving a thin layer of chocolate. Then, is cooled and a hard shell is produced which is then filled and closed with a layer of

liquid chocolate. Finally, it is cooled again before the mould is removed during demoulding. In order for the chocolate to come out of the mould easily, the contraction should be sufficient (Pinschower, 2003). Difficult demoulding may be due to (Nor Aini & Sabariah, 1995):

- (i) Mould is not cleaned properly. There is a possibility that some chocolate and sugar residues are left on the mould leading to the growth of microorganisms and affecting the quality of the upcoming product. Besides the contamination problem, the residues will initiate nucleation for the newly deposited chocolate which can affect the crystallisation and subsequently the demoulding process.
- (ii) Chocolate not properly tempered. The tempering process is aimed to produce the right amount of stable crystal. However, if the chocolate is not properly tempered, the unstable crystals will be formed leading to less contraction and subsequently affect the demoulding process (Tewkesbury *et al.*, 2000).
- (iii) Temperature of the mould when the liquid chocolate is poured into it is not appropriate. The mould should be pre-heated to the temperature around the temperature of the liquid tempered chocolate. If the mould surface is warmer than the liquid chocolate, the crystals that exist will be destroyed. However, if the mould surface is too cold, the production of the desired crystal form would not be achieved (Beckett, 2008).

Chocolate residue on the mould surface after demoulding is caused by the adhesion property of the chocolate to the surface and cohesion between the chocolate elements (Keijbets *et al.*, 2010). Proper mould cleaning which aims to remove any residue on the surface is necessary to maintain the hygiene level and the final product quality, prevent the development of spots and stains on the mould causing the mould to lose its shine, avoid demoulding problems as well as to reduce production wastage. Figure 1.2 shows the example of the moulds with chocolate residues attach to it and need a proper clean. The level of cleanliness can be classified as below (Christian, 2003):

- (i) Atomically clean: clean at nano-scale.
- (ii) Physically clean: none of the deposit can be detected by eye.
- (iii) Biologically clean: microorganisms-free or at sterile condition.
- (iv) Chemically clean: no substances like cleaning chemical.



Figure 1.2: Example of the moulds with chocolate residues.

Prior to cleaning process, it is important to determine the strength of force contributed to the deposit formation so that the best way to clean the surface can be identified. Many researchers have studied the cleaning of food and beverages deposits

from the contact surface. However, less work has been carried out involving the cleaning of crystalline material. Thus, it is hoped that findings from this current work will give some understanding on the removal behaviour of crystalline confectionery material with respect to the crystallisation aspect and the cleaning condition.

#### **1.4 Objectives of study**

The aims of this study were:

- (i) To understand the crystallisation behaviour and its relationship with the chocolate rheology.
- (ii) To investigate the effect of chocolate processing conditions and mould material on the separation force between solid chocolate and the mould.
- (iii) To study the removal behaviour of solid chocolate from the mould material with and without cleaning chemical.

#### **1.5 Thesis outline**

This thesis comprises 7 chapters including this chapter. A brief chocolate history and manufacturing, research background and the aims of this thesis have been given above.

The descriptions of the remaining chapters are given as follows:

Chapter 2 discusses published work relevant to this study including the crystallisation aspect, chocolate processing, chocolate-mould interaction, chocolate rheology and the cleaning work of food deposits from the heat exchange surface.

Chapter 3 describes the materials and all the experimental set-up as well as the procedures to carry out all the experiments throughout this study. The sample preparation and data analysis methods are also described.

Chapter 4 reports the results of the crystallisation study of dark chocolate with respect to some parameters including the surface variations, cooling conditions and also the effect of the tempering process using the DSC. This is followed by the rheological study which focuses on the evolution of the apparent viscosity and the yield stress.

Chapter 5 deals with the work carried out to measure the removal force using two techniques: micromanipulation and texture analyser. The micromanipulation work includes variation of cooling and soaking conditions, surface material, probe speed and also the influence of tempering on the removal force. For the work involving texture analyser, the influence of the probe-chocolate surface distance, contact time, surface material and tempering process on the separation force are presented.

Chapter 6 focuses on the removal behaviour of a solid chocolate layer using a flow cell cleaning rig. The effect of various parameters including the flow velocity and temperature, chemical requirement, surface material, cooling condition and tempering on the cleaning time and removal behaviour were studied.

Chapter 7 gives the conclusions of the results obtained in this study and some ideas for future work to be carried out.

## **2 LITERATURE REVIEW**

### **2.1 Introduction**

Chapter 1 has introduced some background of this thesis and the objectives of the work. This literature review is focusing on the topics which relate to the work reported in this thesis. Initially, some introduction on the chocolate ingredients will be given, followed by basic information on cocoa butter crystallisation. This will include the description on the crystallisation process, polymorphism, crystal arrangement and factors affecting the crystal formation. Some reviews on tempering process, blooming and cooling process will also be given. In addition, it will discuss the methods used to characterise the polymorphs.

Chocolate-mould interaction is discussed by considering the factors contributing to the adherence of chocolate to the mould and some explanation on the micromanipulation technique was included followed by some reviews on chocolate rheology. Finally, cleaning work of fouling deposits that have been conducted previously is discussed.

### **2.2 Chocolate Ingredients**

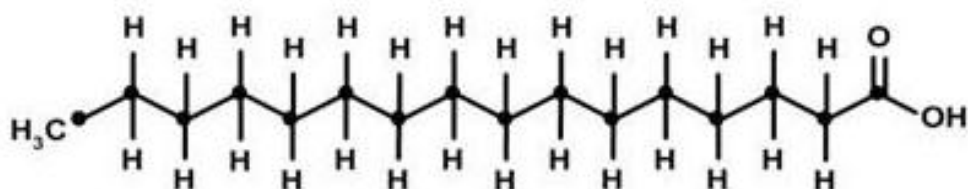
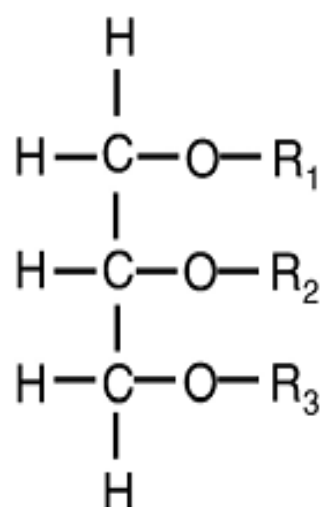
The chocolate formulation depends on the type of chocolate to be produced. Raw ingredients in chocolate making are cocoa solids, cocoa butter, sugar and lecithin for dark chocolate with the addition of milk solids and milk fat for milk chocolate, while for white chocolate no cocoa solids are involved. All these ingredients influence the crystallisation kinetics and the microstructure which will determine the quality of final product. For example, the addition of lecithin can increase the crystal growth rate with more amount of

desired crystals can be produced (Svanberg *et al.*, 2011). (Hartel, 2001) also reported that the dispersion of sugar crystals and cocoa solids throughout the cocoa butter has an impact on the chocolate texture and quality.

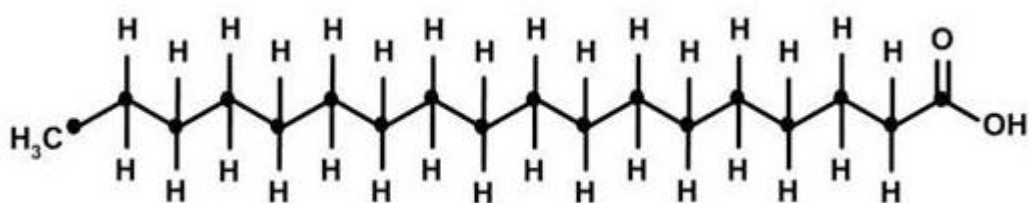
### **2.3 Cocoa butter crystallisation**

Cocoa butter is a pale-yellow fat extracted from the cocoa bean which has a high stability characteristic as it exhibits brittleness below 20°C and will only begin to soften around 30-32°C with the melting point is about 35°C (Minifie, 1989). It is well known that cocoa butter is a mixture of triacylglycerols (TAG) composed of three main fatty acids (R1, R2 and R3) attached to a glycerol backbone as illustrated in Figure 2.1. The three fatty acids are approximately 26% of palmitic acid (C16:0) represented by P, 34% of stearic acid (C18:0) represented by S and 35% of oleic acid (C18:1) represented by O (Beckett, 2008). The 3-letter code is used to identify TAGs. Three main TAGs in cocoa butter are POP, SOS and POS.

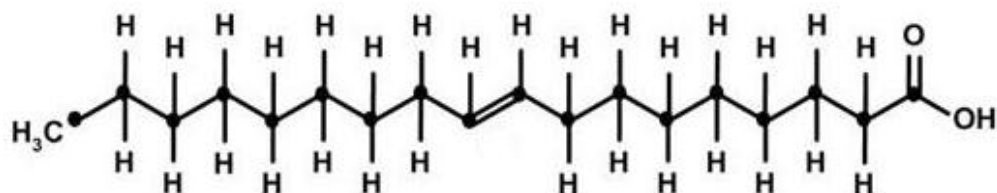
Cocoa butter plays an important role to determine a good texture, appearance and stability of the final product. Crystallisation is defined as a process which involves the formation of a crystalline lattice structure (Hartel, 2001). Crystallisation and polymorphism of cocoa butter have been studied extensively by many researchers all around the world. However, the complexity of the process requires further study to be carried out. If a proper crystallisation is not obtained, it will contribute to a defect in the final product quality.



Palmitic



Stearic acid



Oleic acid

Figure 2.1: Structure of triglyceride and the fatty acids.



### **2.3.1 Basics of crystallisation**

During solidification of cocoa butter, the crystallisation process occurs which involves a liquid to solid transition. During the liquid state, the fat molecules move randomly and are constantly associating and dissociating with each other. When the temperature decreases, the molecules have less energy to move and tend to come together and spontaneously arrange to form nuclei. A stable nucleus is achieved when the radius reaches a critical value which depends on the surface energy and the free energy of the liquid to solid transformation. The crystallisation process consists of three steps (Roos, 1995):

- (i) Nucleation – the most important step to control the crystallisation.
- (ii) Propagation – crystals growth.
- (iii) Maturation – crystal perfection.

Nucleation mechanisms can be classified into primary and secondary, with primary nucleation which is the basic mechanism of the crystal formation can be homogeneous or heterogeneous. Homogeneous nucleation rarely occurs in real life situations. It occurs when the molecules in solution arrange to form a crystal structure and requires a large extent of supercooling to initiate nucleation. Practically, the heterogeneous nucleation is found in fat crystallisation. In this case, the surfaces and particles in contact with the melt promote the formation of a nucleus and initiate nucleation with much lower energy needed (Hartel, 2001). Secondary nucleation can occur when the existing crystals are in contact with each other or the equipment part such as a stirrer or a solid wall causing break up of the crystals which act as a site and source for the formation of new crystals.

The crystals will then continue to grow as long as the molecules have sufficient mobility to move as it requires that the molecules migrate and diffuse through the material to the surface of the growing crystal. Once the molecules reach the surface, they will orient into an arrangement and incorporate into the crystal lattice resulting in some removal of the latent heat of fusion associated with the phase change. When the thermodynamic equilibrium between the liquid and crystalline states has been attained, the growth stops and crystallisation is completed.

### **2.3.2 Polymorphism**

The complication of the cocoa butter crystallisation is contributed by the polymorphic nature as it can crystallize into six different forms depending on the thermodynamic and kinetic factors (Sato, 2001) . This behaviour is called ‘polymorphism’ (Sato *et al.*, 1989). Many researchers have done the characterisation work of the cocoa butter polymorphs and some discrepancies occurred in the number of forms. However, all of them agreed that there is a difference in the melting temperature of the polymorphs. A summary of the identified polymorphs and the melting temperatures are given in Table 2.1. The characterisation was made by using various methods such as microscopy, X-ray diffraction and differential scanning calorimetry. The nomenclature introduced by Wille & Luton will be used throughout this thesis as it is the most well known in the confectionery industry.

Table 2.1: Nomenclature and melting points (°C) of cocoa butter polymorphs reported by previous researchers.

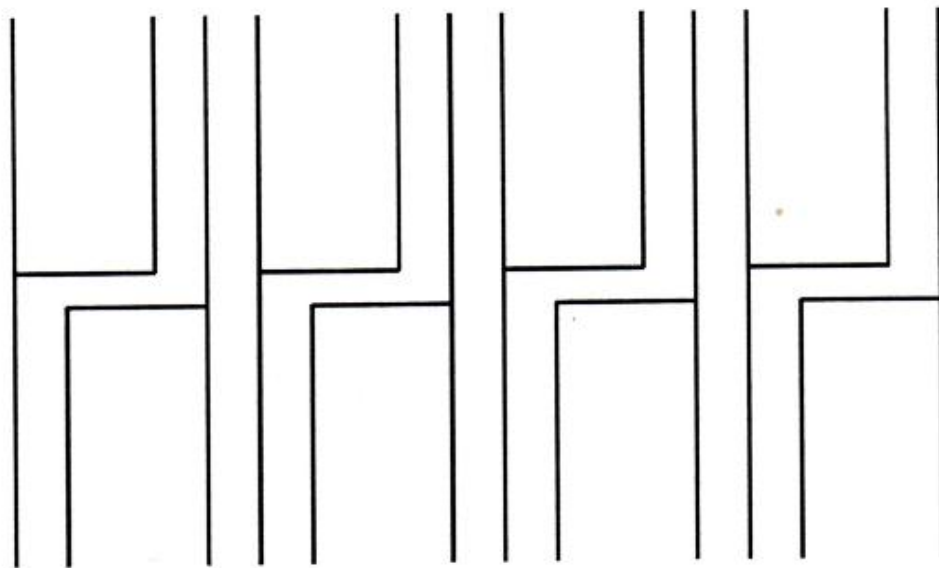
Vaeck (1960)	Duck (1964)	Wille & Luton (1966)	Lovegren <i>et al.</i> (1976)	Davis & Dimick (1986)
$\gamma$ 17.0	$\gamma$ 18.0	I 7.3	VI 13.0	I 13.1
$\alpha$ 21-24	$\alpha$ 23.5	II 3.3	V 20.0	II 17.7
		III 25.5	IV 23.0	III 22.4
$\beta'$ 28.0	$\beta''$ 28.0	IV 27.5	III 25.0	IV 26.4
$\beta$ 34-35	$\beta'$ 33.0	V 33.8	II 30.0	V 34.9
	$\beta$ 34.4	VI 36.3	I 33.5	

The difference in the melting temperature for each polymorphic form is contributed by the variation of crystal structures when the fatty acid chains are arranged differently. Form I, the most unstable form is obtained when cooling is being carried out rapidly to a very low temperature from the molten chocolate. Form III is believed to be a mixture of Form II and IV (Merken and Vaeck, 1980). Even though Form VI is the most stable form, it prone to have bloomy surface which is caused by the migration of fat to the surface. The desired form is form V with a glossy appearance and good contraction to produce a good shape of moulded product. This characteristic is determined by the tempering process which manipulates the temperatures to produce Form V crystals.

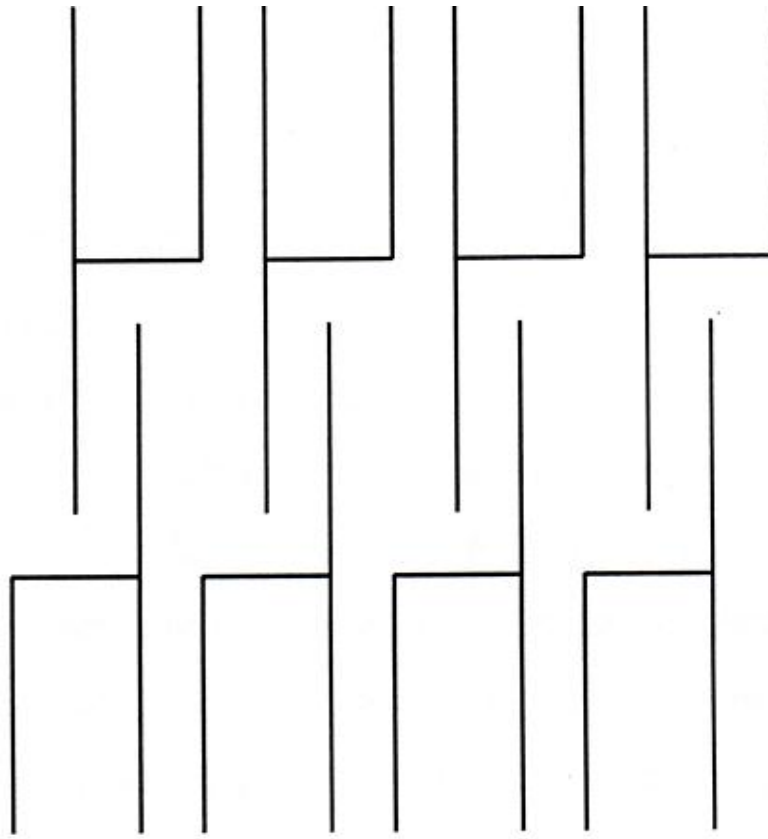
### 2.3.3 Crystal arrangement

As mentioned earlier, the TAG molecules are able to pack in different crystalline arrangements giving different melting temperature. TAG molecules which look like chairs

or tuning forks can be arranged in two ways; double or triple packing as shown in Figure 2.2. Double packing involves the overlapping of the fatty acids of adjacent molecules. Contrarily, the fatty acids of adjacent molecules in triple packing do not overlap. Concerning solidification in chocolate, the cooling rates applied play an important role to determine the molecular arrangement of the TAG. When the cooling process takes place rapidly, the molecules do not have a chance to align in their lowest energy state resulting in a less stable form or polymorph.



(a)



(b)

Figure 2.2: Packing arrangements of (a) double chain and (b) triple chain of TAG.

#### 2.3.4 Factors affecting the crystals formation

As mentioned previously, the crystallization of cocoa butter is a complex process. Thus, a proper handling needs to be taken to ensure the correct polymorph can be obtained. There are several factors that influence the crystals' formation including the chocolate ingredients, crystallisation temperature, cooling rate and shearing.

Chocolate ingredients and pre-crystallisation technique have been reported to have an impact on the kinetics of crystallisation (Svanberg *et al.*, 2011). The effect of sugar, cocoa particles and lecithin on cocoa butter crystallisation in seeding and non-seeding pre-

crystallisation techniques was determined from DSC measurements and image analysis. All ingredients and both pre-crystallisation techniques were found to have a large impact on the crystallisation. Kinta & Hartel (2010) in their study used different seed amounts and observed the crystallisation behaviour by using light microscopy. According to them, too few seeds will lead to the bloom formation. The addition of milk fat for milk chocolate was also reported to retard crystallisation of cocoa butter as the combination of two fats will cause the nucleation rate to decrease (Metin and Hartel, 2005).

The temperature at which the chocolate is cooled also influences the crystallisation. The nucleation rate increases as the temperature increases (Metin and Hartel, 2005). It is well known that cooling rate has a great impact on the crystallisation. Rapid cooling will cause the nucleation rate to increase and lead to formation of small crystals.

Agitation or shear is generally thought to be very important to initiate nucleation. According to Stapley *et al.* (1999) and Metin and Hartel (2005), shear breaks up crystallites producing more seed crystals and secondary nucleation can occur. Shear can also align TAG molecules parallel to each other in the shear field, and then move them past each other. Other than that, shear provides better overall mixing.

### **2.3.5 Tempering process**

Tempering is one of the most crucial stages in chocolate making process which aims to produce sufficient seed crystals to ensure the crystallisation occurs into the right crystal form. The importance of tempering process are to adjust the yield value and viscosity of the chocolate so that is suitable for moulding, coating or enrobing and has

long-term stability of the chocolate flow properties (Beckett, 2008). During tempering, the crystallization process was induced by the addition of seed chocolate to obtain the desired crystal form of Form V. The shearing effect and the temperature history used play an important role for the tempering process to occur successfully (Stapley *et al.*, 1999). Precise controls of the temperature with the help of agitation enhance the nucleation rates (Afoakwa *et al.*, 2007).

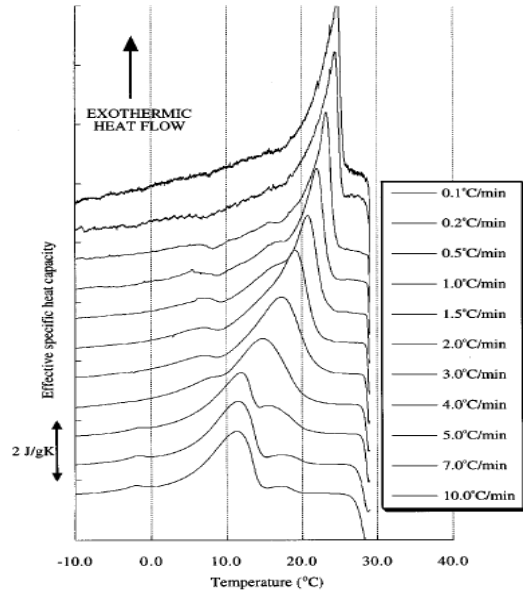
According to Briggs and Wang (2004), the typical tempering process consists of melting of the solid chocolate at 45-50°C followed by cooling of the melted chocolate to 28-29°C in about 20 minutes to initiate crystallization. This temperature will be held constant for a period of time to allow the seed crystals to be formed. Then, the chocolate will be rewarmed to the temperature of 30-32°C to get rid of the crystals with lower melting points and at the same time the Form V crystals will be allowed to form. Finally, the chocolate is ready to be poured into moulds and will be cooled to 18°C to get a final product with the desired appearance.

In general, the shear rate applied is proportional to the crystallization time. Before the development of the tempering machines, chocolate used to be hand-tempered. Nowadays, the use of multistage heat exchangers allows the chocolate to pass through it where shear is applied at different rates. There are many tempering methods that have been used in previous studies to investigate the effect of shear applied on chocolate tempering. For example, Stapley *et al.* (1999) and Dhonsi & Stapley (2006) have used a concentric cylinder geometry shearing rig with a water jacket incorporated to control the temperature of the tempering process. The design used was able to create a uniform shear rate to the chocolate. Another method that has been used for tempering was using a rheometer

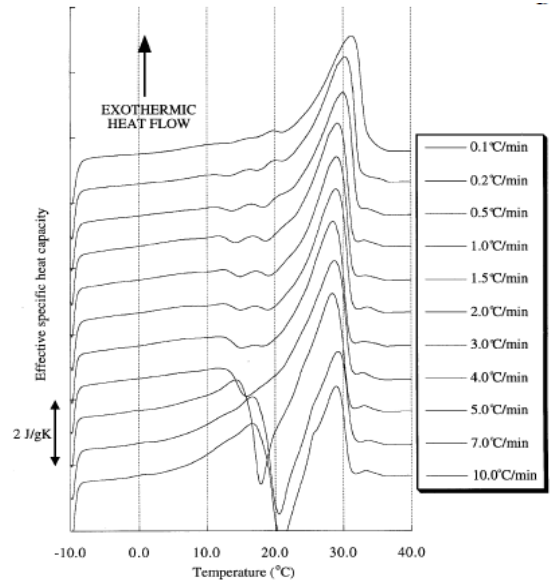
equipped with parallel plate geometry (Briggs & Wang, 2004). The temperature control was done by a Peltier system. A helical ribbon impeller, equipped with a sample container with circulating liquid jacket has also been used to study the crystallisation under stirring conditions compared to the static conditions (Toro-Vazquez *et al.*). It has been found that cocoa butter was crystallised into Form V under stirring conditions, but not under static conditions. According to MacMillan *et al.* (2002), the absence of shear produces Form IV crystals causing the formation of chocolate which will easily bloom.

As stated earlier, tempering process can influence the formation of the polymorph. Stapley *et al.* (1999) has done a comparison based on the DSC scans for the tempered and untempered chocolate. For a tempered chocolate, more unstable crystals will be formed when a higher cooling rate is applied during cooling process as shown in Figure 2.3 (a) and (b). For the untempered chocolate, less stable polymorphs were noticed even at the lowest cooling rate as displayed in Figure 2.3 (c) and (d). The samples cooled at higher cooling rates show multiple subpeaks due to the presence of crystals with variations in sizes, compositions and polymorphs.

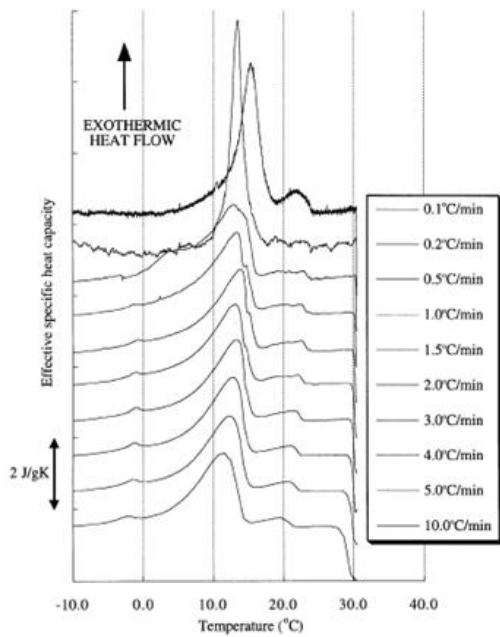




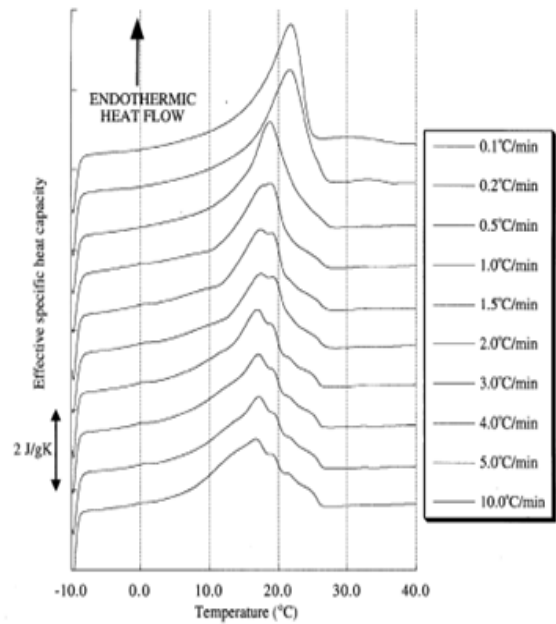
(a)



(b)



(c)



(d)

Figure 2.3: (a) DSC cooling curves of tempered chocolate at different cooling rates. (b) DSC remelting curves of tempered chocolate at 5°C/min for different cooling rates. (c) DSC cooling curves of untempered chocolate at different cooling rates. (d) DSC remelting curves of tempered chocolate at 5°C/min for different cooling rates (Stapley *et al.*, 1999).

### 2.3.6 Blooming

Blooming is a major problem in chocolate production. It refers to the appearance of whitish spots on the chocolate surface which affect the appearance of the product. Figure 2.4 shows the appearance of well tempered chocolate and the untempered chocolate. However, both tempered and untempered chocolates have the tendency to have the bloom formation. There are two types of blooms that have been reported which are fat bloom and sugar bloom. Fat bloom occurs due to the migration of the fat to the chocolate surface, while sugar bloom is caused by the action of moisture on the sugar ingredients (Minifie, 1989). It can be caused by composition, improper processing conditions and storage conditions (Lonchampt and Hartel, 2004).

When two incompatible fats are used, the bloom formation tends to occur. Tempering and cooling are the two crucial steps that need to be done correctly. Chocolate which undergoes a good tempering will have a good resistance to fat bloom. The under-tempering case occurs when the seed crystals are not enough to induce crystallisation. Re-crystallisation can occur due to the generation of new seeds upon cooling which can accelerate the formation of blooms. In the case of over-tempered chocolate, the amount of seed crystals is too large which will affect the contraction of the chocolate as the crystallisation is extended. A good tempering can be achieved by using over 270ppm seeds (fat basis) (Kinta & Hartel, 2010). According to them, similar bloom surface with the untempered chocolate has developed when not enough seed crystals were added, but the bloom on the poorly tempered chocolate appeared just after cooling whereas the bloom on the untempered chocolate took several days to be detected. During cooling, it is essential to control the cooling rate as it can prevent the blooming problem to occur. Rapid cooling

tends to promote bloom formation. Chocolate has a long shelf life of about a year. The development of bloom can also occur during storage. It is necessary to keep the chocolate at low temperature to minimise bloom formation even though the problem can still occur after more than one year of storage. The pictures in Figure 2.5 illustrate blooming problem caused by the factors mentioned above while Figure 2.6 presents the AFM scans of the bloomed dark chocolate.



Figure 2.4: The well-tempered chocolate is on top. It has a glossy surface, but the untempered chocolate will stick to the mould surface (Le Reverend *et al.*, 2008).

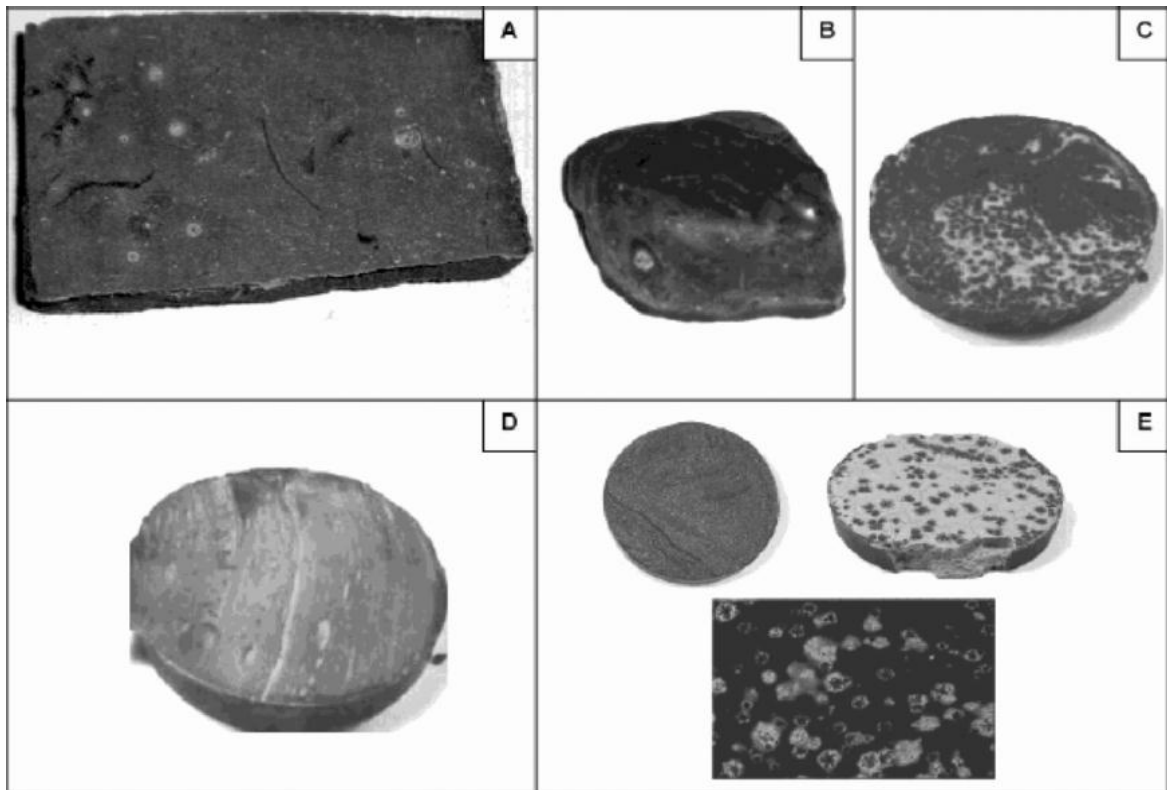
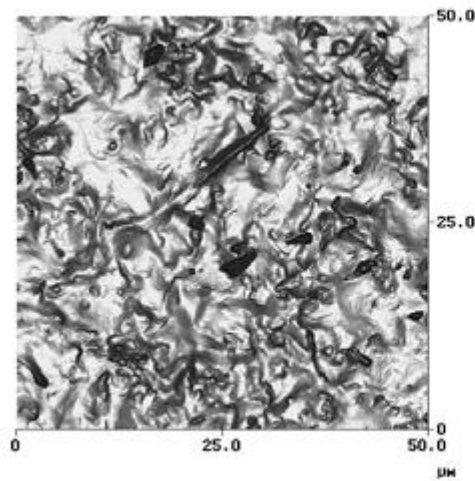
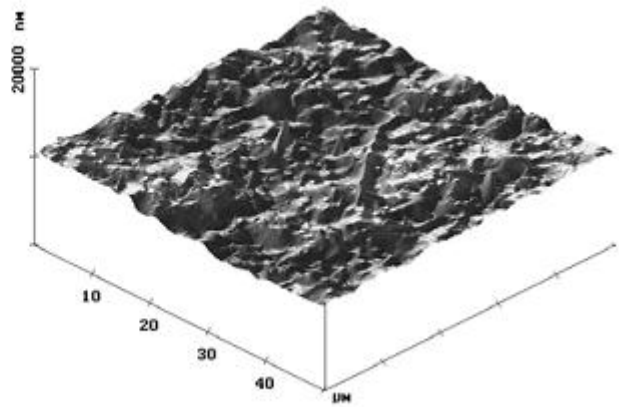


Figure 2.5: Chocolate that has blooming problem due to (A) storage, (B) fat migration, (C) heat hit, (D) over-tempering, (E) non tempering (Lonchampt and Hartel, 2004).



(a)



(b)

Figure 2.6: (a) 2-D and (b) 3-D AFM scans of dark chocolate surface with blooming problem (Hodge and Rousseau, 2002).

### 2.3.7 Cooling process

Chocolate solidification is accomplished by the cooling process. During cooling, there are two types of heat that have to be removed from the product to ensure the chocolate solidifies in the correct polymorphic form; specific heat and latent heat (Beckett, 2008). Tempered chocolate is deposited into a mould, shaken to remove any bubbles and finally cooled. The typical heat transfer mechanisms involved are conduction, convection and radiation. For conductive heat transfer, the heat flows through the material in contact with chocolate. For convective heat transfer, the cold air is blown over the product at varying speed and some heat will be removed. Heat transfer by radiation takes place at a rate determined by the fourth power of the temperature difference between the chocolate and its surroundings ( $\Delta T^4$ ) (Beckett, 2008).

Cooling tunnel and multi-tier coolers are commonly used to cool the chocolate in industry. The cooling rate used need to be controlled properly as it can give a big impact on the crystalline structure of the end product. Properly tempered chocolate can result in a formation of less stable polymorphs if too high cooling rate is applied (Stapley *et al.*, 1999). Besides that, (Campos *et al.*, 2002) in their study found that rapid cooling resulting in a high nucleation rate of anhydrous milk fat and lard. A large number of nuclei are produced instantaneously causing a rapid increase in viscosity, thus limiting molecular diffusion and crystal growth. For that reason, it can be seen in Figure 2.7 (A) and (C) that the crystals size are smaller compared to the crystals shown in Figure 2.7 (B) and (D) which were cooled slowly allowing the crystal aggregation to occur.

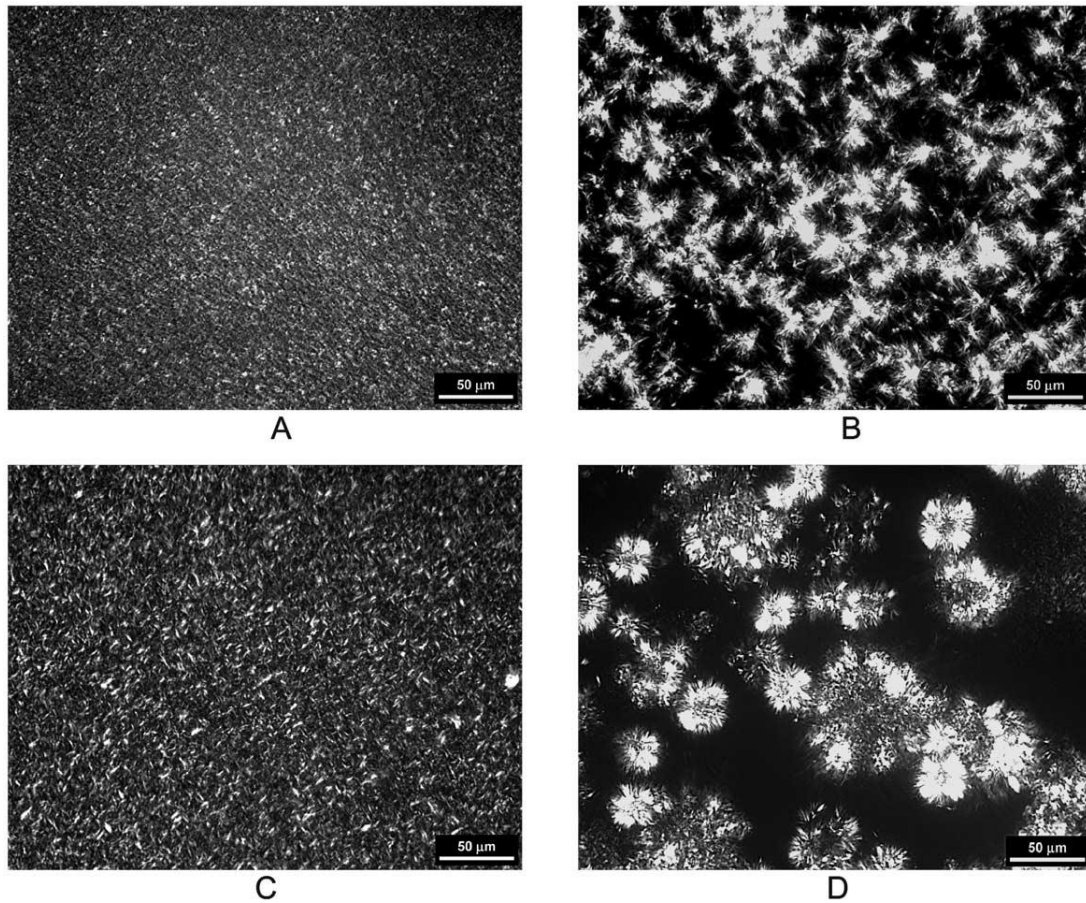


Figure 2.7: Polarized light micrographs of anhydrous milk fat cooled rapidly (A) and slowly (B), and lard cooled rapidly (C) and slowly (D) (Campos *et al.*, 2002).

Recently, rapid cooling process known as FrozenCone is becoming increasingly popular among the chocolate manufacturers especially to produce the Easter eggs. The typical process can be described as follows (Le Reverend, 2009):

- i) Freshly tempered chocolate is deposited into the mould at a temperature around 30°C.
- ii) The cold press at a typical temperature of -10°C is inserted into the molten chocolate for about 3s as illustrated in Figure 2.8. It is enough to allow the chocolate shell to partially crystallise.
- iii) The chocolate is then conveyed in a first tunnel where it sets completely.
- iv) In the case of filling chocolate, a filling can be injected.
- v) A second cooling tunnel is used to cool the filling.
- vi) The shell is then closed by applying molten tempered chocolate at the surface or by combining two shells together.

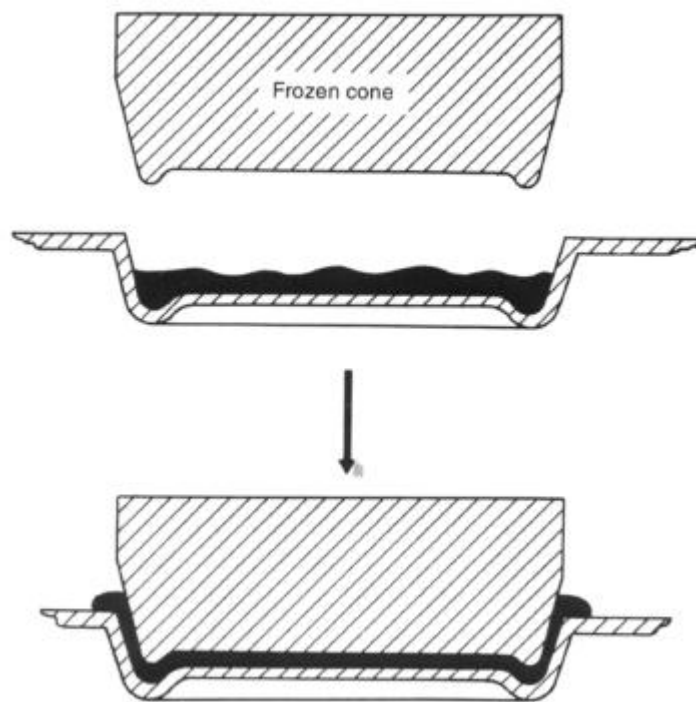


Figure 2.8: The insertion of a frozen plunger into the chocolate during FrozenCone process (Baichoo, 2007).

Some modelling works concerning cooling of chocolate have been carried out by several researchers. (Tewkesbury *et al.*, 2000) have developed a model to predict the temperature distributions in the mould during cooling with respect to space and time. The model can represent the behaviour of chocolate and filling in the chocolate manufacturing industry. In other work, Le Reverend *et al.* (2011) developed a mathematical model of the phase change of cocoa butter and heat transfer for the FrozenCone process. Only a small fraction of the cocoa fats is solidified when rapid cooling is applied and the numerical simulation shows that the rest of the material only crystallise when passing through cooling tunnels. From the model, it has been identified that metal mould can stand the filling deposition temperature up to 45°C without melting of the chocolate shells, but only 36°C for polycarbonate moulds. Different mould materials vary in the thermal resistant and affect the heat transfer whereby metal mould would allow better cooling efficiency compared to polycarbonate mould.

### **2.3.8 Methods to characterise the polymorphs**

There are two common methods to identify the different polymorphs. X-ray diffraction (XRD) is commonly used identify the crystal and determine molecular structure. One advantage of this method is that it allows the presence even small crystalline regions to be identified in complex matrices (Baichoo, 2007). Le Reverend *et al.* (2009) has obtained XRD patterns of chocolate samples and characterized the crystalline state of cocoa butter by using subtraction method of the liquid state pattern from the solid state pattern for the same sample. The area under the curve gave the quantification of the degree of crystallinity for the current system. In a study conducted by MacMillan *et al.* (2005), in-situ XRD has been used to characterise the crystal structure and the relationship with the



growth kinetics of the cocoa butter polymorphs was determined. Figure 2.9 shows the example of the XRD scan.

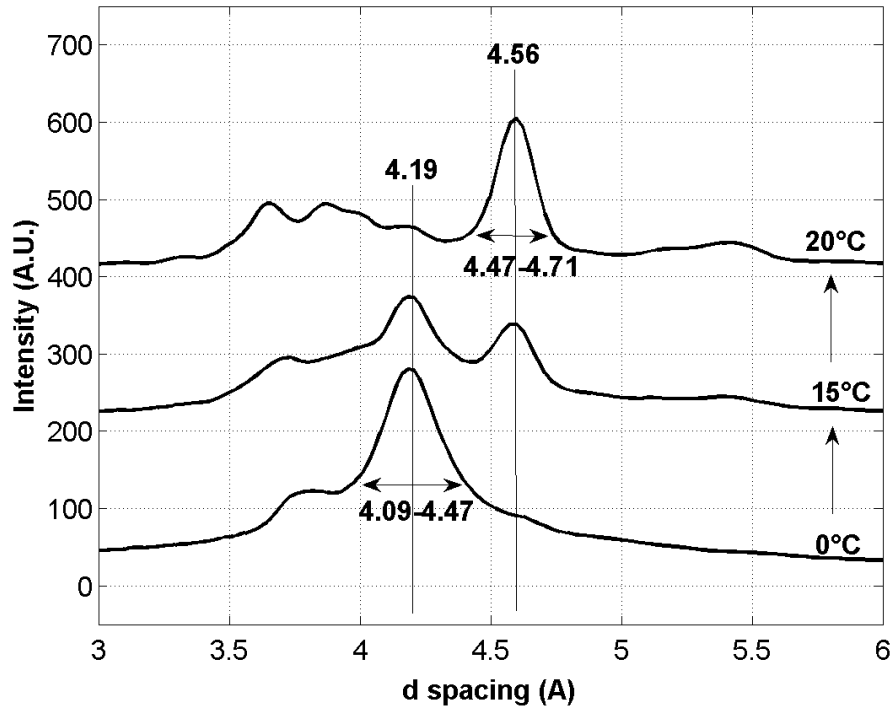


Figure 2.9: Example of XRD scan of cocoa butter cooled rapidly and heated slowly (Le Reverend, 2009).

Differential Scanning Calorimetry (DSC) is another method to characterize the polymorphisms of fats in food products. It measures both endothermic and exothermic processes which can provide the information on the crystallisation and melting of the fats. Stapley *et al.* (1999) conducted a study to determine the effect of tempering process and the temperature history on the crystallization of chocolate by using the DSC to observe the solidification stage of the chocolate. The polymorphous transition in chocolate have also been studied by Fessas *et al.* (2005) using DSC analysis. The work done was aimed to determine the polymorph type resulted from the temperature history applied. Figure 2.10 presents the example of the typical DSC curves.

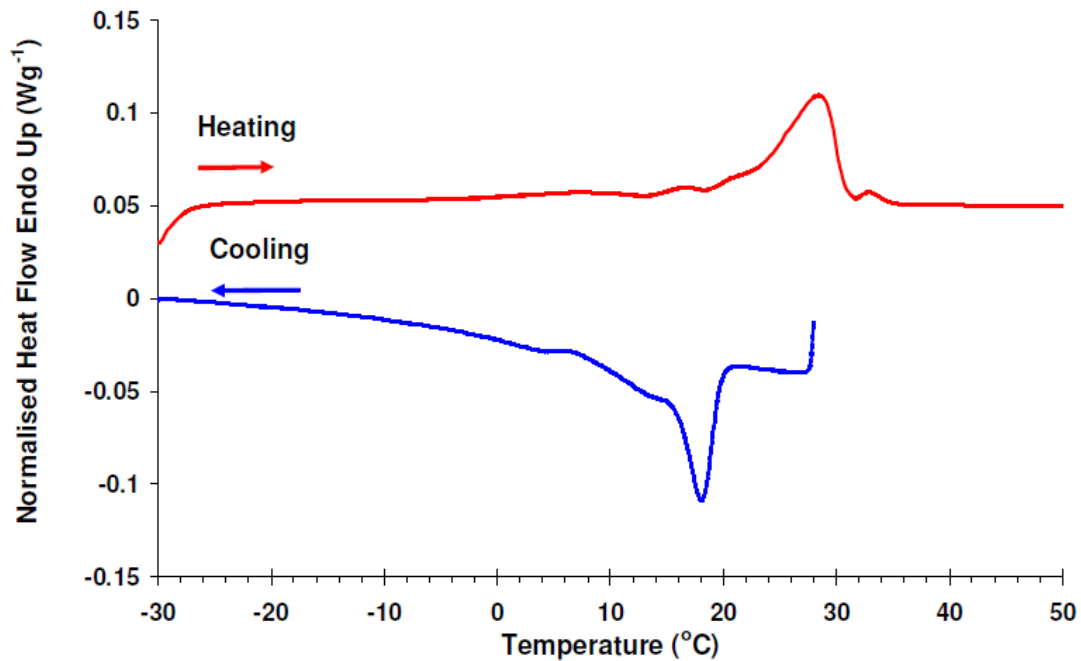


Figure 2.10: Example of the cooling and melting DSC curves for tempered chocolate cooled at 1°C/min to -30°C and rewarmed at 10°C/min (Baichoo, 2007).

## 2.4 Chocolate-mould interaction

### 2.4.1 Factors contributing to the adherence of chocolate to the mould

Foodstuffs adhesion to the industrial equipment is one of the major problems facing by the food processing industry. Adhesion phenomenon will exist when there is a direct contact between food particles and the surface of the equipment. The attraction formed needs to be overcome when separating those two surfaces. Commonly, the adhesion of food components to the equipment will create fouling problems and lead to an increase in the cleaning cost.

After undergoing the tempering process, the cooling process of the tempered chocolate is needed for the crystallization process to take place. The tempered chocolate will be deposited into a mould and allowed to cool at a specific cooling rate. An improper crystallization will result in a bad demoulding process with some deposits left on the mould surface. Well tempered chocolate contracts more and easily detaches from the mould whilst the untempered does not. It has been reported that the initial viscosity, cooling rate and cooling direction affect the contraction of chocolate (Pinschower, 2003). The higher the viscosity of the sample when transferred to the solidification rig the lower the contraction measured. However, the effect of cooling rate on the contraction was found to be diverse. It was expected that slow cooling will result in more contraction as more time available for the molecules to arrange themselves into a closer packing. The opposite effect was possibly due to the direction of heat flow. If cooling process is being carried out from the bottom, the chocolate nearest to the mould will solidify first and solidification will continue towards the centre of the chocolate. The surface movement follows a direction towards the source of cooling and thus, chocolate will stick to the mould surface. On the other hand, if it is cooled from the top, the chocolate surface moves upwards resulting an easy detachment from the mould.

Different mould surfaces will influence differently the detachment behaviour of the chocolate during the solidification stage. The properties of the mould surface will determine the failure mechanisms during demoulding stage, whether it is prevailed by adhesion failure or cohesive failure. By comparing four different mould materials, Keijbets *et al.* (2009) suggested that a suitable mould material for chocolate moulding should have a surface energy below  $30 \text{ mN m}^{-1}$ . Michalski *et al.* (1999) reported that the surface hydrophilicity will influence the adherence of food emulsions to the equipment. A

hydrophilic surface which can easily wet will reduce the adhesion forces with the emulsion droplets. The surface should have a higher surface energy than the adhesive to create a low contact angle and ease of cleaning (Bhandari, 2007). Another factor contributing to different failure mechanisms during demoulding is the processing conditions including the temperature, contact time and relative humidity of the surrounding environment (Keijbets *et al.*, 2010).

#### **2.4.2 Micromanipulation**

The micromanipulation rig is an apparatus that gives a direct measurement of force required to remove fouling deposits from a substrate surface. It has been widely used to study the adhesion of biofouling deposits (Chen, 2000; Chen *et al.*, 2005) and food fouling deposits (Liu *et al.*, 2006b; Liu *et al.*, 2006a; Liu *et al.*, 2002; Liu *et al.*, 2006c; Liu *et al.*, 2007; Othman *et al.*, 2009; Akhtar, 2010; Goode, 2011). This technique has also been used to measure the pulling energy for toothpaste removal from stainless steel surface (Akhtar, 2010; Cole, 2011). The term ‘pulling energy’ was introduced by (Liu *et al.*, 2006a) to compare the adhesive and cohesive forces in the case whereby total removal of the deposits from the surface could not be achieved. Adhesion refers to the attraction between two surfaces of different material in contact, while cohesion is the attraction the molecules in the same material. The detail explanation of the rig and its operation will be given in section 3.4.

The removal of fouling deposits from a surface is dependent on the nature of the deposits and the characteristic of the fouling surface (Liu *et al.*, 2006b). For example, tomato paste can be removed in large chunks by hydration of the deposit-substrate surface.

Contrarily, protein deposits are removed in small pieces from the surface. In some cases, the combination of both types of removal can be observed when the deposit breaks at the surface and the bulk deforms. In a study conducted by Akhtar (2010), the pulling energy to remove toothpaste from stainless steel surface was found to be the largest, followed by glass and PTFE. Similar behaviour observed for the removal of Turkish delight and SCM. Interestingly, reverse behaviour can be seen in removal of caramel deposit. The amount of energy needed for the deposit removal is also affected by the process variables including the soaking time, medium temperature and chemical concentration as the deposit is normally soaked in water or chemical solution (used when water alone cannot remove the deposit) prior to micromanipulation measurement in order to identify the adhesive and cohesive effects in the cleaning of fouling deposits. The effect of adding cleaning chemicals has been studied by Liu *et al.* (2007) in the removal of egg albumin from a metal disc. The SEM pictures of the deposits show that swelling and dissolution occurs when it was submerged in 0.5% NaOH solution for 60 min at 20°C. It can be observed in Figure 2.11 (b) that the protein dissolving away and amorphous clumps are formed.

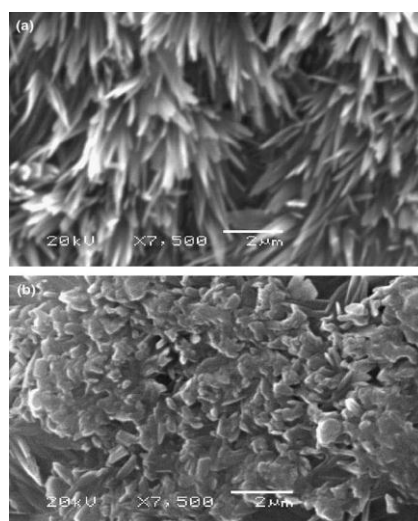


Figure 2.11: SEM images of egg albumin deposits (a) before and (b) after contacting with 0.5% NaOH solution for 60 min at 20°C (Liu *et al.*, (2007)).

A comparison between the use of fluid dynamic gauging and a micromanipulation probe to measure force and removal behaviour of baked tomato puree deposits from stainless steel surfaces has been studied by Hooper *et al.* (2006). The fluid dynamic gauging technique uses the principle of pressure difference to determine the flow characteristics of the liquid through a nozzle which is placed perpendicularly with the surface. The details of this technique was described by Tuladhar *et al.* (2000). The micromanipulation technique showed an advantage over the fluid dynamic gauging even though both techniques exhibit the same removal characteristic. This technique gave a separate analysis of the adhesive and cohesive interactions, while the dynamic gauging technique only showed the deformation changes due to the differences in adhesive and cohesive strength and the results obtained exhibited a greater scatter.

Even though the micromanipulation measurement has been used to study a wide range of deposits removal, there is no literature found that involves the deposits which has been crystallised.

#### **2.4.3 Texture analyser**

The use of texture analyser to study adhesion was established by Walewijk *et al.* (2008). In their study, the adhesion between alginate gel surfaces was measured in air, distilled water and a 1 M calcium chloride solution. The maximum force upon retraction was considered as the adhesive force. An increase in applied force for a range of contact times and increase in contact time for a range of applied forces were found to increase the adhesive forces between the alginate gel surfaces.

In a study conducted by Keijbets *et al.* (2009) who investigate the effect of surface energy to the chocolate-mould adhesion, a texture analyser has been used to mimick the demoulding process. A pull off method was employed whereby a probe made of four different materials was brought into contact with a surface of liquid chocolate which then solidified. The two surfaces were then separated when the probe was pulled vertically. The same experimental set up was used by Keijbets *et al.* (2010) to determine the effects of processing conditions on chocolate demoulding. Temperature, contact time and relative humidity of the surrounding environment were reported to significantly affect the demoulding process.

## **2.5 Chocolate rheology**

Rheology is defined as a study of deformation and flow of matter (Rao, 2006). It is essential to know the rheological behaviour to control the product quality. Liquid chocolate which is classified as a non-Newtonian contains the dispersion of solid particles throughout the continuous fat phase and the interaction between them determines the rheological properties. There are two parameters normally used to quantify rheology; yield stress and apparent viscosity (Goncalves and Lannes, 2010). Yield stress refers to the amount of energy required to initiate flow, while the energy needed to maintain the flow is represented by the apparent viscosity (De Graef *et al.*, 2011). Chocolate rheology is commonly described with the Casson equation whereby the Casson viscosity and Casson yield stress can be obtained by conducting linear regression for the plot of the square root of the shear stress versus the square root of the shear rate.

Some studies found that the flow properties are determined by several factors including the processing (refining, conching and tempering) and the formulation (particle size distribution, amount of fat and type of emulsifiers) (Afoakwa *et al.*, 2009; Afoakwa *et al.*, 2007; Afoakwa *et al.*, 2008b; Afoakwa *et al.*, 2008a). The influence of cooling rate on the rheological properties has also been studied by (Baldino *et al.*, 2010).

There are several methods that can be used to determine the yield stress value. A summary of the methods is given below:

- (i) Data from shear rheology experiments which are plotted as viscosity versus shear stress or shear stress versus shear rate. In the viscosity plot, the yield stress is estimated as the stress at which the viscosity starts to decrease (Walls *et al.*, 2003). Two approaches can be used to determine the yield stress value from the shear stress versus shear rate plot. Firstly, model fitting can be carried out to any established models and secondly, log plot that shows Newtonian behaviour at very high shear rates and “stress plateaus” at low stresses that are taken as the yield stress can be used (Evans, 1992).
- (ii) Creep measurements which involves the application of constant stress for a period of time and the strain resulted is recorded. The strain increases dramatically beyond the yield stress (Walls *et al.*, 2003).
- (iii) Oscillatory or dynamic strain or stress experiments, whereby the oscillation stress is increased and the resulting strain is recorded. This method can determine the



linear viscoelastic region with no structure damage occurs within this region. The flow only initiates when there is structure damage (Wall et al., 2003).

Rheological data can provide the information not only on the flow behaviour, but also the crystallisation of fat indirectly. De Graef *et al.* (2008) have developed a rheological method to study the palm oil crystallisation with the presence of shear. The method can be divided into two parts. Firstly, continuous shear is applied for a pre-defined period and crystallisation is observed from the apparent viscosity measurement with respect to isothermal time under shear. Secondly, shear is halted and oscillation is used during 30 s, thus recording modulus and phase angle. A comparison with time-resolved X-ray diffraction and polarized light microscopy was then made to confirm the results. Figure 2.12 presents the apparent viscosity evolution when crystallising the palm oil at 18°C under different shear rates. According to them, the increase in viscosity during crystallisation can be due to the increase in amount of fat crystals exist and thus to the degree of crystallinity.

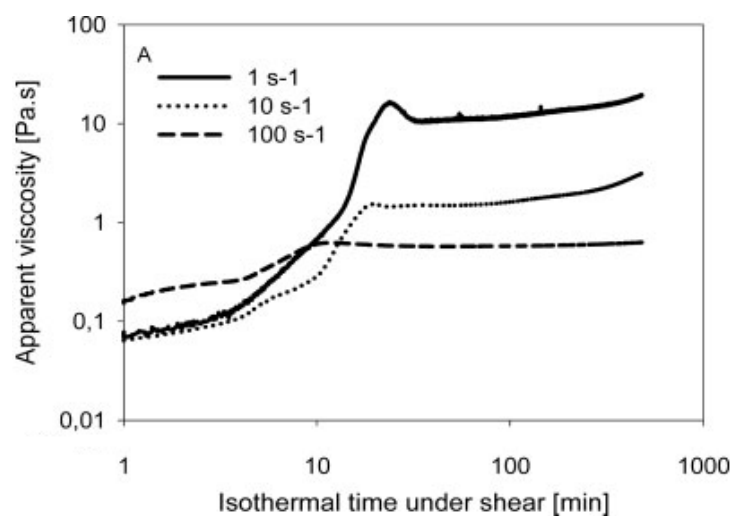


Figure 2.12: Apparent viscosity of palm oil under different shear rates (De Graef *et al.*, 2008).

## **2.6 Cleaning of formulated food products**

Recently, reducing the environmental impact of processes has become a primary focus in the production of formulated food products. Cleaning of the equipments used will generate large volume of effluent with highly acidic or alkaline based on the cleaning chemical involved. Fouling deposits developed on the surface of the equipment need to be removed to ensure the desired quality of the products can be achieved. On the other hand, the energy consumption can be minimized as the deposits formation can increase pressure drop and eventually reduce the effectiveness of the heat transfer.

The cleaning problems need to be clearly identified in order to select a suitable cleaning procedure. Fryer and Asteriadou (2009) have demonstrated a cleaning map as shown in Figure 2.13 which classifies the cleaning problem by considering the type of cleaning fluid and the soil complexity. The three types of soil in the shaded area need to have a special attention in cleaning work.

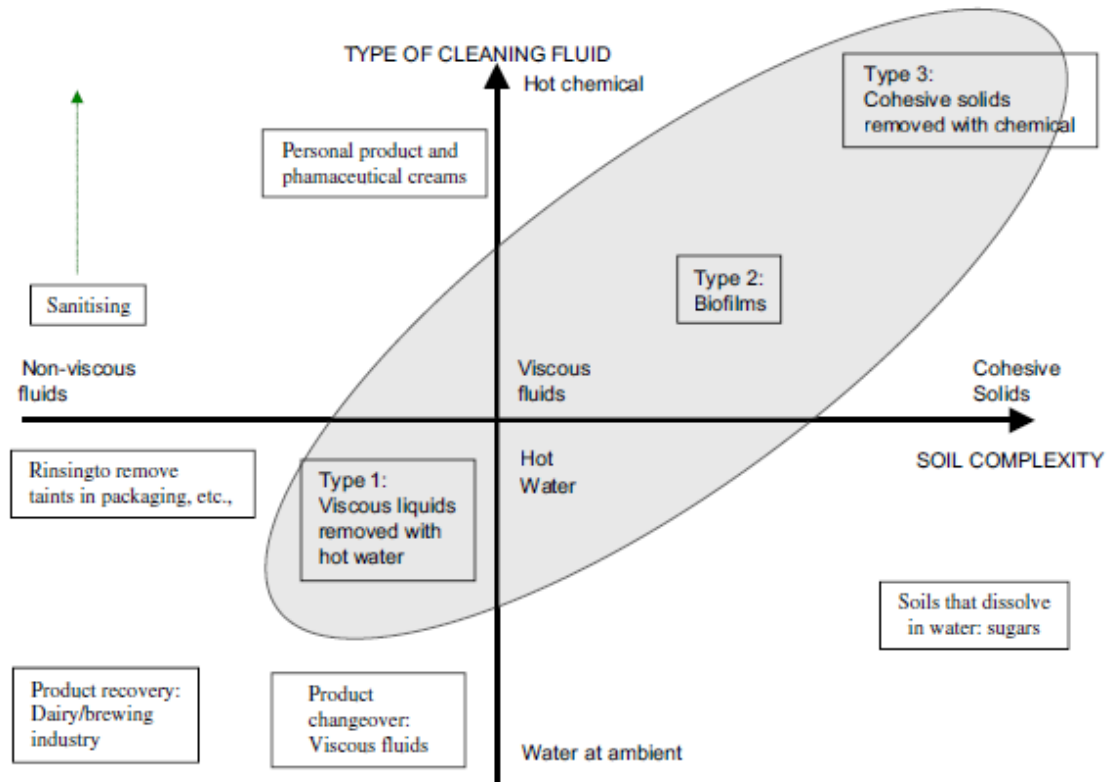


Figure 2.13: Cleaning map which consider the type of cleaning chemical and soil complexity to classify the cleaning problems (Fryer & Asteriadou, 2009). The soil involved in current study is classified as Type 3.

In the current work, the cleaning of chocolate layer from various types of surfaces will be studied using a flow cell rig that has been developed at University of Birmingham which has been used by several researchers previously. A detailed explanation of the rig will be given in section 3.6. Christian (2003) has used the same rig to conduct cleaning work of carbohydrate and dairy protein deposits. It has also been used to study the cleaning behaviour of other fouling deposits such as egg albumin (Ab. Aziz, 2007), sweet condensed milk (Asteriadou *et al.*, 2009), brewery foulants (Goode, 2011) and toothpaste (Cole, 2011). Various process conditions have been taken into account including the temperature and fluid flow.

## **2.7 Conclusions**

This chapter has discussed the overall topics involved in the current work. Crystal formation is determined by the chocolate ingredients, crystallisation temperature, cooling rate and shearing. These factors will also give an impact on the interaction of chocolate with the mould surface which subsequently affects the removal behaviour. In the next chapter, the preparation of the sample and methods involved in the experimental work of this study will be described.

### **3 MATERIALS AND METHODOLOGY**

#### **3.1 Introduction**

In Chapter 2, the basic information on the tempering and cooling processes, as well as the methods commonly used for crystals characterisation have been discussed. A review of the chocolate-mould interaction including the micromanipulation technique was also given. There are several factors that influence the adherence of chocolate to the mould discussed in Chapter 2. Besides that, the chocolate rheology and some cleaning aspect have also been reviewed.

This chapter describes the materials and methods involved in completing this study which started by the hard surface characterisation, followed by the sample preparation. The study can be divided into three investigations:

- (i) Characterisation of crystals using the DSC and some rheological data that was obtained using a rheometer with parallel plate geometry.
- (ii) Force measurement using micromanipulation technique and texture analyser.
- (iii) Determination of removal behaviour of solid chocolate layer from hard surfaces using a flow cell cleaning rig. Image analysis was conducted to determine the cleaning time.

## 3.2 Surface characterisation

Three surface materials were investigated namely stainless steel 316, polycarbonate and PTFE. The mould materials were chosen as they are commonly used for chocolate moulds.

### 3.2.1 Contact angle measurement

An apparatus specially designed at University of Birmingham to measure contact angle was used to carry out the water contact angle measurements at room temperature as shown in Figure 3.1. The contact angles were determined using sessile drop technique with approximately 25 $\mu$ L of deionised water was dispensed onto the dry solid surfaces and the images were recorded by the CCD camera. Image analysis was performed using FTA32 software (FTA, UK). Six surfaces were used for each material to give the mean contact angle.

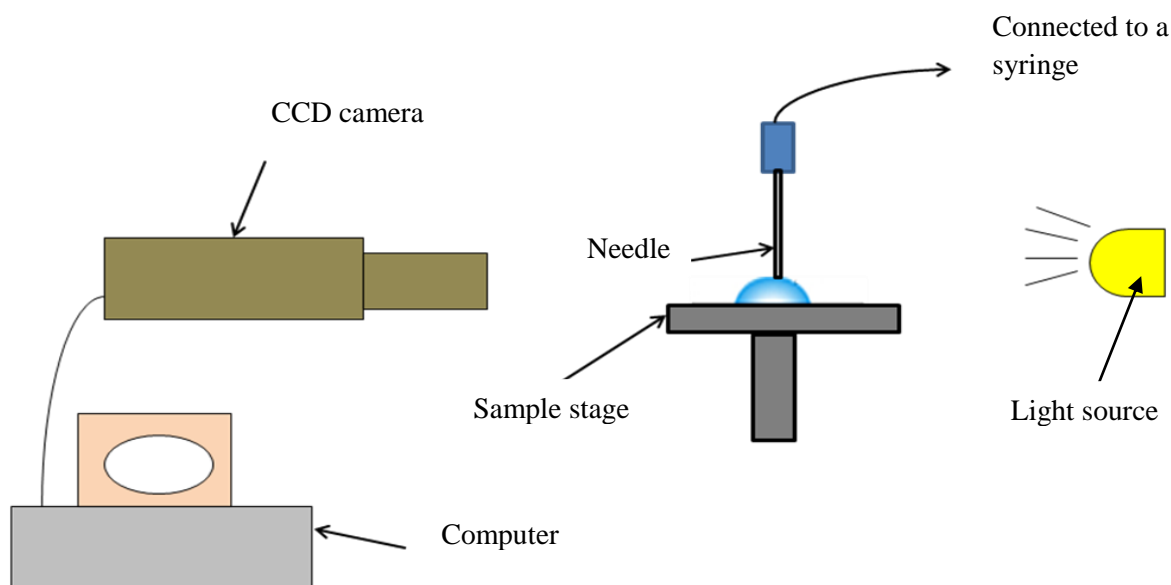


Figure 3.1: Contact angle measurement apparatus.

### **3.2.2 Surface roughness measurement**

Surface roughness measurements were performed using a MicroXAM2 vertical scanning interferometer (Omniscan, UK). A 10X objective lens was used to capture the images which were then analysed using SPIP software (Image Metrology, Denmark). Three surfaces were measured for each material with five different points on a surface giving a total of 15 measurements. The reported values are the mean surface roughness of those measurements as given in Table 5.1.

## **3.3 Chocolate crystallisation**

### **3.3.1 Materials**

Solid chocolate used in this study was supplied by Mondelez. Commercially available high cocoa chocolate was used in this study. The ingredients of dark chocolate used throughout this study unless stated were organic cocoa mass with minimum cocoa solids of 70%, organic raw sugar, organic cocoa butter, soya lecithin and organic vanilla extract.

#### **3.3.1.1 Preparation of untempered dark chocolate**

Solid dark chocolate was melted at 42°C using a double boiling system with repeated stirring. The temperature was measured by using a thermometer.

### 3.3.1.2 Preparation of tempered dark chocolate

For the preparation of tempered chocolate, the Temperer Revolution 2 manufactured by ChocoVision Corporation was used as shown in Figure 3.2. It is a tabletop-tempering machine which has been programmed to temper dark, milk or white chocolate. The main components of the temperer are bowl, baffle, scraper, exhaust air, intake air, heat duct, and probe. The presence of the baffle will form two compartments (A and B) with the scraper attached to one of the baffle ends to prevent backflow of the chocolate. 200g of solid dark chocolate was initially loaded into compartment A. When the temperer started, the melted chocolate was heated up to 42°C and collected in compartment B. After completing the melting process, 5g of solid chocolate which is already in Form V was added into compartment A as a seed aiding the formation of crystal structure. The chocolate was then cooled down to 32.2°C and after the temperature has been reached, the remaining seed was removed from compartment A. Finally, the chocolate was further cooled to 30.4°C and the tempering process was completed.

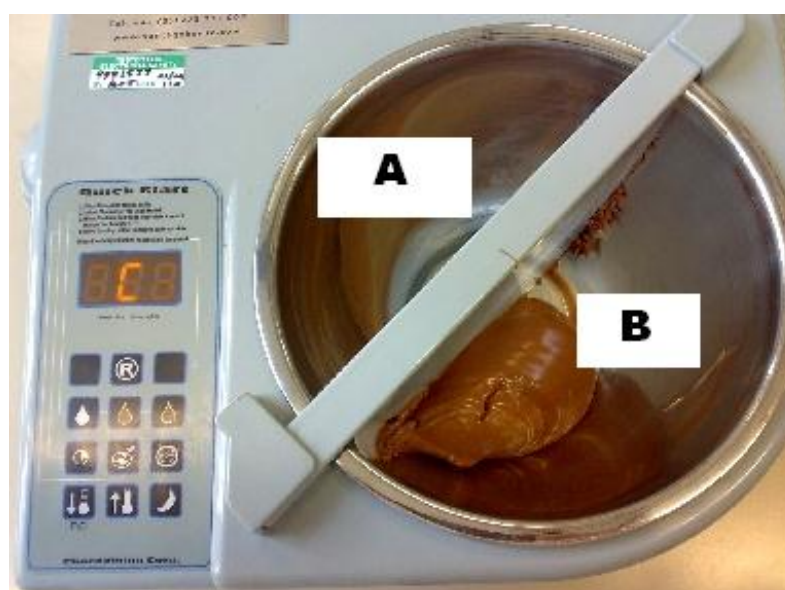


Figure 3.2: Temperer Revolution 2.



### 3.3.2 Differential scanning calorimetry (DSC)

The DSC was used to monitor heat effects associated with phase changes as a function of time and temperature. In this study, a Perkin Elmer PYRIS Diamond DSC was used which consists of four main components which are furnace, auto sampler, cooling system and computer.

Chocolate sample of  $10 \pm 0.02$  mg was put into a 50  $\mu$ L aluminium pan using a metal microspatula. It was then weighed and sealed using a sample press. Then, the aluminium pan was inserted into a PC-driven DSC together with an empty pan as a reference using an auto sampler system. Both of the pans were put on separate furnaces heated by separate heaters and ready to be scanned at specified rates. This procedure was done quickly to reduce the effect of temperature changes towards the crystals formation.

During the characterisation study, the sample was scanned based on the program showed in Figure 3.3. The chocolate was cooled from 32°C (for tempered chocolate) and 42°C (for untempered chocolate) to 10°C with the cooling rates of 1°C/min (slow cooling) and 10°C/min (fast cooling). After the cooling process took place, the sample undergoes an isothermal process for one minute followed by a remelting step at a constant rate of 5°C/min. The remelting step was carried out to get the information of the melting point of the solidified sample. The remelting rate was kept constant for all experiments involving the characterisation of solidified chocolate on different surfaces by using a Peltier stage (Section 3.3.3).

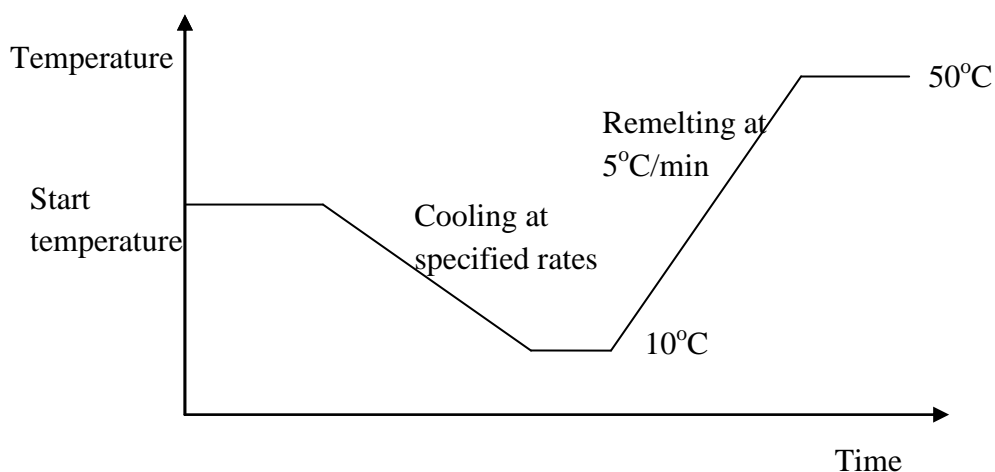


Figure 3.3: Temperature history for DSC.

The profile obtained was the difference of heat output of the two furnaces with respect to the temperature for both cooling and remelting steps. These scanning steps were used for both tempered and untempered chocolate.

DSC was calibrated using an empty pan as a reference and two pans with 4-10mg of indium and octadecane respectively have been scanned with the heating rate of 10°C/min. The melting peak temperatures were examined to ensure the reliability of the data obtained from the scanning of chocolate samples.

### 3.3.3 Solidification using a Peltier stage

Prior to DSC measurement, chocolate solidification was achieved by using a Peltier stage (Linkam, UK) which can deliver accurate temperature profiles for cooling process to be carried out. Linksys 32 software was used to control the Peltier stage. In this study, this apparatus has been used to create a solid chocolate on a square disc made of different materials (stainless steel 316, polycarbonate and PTFE) to determine the effect of materials

used to the crystal formation. This apparatus was used to solidify chocolate in all experiments through this study unless stated.

The Peltier stage was initially heated up to 32°C for solidification of tempered chocolate as it is the temperature at which the tempering process completes and 42°C for solidification of untempered chocolate as it is the temperature at which the melting process accomplished and all the crystals have completely melted. Before applying the temperature profile, approximately 0.5g of liquid chocolate (tempered and untempered) was spread evenly on the surface of the disc which was then put on the Peltier stage. It was covered by the cooling rig cover to prevent any temperature disturbance from the environment during cooling process. Figure 3.4 and 3.5 illustrate the cooling rig and the schematic diagram. Cooling process was carried out at rates of 1°C/min (slow cooling) and 10°C/min (fast cooling) from 32°C (tempered chocolate) and 42°C (untempered chocolate) to 10°C.



Figure 3.4: Cooling rig.

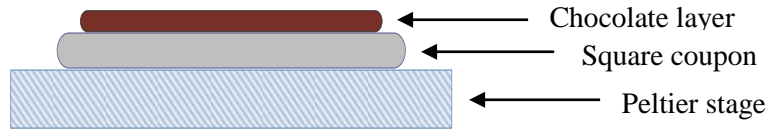


Figure 3.5: Schematic view of the cooling rig.

### 3.4 Rheological characterisation

Rheological studies were carried out on a controlled stress AR1000 rheometer (TA Instruments, UK) equipped with parallel plate geometry (40mm upper plate diameter) and a Peltier plate system to achieve accurate control heating and cooling. Experiments were performed under the steady state shear flow mode, temperature ramp and dynamic oscillatory mode. Reproducibility of all the tests was determined by executing at least three replicates of each measurement.

#### 3.4.1 Steady flow study

Solid dark chocolate was melted directly on the rheometer plate for 5 minutes at 35, 50 and 70°C. The upper plate was then lowered to its testing position with the gap of 500µm from the lower plate. The chocolate sample was equilibrated for another 2 minutes before increasing the shear rate from 0 to 100s<sup>-1</sup>. A moisture trap was used to cover the samples to avoid moisture loss. Finally, the flow curve was obtained by plotting the shear stress (Pa) as a function of the shear rate applied (1/s).

Flow temperature ramp was also performed to investigate the influences of shearing and cooling rate on the viscosity whilst the liquid chocolate was cooled from 50 to 10°C (untempered chocolate) and 31 to 10°C (tempered chocolate). The shear rates used were 15 and 50s<sup>-1</sup> while the cooling rates applied were 1, 5 and 10 °C/min. The viscosity was measured in relation to the temperature and the viscosity evolutions during cooling were monitored for all tests.

### **3.4.2 Dynamic oscillatory test**

Stress sweep measurements were carried out at oscillatory stress of 0.01 to 500 Pa and a constant frequency of 0.1 Hz to determine the linear viscoelasticity region (LVR) which was obtained from the log-log plot of the complex modulus (Pa) versus the oscillation stress. The yield stress value which indicates the stress that will cause the material starts to flow when destruction of the structure occurs was measured from the interception of  $G'$  and  $G''$  curves. The influence of temperature on the LVR and the yield stress has been studied at 35, 40 and 70°C. An attempt has also been made to compare the modulus evolution for dark and milk chocolates at 35°C.

## **3.5 Force measurement using micromanipulation technique**

### **3.5.1 Micromanipulation rig**

The micromanipulation rig was used to measure the pulling energy required to remove a chocolate layer from a hard surface. This technique was chosen as it has been used to measure adhesion and cohesion of various fouling deposits as discussed in section 2.4.2.

The schematic diagram of micromanipulation rig is shown in Figure 3.6 and 3.7. A T-shaped probe made of stainless steel chip with the dimension of 30 x 6 x 1mm as shown in Figure 3.8 was attached to the output end of a force transducer (Model BG-1000, Kulite Semiconductor, Leonia, NJ, USA) which moved horizontally over the rectangular coupon. The force transducer was mounted on another micromanipulator and it sensed the force exerted on the probe by measuring the resulting voltage at 100 Hz by a multifunctional data acquisition board (Amplicon Liveline, Brighton, UK) when scraping the sample from the surface at a constant speed of 1.1 mm/s. Before the experiment started, the probe was lowered so that the gap between its bottom edge and the surface of the disc was 100 $\mu$ m. This gap was used throughout the work. Othman *et al.* (2009) used the same gap for total removal measurement and 700 $\mu$ m for partial removal. The gap adjustment was done by fine tuning the digital level indicator (Model 10-CP12MS) with the help of the side-view microscope, while the top view microscope was used to monitor the removal of the sample.



Figure 3.6: Micromanipulation rig.

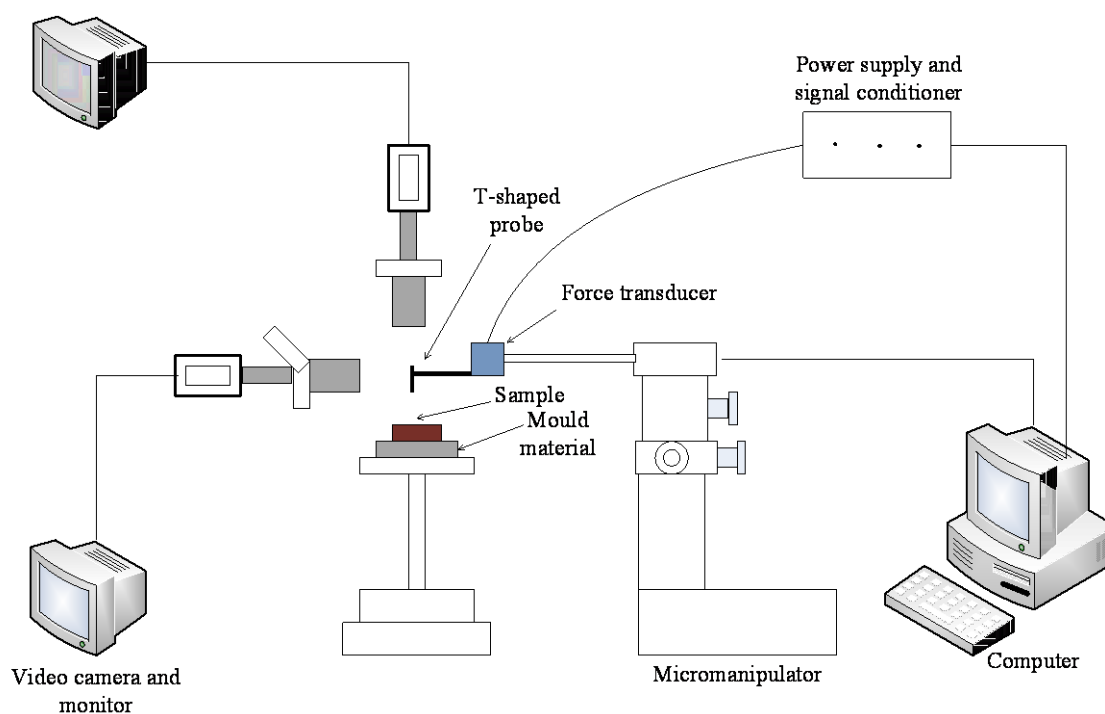


Figure 3.7: Schematic diagram of the micromanipulation rig.

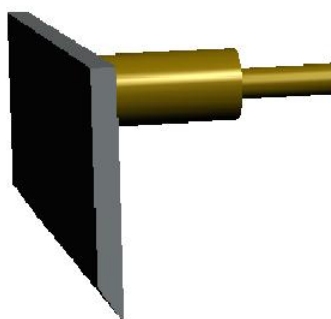


Figure 3.8: T-shaped probe.

### 3.5.2 Force transducer

A BG-1000 transducer shown in Figure 3.9 was used throughout this study which can measure a bi-directional tension force applied to the end of an ultraminiature cantilever beam. It was designed with a combination of high sensitivity and high spring constant

which permit a measurement of high frequency force fluctuations. It is insensitive to cross axis or lateral force inputs. It was decided to use this high range transducer because the measurement using a 10g transducer produced an output voltage exceeded the maximum value.



Figure 3.9: BG-1000 force transducer.

### 3.5.3 Calibration of force transducer

The force transducer was calibrated after the T-shaped probe has been attached to it to ensure the accuracy of the measurement. It also gave the calibration factor needed for the calculation of the pulling energy. Two weight hangers and 20 weights with 50g each were used to calibrate the force transducer. The two hangers were hung at both end of the T-shaped probe. The output voltage was recorded for each additional weight. Figure 3.12 displayed an example of the output voltage when 700g of weights were hung at the T-shaped probe. The resulted calibration curve has been shown in Figure 3.13 which gives the calibration value of 6.5195 V/kg.





Figure 3.10: Weights and weight hanger.

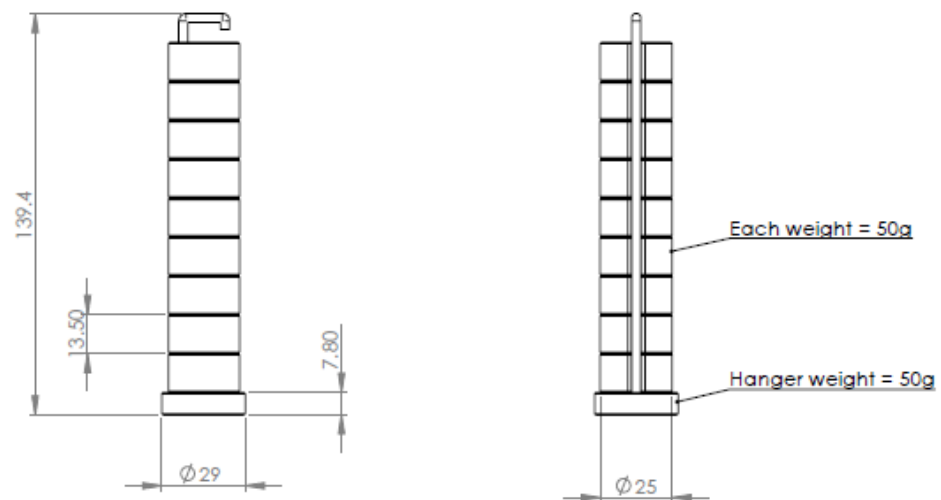


Figure 3.11: Schematic diagram of weights and weight hanger.

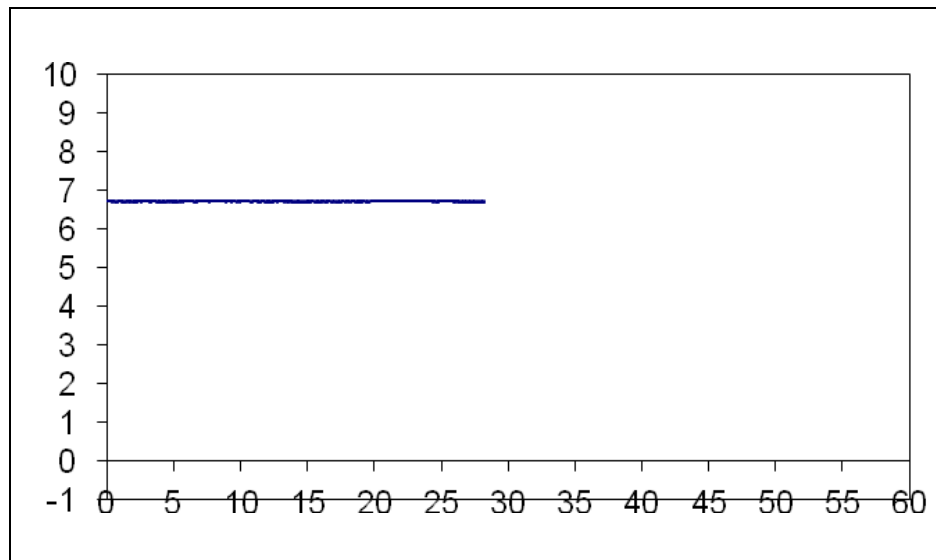


Figure 3.12: Example of the output voltage when 700g weights were hung at the T-shaped probe.

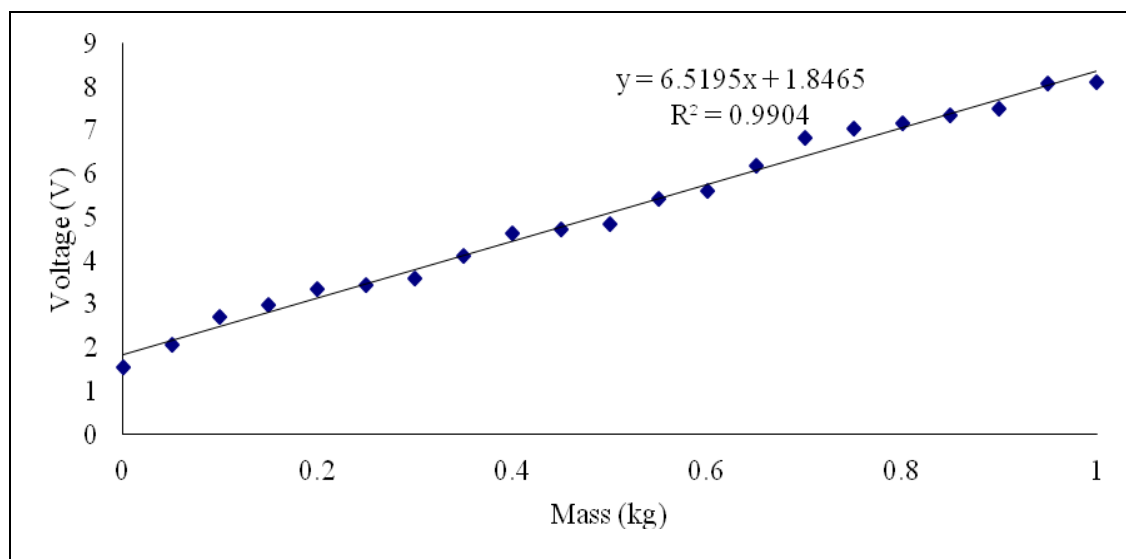


Figure 3.13: Calibration curve for 1000g transducer.

### 3.5.4 Micromanipulation measurement

A layer of solid chocolate on the surface of mould material was prepared as described in sections 3.3.1 and 3.3.3 prior to micromanipulation measurement. The surface coated with solid chocolate (tempered or untempered) was first placed on the stage held by a micromanipulator. Most of the experiments involved soaking the chocolate coated surface in water or 0.1% NaOH solution at specified temperature for a certain period of time before being placed on the stage.

The measurement can be started after the above procedures have been set. The probe speed and the distance of the movement (depending on the length of the square coupon) can be controlled via relevant software (Prior). Data acquisition was always first activated before the motor was set to move. Figure 3.14 shows the sequence of the pulling process from A to D. The measurement was completed when the probe stopped and the file was then saved. The coupon and remaining chocolate was weighed to determine the removal percentage.

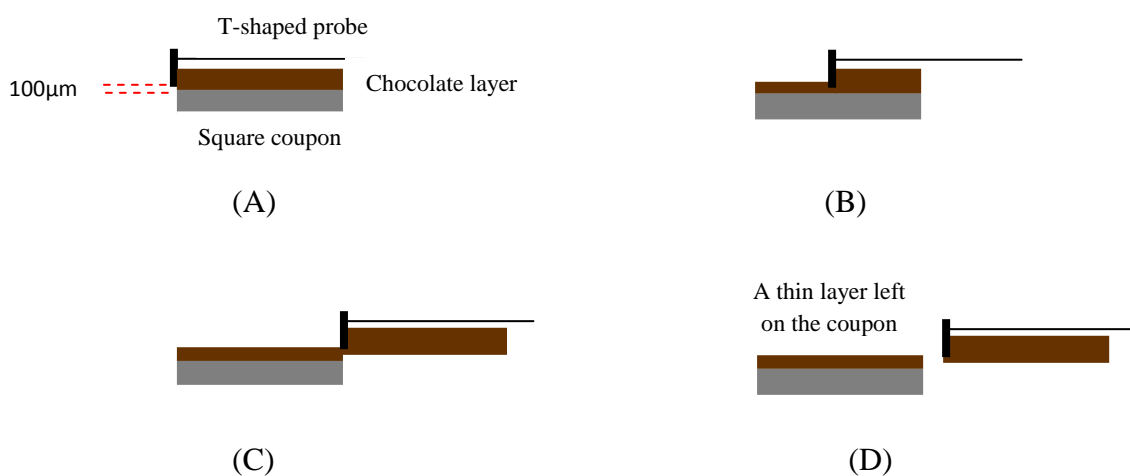


Figure 3.14: The chocolate layer was pulled away leaving a thin layer on the coupon.

### 3.5.5 Data analysis of micromanipulation

The data collected after each measurement was displayed in a curve showing voltage (volt) versus sampling time (second). The voltage can be converted into force to give the value of Y-axis of the graph according to the calculation below. Figure 3.15 shows the typical curve for pulling a sample from a surface.

Calibration factor = transducer calibration value (slope of the calibration curve) x 9.8

Force = voltage x calibration factor

It is based on: 1kg (force) = 9.8N or 1g (force) =9.8mN

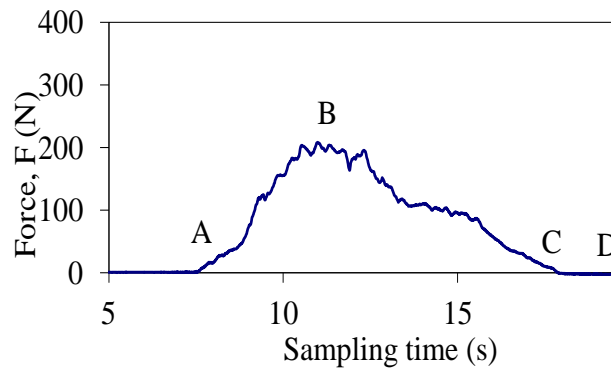


Figure 3.15: Typical curve obtained when pulling a chocolate layer from a surface (the voltage has been converted to force for Y-axis).

The total work done by the applied force can be estimated by the integral of

$$dW = Fdx \quad 3-1$$

where  $dx = vdt$ , giving

$$W = \frac{L}{(t_C - t_A)} \int_{t_A}^{t_C} F dt \quad 3-2$$

where L is the length of the coupon, and  $t_A$  and  $t_C$  the first and last times at which the probe touched the surface.

The apparent adhesive strength of a fouling sample,  $\sigma$  (J/m<sup>2</sup>), defined as the work required to remove the sample per unit area from the surface to which it is attached, is then given by:

$$\sigma = \frac{W}{\alpha A} \quad 3-3$$

where A (m<sup>2</sup>) is the coupon surface area, and  $\alpha$  is the fraction of that area covered by the sample.

### 3.6 Force measurement using texture analyser

Chocolate-mould interaction was also studied using a TA-XTplus Texture Analyser (Stable Micro Systems, UK) with 30kg load cell controlled by the Exponent software. A pull-off method was performed to determine the adhesion between the solidified chocolate and the flat surface cylindrical probe made of different material (20mm in diameter and 10mm thickness). The picture of the texture analyser used in this study is shown in Figure 3.16. The principal of this method is the same as that used by Adhikari *et.al* (2007), Walewijk *et.al* (2008) and Keijbet *et.al* (2009) whereby the separation force was measured by pulling the probe off from a chocolate surface. The force and probe height calibration

were made every day before performing any measurement to ensure the accuracy of the data using standard method.

Liquid tempered/untempered chocolate prepared as described in section 3.3.1 was poured into a sample holder made of Plexiglas until the height reached 1cm with the volume was approximately 30cm<sup>2</sup>. The sample holder was then placed on the stage and clamped to avoid any movement which can affect the force measurement. The flat probe was then brought into contact with the liquid chocolate to create the chocolate-probe interface. In all experiments, the distance of the probe surface and the liquid chocolate, X was kept constant at 0mm unless stated. This setting was left at room temperature for a specific time with the liquid chocolate turned into solid with the increasing of contact time. The probe was finally pulled off at 0.1mm/s over the distance of 15mm. This procedure is represented in the diagram shown in Figure 3.17.

The peak separation force given by the force versus distance profile of the pulling test was taken as the adhesion force and the experimental adhesion force,  $E_a$  is defined as the force per surface area,

$$E_a = \frac{\text{adhesion force}}{\text{surface area}} \quad 3-4$$

where the surface area is the contact area at which the chocolate-probe interface was created.

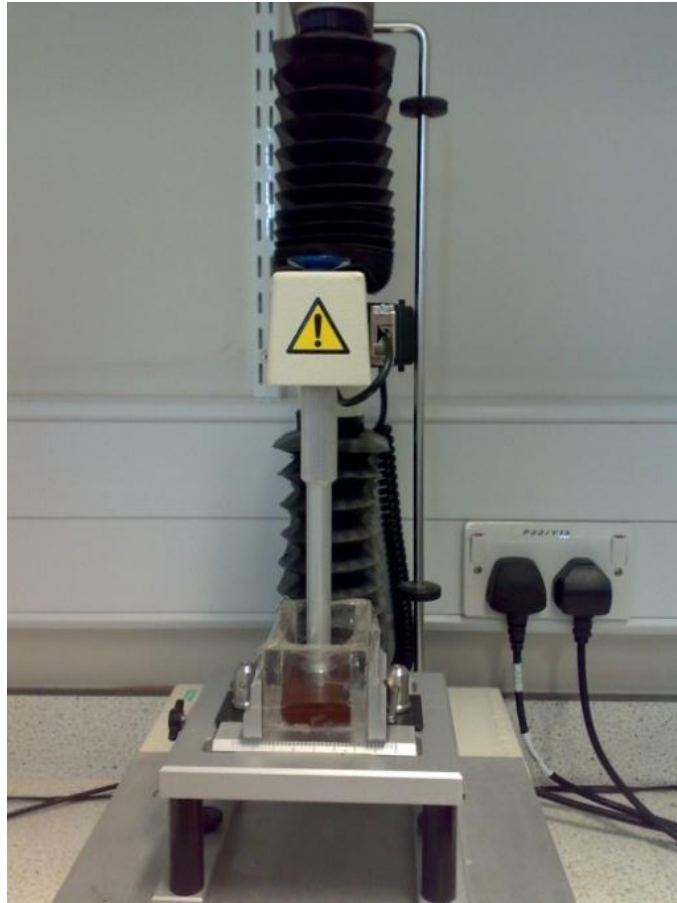
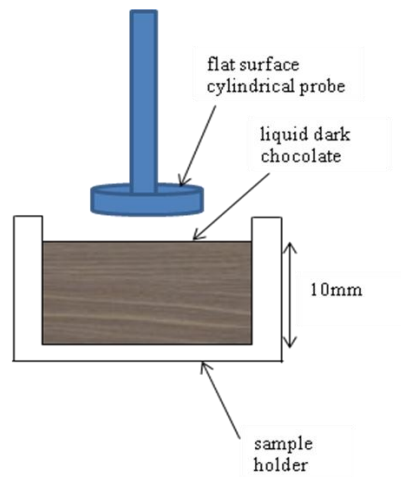
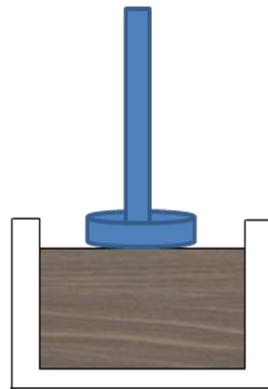


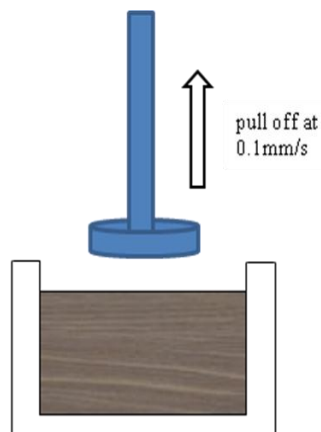
Figure 3.16: TA-XTplus Texture Analyser.



(a)



(b)



(c)

Figure 3.17: Schematic diagram of the pulling test; (a) liquid dark chocolate in the sample holder, (b) the chocolate-probe interface was created and (c) the probe was pulled off from the chocolate surface.



### 3.7 Cleaning rig

The flow cell cleaning rig was used to study the removal behaviour of a solid chocolate layer from the same square coupon used in section 3.5. It has been used in cleaning work for other fouling deposits as has been discussed in section 2.6. Figures 3.18 and 3.19 show the cleaning rig and a schematic diagram respectively. The rig consists of a rectangular flow channel (height 7 mm and width 32mm) made of stainless steel with the test section containing the fouled coupon was positioned in the middle of the flow channel. The test section as shown in Figure 3.20 was made of stainless steel base and glass top and side. It was designed with a removable base to allow the insertion of the coupon. The fouled coupon which was fitted to the test section using silicon grease was visible through the 3-sided glass section (100mm length).

Other parts of the rig were heating tank, chemical tank, flow transmitter PD340, temperature meter, thermocouples, centrifugal pump, valves and data logger. A Canon EOS 30D camera which was mounted on a tripod stand was also used to capture images throughout the experiment which controlled by a timer. The images were needed for image analysis to monitor the removal behaviour of the solid chocolate layer for all experiments which will be described in section 3.7.3. Experiments carried out using the cleaning rig were:

- a) Water rinsing to determine the condition which can give removability.
- b) Chemical cleaning at different temperatures and velocities.
- c) Surface material variations: stainless steel 316, polycarbonate and PTFE  
(characterisation has been carried out as described in section 3.2)

- d) Sample: tempered and untempered chocolate with cooling rates of 1 and 10°C/min and different cooling methods (preparation of the samples were the same as described in section 3.3.1)



Figure 3.18: Cleaning rig.

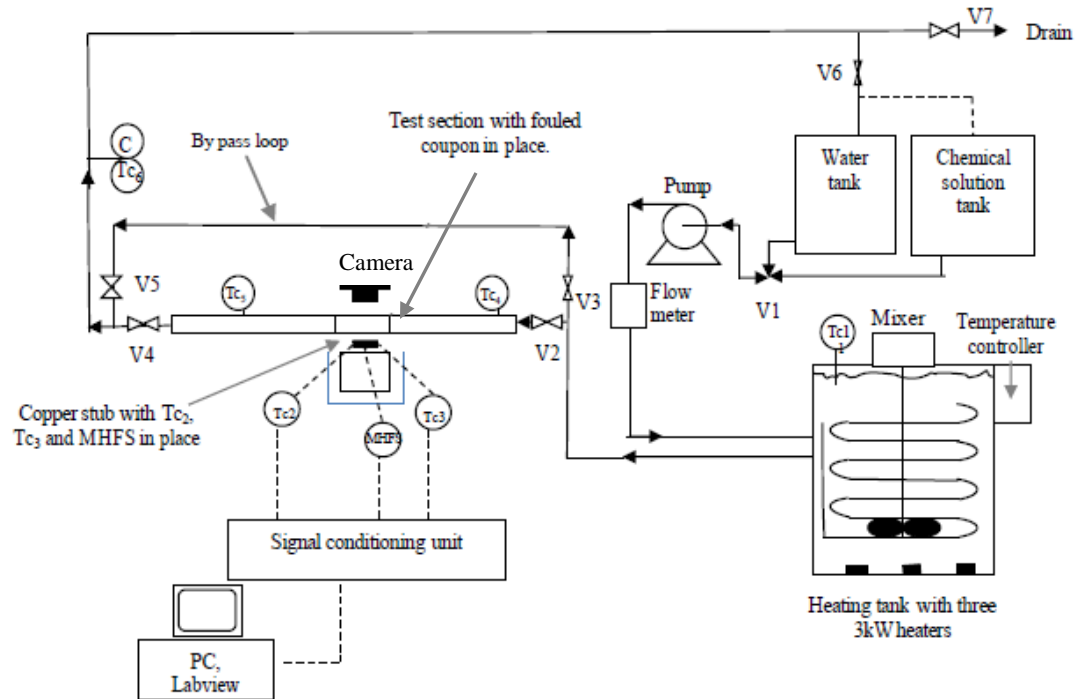


Figure 3.19: Schematic diagram of the cleaning rig (Goode *et al.*, 2010) with some modifications.

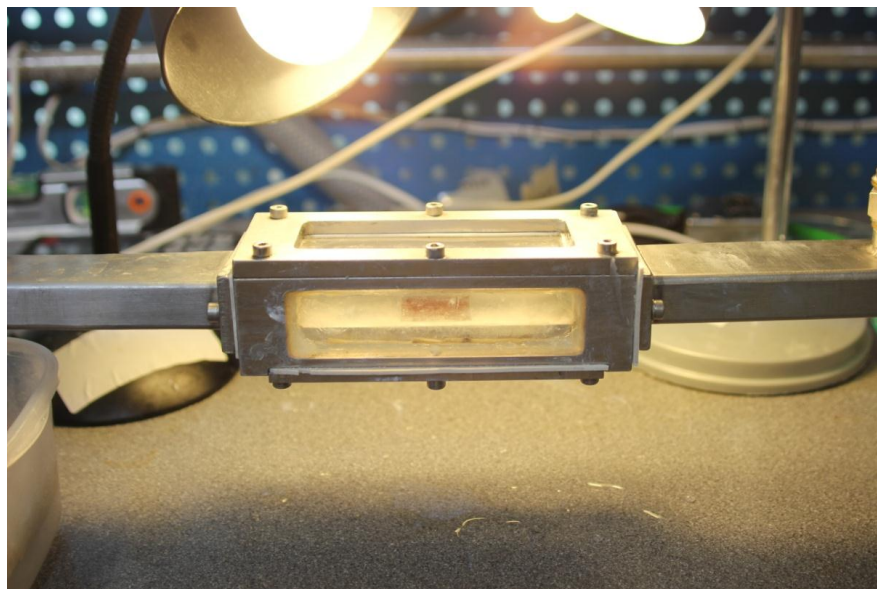


Figure 3.20: Test section with fouled coupon attached to it.

### **3.7.1 Water rinsing**

A series of water rinsing experiments was carried out to investigate the clean ability without chemical usage. Water from the water tank was heated in the heating tank before passing through the test section and finally recirculation back to the water tank. The experiments started with 50°C and 0.25m/s and manipulated throughout the work. The circulation was performed until the coupon surface was visually clean, otherwise it was stopped after one hour. All experiments were repeated at least two times.

### **3.7.2 Chemical cleaning**

In experiments involving the chemical, 0.1% NaOH was passed through the system until the coupon was visually clean. Valve V1 (refer Figure 3.19) played an important role to control the flow from either the water tank or the chemical tank. After each experiment the cleaning fluid was then passed to the drain and the system was rinsed to be used for the next experiment.

### **3.7.3 Image analysis**

Image analysis was chosen to study the removal behaviour of the solid chocolate from the surface because it clearly gave the cleaning point by naked eye. For that reason, there was no heat transfer analysis involved in this study as has been used by Palabiyik (2013). Images captured continuously for every 10 seconds throughout the experiments were used to calculate the area covered with the chocolate on the surface at each time interval. All the images were downloaded and analysed using ImageJ software.

Multiple images evaluation has been used as all the images were taken at the same focal distance. The area considered for the calculation is 80% of the area of the coupon and labelled as A in Figure 3.19. The area percentage was chosen as it can eliminate the influence of the silicon grease used to avoid the leakage. For that reason, the images need to be cropped before further analysis being carried out. Threshold setting would be very crucial to get the most distinguishable between the surface and deposit. A clean surface was achieved when the remaining covered surface was 1%. The calculated area was plotted over time to get the area reduction profile for the experiment.

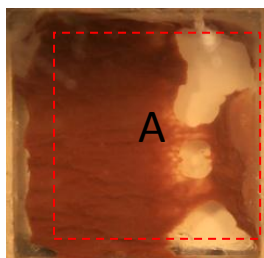


Figure 3.19: Area considered for the calculation.

#### **3.7.4 Film characterisation**

In chemical cleaning at room temperature, there was a thin film left on the surface after the circulation for one hour. An attempt has been made to identify the film using Confocal Raman Microscope (WITec). It was expected that the thin film was a layer cocoa butter. For that reason, cocoa butter was used as a reference. Peaks exist at certain wave numbers gave the information on the components of the film.

### **3.8 Conclusions**

This chapter has described the procedures and methodology in details for all the investigations carried out in current work. The results and discussions will be reported in the following chapters.

## **4 CRYSTALLISATION AND RHEOLOGICAL STUDY**

### **4.1 Introduction**

Crystallisation of cocoa butter is a complex process associated with the polymorphism behaviour of the material. It is essential to study the crystallisation in order to produce the desired crystalline microstructure. There are several factors that affect the formation of the crystals as described in Chapter 2 and one of the best methods to study the crystallisation is to use the DSC. In addition, a rheological study can also give data that can be correlated to the microstructure of chocolate. Chocolate rheology is usually quantified using two parameters: apparent viscosity and yield stress which have been explained in Chapter 2. Chapter 3 outlined the principle of DSC operation and the temperature history applied for all the experiments conducted in this chapter as well as the experimental procedure for the rheological study using a rheometer. The objectives of the work presented in this chapter were to (i) obtain a better understanding of the crystallisation behaviour of chocolate, (ii) check for the effectiveness of the lab scale tempering and characterise the polymorphs present and (iii) determine the rheological properties of dark chocolate.

This chapter details characterisation of chocolate polymorphism after solidification has taken place. The influence of the tempering, cooling rate and material variation have been investigated. The rheological study comprises of three different experiments which includes the steady flow behaviour, temperature ramp and dynamic measurements.

## **4.2 Crystallisation study using the DSC measurements**

DSC experiments were carried out for several purposes including checking whether the tempering process performed by the lab scale apparatus was capable to produce the desired crystal form, characterising of the polymorph present after cooling the tempered and untempered chocolate using the Peltier stage since the melting temperature depends on the crystals exist and determining the influence of the mould surface variations on the crystallisation.

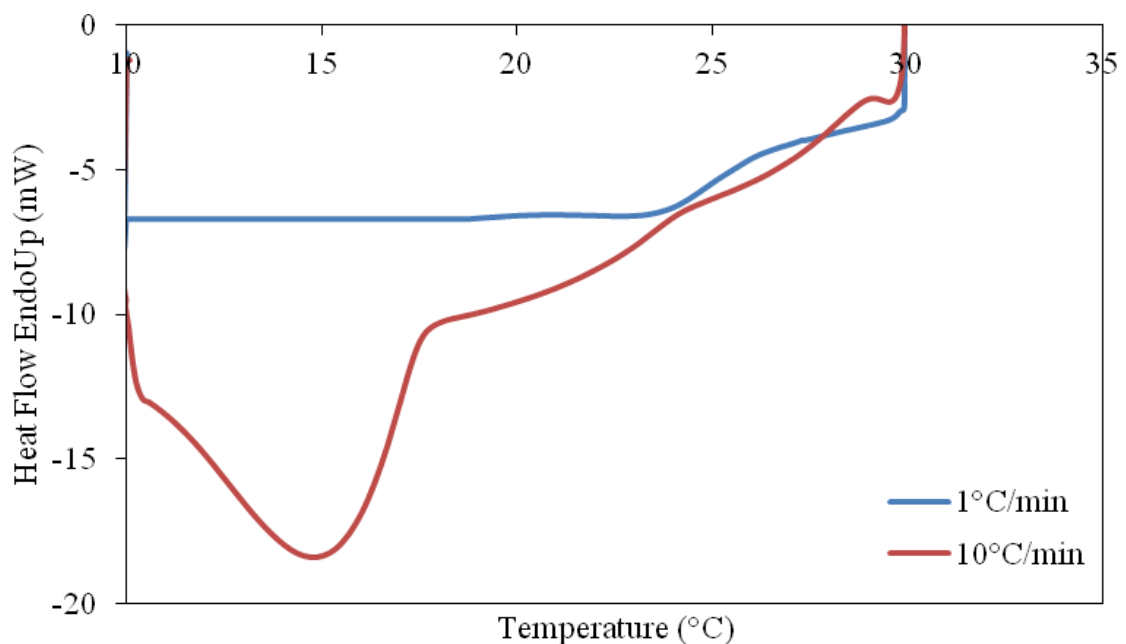
### **4.2.1 Checking the effectiveness of the lab scale tempering process**

Only freshly tempered chocolate was used for all the experiments, as chocolate which had been stored for a certain period of time could contain different crystal forms. Baichoo (2007) compared the melting profile of freshly tempered and ageing samples and found out that upon storage, the Form V crystals will transform to Form VI, which has a higher melting point. It is necessary to ensure that the correct lab scale tempering (an appropriate tempering profile) has been carried out to produce Form V crystals to be used in all experiments. For that reason, a DSC profile was obtained to check the behaviour of the liquid chocolate coming out from the temperer.

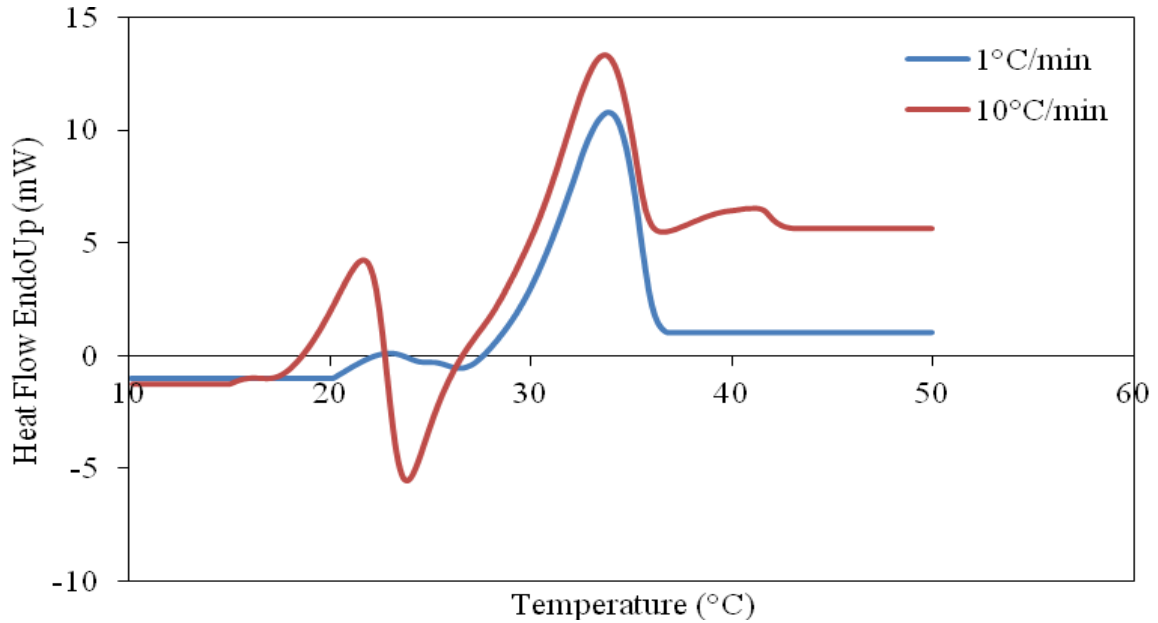
Figure 4.1 illustrates the cooling and melting curves for tempered chocolate from the DSC scan with slow and fast cooling applied. It can be seen from the figure that at slow cooling rate (1°C/min), a main peak is visible at about 24°C during cooling. Upon heating this sample, there is a major peak at 33°C, which is attributed to the melting of Form V crystals, with a small peak at about 23°C. At fast cooling rate (10°C/min) one can



see that during cooling phase, there are two peaks: a small peak at 22°C (stable crystals) and much larger peak at 15°C (unstable crystals). During reheating, the unstable crystals melt first at about 21°C and the stable crystals melt at 33°C. There are two possible reasons for this phenomenon; recrystallisation of the melt into stable crystals or a solid-solid transition from unstable to stable forms (Le Reverend, 2008). This behaviour suggests that during rapid cooling, a significant amount of chocolate crystallised into unstable crystals which melted at low melting temperature and subsequently recrystallised into stable crystals which then melted at higher melting temperature. There is also a small peak at 40°C which is believed to be due the existence of Form VI. These DSC results are in agreement with the literature. Thus, it can be concluded that the lab scale tempering applied in this study is able to generate tempered material.



(a)



(b)

Figure 4.1: DSC curves for tempered chocolate (a) cooled at 1°C/min and 10°C/min and (b) remelted at 5°C/min.

#### 4.2.2 Characterisation of the polymorphism after cooling by using the Peltier stage

Besides tempering, the cooling process is also a crucial step to be investigated to ensure the effectiveness of the system to produce Form V crystals. A well-tempered chocolate can turn into a product with a bloomy surface if the chocolate is cooled too rapidly resulting from the nucleation of the cocoa butter in a less stable crystal form which then transformed to a more stable crystal (Hartel, 2001). Therefore, it is very important to apply correct cooling to produce the desired product quality. Hence, the capability of the cooling system which involved the Peltier stage described in section 3.3.3 was studied. The Peltier stage employs conduction cooling which can remove the specific and latent heat.

The rate of heat conduction through chocolate is low, thus requires significant cooling time to allow heat to be conducted to the surface where it can be removed. In industry, liquid tempered chocolate (28–32°C) is deposited into pre-heated polycarbonate moulds (25°C), which are subsequently placed in a cooling tunnel. The air temperature used in commercial cooling tunnels during chocolate manufacturing is usually 10–15°C. The provision of cold air flow is to remove both sensible and latent heat from the liquid chocolate sample, so that a solid product could be formed for easy handling during packaging. On average, a temperature decrease of 10°C is required. From the assumption that the specific heat capacity of chocolate to be about  $1.6\text{kJ kg}^{-1}\text{°C}^{-1}$  and the latent heat to be  $45\text{kJ kg}^{-1}$  (Beckett, 2008), a total of 60J need to be removed to cool and solidify each gram of chocolate (Keijbets *et al.*, 2009).

#### **4.2.2.1 Effect of tempering and cooling rate on the crystallisation**

As discussed in the literature review, the aim of the tempering is to pre-crystallise the cocoa butter so that a small amount of seed crystals are present and the remaining fat can solidify on them during cooling to produce Form V crystal. In this section, the crystal type produced when tempered and untempered chocolate cooled on the Peltier stage was studied. DSC melting curve was used to determine the types of crystal present after being cooled on the Peltier stage. Thermal method was chosen instead of microscopy techniques because the complexity of chocolate makes the later techniques incapable of distinguishing individual cocoa butter crystals (Hartel, 2001). Rapid and slow cooling was applied to both tempered and untempered chocolate by changing the temperature profile in the Linksys software which controls the Peltier stage.

Figure 4.2 shows the DSC melting curves for tempered and untempered chocolate cooled at 1 and 10°C/min. For tempered chocolate, a single peak predominates for both cooling rates with rapid cooling giving a slightly higher peak temperature at about 34°C compared to 33°C with slow cooling. This is the melting point for Form V crystal. This suggests that both cooling rates produce Form V crystals. When compared to the melting curve for Figure 4.2, it is noticed that the recrystallisation peak existing when the chocolate cooled at 10°C/min has disappeared. This is probably due to the heat transfer mechanism applied by the Peltier stage that prevents the recrystallisation occurring.

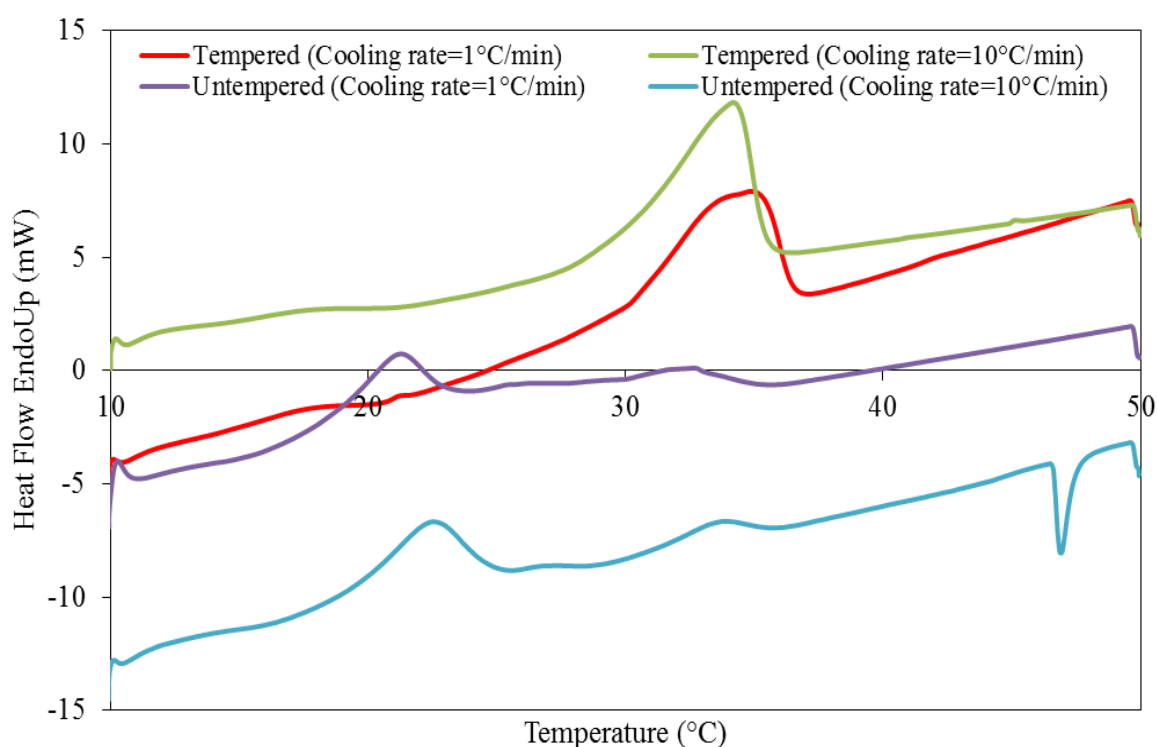


Figure 4.2: DSC melting curves (melting rate 5°C/min) for tempered and untempered chocolate cooled at 1°C/min and 10°C/min.

From the same figure, it can also be observed that for untempered chocolate, there are two peaks for both cooling rates. Major peaks for slow and rapid cooling are visible at

21 and 23°C respectively and a small peak is visible at about the same peak temperature as the tempered chocolate (33°C for rapid cooling and 34°C for slow cooling). The graph shows that there is a competition between rapid nucleation and growth of lower stability polymorph and slow growth of high stability polymorph. However, lower stability polymorphs predominate the crystallisation process even at low cooling rate. This suggests that without the seed crystals produced during tempering, the nucleation and crystal growth into a high stability polymorph cannot be achieved. Both tempered and untempered chocolate show little dependence on the speed of cooling by the Peltier stage. However, the effect of tempering on the crystallisation can be seen clearly from the melting curves and the combination of tempering and slow cooling on the Peltier stage can definitely produce Form V polymorph.

The effect of tempering and cooling can also be seen from Figure 4.3 which demonstrates the melting curves for tempered and untempered chocolate where no controlled cooling was applied. The liquid tempered and untempered chocolates were left at room temperature for one hour. There is one major peak for tempered chocolate at 40°C and multiple peaks for untempered chocolate at 23°C, 32°C and 34°C. These results show that it is necessary for a proper cooling to be applied to obtain the desired crystal form even though proper tempering has been carried out. Without the combination of tempering and proper cooling, the correct crystal type cannot be produced.

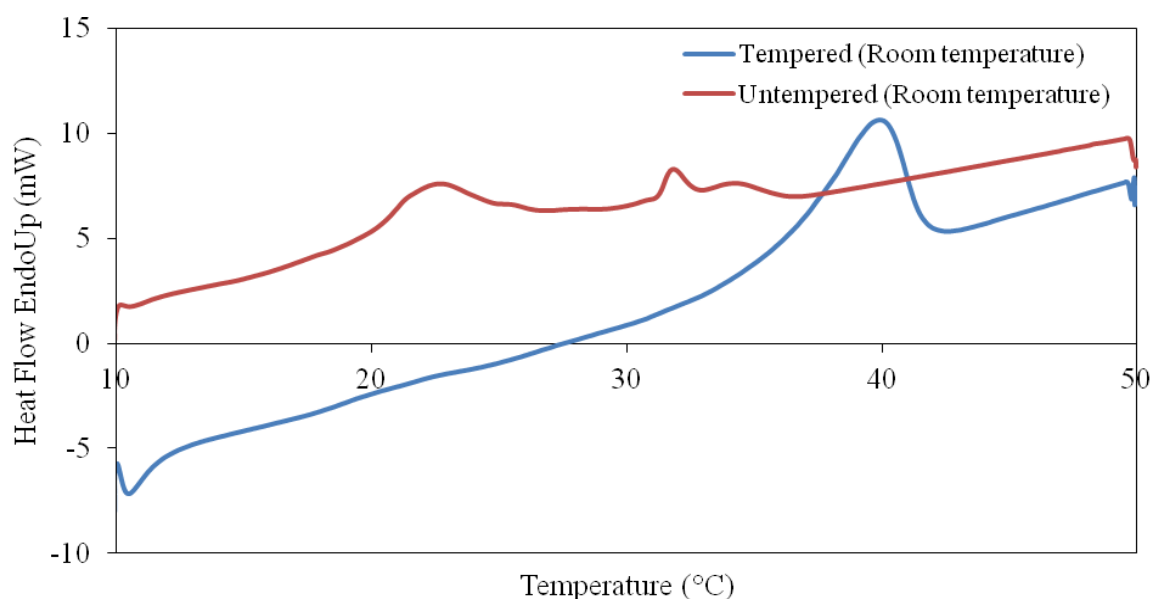


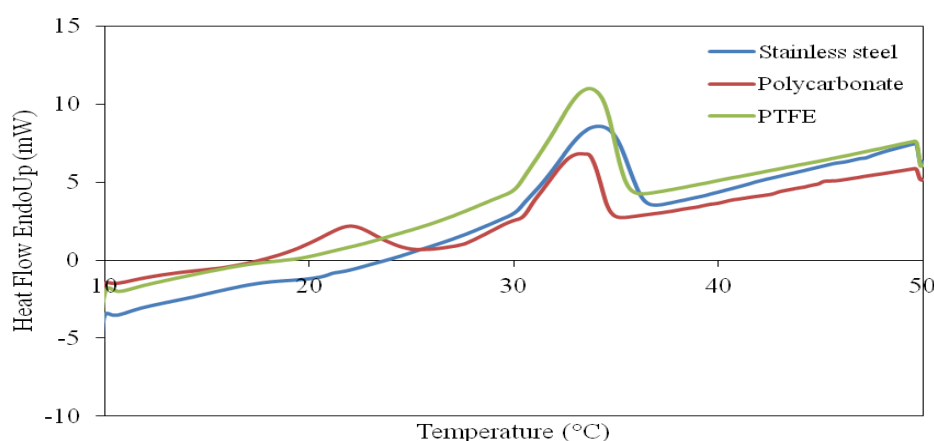
Figure 4.3: DSC melting curves (melting rate 5°C/min) for tempered and untempered chocolate left at room temperature for 1 hour.

#### 4.2.2.2 Effect of material variations on the crystallisation

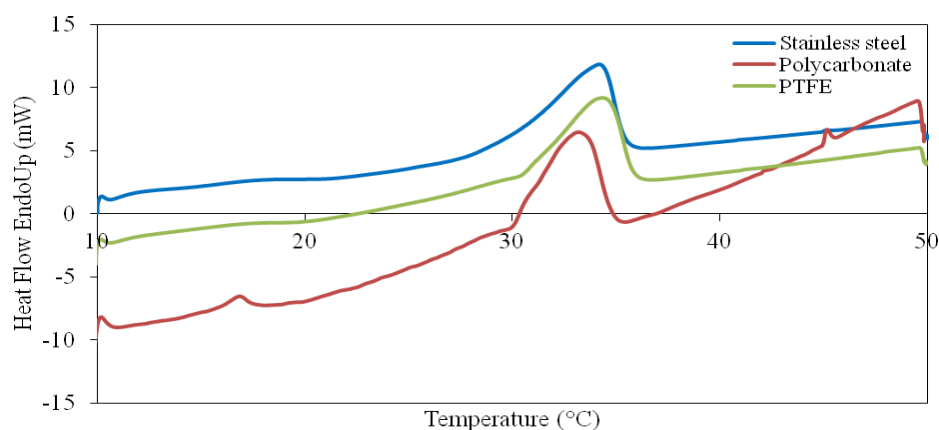
Different materials have varying abilities to conduct heat during cooling of a chocolate layer on the Peltier stage. The thermal conductivities of the materials used in this study are different giving different rate of heat transfer. Thus, a study has been carried out to determine whether the material influences crystallisation. Approximately 0.5g of the liquid tempered chocolate was poured on square hard surfaces made of stainless steel, polycarbonate and PTFE with the area of 400mm<sup>2</sup> and thickness of 4mm before it was placed on the Peltier stage and further cooled at slow and rapid cooling rate. The cooling rates applied were 1 and 10°C/min and the DSC melting curve was again used to identify the polymorphic forms that resulted.

The melting curves shown in Figure 4.4 (a) and (b) were obtained when approximately 10mg of solidified chocolate was put into the DSC and the heating rate

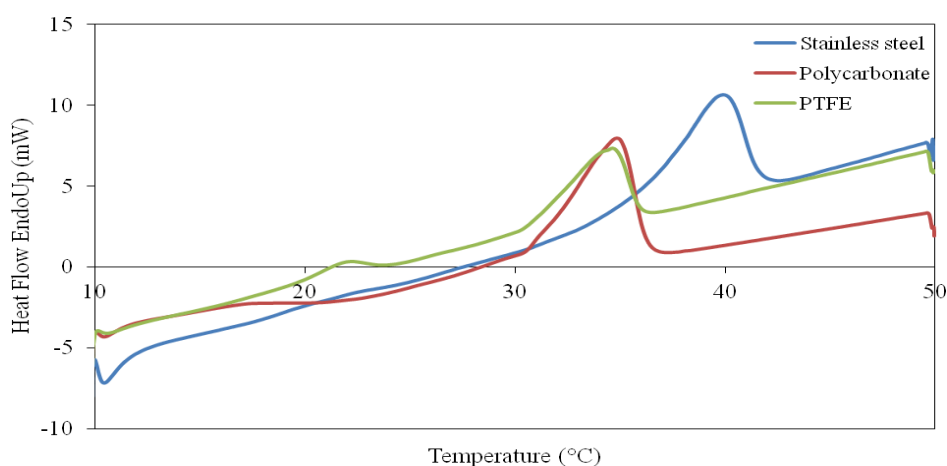
applied was 5°C/min. Figure 4.4 (a) and (b) illustrate the melting curves when the chocolates were cooled on the Peltier stage at 1 and 10°C/min respectively. Both figures show that the formation of the solid chocolate on those three materials were in correct polymorphic form with the peak temperature at around 34°C indicating the cooling rate applied gives proper control of crystallisation. However, melting curves for the chocolate on polycarbonate cooled at slow and fast cooling rates show another peak at lower temperature. This is possibly due to the thermal conductivity of the polycarbonate which is the lowest among the three materials. Different behaviour can be seen in Figure 4.4 (c) when the chocolate underwent no controlled cooling. Polycarbonate and PTFE give one minor peak at lower melting points and one major peak at about 34°C, but the stainless steel gives one major peak at 40°C which indicates that the formation of type VI crystals has occurred. This behaviour is believed due to the fluctuation of the room temperature in that there was no control on the heat released from the liquid tempered chocolate and thus on the cooling rate.



(a)



(b)



(c)

Figure 4.4: DSC melting curves (melting rate 5°C/min) for tempered chocolate on different surfaces cooled to 10°C at 1°C/min (a), 10°C/min (b) and left at room temperature for 1 hour (c).

In overall, it can be concluded that the lab scale tempering apparatus that has been used for sample preparation throughout this study is dependable to ensure that the correct crystal form was produced. Besides, the polymorphism was found to be influenced by the tempering process as well as the cooling rate applied. For the solidification carried out on different surface materials at different cooling rate, it was noticed that no dependency for proper cooling at 1 and 10°C/min for stainless steel and PTFE. Only polycarbonate gave a



extra peak at lower temperature for both cooling rates. The results obtained was not as expected. This is possibly due to the cooling rates applied, which able to produce Form V crystals. However, the sample left at room temperature gave a different behaviour.

### **4.3 Rheological study of dark chocolate**

The rheological approach was divided into 3 parts with the experimental details were described in section 3.4:

- Steady flow measurement was carried out to study the influence of temperature on the viscosity of dark chocolate.
- Temperature ramp which aims to evaluate crystallisation by monitoring the apparent viscosity. The changes in apparent viscosity at different process conditions were monitored. Only the untempered chocolate was used for this study except for the investigation of the effect of pre-crystallisation on the viscosity evaluation of dark chocolate.
- Dynamic measurement involving stress sweep test was performed to determine the linear viscoelasticity region (LVR). The oscillatory parameters used to compare the elastic properties of dark chocolate were storage modulus ( $G'$ ), loss modulus ( $G''$ ) and phase shift angle ( $\delta$ ).

### 4.3.1 Steady flow behaviour of the molten dark chocolate

Figure 4.5 shows the flow curve of molten dark chocolate prepared as described in section 3.3.1 with varying temperature. In steady flow study, all temperatures show an increase in apparent viscosity with decreasing of shear rate showing the shear thinning behaviour. Generally there are two flow profiles-low shear and high shear regions. It can be seen that at shear rate below  $20\text{s}^{-1}$ , a small change in shear rate applied produced a large change in apparent viscosity determined by the slope. However, at higher shear rate the viscosity was found to be nearly independent of shear rate.

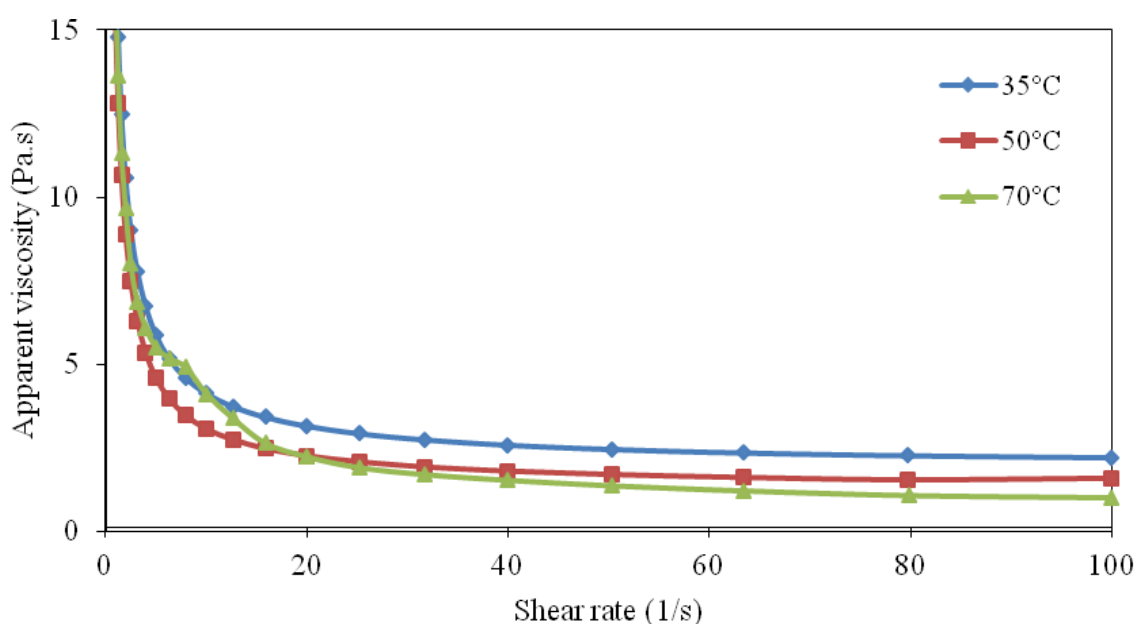


Figure 4.5: Apparent viscosity of liquid dark chocolate sheared from 0 to  $100\text{s}^{-1}$  at different temperatures

The Casson model which is a standard model in the chocolate industry has been used internationally to characterise the rheological behaviour of the dark chocolate with the shear rate in the range of 0-100 s<sup>-1</sup>.

$$\sigma^{0.5} = K_1 \left( \dot{\gamma} \right)^{0.5} + \sigma_o^{0.5}$$

where  $\sigma$  = shear stress (Pa),  $K_1$  = Casson viscosity [(Pa.s)<sup>0.5</sup>],  $\sigma_o$  = yield stress (Pa) and  $\dot{\gamma}$  = shear rate (s<sup>-1</sup>).

A plot of the square root of the shear stress vs the square root of the shear rate (Figure 4.6) was used to determine the Casson yield value and viscosity based on the linear regression as given in Table 4.1. The yield stress ranged from 7.69 to 9.16 Pa and the Casson viscosity ranged from 0.76 to 1.16 (Pa.s)<sup>0.5</sup>. It was found that Casson viscosity decreased with the increasing of temperature. The yield value and Casson viscosity obtained in this study is lower than the values for milk chocolate at higher shear rate as reported by Briggs and Wang (2004).

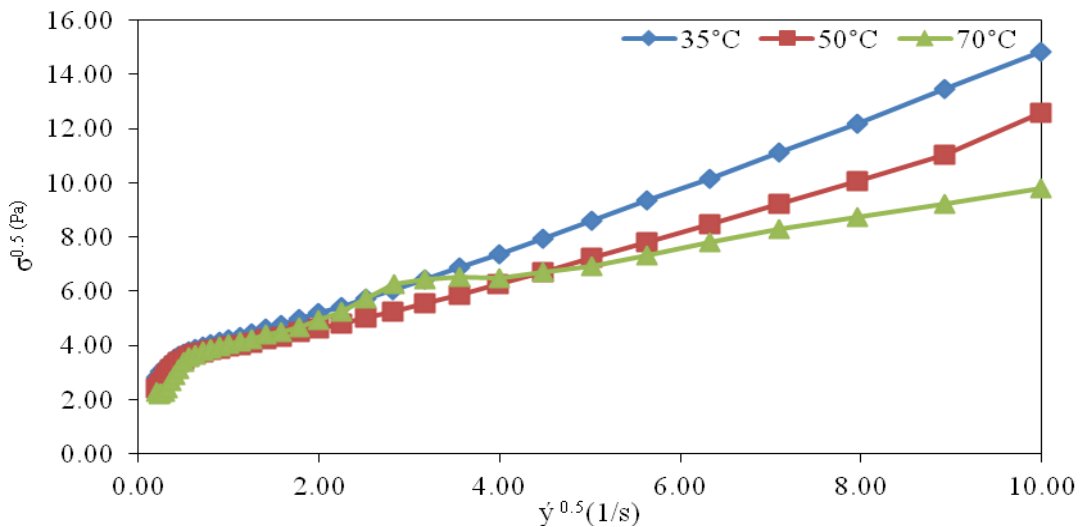


Figure 4.6: Square root of the shear stress vs square root of the shear rate for different temperatures.

Table 4.1: Rheological parameters of the Casson Model for dark chocolate. The errors represent the standard error of the mean from 3 replicates.

Temperature (°C)	Yield stress (Pa)	Casson viscosity (Pa.s) <sup>0.5</sup>
35	8.51±0.02	1.16
50	7.69±0.06	0.92
70	9.16±0.17	0.76

#### 4.3.2 Effect of cooling on the viscosity evolution of dark chocolate

When cooling is taking place, the fat solidifies and accompanied by an increase in viscosity as the level of solid fat increases (De Graef *et al.*, 2008). The viscosity evolution of liquid untempered chocolate was studied at three different cooling rates with different behaviour observed. From the curves obtained, additional information can be derived which related to the crystallisation point and the solidification rate.

The viscosity evolution during cooling from 50°C to 10°C at different cooling rates whilst sheared at 15s<sup>-1</sup> with the parallel plate geometry is given in Figure 4.7. The curves can be divided into two zones; A and B and can be described as follows:

Zone A: When cooling from 50°C, the apparent viscosity for all cooling rates applied were low and exhibit a similar change in apparent viscosity. A slow increment with the reduction of the temperature during cooling can be seen between 50 and 25°C. Chocolate was still in the liquid state in this temperature range. This region can be described as the so called “crystallization induction period” because the nucleation has started at this stage.

Induction time measures the time at which the first nuclei can be detected, means that the crystallisation has started (Hartel, 2001).

Zone B: When the sample was cooled at 1°C/min, it can be observed that there is a sudden increase of the viscosity at about 24°C which is related to the crystallization and aggregation of cocoa butter. This corresponds to the crystallization seen by the DSC (Figure 4.1 (a)). The temperature at which sudden change occurs corresponds to the crystallization temperature during cooling step and generally lower at higher cooling rate. Higher viscosity represents more interparticle friction between the crystals as many small crystals present. At 5°C/min, a viscosity jump occurred around 20°C which indicates that a lower polymorph exists. For cooling rate of 10°C/min, the sudden change in viscosity occurs the earliest of the three cooling rates used.

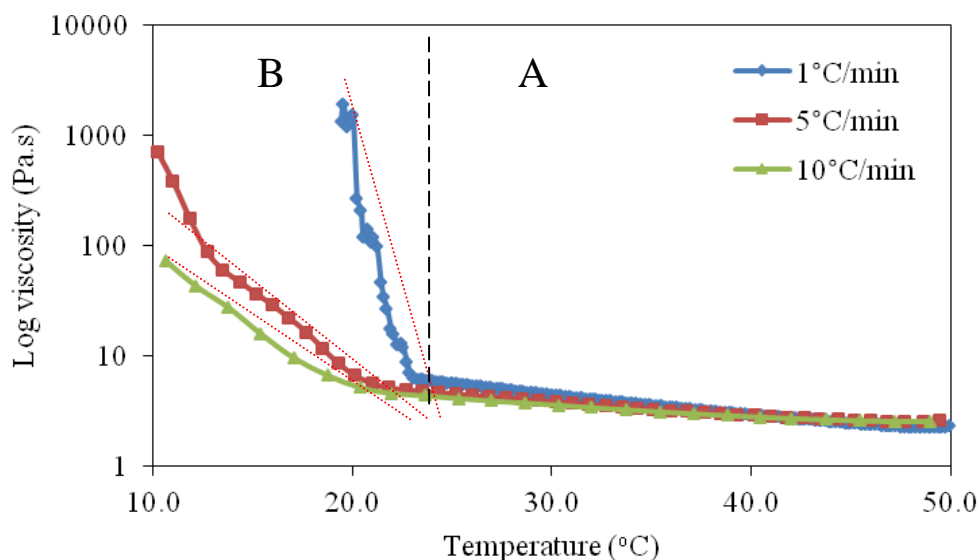


Figure 4.7: Viscosity evolution of untempered dark chocolate cooled from 50 to 10°C at different cooling rates whilst sheared at  $15\text{s}^{-1}$ . Zones A and B are corresponding to the different states of cocoa butter and described in the text.

The relation between the rate of change in apparent viscosity (representing the crystallisation rate) and the temperature at which sudden change occurs with respect to the cooling rate is displayed in Figure 4.8. Rate of change in apparent viscosity for zone A has been calculated from the slope of the red dotted lines shown in Figure 4.7. At the lower cooling rate, the viscosity increased more rapidly compared to the higher cooling rate which viscosity climbed slowly as the temperature decreased. It is well known that slow cooling will give more time for the chocolate to crystallize into small crystals leading to an acceleration in the apparent viscosity. Meanwhile, the major increase in apparent viscosity occurred earlier when cooling at slow cooling rate, showing that the sample crystallized faster. Sudden viscosity change can be observed at around 23°C at cooling rate of 1°C/min and around 19°C at cooling rate of 10°C/min. When compared to the DSC data in Figure 4.1 (a), the onset temperatures were quite close to the crystallization temperature illustrated in the DSC curves confirming that the temperature at which the sudden increase in apparent viscosity occurred is the starting point whereby the crystals start to form. Slight difference between those two crystallization temperatures was probably due to the existence of shear at the rate of 15s<sup>-1</sup>. Higher cooling rate displayed a lower onset temperature with the crystals produced were not in the desired form (Form V).

It is well known that suspended particles influence the flow behaviour of a fluid. The increase in viscosity of the sample during crystallization can be related to the increase in the amount of the fat crystals present and thus to the degree of crystallinity. Reddy *et al.* (1996) reported that fat components and composition influence the crystallisation rate, but this experiment involved the same material which did not affect the measurement. Method of pre-crystallisation also gives an influence in the rate of change in apparent viscosity as investigated by (Bolliger *et al.*, 1998) who found that chocolates precrystallised using

conventional equipment exhibited an increased rate of change in apparent viscosity compared with chocolates precrystallised using the lab scale scraped surface heat exchanger (SSHE). The effect of pre-crystallisation on the viscosity evolution will be discussed later.

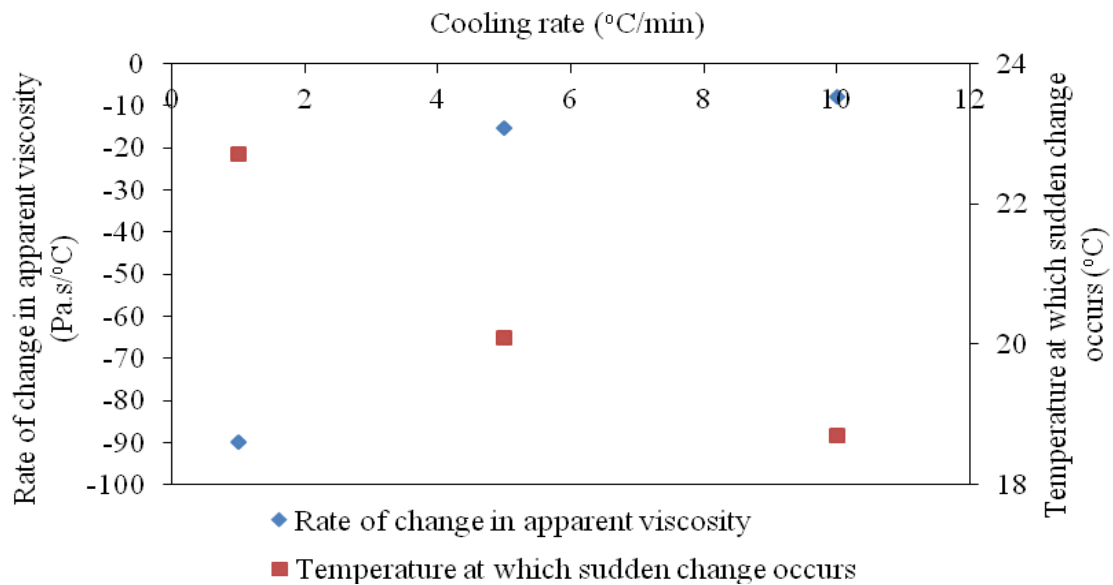


Figure 4.8: Rate of change in apparent viscosity and the temperature at which sudden change occurs subjected to cooling rates.

#### 4.3.3 Effect of shearing whilst cooling on the viscosity evolution of dark chocolate

Cooling is aimed to remove the specific and latent heat, contract the chocolate so that it can be removed from the mould without any residue left on the mould surface and produce a stable and attractive product that meet the customer requirement. This part of study determines the influence of shearing on the rheological properties of dark chocolate whilst cooling. The existence of shear can affect the nucleation and furthermore promote the aggregation of the crystals. Continuous shearing has been applied when the sample was cooled from 50 to 10°C.

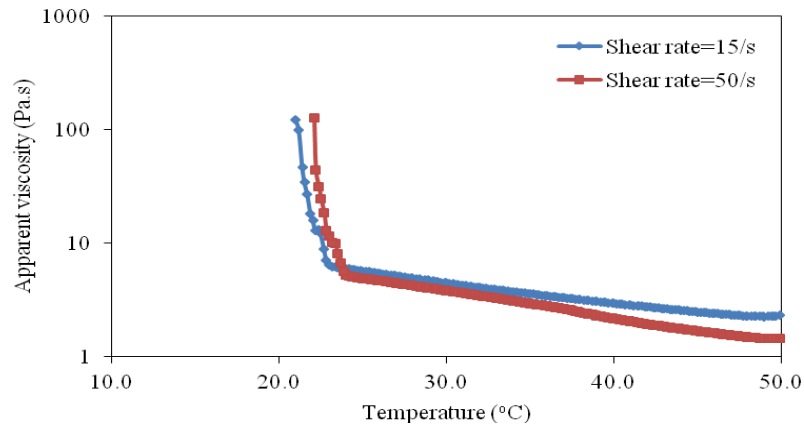
Figure 4.9(a), (b) and (c) show the viscosity evolution during cooling with shear at the rate of 15 and 50s<sup>-1</sup>. The higher the shear rate, the rapid increase in apparent viscosity with shorter induction time of nucleation can be observed at cooling rate of 1°C/min as displayed in Figure 4.9 (a). From the figure, it can be seen that at the beginning of the cooling process, shear rate of 15s<sup>-1</sup> gave higher viscosity than 50s<sup>-1</sup>. From about 35°C, both lines were overlapping until they reached the onset temperature and the apparent viscosity started to increase rapidly. Results indicate that the presence of shear can accelerate the crystallization by producing a large number of small crystals leading to more compact crystal aggregates whereby they are attracted to each other due to Van der Waals forces as described by Kloek *et. al* (2005). The onset temperature of about 25°C when the chocolate was sheared at 50s<sup>-1</sup> shows that less stable polymorph has been formed as this part of study only involves the untempered chocolate. The original aim was set to measure the viscosity until the cooling temperature reached 10°C, but the measurement stopped at about 20°C probably due to the formation of larger crystals and for the safety purpose to prevent the bearing of the rheometer from damage.

According to De Graef *et al.* (2008) and Kloek *et al.* (2005), the application of shear during crystallisation can increase the rate of nuclei formation and accelerate polymorphic transitions during primary crystallisation. Besides, shear can also induce the orientation of crystallites and produce a large amount of small crystals as shearing can cause fracture of crystals. Crystal growth can be enhanced as the aggregation is also affected by shear. Fat crystals attract each other due to van der Waals forces and under static conditions, meet due to Brownian motion. Shear increases the collision frequency to an extent proportional to the shear rate. Above a critical shear rate, which depends on particle size and viscosity, collision of crystals due to shear dominates over that caused by

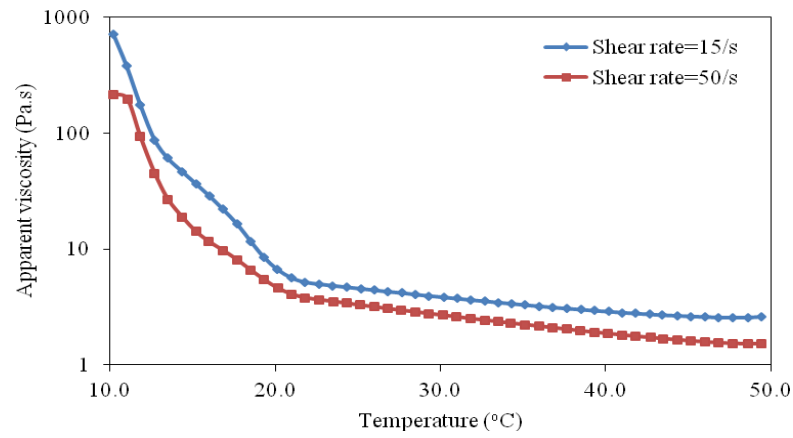


Brownian motion. Aggregating crystals tend to form voluminous aggregates with a volume much greater than the total volume of the primary crystals, causing viscosity to increase. However, increasing the shear rate may cause aggregates to break up because of the shear forces acting upon them. Furthermore, shear may also induce internal rearrangement of the aggregates, which as a result, may become more compact. Tarabukina *et al.* (2009) reported that the application of low shear rates upon cooling produces two viscosity jumps with the first sharp increase is related to the crystallisation of palm oil and further shearing leads to the second viscosity jump caused by the motion of larger crystalline aggregates. However, for shear rates higher than  $300\text{s}^{-1}$  the second viscosity jump was invisible. This is due to the fact that aggregation is not possible at high shear rate and the crystallised palm oil formed a suspension of aggregated crystals.

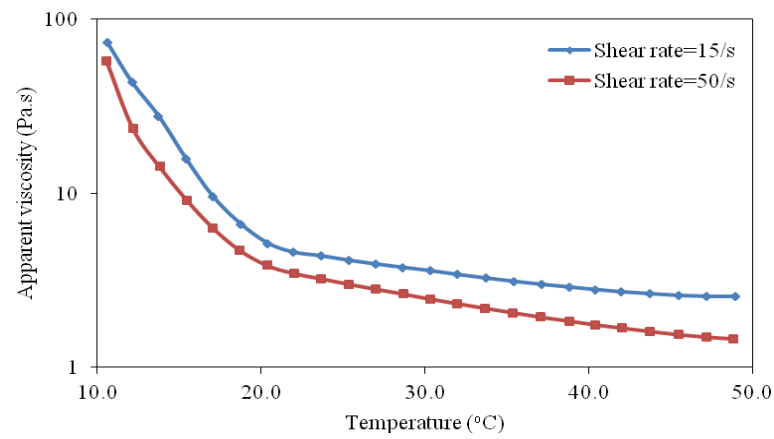
In contrast, Figure 4.9 (b) and (c) with cooling rate of 5 and  $10^{\circ}\text{C}/\text{min}$  respectively do not illustrate the same behaviour. There was no sharp increase in apparent viscosity for both shear rates applied even though the viscosity were still increased when the temperature decreased. The apparent viscosity resulted from shearing at  $15\text{s}^{-1}$  was greater than that  $50\text{s}^{-1}$  throughout the cooling process due to the shear thinning nature of chocolate, with the shape of the curves was similar. This behaviour shows that the effect of cooling rate dominates over that the shear applied. Even though shearing has been suggested to promote aggregation and speed up the nucleation, the rapid cooling rate used did not provide enough time for the crystal formation as have been discussed previously. For higher cooling rate, the measurement stopped at  $10^{\circ}\text{C}$  as has been set.



(a)



(b)



(c)

Figure 4.9: Viscosity of untempered dark chocolate cooled from 50 to 10°C at 1°C/min (a), 5°C/min (b) and 10°C/min (c) whilst sheared at 15 and 50s<sup>-1</sup>.

#### **4.3.4 Effect of pre-crystallisation on the viscosity evolution of dark chocolate**

Pre-crystallisation is a very important step to obtain Form V crystals to ensure the final product quality meets the customer requirement. Tempering involves the action of shear with controlled cooling and melting with the addition of seed crystals to induce the formation of desired polymorph. Liquid tempered or untempered chocolate (used as a control to assess the role of tempering) was placed on the Peltier stage of the rheometer before the upper plate was lowered down to the gap of 500 $\mu$ m from the base. The liquid chocolate was then cooled from 50 to 20°C (untempered chocolate) and 31 to 20°C (tempered chocolate). The effect of tempering process on the evolution of apparent viscosity was studied and the results are shown in Figures 4.10 and 4.11.

From Figure 4.10, the cooling process of tempered dark chocolate can be represented by two distinct regions. There was an induction period observed indicated by a plateau region showing relatively constant apparent viscosity as the temperature was decreased from 31°C to 26°C (subjected to the cooling rate of 0.5°C/min) and 24°C (subjected to the cooling rate of 1°C/min). Another region (below the temperature mentioned above) shows a linear increase in apparent viscosity most probably due to the crystals formation during tempering process. There was no sharp increase in viscosity observed for both cooling rates applied. The possible reason for this behaviour is that there were already seed crystals exists in the liquid tempered chocolate. Gradually, the presence of stable polymorph started to nucleate the bulk of remaining liquid chocolate when the onset temperature has been reached. Once again, the cooling rate applied gives an impact on the onset temperature for both tempered and untempered chocolate as has been discussed in section 4.2.2.1

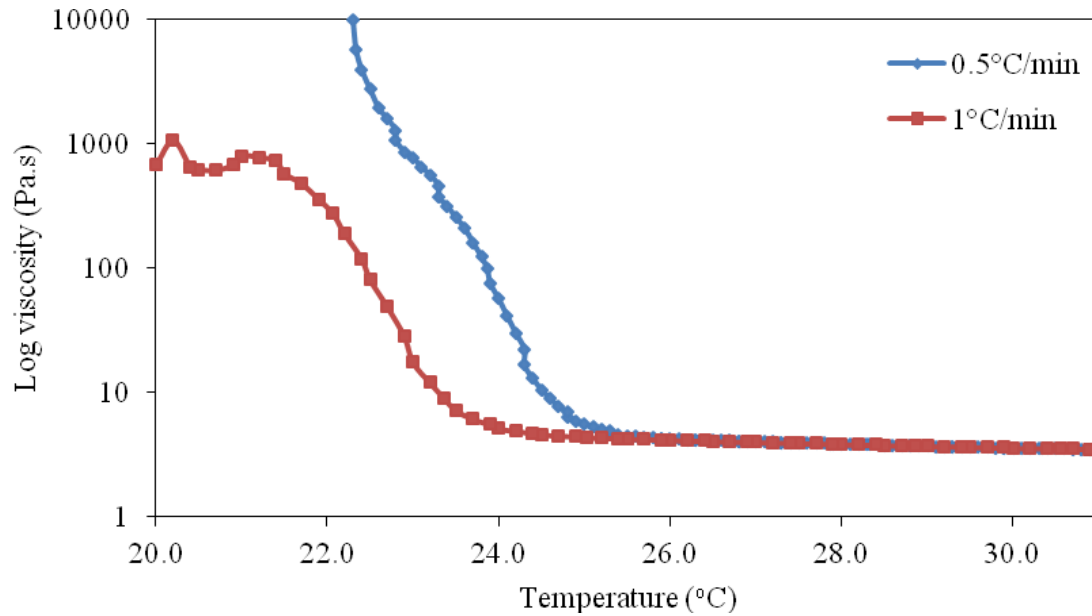


Figure 4.10: Viscosity of tempered dark chocolate cooled from 31 to 20°C at 0.5 and 1°C/min whilst sheared at 15s<sup>-1</sup>.

Figure 4.11 portrays the viscosity evolution for untempered chocolate which exhibits similar behaviour to the tempered chocolate at the beginning of cooling process. However, there were sharp increases in apparent viscosity showing that the crystallization has just started and the crystals were only beginning to exist. The crystallization may still occur but only large crystals formed which prevent compact packing.

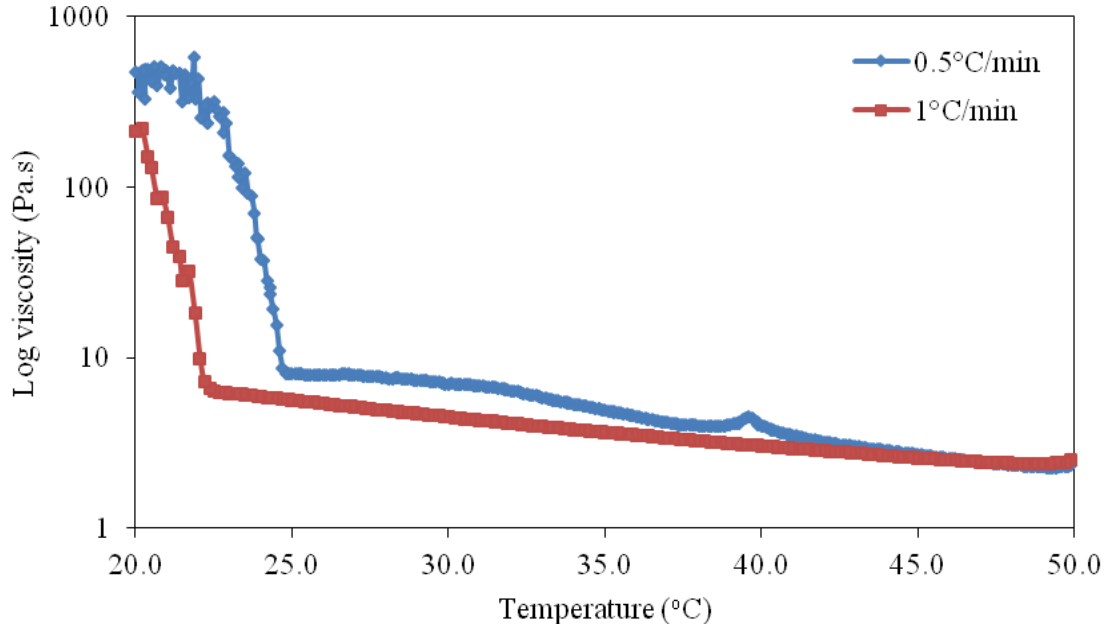


Figure 4.11: Viscosity of untempered dark chocolate cooled from 50 to 20°C at 0.5 and 1°C/min whilst sheared at 15s<sup>-1</sup>.

#### 4.3.5 Dynamic measurements

Dynamic measurement was carried out to obtain a better description of rheological properties of dark chocolate. The influences of temperature and chocolate type on the modulus evolution were studied. From the rheogram, the linear viscoelastic region (LVR) and the yield stress were determined.

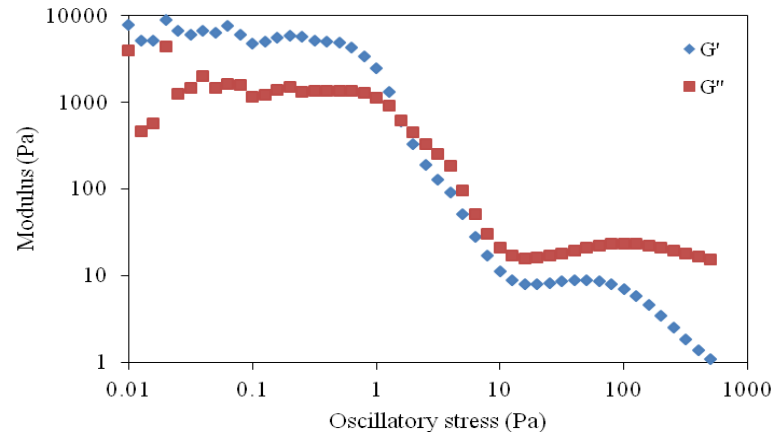
##### 4.3.5.1 Influence of temperature on the modulus evolution

A stress sweep test was conducted at oscillatory stress of 0.01 to 500 Pa at 35, 40 and 70°C. Storage modulus ( $G'$ ) and loss modulus ( $G''$ ) were used as a measure of the elastic and viscous component of the chocolate. Whichever modulus is dominant at a particular

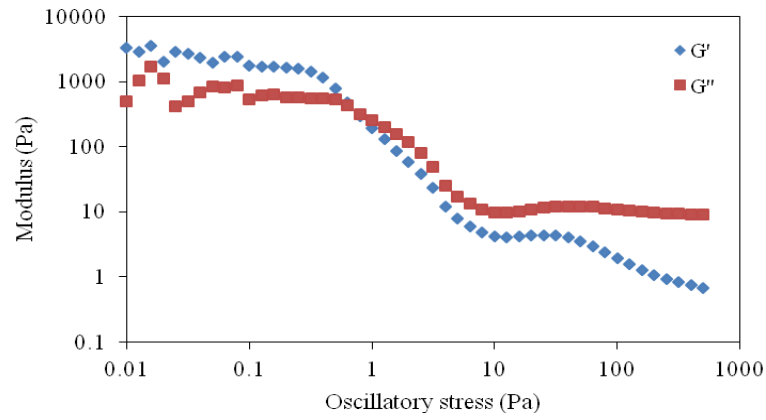
stress will indicate whether the chocolate appears to be elastic or viscous. The results are shown in Figure 4.12(a-c). All figures show the similar trend as follows:

- (i)  $G'$  was greater than  $G''$  at lower oscillatory stress for all temperatures and both are nearly independent of oscillatory stress. This indicates that the sample was elastic at all temperatures studied. The linear viscoelastic region (LVR) was identified.
- (ii) Beyond the LVR, the modulus decreased as the oscillatory stress was increased. There was a crossover point subjected to increasing oscillatory stress in which the  $G'$  crossed the  $G''$ .
- (iii)  $G''$  was greater than  $G'$  at higher oscillatory stress showing that the energy used to deform the material was dissipated viscously and the materials behaviour is liquid like.

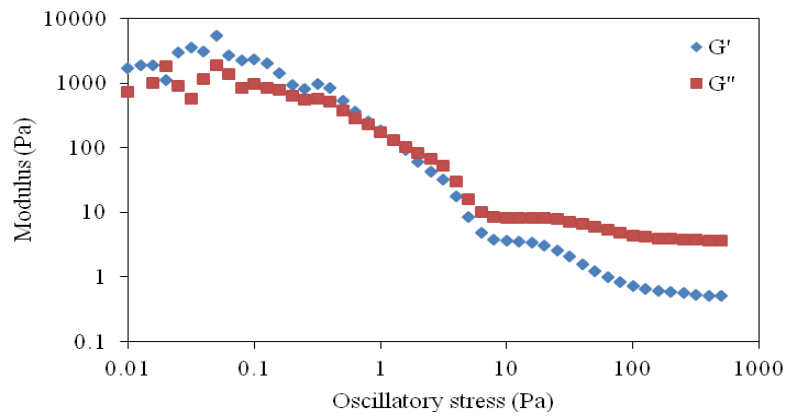
Oscillatory stress sweeps done revealed the modules were constant at oscillatory stresses less than the LVR values given in Table 4.2. LVR is a region where the increase in stress does not influence the modulus showing that the structure remains unchanged. The table shows that the LVR decreased when the temperature increased. A longer LVR at low temperature indicates that the chocolate structure is able to withstand great deformation before rupture. The yield stresses determined from the crossover point of  $G'$  and  $G''$  are also listed in Table 4.2. At higher temperature, material components have more thermal energy and hence a lower stress input is required to initiate flow. Consequently, yield stress tends to decrease with increasing temperature. This suggests that less force would be needed to remove the chocolate at higher temperatures. The yield value obtained from the oscillatory test sweeps agree with the literature.



(a)



(b)



(c)

Figure 4.12: Complex modulus as a function of oscillation stress for dark chocolate at 35°C (a), 40°C (b) and 70°C (c) (average of three measurements).

Table 4.2: LVR and yield value of dark chocolate at different temperatures.

Temperature	LVR	Yield value
(°C)	(Pa)	(Pa)
35	0.6310	1.5850
50	0.5012	1.0000
70	0.1259	0.7943

#### 4.3.5.2 Influence of chocolate type on the modulus evolution

It is believed that the formulations used to make a specific type of chocolate can affect the rheological behaviour. For that reason, an attempt was made to investigate the influence of chocolate type on the modulus evolution. A stress sweep test was conducted at oscillatory stress of 0.01 to 500 Pa at 35°C for both untempered dark and milk chocolates (also supplied by Mondelez). The ingredients of the milk chocolate were organic raw cane sugar, organic whole milk powder with minimum milk solids of 25%, organic cocoa mass with minimum cocoa solids of 34%, organic cocoa butter, soya lecithin and organic vanilla extract.

Figure 4.13 displays the evolution of complex modulus for both types of chocolate. In general, both types exhibit a similar trend to the results obtained for the temperature effect investigation previously discussed in section 4.3.6.1. It can be seen from the figure that  $G'$  was greater than  $G''$  at lower oscillatory stress for both dark and milk chocolates. When the LVR ended, the modules decreased when the oscillatory stresses were increased. In both cases there were the cross over points between the  $G'$  and  $G''$ . At higher oscillatory stress,  $G''$  was greater than  $G'$ . From the figure, it is clearly observed that the



length of LVR for dark chocolate was less than that for milk chocolate and the yield stress for dark chocolate was considerably lower as compared to milk chocolate. The yield value appears to contradict a study carried out by Gaikwad (2012) who compared dark and milk chocolate and found that the yield stress for milk chocolate was lower than for dark chocolate. The presence of finer particles in dark chocolate used in that study contributes to the higher yield stress as they can form more compact aggregates under low shear or no-flow conditions.

Besides the temperature-dependent characteristic, the yield value is also influenced by the particle size distribution, fat content, quantity of lecithin, moisture content and conching time. The possible reason for the higher value of yield stress of milk chocolate in this study as compared to dark chocolate is the particle size distribution. It is expected that the particle size of milk chocolate was smaller than that of the dark chocolate producing a well packed structure which needs to be broken to create a flow.

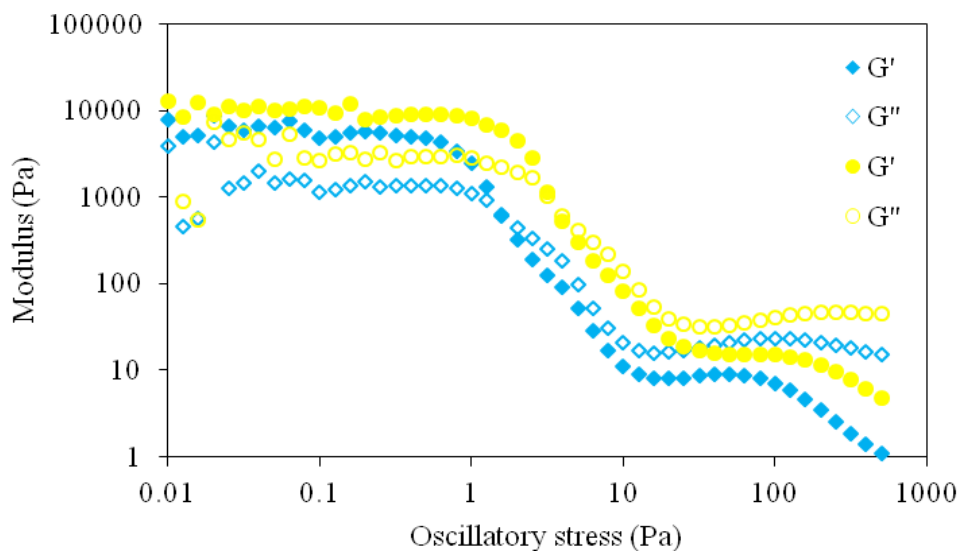


Figure 4.13: Complex modulus as a function of oscillation stress for untempered dark (blue) and milk (yellow) chocolates at 35°C (average of three measurements).

#### **4.4 Conclusions**

From the DSC curves, it can be concluded that the lab scale tempering machine which was used to prepare the samples for all the experiments throughout this study is able to produce Form V crystals. Solidified chocolate cooled on the Peltier stage was also examined in the DSC. Tempered chocolate cooled at slow and fast cooling rates resulting in more stable crystals compared to the untempered chocolate. All the materials used gave the same crystal form if the chocolate cooled on the Peltier stage at both cooling rate applied. The information of crystallisation obtained from the viscosity evolution in rheological study can be compared with the DSC data. Sudden increase in viscosity was observed to occur at the crystallisation temperature. Cooling, shearing and tempering gave an impact to the viscosity evolution as well as the crystallisation of chocolate. In dynamic measurement, the yield stress decreased when the temperature increased which is useful information in the cleaning work.

## **5 FORCE MEASUREMENT USING MICROMANIPULATION TECHNIQUE AND TEXTURE ANALYSER**

### **5.1 Introduction**

This chapter reports the application of two techniques to study the interaction between chocolate and mould materials. When the chocolate is in direct contact with mould materials, adhesion phenomena caused by the factors discussed in Chapter 2 will make the chocolate stick to the surface. To remove the chocolate from a surface, both adhesive and cohesive forces need to be overcome. Both a micromanipulation rig and a texture analyser have been used to measure the force required to remove a solid chocolate layer from the surface. Hence, the aims of the experiments reported in this chapter were (i) to determine the ease of removal of a solid chocolate layer from the surface and (ii) to identify the capability of both the micromanipulation rig and the texture analyser to separate the chocolate layer from the surface materials in different directions. Three different surface materials were used: stainless steel 316, polycarbonate and PTFE. The characterisation of these three surface materials including the contact angle and surface roughness measurements was made prior to the force measurement. Only dark chocolate was used throughout the experiments for this chapter.

The micromanipulation technique was used to study the effect of chemical usage, soaking time, medium temperature, surface material variation, T-probe speed, pre-crystallisation and cooling condition on the pulling energy. Besides, the use of texture analyser in a separate study later in this chapter will emphasise on the effect of the distance

between the probe surface and the chocolate surface, chocolate-probe contact time, pre-crystallisation and surface material variation on the separation force of the two surfaces.

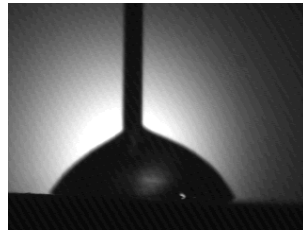
## **5.2 Surface characterisation**

The properties of the surface are very important to determine as they may affect the ease of removal of the chocolate layer from the surface material. Water contact angle and average roughness for the 316 stainless steel, polycarbonate and PTFE used in this study are summarised in Table 5.1. Figure 5.1 shows the images recorded by the video contact angle device, while the surface topography images scanned by the interferometer are shown in Figure 5.2.

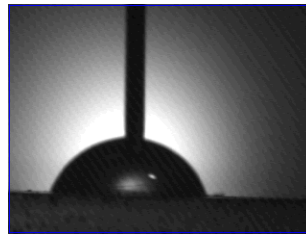
It is clearly seen from the table and the images that stainless steel was the most hydrophilic among the three surfaces with the water contact angle of  $66\pm4^\circ$  while the PTFE was the most hydrophobic among the three surfaces with the water contact angle of  $88\pm4^\circ$ . A small contact angle can be observed from Figure 5.1 (a) when water spread over a large area on the stainless steel surface. In contrast, water dropped on the PTFE surface did not spread over the surface, but a bead was formed as can be seen in figure 5.1 (c). However, stainless steel and polycarbonate were the smoother surfaces with the mean surface roughness of  $1.5\pm0.2\text{nm}$  and  $1.3\pm0.2\text{nm}$  respectively compared to PTFE which had a rougher surface with the mean surface roughness of  $4.3\pm1.3\text{nm}$ . Figure 5.2 (c) reveals that there were deep crevices on the PTFE surface. Therefore, maybe the chocolate could be trapped within the crevices which might subsequently affect the removal behaviour.

Table 5.1: Water contact angle,  $\theta_w$  ( $^\circ$ ) and average surface roughness,  $S_a$  (nm) of the surfaces. The errors represent the standard error of the mean from 6 replicates (water contact angle) and 3 replicates (average surface roughness).

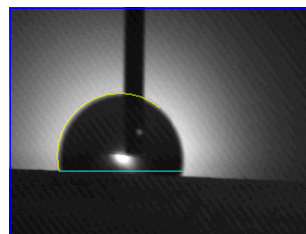
Surface materials	$\theta_w$ ( $^\circ$ )	$S_a$ (nm)
Stainless steel 316	66 $\pm$ 4	1.5 $\pm$ 0.2
Polycarbonate	72 $\pm$ 3	1.3 $\pm$ 0.2
PTFE	88 $\pm$ 4	4.3 $\pm$ 1.3



(a)

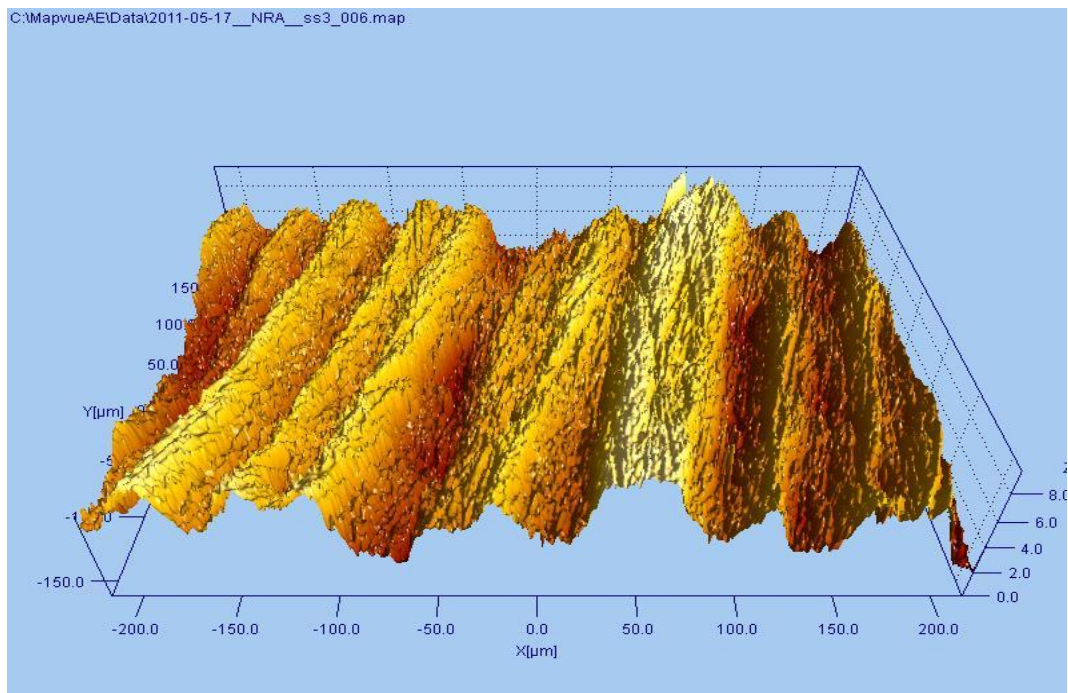


(b)

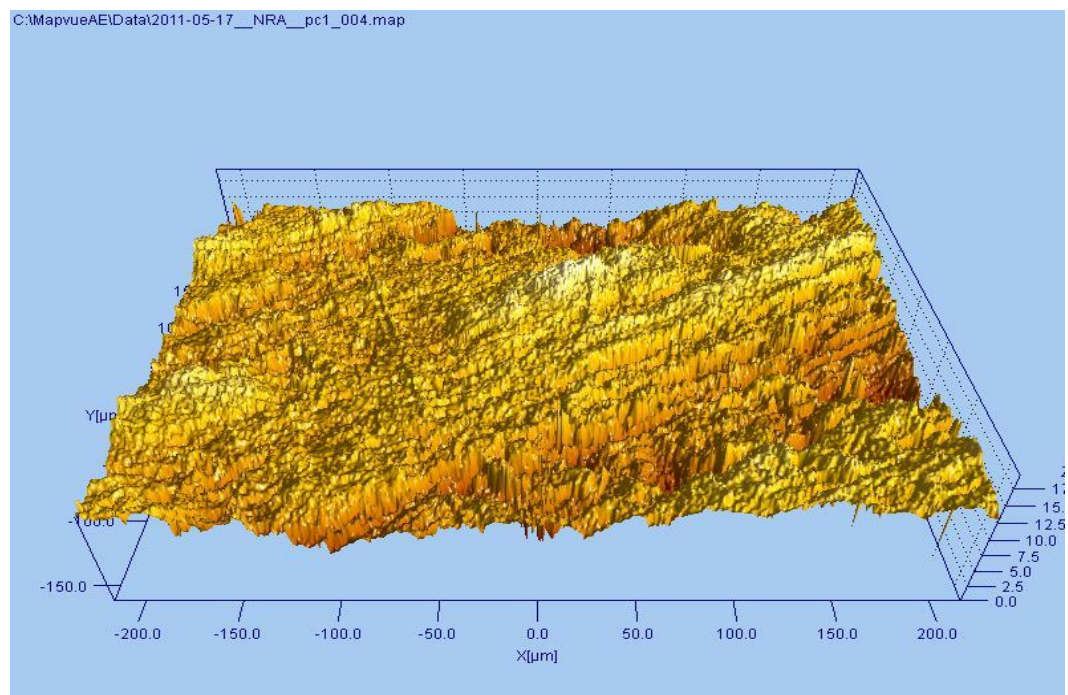


(c)

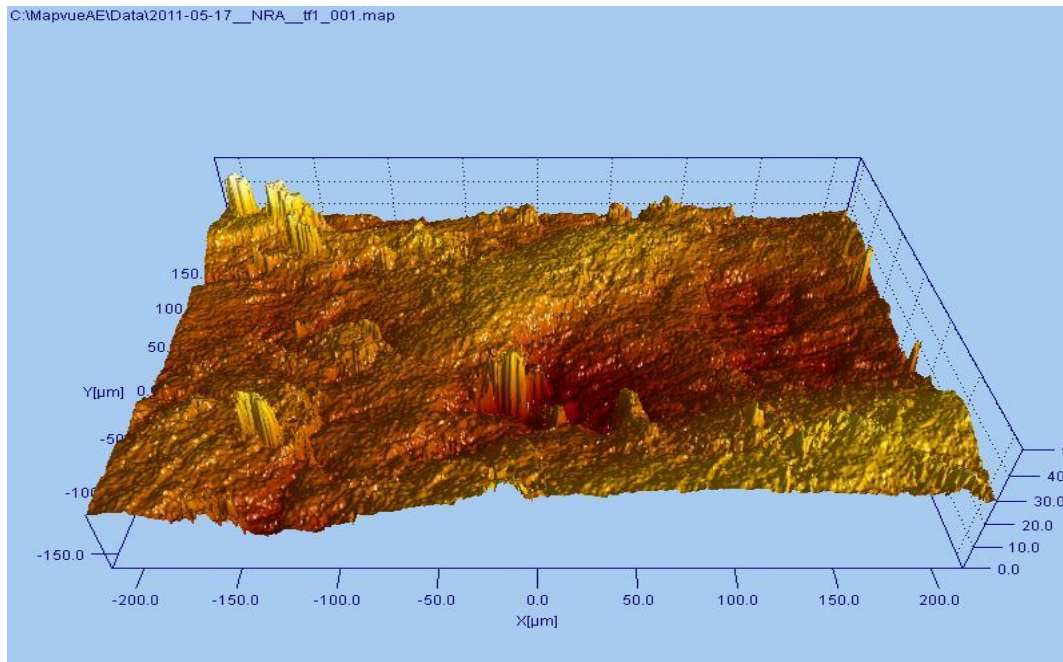
Figure 5.1: Images from video contact angle device; (a) stainless steel, (b) polycarbonate, (c) PTFE.



(a)



(b)



(c)

Figure 5.2: Surface topography images of (a) stainless steel, (b) polycarbonate and (c) PTFE scanned by using interferometer.

### 5.3 Measurement of removal force using micromanipulation technique

The background of this technique was described in Chapter 2. Operation of the micromanipulation rig was described in section 3.5 and the preparation of the fouled surface was given in section 3.3.1 and 3.3.3. The same procedure was used throughout the experimental work in this section and only dark chocolate was involved. The effect of soaking conditions including the chemical usage, time and medium temperature, material variations, probe speed, tempering and cooling on the pulling energy and removal of chocolate layer from the surface were studied. The term ‘pulling energy’ will be used throughout this section instead of adhesive strength as it represents the energy required to break the cohesive bonds between the chocolate sample and to remove the chocolate mass

from the surface. It is due to the removal behaviour observed as will be discussed in section 5.3.1.

### **5.3.1 Typical behaviour of scraping process**

When the T-shaped probe was moved horizontally across the chocolate layer surface, the measured force versus sampling time was recorded simultaneously. The typical curve is shown in Figure 5.3 and the corresponding scraping process behaviour is illustrated in Figure 5.4 which can be divided into four steps (A-D).

Initially, the gap between the bottom edge of the T-shaped probe and the surface of the square coupon was adjusted to be 100 $\mu$ m and it was kept consistent for all experiments. The movement of the T-shaped probe was initiated until it reached point A where the T-shaped probe started to contact the chocolate deposit. Then, the scraping process began and the measured force started to increase until it reached point B (centre of the coupon). Some of the chocolate deposit moved together with the probe but some remained on the surface. The measured force was then decreased to point C (final edge) where the probe left the surface and pulled the scraped deposit away from the surface. No force was detected once the probe was pulled away from the surface as shown by C to D in Figure 5.3. For all experiments carried out, no clean surface left after the micromanipulation measurement with a thin layer of chocolate left on the surface. This indicates that for dark chocolate, the cohesive forces between chocolate elements are weaker than the adhesive strength between the chocolate layer and the coupon surface. Scraping only involves the breakage of the bonds within the chocolate crystals. For that



reason, all the results in this section will be reported using the term “pulling energy” with respect to the parameters investigated.

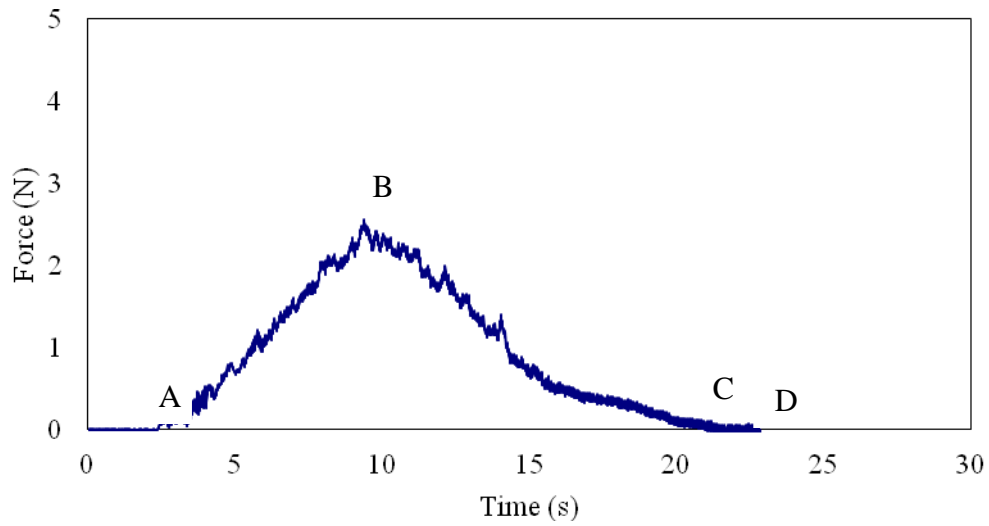


Figure 5.3: Typical curve of force versus sampling time for scraping a chocolate layer from a surface (probe moving at 1.1mm/s).

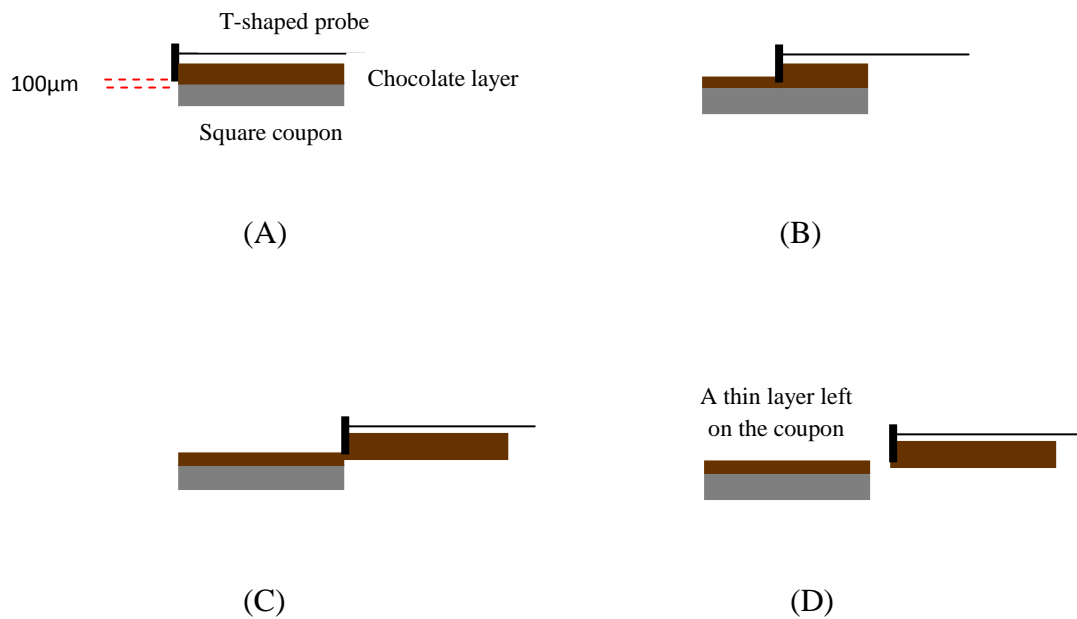


Figure 5.4: Schematic diagram of scraping process by the T-shaped probe.

### **5.3.2 Effect of chemical usage, soaking time and temperature on the pulling energy and removal**

Before the micromanipulation measurements were carried out, the square polycarbonate coupon with 0.5g solid chocolate layer on the surface was soaked in water for 10 minutes at different water temperature to aid the removal of the chocolate deposit. Only tempered chocolate was used for the experiments carried out in this section.

From Figure 5.5, it can be seen that a very high pulling energy was needed to remove the solid chocolate soaked in water at 25°C for 10 minutes. It was observed that at 25°C, the chocolate layer was still solid. For that reason, the scraping process was almost impossible. The pulling energy reduced slightly when the water temperature increased to 30°C. At 30°C, solid chocolate started to become softer and a small amount of chocolate was removed. However, when the water temperature increased to 35°C, the pulling energy needed to scrape the chocolate from the polycarbonate surface decreased from 2000J/m<sup>2</sup> to 250J/m<sup>2</sup> giving almost 90% reduction. Based on the melting curve obtained from the DSC study discussed in section 4.2, the melting temperature for tempered chocolate cooled at 1°C/min was about 34°C. Therefore it makes sense that a low pulling energy required to remove the chocolate from the surface. However, it was found that after the measurement was carried out there was small amount of chocolate in liquid form stuck on the polycarbonate surface. At 40°C, the pulling energy remained constant which was also supported by the DSC results. The effect of water temperature on the baked tomato paste hydrated for 10 minutes at different temperatures was studied by Liu *et al.* (2002). The apparent adhesive strength decreased with the hydration temperature increased in an exponential form. That result was not due to the melting of the deposit, but gradual

hydration of the surface. In current study, the water temperature contributes to the melting of the solid chocolate layer. The gap between the bottom edge of the probe and the solid surface might be the cause of the liquid chocolate left on the surface.

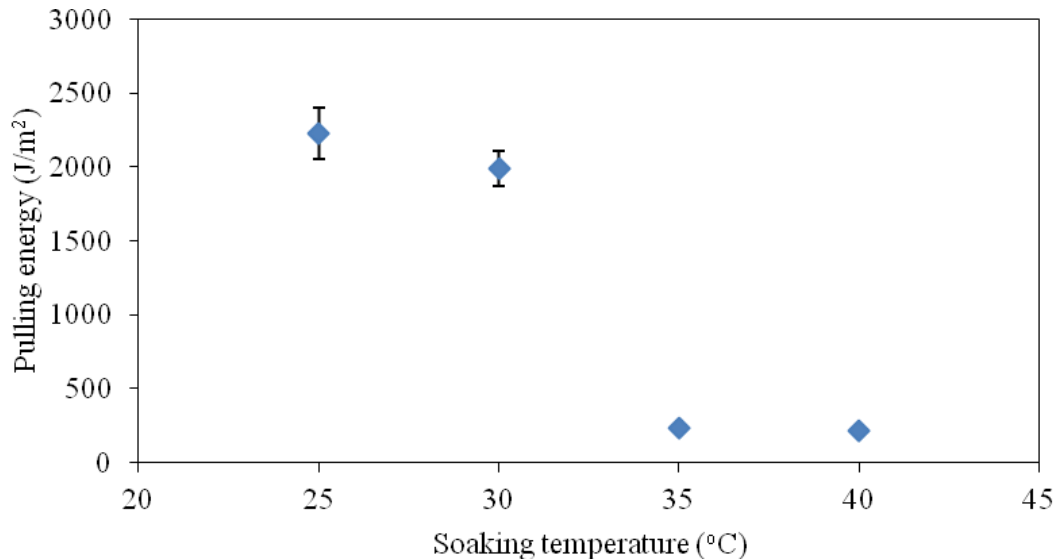


Figure 5.5: Pulling energy as a function of water temperature when the sample was submerged in water for 10 minutes prior to the measurement. Data are average of three repeats with the pulling speed of 1.1mm/s and the standard deviation plotted as error bars.

Besides the temperature, the soaking time was also believed to affect the pulling energy. Therefore, an experiment involving the variation of soaking time was conducted. The square coupon fouled with 0.5g solid chocolate was soaked in water at 30°C with the soaking time in the range of 5 to 30 minutes. Figure 5.6 shows interesting behaviour, in that an increase in the pulling energy was observed after the chocolate being soaked in water at 30°C after 10 minutes. The pulling energy increased from ca 600J/m<sup>2</sup> to 2000J/m<sup>2</sup> between 7-10 minutes. There was a further slight increase at 20 minutes soaking time whilst at 30 minutes, the pulling energy was slightly reduced to about 1800J/m<sup>2</sup>. A reduction in pulling energy with soaking time was expected. A possible reason for this

result is that the amount of chocolate scraped away gave an impact on the pulling energy as the solid chocolate would have turned into a softer form after being exposed to that temperature for a longer time. As more solid chocolate turned into a semi solid form, the mass of chocolate need to be scraped increased and consequently more energy required to remove them away. To support this, an experiment has been carried out with an increase in mass of chocolate which will be discussed later in this section. In a study conducted by Liu *et al.* (2002), the adhesive strength of baked tomato paste soaked in water decreased with the increasing of hydration time and eventually remained constant after 30 minutes. The same was obtained by Cole (2011) who measured the pulling energy of toothpaste after soaking in water for a range of time. The different with respect of soaking time will be determined by the interaction of the sample with water when soaking takes place.

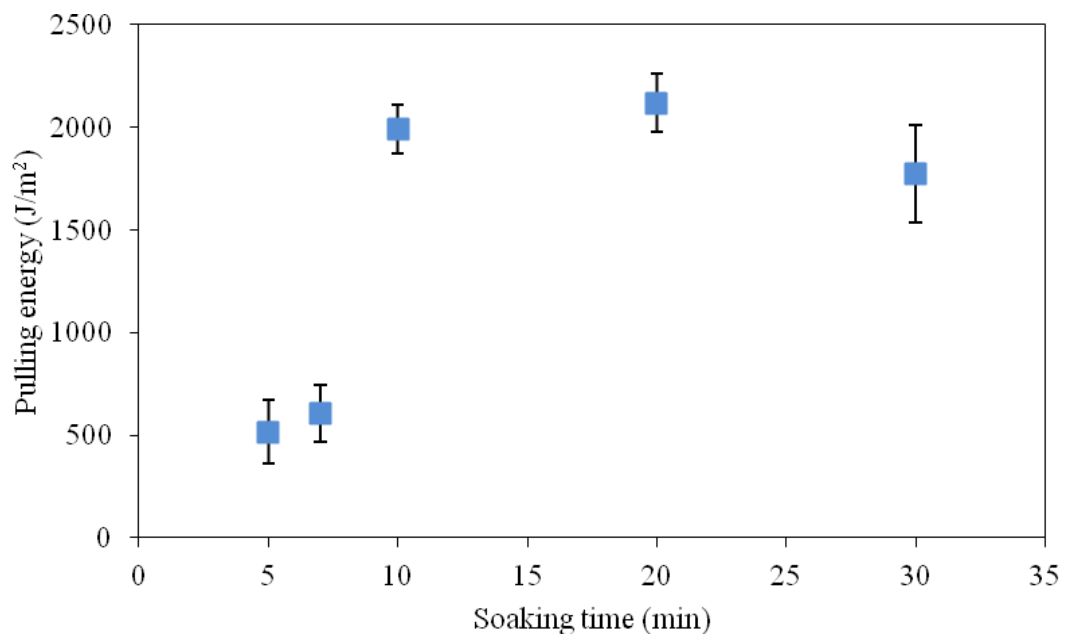


Figure 5.6: Pulling energy as a function of soaking time when the sample was submerged in water at 30°C prior to the measurement. Data are average of three repeats with the pulling speed of 1.1mm/s and the standard deviation plotted as error bars.

Figure 5.7 shows the percentage of the chocolate removed from the polycarbonate surface for a range of soaking times after the solid chocolate was soaked in water at 25, 30, 35 and 40°C. The percentage was determined from the ratio of mass reduction after the measurement being made to the initial mass. Results indicate that in all cases, removal increased by a factor up to four times when the water temperature increased from 30°C to 35°C. At 25 and 30°C, the removal percentage shows a slight increment at 10 minutes soaking time with the removal for 30°C is corresponding with the increase of pulling energy at 10 minutes. When prolonging the soaking time, the removal percentage remained constant. However, at a temperature greater than the melting temperature, the increasing of soaking time did not show any significant change in removal percentage. Almost 90% reduction was achieved even after being soaked only for 5 minutes. This is again due to the melting behaviour of the solid chocolate as shown by the DSC study.

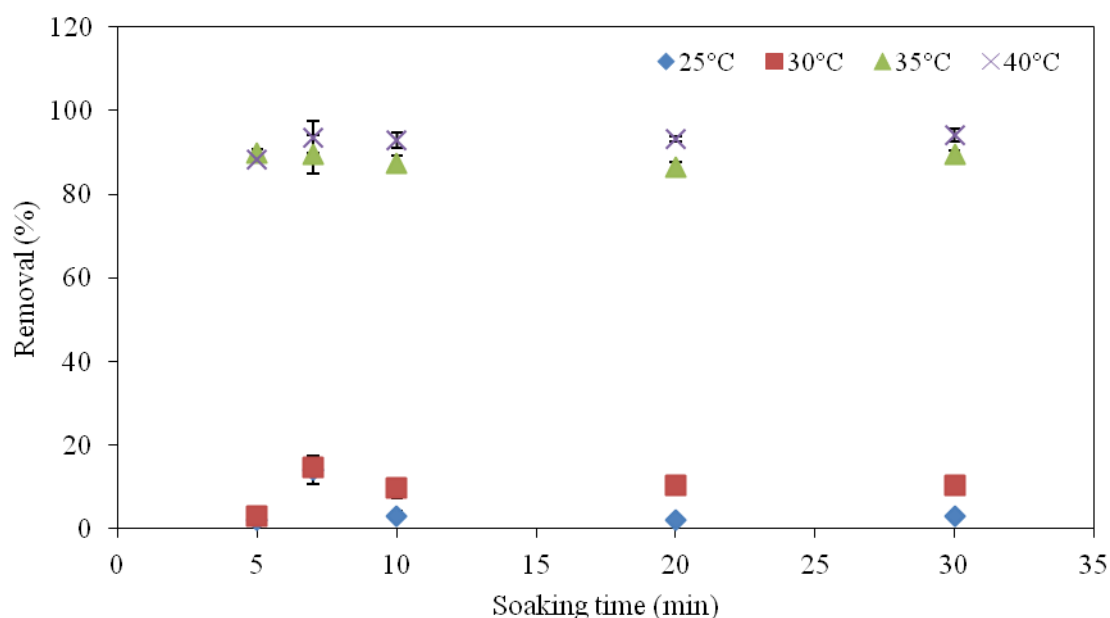


Figure 5.7: Removal percentage as a function of soaking time for different water temperature.

After looking at all the results obtained, it was noticed that complete removal could not be achieved even after soaking the solid chocolate in water at temperature higher than the melting point. It might be possible to remove the chocolate completely from the polycarbonate surface when the cleaning chemical detergent is used. A trial experiment was carried out to test this hypothesis. Figure 5.8 highlights the difference of the typical curve of the force versus sampling time for scraping the chocolate layer after it was soaked in water and 0.1% NaOH. The area under the curve reflects the energy used to scrape the chocolate from the surface. It can be seen that the area under the curve for water was much larger compared to the area under the curve for NaOH. Furthermore, the removal percentage was also higher compared to the removal after soaking in water. Soaking the chocolate in 0.1% NaOH did not only change the internal structure of the chocolate crystals, but also cause dissolution to occur. The presence of three fatty acids attached to the glycerol backbone in the cocoa butter molecule has also resulted in soapy effect (Beckett, 2008). In a study conducted by Liu *et al.* (2006, 2007) the morphology of whey protein concentrate and egg albumin respectively after being submerged in 0.5% NaOH solution were examined using SEM. Both deposits swelled and increased in thickness after contact with NaOH solution and this followed by the dissolution. The thickness and dissolution rate were affected by the contact time, concentration and temperature of the NaOH solution. SEM pictures showed that the chemical did not only break the chemical bonding within the deposits but also changed the internal structure. From that findings, it was therefore decided to soak the solid chocolate in 0.1% NaOH instead of water for the following experiments.

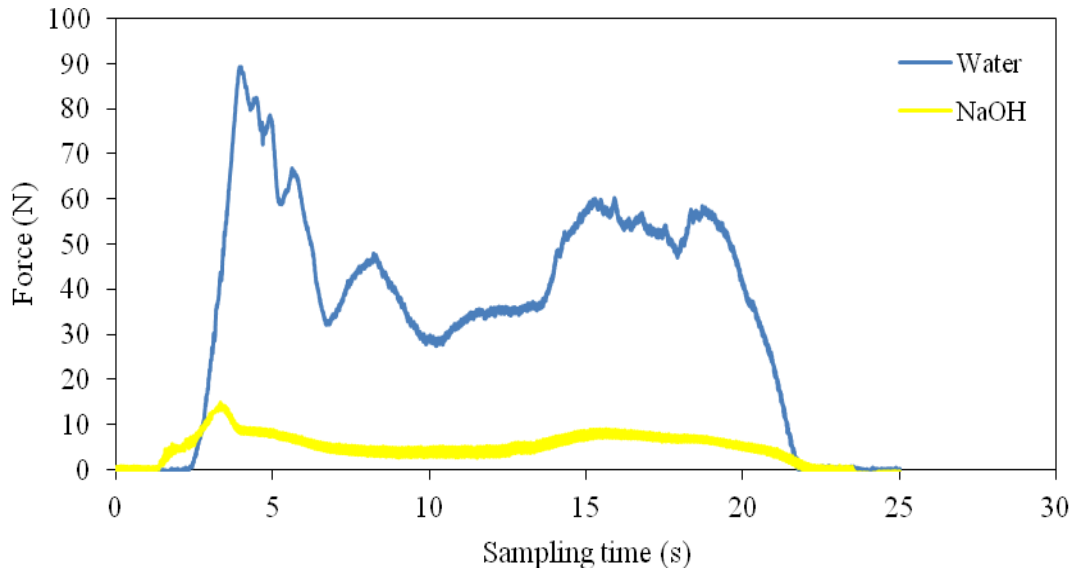


Figure 5.8: Typical curve showing force versus sampling time for pulling a chocolate layer from coupon surface under two conditions: after submerging in water and that after submerging in 0.1% NaOH. Data are average of three repeats with the pulling speed of 1.1mm/s.

To study the effect of combination of the temperature and the chemical usage, three samples were put into 0.1% NaOH at 25, 30 and 40°C respectively for 10 minutes. From Figure 5.9, it was found that the pulling energy decreased when the temperature of the solution increased from 25°C to 40°C. The pulling energy of 350J/m<sup>2</sup> at 25°C reduced to 75J/m<sup>2</sup> at 40°C. The reduction was also observed when no chemical was involved (see Figure 5.5), but the amount of energy needed when the chemical used was much lower than that without chemical. The removal percentage shown in Figure 5.9 increased up to 90% at 40°C.

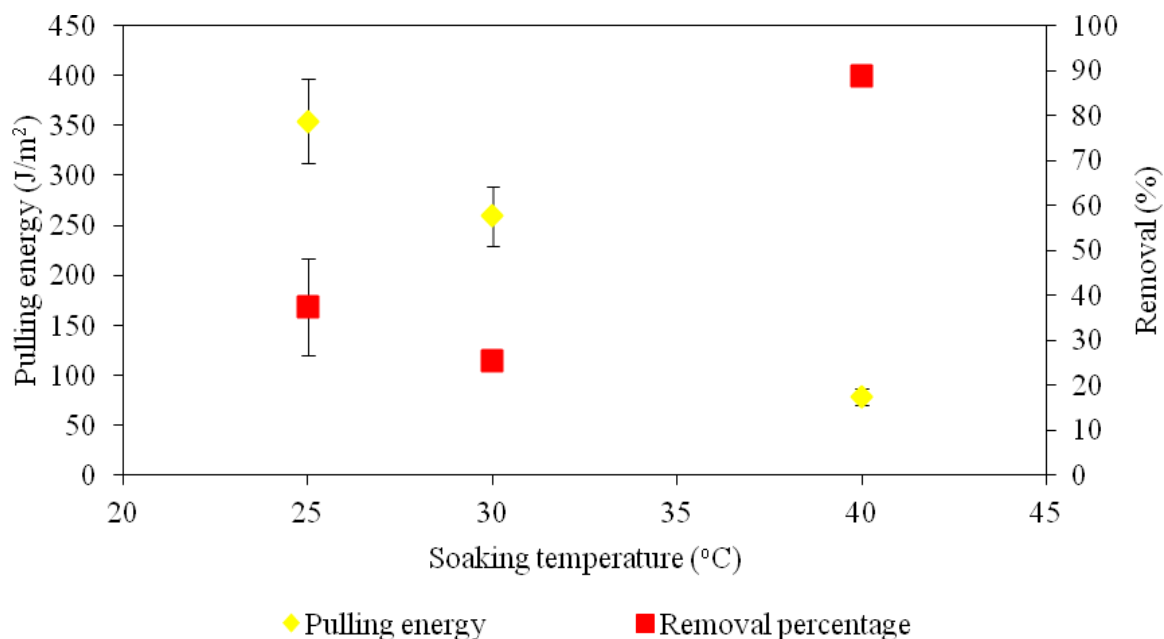


Figure 5.9: Pulling energy and removal percentage as a function of solution temperature (the sample was submerged in a 0.1% NaOH solution for 10 minutes prior to the measurement). Data are average of three repeats with the pulling speed of 1.1mm/s.

In all cases, the solid chocolate on the material surfaces were submerged in either water alone or chemical solution prior to micromanipulation measurements. The dissolution phenomena mentioned earlier was illustrated in Figure 5.10. There was no dissolution observed in Figure 5.10 (a) which shows chocolate immersed in water alone, even though the water temperature (40°C) exceeded the melting temperature of the tempered chocolate cooled at 1°C/min. However, in Figure 5.10 (b) (soaked in 0.1% NaOH at 25°C), small particles can be seen in the solution showing that the chocolate structure has been disturbed. The chemical used weakens the intermolecular forces even at room temperature. When the temperature increased to 30°C, the amount of small particles also increased as shown in Figure 5.10 (c) and some of them had dissolved in the solution. The dissolution was fastest at 40°C as after 10 minutes of soaking, no particles can be seen



in Figure 5.10 (d). The diffusion of chemical agent into the chocolate deposit is a function of temperature. An increase in the temperature will result both in an increase of dissolution rate and decrease in the deposit strength. This is in agreement with Liu *et al.* (2007) who also found that the concentration of NaOH solution also influenced the dissolution rate of egg albumin deposits.

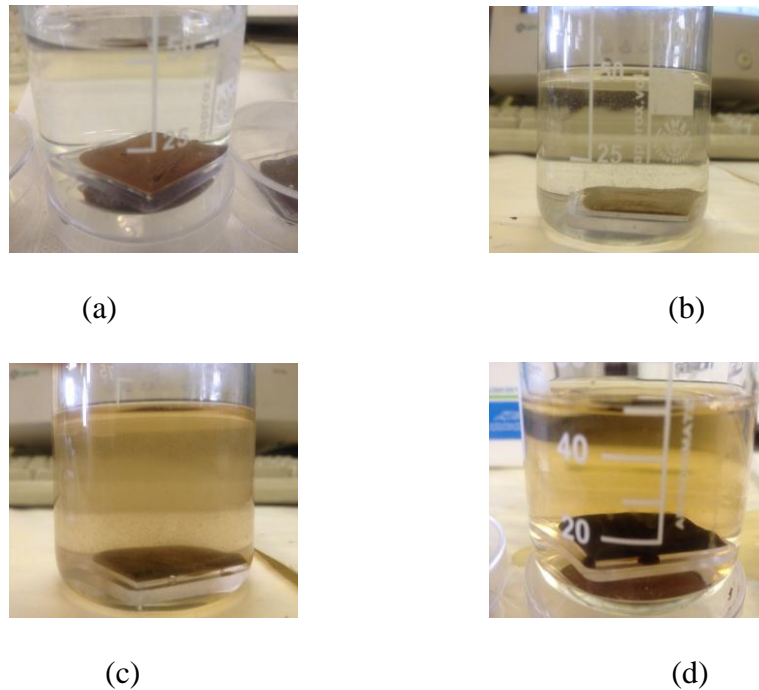


Figure 5.10: Dissolution occurred when soaking in 0.1% NaOH for 10 minutes. (a) Soak in water at 40°C, (b) Soak in 0.1% NaOH at 25°C, (c) Soak in 0.1% NaOH at 30°C and (d) Soak in 0.1% NaOH at 40°C.

Before further investigation, it was decided to have a look at the influence of the amount of chocolate to the pulling energy. Therefore, 0.6g of chocolate was placed on the square coupon instead of 0.5g used in the other experiments. The solid chocolate was soaked in 0.1% NaOH at 30°C for 10 minutes prior to micromanipulation measurement. Figure 5.11 shows that the pulling energy increased from 250J/m<sup>2</sup> to 430J/m<sup>2</sup> when the

amount of chocolate increased by 20%. The amount of chocolate to be scraped influences the pulling energy. Liu *et al.* (2007) in their study involving the variation of heating temperature for egg albumin reported that at higher heating temperature, the adhesive strength between the deposits and the stainless steel surface increased caused by the production of more deposits as more proteins had been denatured. No chemical was involved in that study.

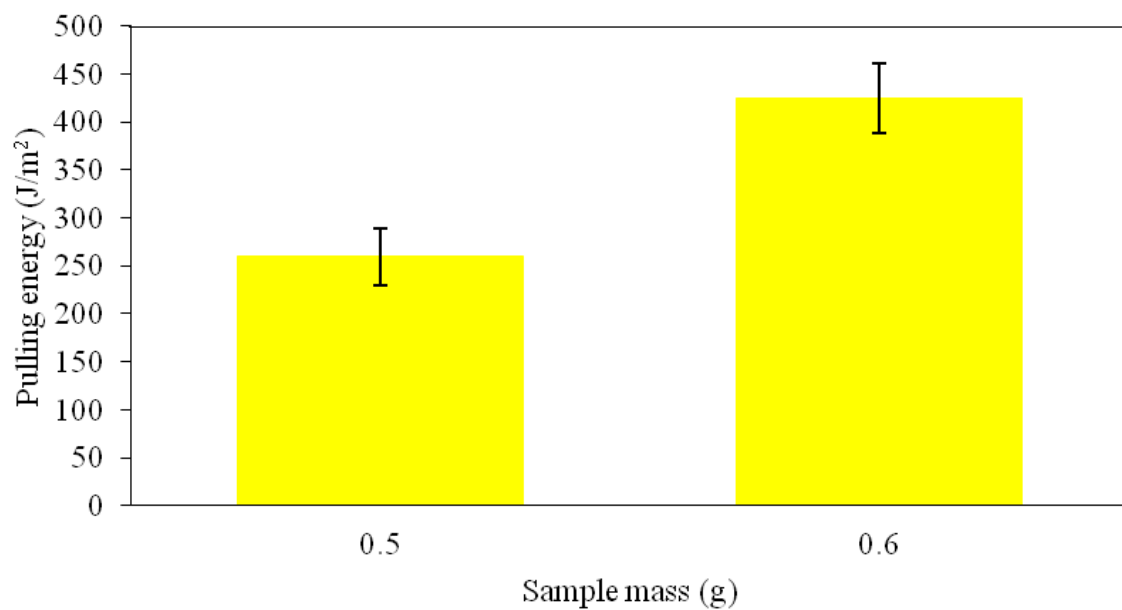


Figure 5.11: Pulling energy as a function of chocolate mass. Data are average of three repeats with the pulling speed of 1.1mm/s.

A new plot of the amount of energy required to remove a gram of chocolate (the energy measured divided the amount of chocolate removed) as function of temperature has been created as displayed in Figure 5.12. It remains unchanged at 25 and 30°C and decreased by 90% at 40°C as the chocolate was in liquid form at this temperature.

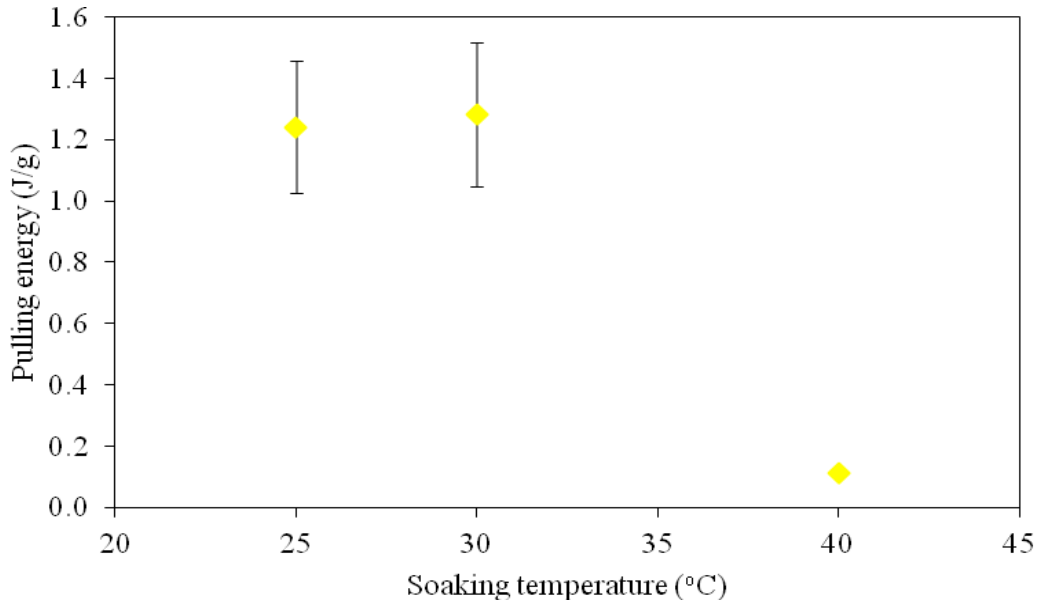


Figure 5.12: The amount of energy per unit gram as a function of temperature.

The chemical concentration is believed to give an impact to the removal process as has been studied by Liu *et.al* (2006) and Bird and Fryer (1991). However, it was not included in the scope of this study. Pulling energy has been measured for the sample soaked in 0.1% NaOH solution at 30°C for a range of time. The pulling energy and removal percentage are shown in figures 5.13 and 5.14 respectively. Instead of increasing with soaking time, the pulling energy only increased slightly after being soaked for 7 minutes from 350J/m<sup>2</sup> to 390J/m<sup>2</sup>, probably due to the experimental error. Then, it decreased to 250J/m<sup>2</sup> and remained constant until 20 minutes soaking time. Further reduction to 150J/m<sup>2</sup> can be seen when the soaking time increased to 30 minutes. Even though it has been shown that the amount of chocolate to be scraped affects the pulling energy, the longer the soaking time the greater the dissolution will occur. Removal percentage increased linearly with the increase of soaking time, and almost 90% reduction was achieved for 30 minutes soaking time. Results suggest that the removal process was actually started during soaking whereby some of the chocolate has dissolved in the chemical solution.

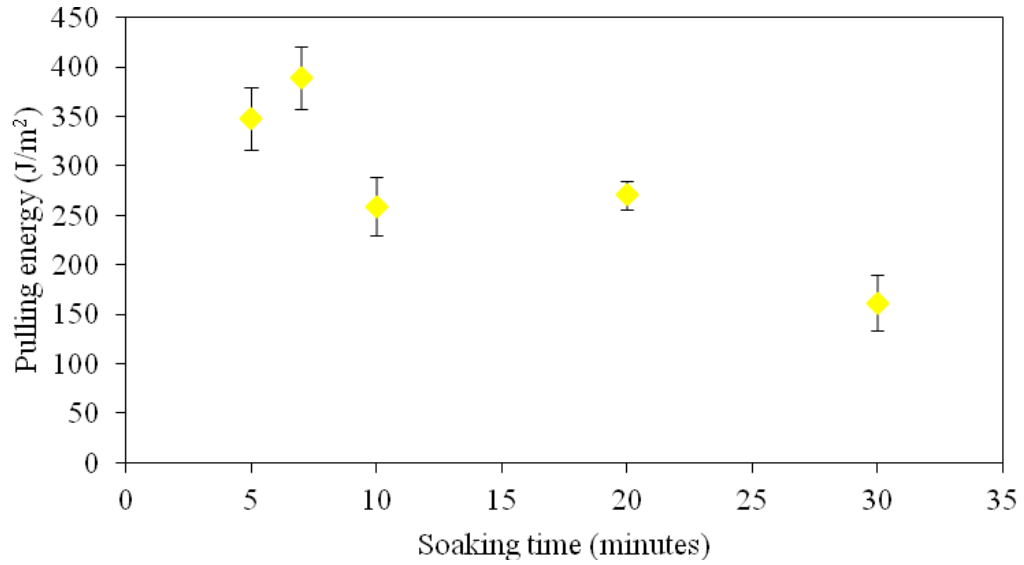


Figure 5.13: Pulling energy as a function of soaking time when the sample was soaked in 0.1% NaOH solution at 30°C prior to the measurement. Data are average of three repeats with the pulling speed of 1.1mm/s.

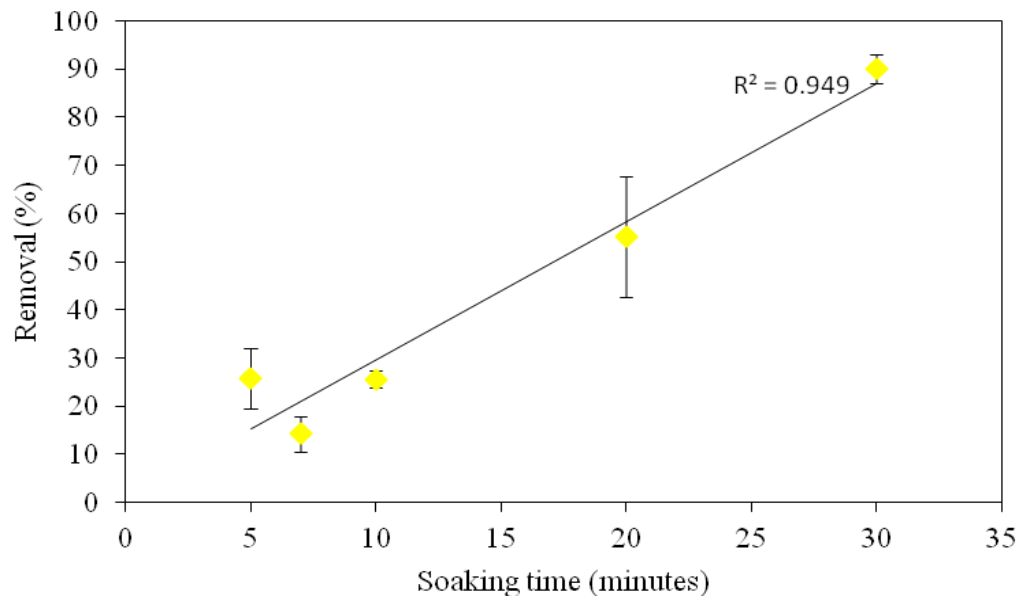


Figure 5.14: Removal percentage as a function of soaking time when the sample was submerged in a 0.1% NaOH solution at 30°C prior to the measurement. Data are average of three repeats with the pulling speed of 1.1mm/s.

In addition to the NaOH solution, a series of experiment has also been conducted with the use of 0.12% v/v cleaning solution as it is the normal concentration used in the industry. A commercial dishwashing liquid was chosen containing 15-30% anionic surfactants, 5-15% non-ionic surfactants, phenoxyethanol, methylisothiazolinone and perfume. To give a comparison, the solid chocolate was soaked in 0.12% v/v cleaning solution at the same temperature (30°C) for 7, 10 and 30 minutes. The pulling energy and the removal percentage are shown in Figure 5.15. A reduction in the strength of pulling energy from 580J/m<sup>2</sup> to 480J/m<sup>2</sup> was observed when the soaking time was increased from 7 to 10 minutes. However, it increased slightly to 500J/m<sup>2</sup> at soaking time of 30 minutes. This is higher compared to the amount of energy required after being soaked in 0.1% NaOH but lower than the amount of energy measured after soaking in water at the same temperature. An increase in the removal percentage was observed from the plot, but only 45% of the chocolate was removed even after 30 minutes exposure to the 0.12% commercial cleaning solution compared to 90% removal after soaking in 0.1% NaOH solution.

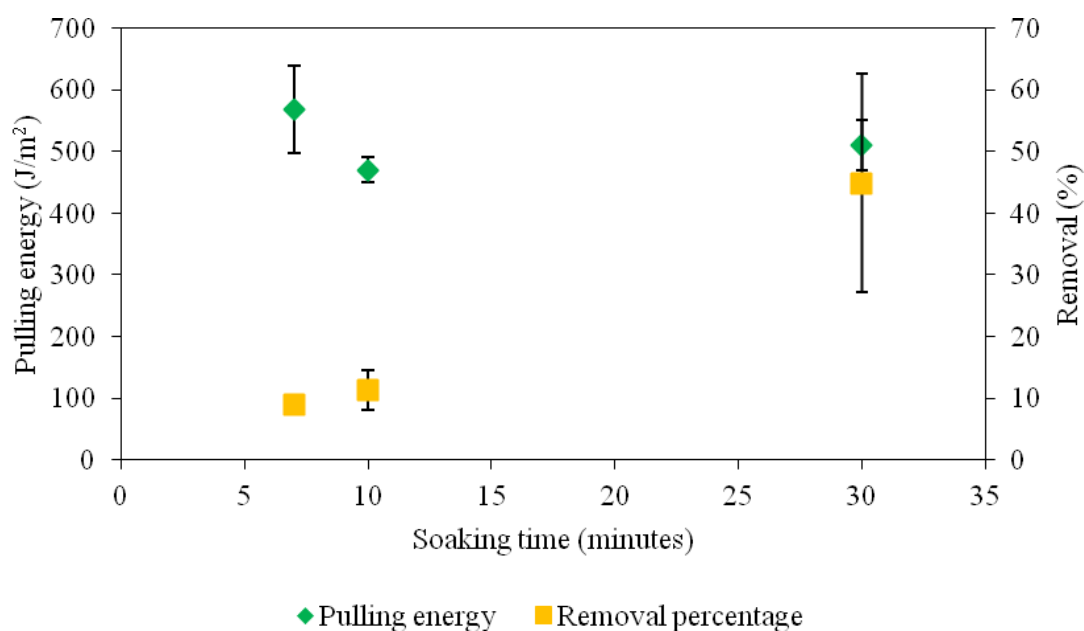


Figure 5.15: Pulling energy and removal percentage as a function of soaking time when the sample was submerged in a 0.12% commercial cleaning solution at 30°C prior to the measurement. Data are average of three repeats with the pulling speed of 1.1mm/s.

The amount of energy required to remove a gram of chocolate as a function of soaking time for both 0.1% NaOH and 0.12% commercial cleaning solutions are shown in Figure 5.16. As expected, it decreased with the soaking time increase. However, the rate of reduction in pulling energy when the solid chocolate was soaked in 0.12% commercial cleaning solution was higher than for the 0.1% NaOH. This is probably due to the ingredients used to produce the solution which aims to clean a wide range of dirt.

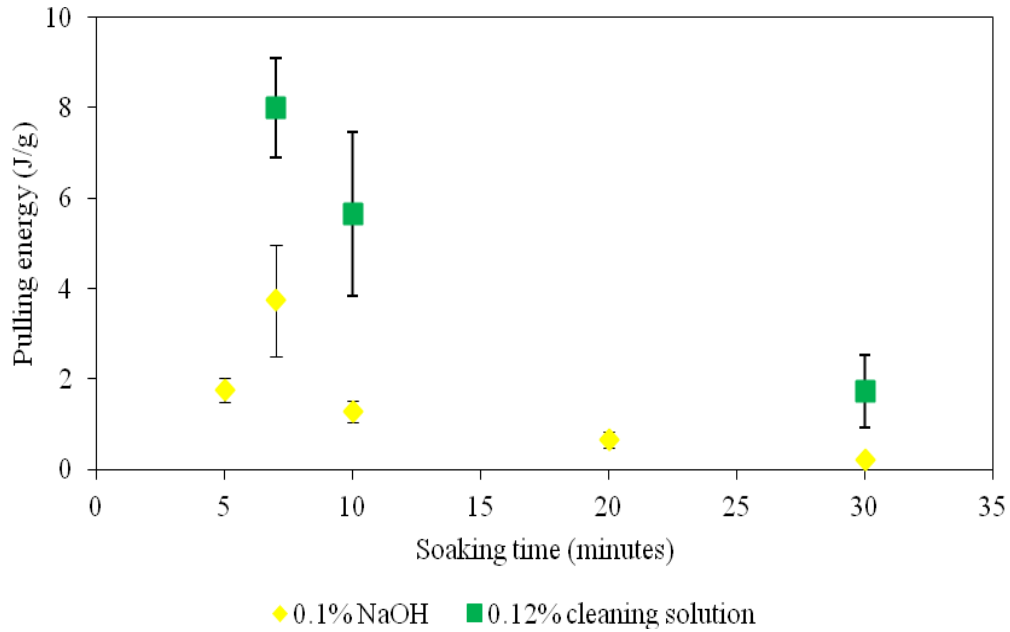


Figure 5.16: Amount of energy per unit gram as a function of soaking time for removal of chocolate soaked in 0.1% NaOH and 0.12% commercial cleaning solution.

### 5.3.3 Effect of probe speed on the pulling energy and removal

The variation of probe speed was studied to identify the influence of the shear rate variation on the removal of the chocolate layer from polycarbonate surface. A constant speed was used (1.11mm/s) in all experiments for other sections in this chapter, but probe speeds in the range of 0.59 to 2.22mm/s were used for the experiments in this section. Rate dependence was expected because of the viscoelastic behaviour of the chocolate as determined in Chapter 4.

The pulling energy and removal percentage for four different speeds are shown in Figure 5.17. Pulling energy did not show any specific trend when the probe speed increased from 0.59 to 2.22mm/s showing that the speed did not affect the amount of energy required to scrape the chocolate layer from polycarbonate surface. However, a

small increment in the removal percentage was observed when the speed increased from 0.59 to 1.82mm/s. It then remained constant when the speed was further increased to 2.22mm/s. This result suggests that the effect of elastic properties is not significant over this range. The effect of probe speed had also been studied by Liu *et al.* (2007) which the adhesive strength of the egg albumin did not show any significant difference with the increasing of probe speed although it was expected to show some dependency due to the viscoelastic behaviour of the egg albumin. Similar results are obtained in this study.

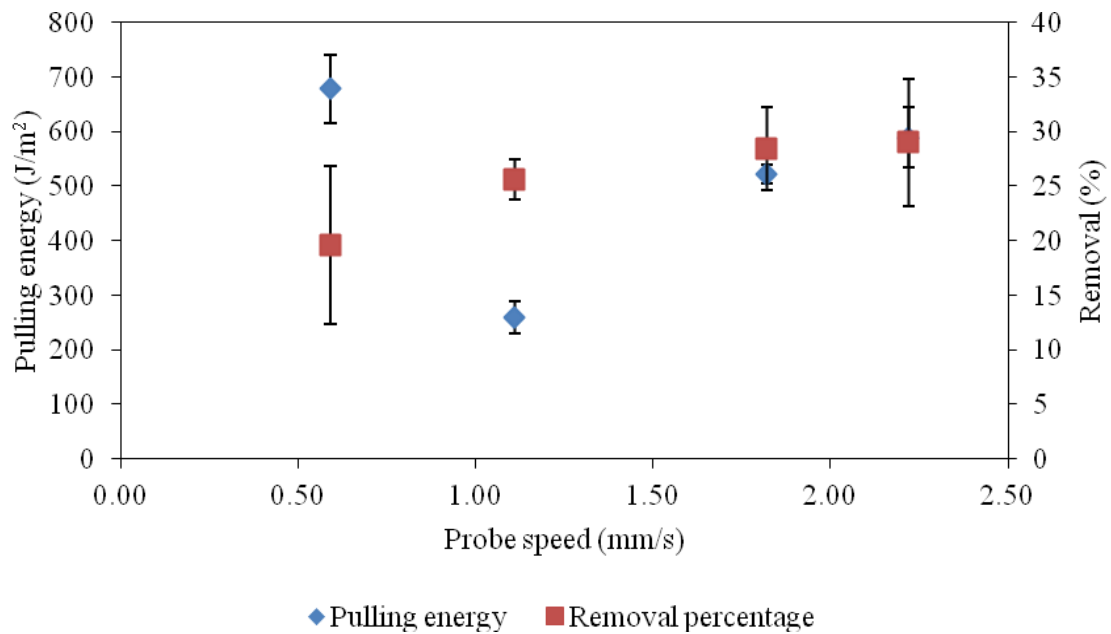


Figure 5.17: Pulling energy and removal percentage as a function of probe speed (the sample was submerged in a 0.1% NaOH solution at 30°C for 10 minutes prior to the measurement). Data are average of three repeats.



### 5.3.4 Effect of surface material on the pulling energy and removal

In section 5.2, the characteristics of the three surface materials used have been studied. This section will involve a series of experiments to measure the force required to remove a solid chocolate layer from these materials. Square coupons made of stainless steel, polycarbonate and PTFE with the same dimension (20mm x 20mm) were coated with 0.5g tempered chocolate, that was then cooled on the Peltier stage to 10°C at 1°C/min. Before micromanipulation measurement was carried out, it was soaked in 0.1% NaOH solution at 30°C for 10 minutes. This condition was chosen as a standard because it can be compared to the results obtained in section 5.3.2. The results are shown in Figures 5.18- 5.20.

As shown in Figure 5.18, the pulling energy for removal of chocolate from stainless steel was the lowest followed by polycarbonate and PTFE. One possible reason for that behaviour is that the surface roughness influences the pulling energy. The rough surface (PTFE) had the highest value (300J/m<sup>2</sup>) compared to 150J/m<sup>2</sup> and 250J/m<sup>2</sup> for stainless steel and polycarbonate respectively. Liu *et al.* (2002) compared the adhesion of baked tomato paste to the rough and smooth stainless steel surfaces and found out that the adhesive strength for rough surface was nearly twice of the smooth surface after 10 minutes of hydration. Deep crevices on the PTFE surface as seen from the image scanned by the interferometer can cause the chocolate trapped in it and subsequently the removal became very difficult. For that reason, high amount of energy is required to scrape even a small amount of chocolate.

Only 13% of the chocolate has been removed from the PTFE surface compared to 37% and 25% removal from the stainless steel and polycarbonate surfaces respectively as

shown in Figure 5.19. Figure 5.20 displays the amount of pulling energy per unit gram for the three surfaces while Figure 5.21 shows the images of the chocolate remaining on the three surfaces captured at the end of the micromanipulation measurements. Even though the magnitude of pulling energy for PTFE was the greatest, only a small amount of chocolate had been removed. In this case, the pulling energy required does not reflect the amount of chocolate needing to be scraped away. The surface roughness seemed to control the removal of chocolate from the three surfaces. Akhtar (2010) who used both AFM and micromanipulation to measure the removal force of caramel, SCM, Turkish delight and toothpaste from glass, PTFE and stainless steel surfaces respectively found that Turkish delight was the most difficult deposit to be removed from PTFE surface due to the cross linking of the agar and low water content of Turkish delight. Caramel, SCM and toothpaste exhibited the same behaviour with the adhesion to the glass surface was the greatest followed by stainless steel and PTFE surfaces. In that case, the removal seemed to be controlled by the characteristic of the deposit.

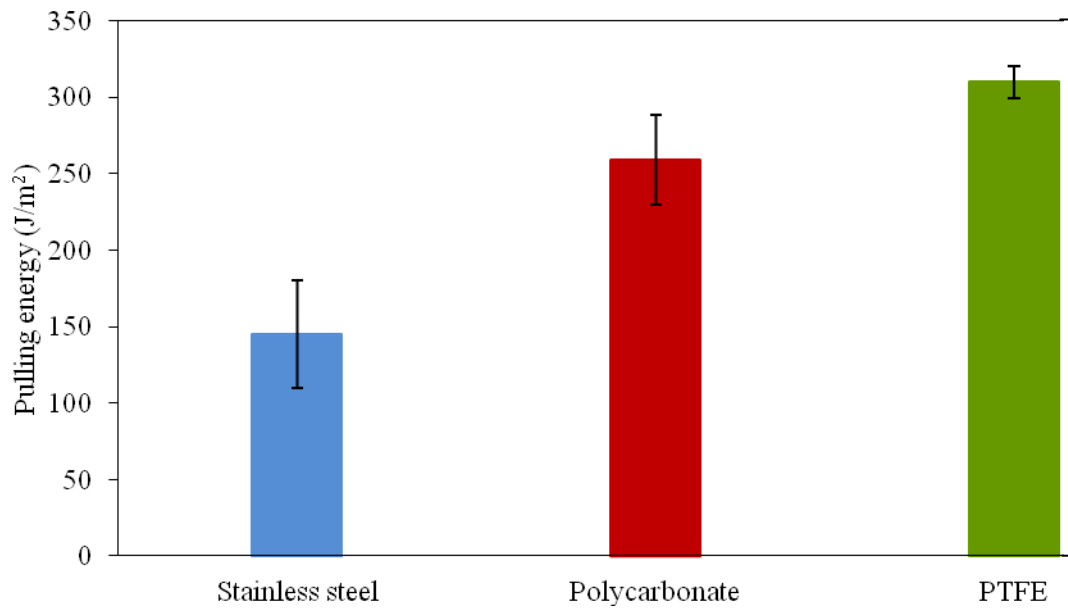


Figure 5.18: Pulling energy for removal from different material surfaces (the sample was submerged in a 0.1% NaOH solution at 30°C for 10 minutes prior to the measurement). Data are average of three repeats with the pulling speed of 1.1mm/s.

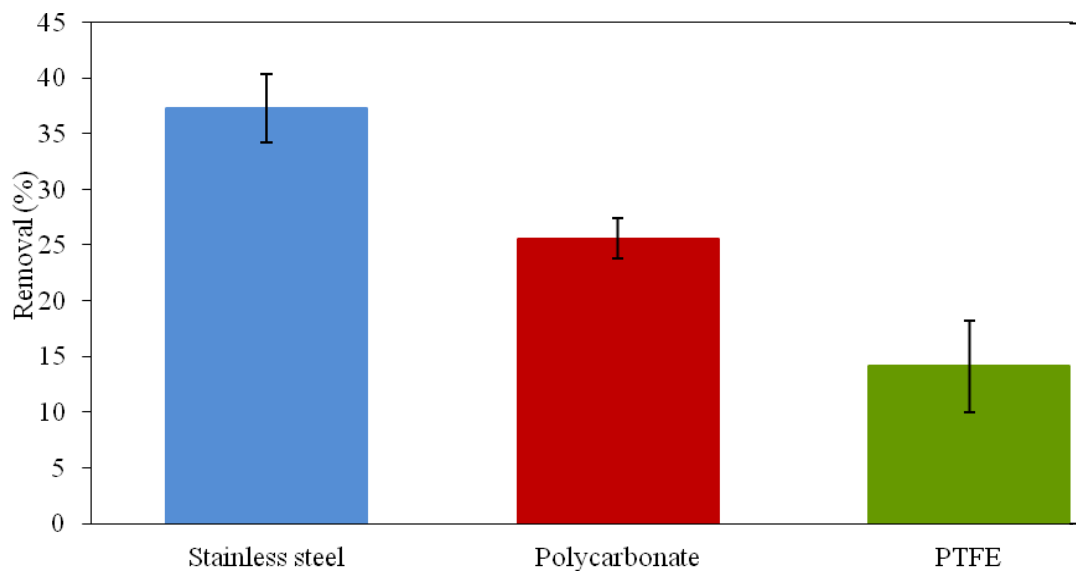


Figure 5.19: Removal percentage for different materials (the sample was submerged in a 0.1% NaOH solution at 30°C for 10 minutes prior to the measurement).

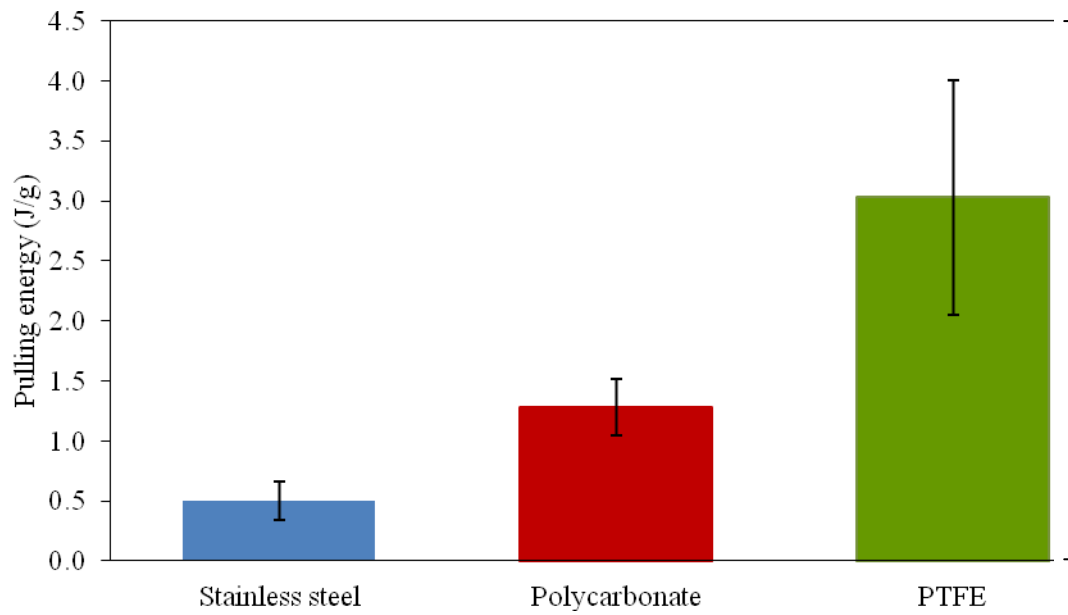


Figure 5.20: The amount of pulling energy per unit gram for different material.

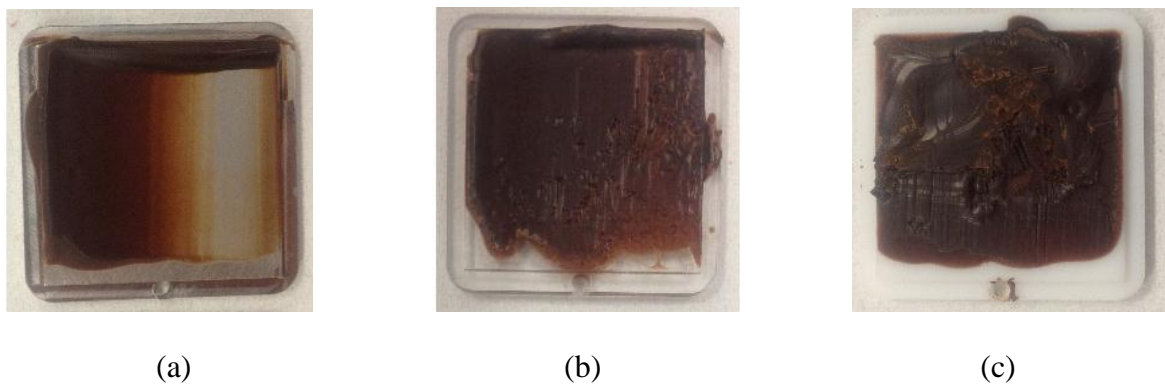


Figure 5.21: Chocolate residue on (a) stainless steel, (b) polycarbonate and (c) PTFE surfaces.

### 5.3.5 Effect of tempering and cooling on the pulling energy and removal

A comparison was made between the strength of energy required to remove tempered and untempered chocolate layers from polycarbonate surfaces. At the same time the effect of slow and rapid cooling on the amount of energy required to remove the chocolate layer

was investigated. 0.5g liquid chocolate (tempered or untempered) was spread evenly on polycarbonate surfaces and cooled on the Peltier stage either slowly (1°C/min) or rapidly (10°C/min). Then, it was soaked in 0.1% NaOH solution at 30°C for 10 minutes before measuring the energy needed to scrape the chocolate layer from the polycarbonate surface.

From Figure 5.22, the influence of cooling rate can be seen for tempered chocolate. Rapid cooling resulted in a higher pulling energy of 400J/m<sup>2</sup> compared to 250J/m<sup>2</sup> for slow cooling. On the contrary, the cooling rate did not affect the pulling energy for untempered chocolate. Tempering will produce a large number of small crystals to induce nucleation of stable polymorphs. Further slow cooling will provide enough time for the chocolate to be arranged in three-dimensional crystal network structure. Rapid cooling will produce higher levels of solid fat content as reported by Campos *et. al* (2002). These two factors; tempering ((Lonchampt and Hartel (2006)) and cooling rate ((Stapley *et al.* (1999))) play an important role in determining the crystal structure. It is because more liquid fat is adsorbed to the crystal surfaces, leading to less liquid fat present in the continuous phase (Boudreau and Saint Amant, 1985). The difference in the crystal structure can be supported by the DSC melting curve for both tempered and untempered chocolate cooled at slow and rapid cooling rates obtained in Chapter 4.

When the solid chocolate was soaked in NaOH solution at 30°C, the crystals were melted and then dissolved in the solution. Melting involves a breakdown in the rigid, solid structure of fat molecules to an amorphous, less ordered system. The attractions between the fat molecules are weakened, but the bonds within the fat molecules are not broken. Stronger intermolecular attraction between crystals in tempered chocolate cooled slowly resulting in only 25% of the chocolate being scraped from the polycarbonate surface. For

that reason, low pulling energy was observed compared to the untempered chocolate with the removal percentage of almost 90%. On the other hand, rapid cooling shows reverse behaviour with the pulling energy for tempered chocolate greater than for the untempered chocolate. It is still unclear about this reverse behaviour. From Figure 5.23, the removal percentage of untempered chocolate is higher than that of tempered chocolate. It can be suggested that untempered chocolate is softer and has less crystal structure. So, more chocolate can be removed.

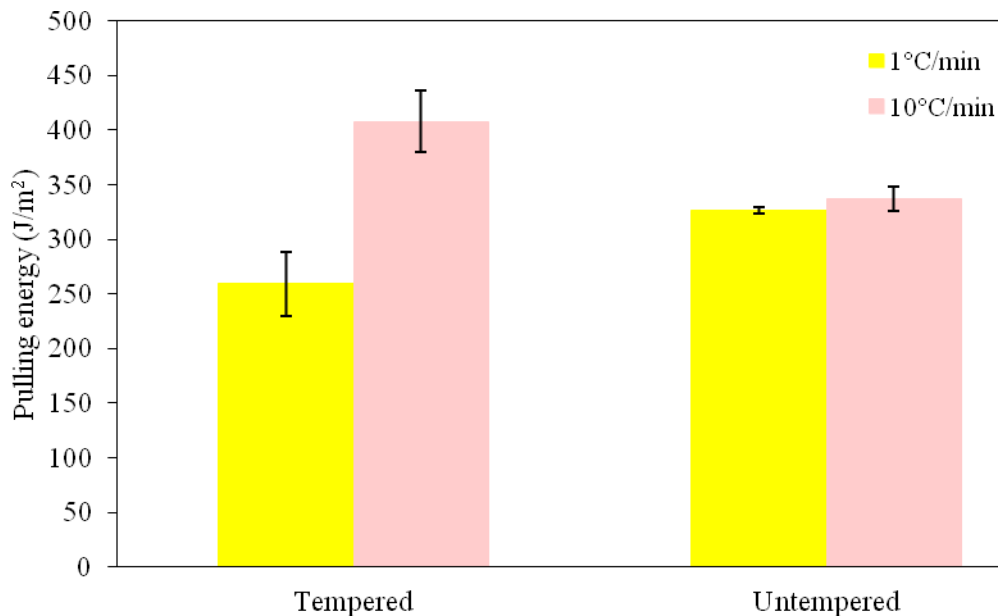


Figure 5.22: Pulling energy for tempered and untempered chocolate (the sample was submerged in a 0.1% NaOH solution at 30°C for 10 minutes prior to the measurement). Data are average of three repeats with the pulling speed of 1.1mm/s.

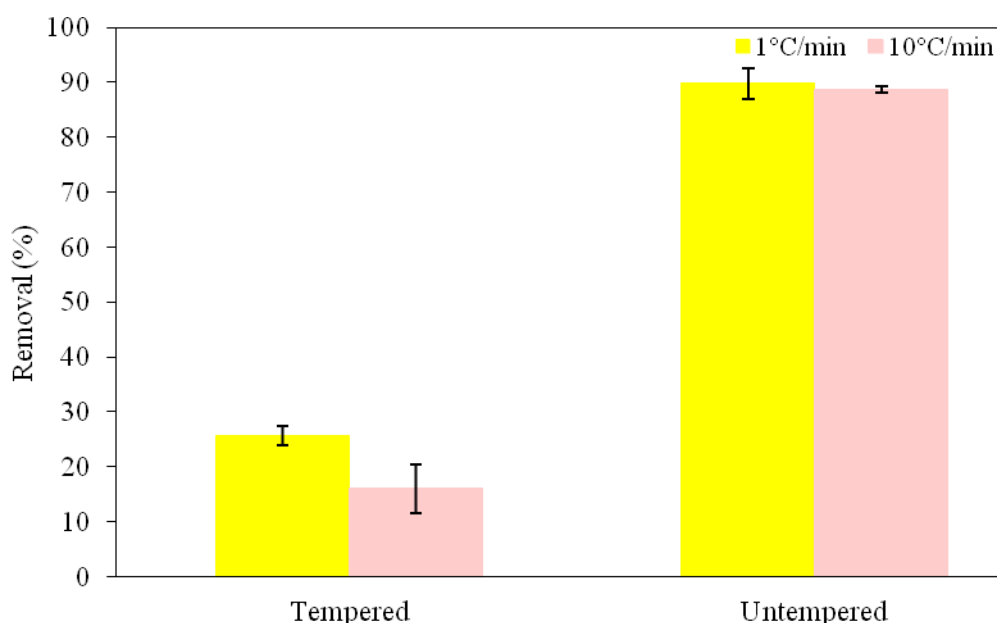


Figure 5.23: Removal percentage for tempered and untempered chocolate (the sample was submerged in a 0.1% NaOH solution at 30°C for 10 minutes prior to the measurement).

The amount of energy required to remove a gram of tempered and untempered chocolate for both cooling rates is shown in Figure 5.24. It is clearly seen that more energy is needed to scrape 1 gram of tempered chocolate compared to the untempered chocolate regardless of the cooling rate applied. The cooling rate seems to affect the amount of energy for tempered chocolate but not for the untempered chocolate as a precise control of cooling rate is needed to create temper. The result obtained suggests that the combination effect of tempering and cooling rate will determine the ease of removal of the chocolate layer from the polycarbonate surface. Even though the untempered chocolate needs less energy to remove, the quality of the product is very poor with the tendency to having a blooming problem caused by the separation of cocoa butter towards the surface (Lonchamp and Hartel, 2004).

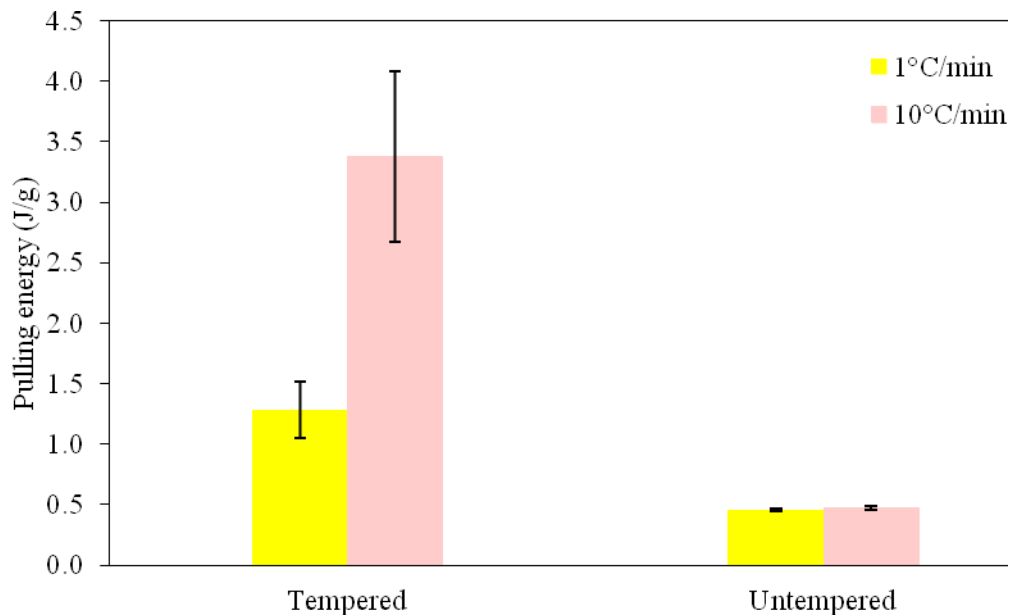


Figure 5.24: The amount of energy for removal of a gram of tempered and untempered chocolate.

In addition to the use of the Peltier stage to cool the liquid chocolate on the polycarbonate surface, an attempt has been made to use another cooling method. The liquid tempered chocolate was poured on the polycarbonate surface and cooled in the refrigerator and at room temperature for one hour respectively. A comparison of the pulling energy was made for four samples; liquid tempered chocolate cooled at (i) 1°C/min and (ii) 10°C/min on the Peltier stage from 32°C to 10°C, (iii) cooled in refrigerator at 4°C for one hour and (iv) cooled at room temperature at 20°C for one hour. From Figure 5.25, it can be observed that the pulling energy for the chocolate solidified in the refrigerator was the greatest. This was first thought to be due to the effect of cooling direction which determines the contraction and subsequently the ease of detachment of the chocolate from the polycarbonate surface. Pinschower (2003) found that the source of cooling will affect the direction of heat flow and the surface movement. Cooling from the bottom of the mould will result in a difficult detachment as the solidification occurs from the mould



surface towards the centre. However, in current study, the Peltier stage which applied cooling from the bottom of the polycarbonate surface shows lower pulling energy compared to the refrigerator which applied cooling from both top and bottom. The amount of energy per unit gram shown in Figure 5.26 also displays the same trend. The reason of this pattern is possibly due to the combination of both heat transfer mechanism and the cooling temperature as the temperature in the refrigerator was lower than the cooling temperature used to solidify the chocolate on the Peltier stage .

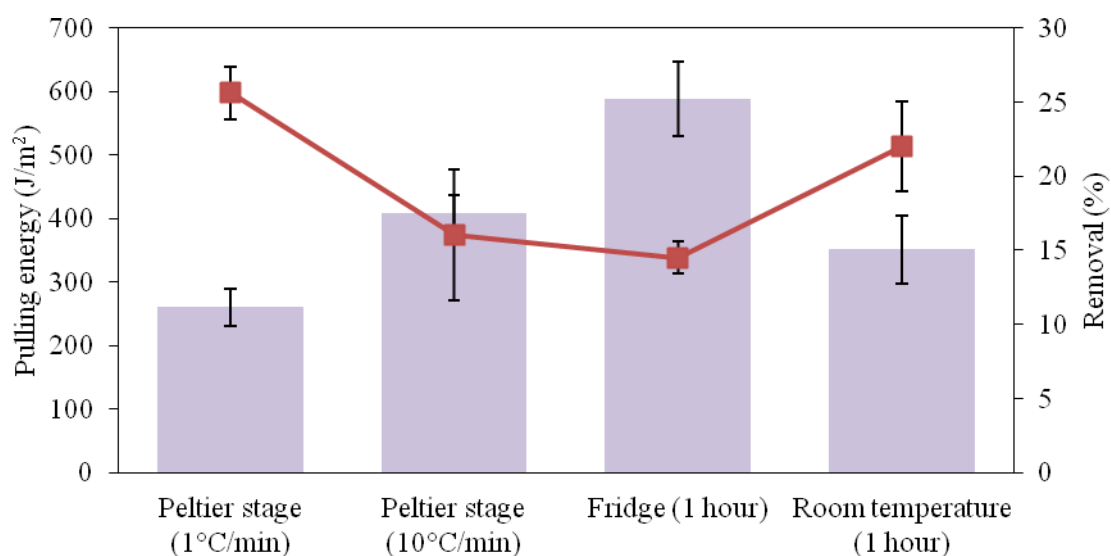


Figure 5.25: Effect of cooling on the pulling energy and removal percentage of tempered chocolate (the sample was submerged in a 0.1% NaOH solution at 30°C for 10minutes prior to the measurement). Data are average of three repeats with the pulling speed of 1.1mm/s.

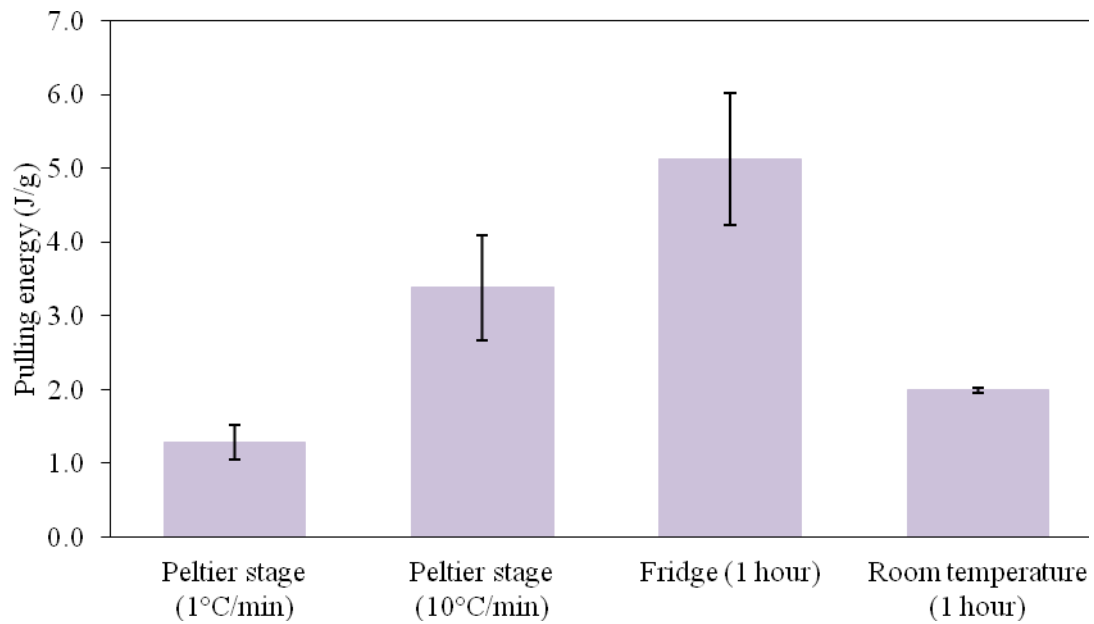


Figure 5.26: The amount of energy per unit gram for different cooling condition.

#### 5.4 Separation force measurement using texture analyser

In this section, the influence of the tempering process, contact time of probe-chocolate and the distance between the probe and the chocolate surface to the separation force were determined. The pull-off method was applied using a texture analyser and all the measurements were made in air at room temperature. Force measurement using this method was carried out when the cylindrical probe was pulled up from a chocolate surface. Only dark chocolate was involved in all experiments for this section. The experimental work was conducted as described in section 3.6.

#### **5.4.1 Effect of the distance between the probe and the chocolate surface on the separation force**

The variation in the distance between the bottom surface of the probe,  $X$  and the chocolate surface was studied with three different values (0, 2 and 5mm). From the results shown in figure 5.27, the change in  $X$  value did not lead to any specific trend neither in the amount of force per unit area nor the amount of chocolate residue on the surface. It was nonetheless found that, the highest value of force per unit area and the least residue on the polycarbonate surface were obtained for  $X=0\text{mm}$ . A possible explanation for this behaviour is that the bottom surface of the probe did not penetrate the liquid chocolate, so during the separation only the adhesion between the two surfaces need to be overcome. Keijbet *et.al* (2010) in their work found out that after 60 minutes contact, the liquid chocolate had turned to a strong crystal network and cohesive enough to withstand the separation force of demoulding when the chocolate-mould interface was created at  $30^{\circ}\text{C}$  and cooled to  $15^{\circ}\text{C}$ . A small amount of residue on the probe surface was probably due to no adjustment in cooling rate was made and the liquid chocolate was left to solidify at room temperature without specific cooling condition.

On the other hand, when the probe penetrated the liquid chocolate and solidification took place, the separation did not only occur between the solid chocolate and the bottom surface of the probe but also the probe sides. The force measured includes the amount of force required for the separation of two surfaces and the cohesive forces between the fat molecules.

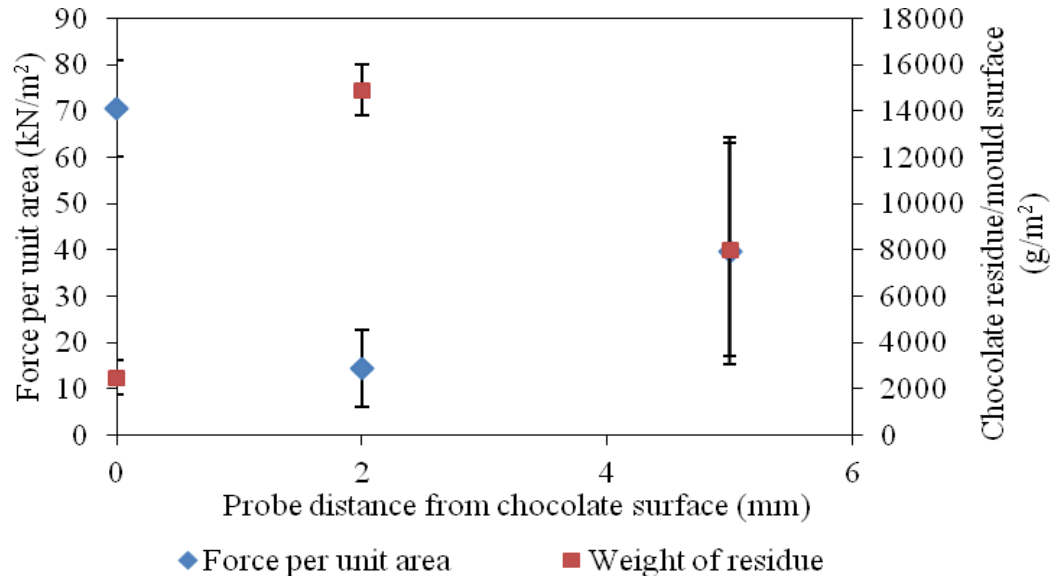


Figure 5.27: Force per unit area for separation of solid tempered chocolate from polycarbonate surface with respect to distance between the probe and the chocolate surface at room temperature. Data are the average of three repeats.

#### 5.4.2 Effect of the chocolate-probe contact time on the separation force

The term ‘contact time’ refers to the time from the creation of the chocolate-probe interface until the separation being carried out. A range of contact time between 10 to 180 minutes was studied. Figure 5.28 shows the force per unit area resulted from the separation of the probe from the solid chocolate together with the amount of residue stuck on the probe surface after the separation took place. A constant value of  $X=0\text{mm}$  was used throughout the experiments in this section.

Figure 5.26 indicates that at  $t_{10}$ , the separation force is zero and after 30 minutes the separation force remained unchanged. A bridge formed when the probe was pulled off from the chocolate surface due to the liquid character at that time led to a low force needed

for the separation of the two surfaces and small amount of residue on the surface after the separation. When the time increased, the liquid chocolate transformed into solid as the latent heat removed allowing the crystallisation process took place. At 60 minutes, the force started to increase almost linearly until the contact time reached 180 minutes as the solidification continued. The force increment up to  $110\text{kN/m}^2$  with time can be attributed by the hardness of the chocolates. The amount of solid fat present increased at each contact time causing an increase in hardness which subsequently led to an increase in adhesion between the surfaces. This is in agreement with Keijbet *et. al* (2010) who measured the surface adhesion and hardness of chocolate for different contact time. The same trend was obtained for both surface adhesion and hardness. Liang and Hartel (2004) agreed that the mechanical properties such as hardness are affected by the packing arrangement of the crystals. Form V crystals will be crystallised in a triple chain which can be packed closer resulting in a harder structure (Afoakwa *et. al*, 2007). The effect of contact time for a similar experimental setup has also been studied by Walewij *et.al* (2008) who measured the adhesion between the alginate gel surfaces immersed in a calcium chloride solution and found out that an increase in contact time resulted in an increase in adhesion between the two surfaces. In this study, the contact time has not been further increased as a matter of time restriction and applicability.

The amount of chocolate residue on the polycarbonate increased initially, but after reaching a maximum value of about  $3000\text{g/m}^2$  at 60 minutes it reduced gradually and started to level off at  $1000\text{g/m}^2$  after 120 minutes contact. The reduction was probably due to the fact that the cohesive strength of the solidified chocolate increased with the presence of more extensive crystal network. However, the fact that there was no clean surface for all the experiments indicates that the cohesive-adhesive failure occurred for all contact time

studied resulting in a break of the chocolate structure leaving an amount of chocolate stuck on the probe surface. This behaviour was expected as improper cooling was used to control the crystallisation process.

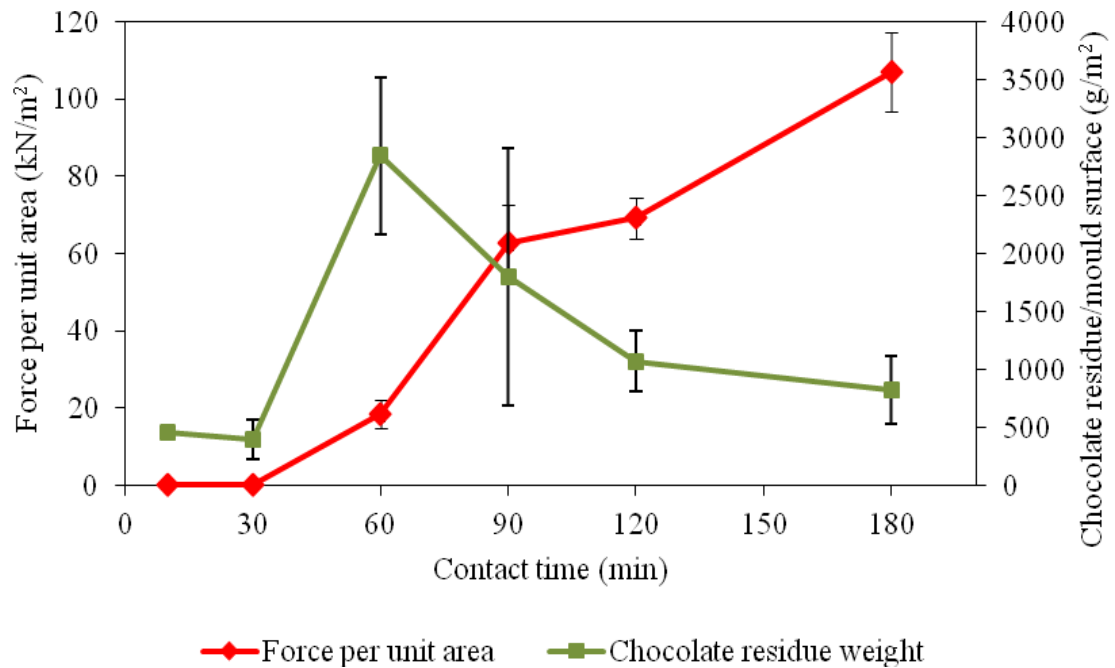


Figure 5.28: Force per unit area for separation of solid tempered chocolate from polycarbonate surface with respect to contact time at room temperature. Data are the average of three repeats.

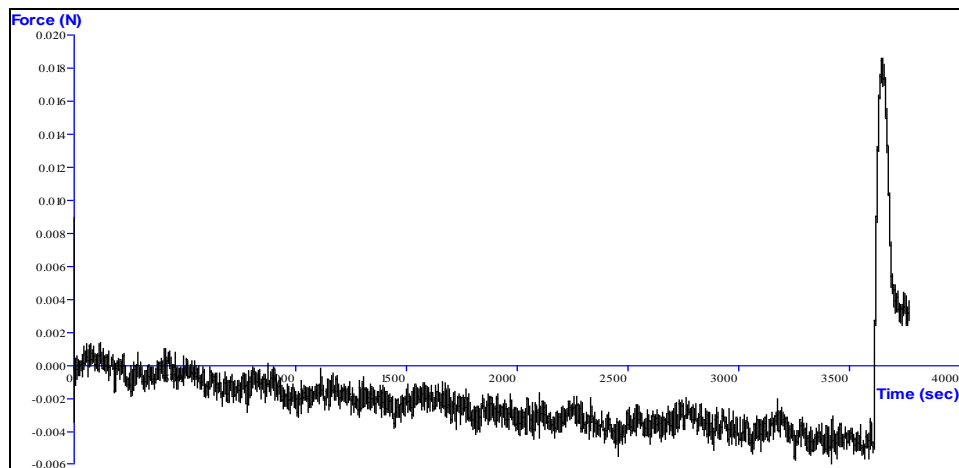
#### 5.4.3 Effect of the tempering and surface material on the separation force

The influence of tempering process and surface material variation on the separation force were studied. Tempered and untempered chocolates were brought into contact with three different materials (stainless steel, polycarbonate and PTFE) for 60 minutes at room temperature before measuring the separation force.

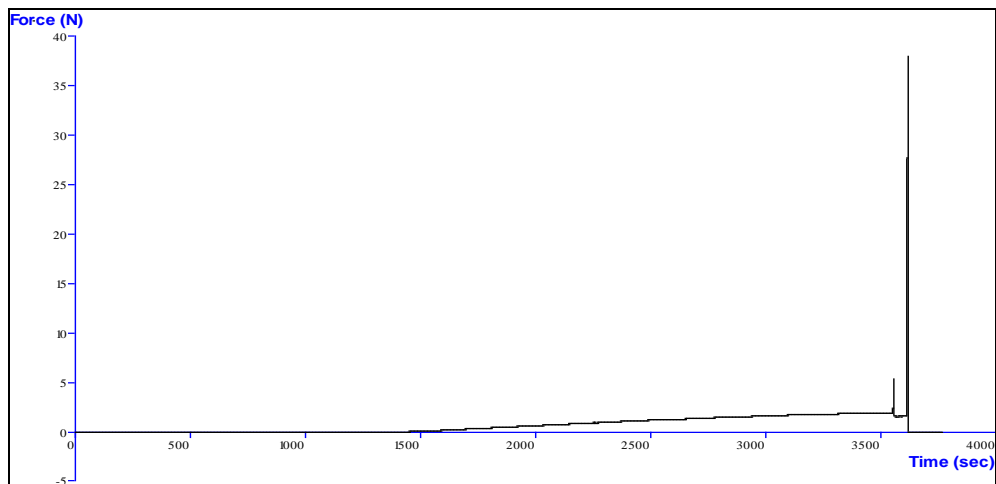
Figure 5.29 (a) and (b) show the typical plot of force versus time obtained when measuring the separation force of the probe surface from the untempered and tempered chocolate respectively. The maximum peak value was taken as the amount of force needed to separate the two surfaces. The presence of noise in Figure 5.29 (a) is due to the liquid characteristic of the untempered chocolate. A possible explanation for a decline in the amount of force before the probe was pulled off is that an expansion occurred when the untempered chocolate solidified. On the other hand, the force for the separation of the probe surface and tempered chocolate started to increase before the pulling step because of the contraction of tempered chocolate when it solidified and then pulled against the probe surface. Figure 5.30 shows the expansion and contraction phenomena of the untempered and tempered chocolate respectively.

From the two plots in Figure 5.29, it is noticed that the peak value for the tempered chocolate is much higher than for the untempered chocolate. This can also be related to the hardness of chocolate which influenced by several factors including composition, manufacturing conditions and tempering and consequently fat crystal polymorphism (Afoakwa *et al.*, 2008 and Beckett, 2000). Afoakwa *et al.* (2008) compared hardness for the optimally-tempered, over-tempered and under-tempered dark chocolate and found that the under-tempered sample was the hardest followed by the over-tempered and optimally-tempered samples. The current study however suggests that the tempered chocolate is harder than the untempered chocolate. It is strongly believed that the cooling process needs to be controlled especially the cooling rate and temperature to ensure that the crystals produced will allow a good separation from the mould material. From the DSC curve shown in section 4.2.2, the polymorph existing on the surface of square coupon after being left at room temperature for 60 minutes had a melting temperature of about 40°C

indicating that type VI crystals were produced. According to Keijbets *et al.* (2010), an increase in cooling temperature had reduced the surface adhesion with clean surface obtained for all cooling temperatures. The chocolate hardness was also found to decrease with the cooling temperature increase as the packing arrangement of the crystals is denser when lower cooling temperature applied.



(a)



(b)

Figure 5.29: Typical plot of force versus time obtained from the output of the texture analyser for separation of probe surface from the (a) untempered and (b) tempered chocolate.





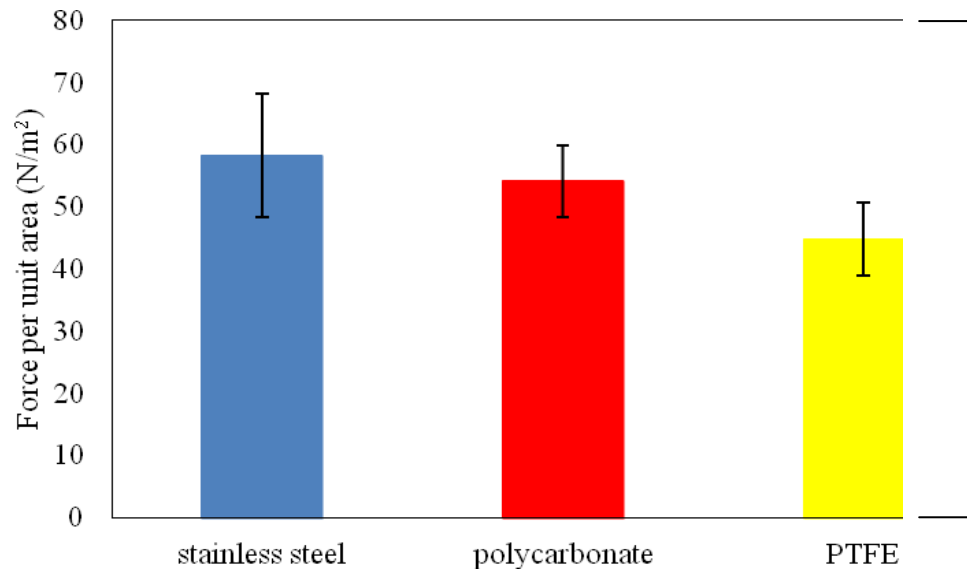
Figure 5.30: Schematic diagram showing the (a) expansion of the untempered chocolate and (b) contraction of the tempered chocolate.

The effect of surface material is displayed in Figure 5.31 with the amount of force measured when the probe was pulled upwards from the untempered and tempered chocolate surfaces are shown in Figure 5.31 (a) and (b) respectively. The values of the separation force can be ranked as follows: PTFE < polycarbonate < stainless steel. The trend is similar for both samples and exactly the same order as for the water contact angle of the probe materials discussed in section 5.2. Interestingly, even though the PTFE surface is rougher than the stainless steel as has been reported in section 5.2, but the separation force is higher compared to the stainless steel. It is expected that this behaviour is caused by the influence of surface hydrophilicity is more significant rather than the surface roughness when studying the surface interaction in vertical direction. The hydrophilicity can be related to the surface energy which is defined as the work required to increase the surface area of a substance by unit area. Hydrophilic surfaces such as glass have high surface energies, whereas hydrophobic surfaces such as PTFE have low surface energies. It is because a material with high surface energy will have a higher bonding potential and more interactions with water can be occurred. (Adhikari *et al.*, 2007) Adhikari *et al.* (2001) mentioned that the lower the contact angle of a liquid on a solid surface, the force needed to separate these surfaces will be greater due to the stronger attraction. Recently, Keijbets *et al.* (2009) reported that a high surface energy material is not suitable

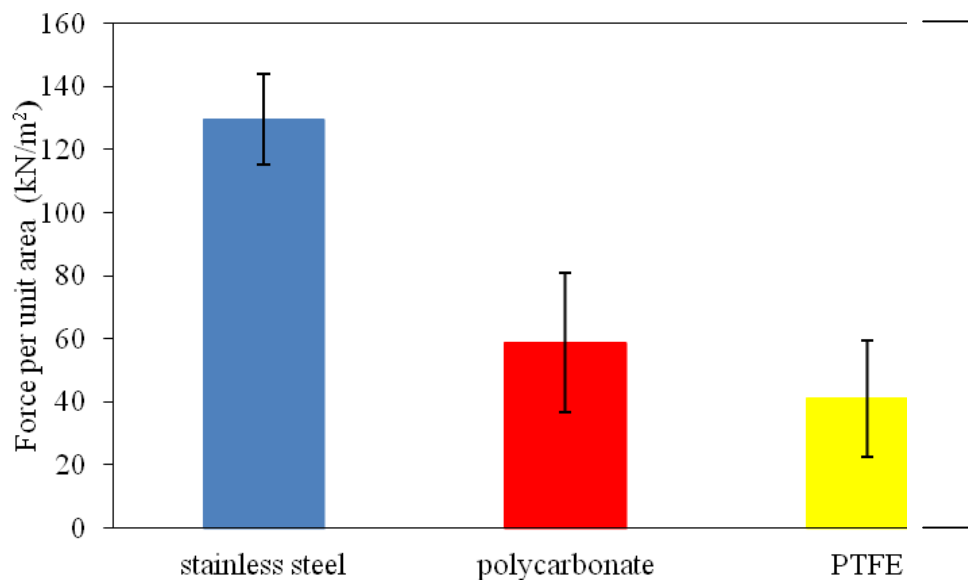
to be used as a mould material as it can cause the demoulding process to be more difficult due to the strong interactions between crystals in the interface region. In the study, the relationship between the surface energy and surface adhesion has been investigated and discovered that both are strongly correlated. A conclusion was made that the maximum surface energy of the material which will provide a good separation is  $30 \text{ mN m}^{-1}$ .

The results suggest that the variation in the amount of force for the separation is determined by the surface energy of the material which essentially affects the crystal polymorphisms. Different surface materials will result in different polymorph leading to the variation in the crystal types exist at the surface region. For that reason, the magnitude of the separation force will be different. The effect of substrate surface energy has been studied by Cho *et al.* (2003) who found that it influenced the crystallisation behaviour of isotactic propylene. Transcrystallites was formed on the substrate with high surface energy, whereas the substrate with low surface energy was dominated by spherulites with some transcrystallites were exist. The surface adhesion was found to be higher for the substrate with high surface energy and further observation was carried out to check the fracture for both cases. The fracture of transcrystallites on high surface energy substrate happened at the interface, but the fracture at the boundary between the transcrystallites and the spherulites was observed for low surface energy substrate.

The same behaviour occurred as no clean surface was observed for all experiments due to the same reason as described previously. Based on the above results and discussions, one may conclude that the pre-crystallisation step, cooling conditions and the surface characteristics affect the separation of the chocolate and the probe surfaces.



(a)



(b)

Figure 5.31: Force per unit area for the separation of solidified (a) untempered and (b) tempered chocolate from different surface materials at room temperature. Data are the average of three repeats.

## 5.5 Conclusions

In micromanipulation measurement, the removal of solid chocolate layer from a surface required a soaking in a chemical solution. In this case, 0.1% NaOH solution was used to aid the removal. The longer the soaking time and the higher the temperature, the lower the pulling energy required to remove chocolate during scraping process. Pulling energy was found to be independent to the probe speed in the range of 0.59 to 2.22mm/s. With respect to surface material, PTFE gave the highest pulling energy followed by polycarbonate and stainless steel. For tempered chocolate, the pulling energy was influenced by the cooling rate, but not for the untempered chocolate. However, in all cases there was no clean surface observed. A thin chocolate layer left indicating that there was still an interaction between the chocolate and the surface material even though it was soaked in a chemical solution. Force measurement has also been conducted using a texture analyser. Instead of scraping, a pull-off method was employed to separate the probe from the chocolate surface. The separation force was found to be dependent on the contact time, tempering and surface material.

## **6 REMOVAL BEHAVIOUR OF SOLID CHOCOLATE LAYER USING FLOW CELL CLEANING RIG**

### **6.1 Introduction**

This chapter reports the time to clean and the removal behaviour of a solid chocolate layer with respect to a number of parameters including the flow temperature, velocity, chemical requirement, surface material, tempering and cooling condition. From the results reported in Chapter 5, the influence of the factors mentioned above on the pulling energy was determined. In this chapter, the cleaning behaviour of solid chocolate layer from hard surfaces will be observed. Essentially, the aims of the experiments conducted in this chapter were to (i) determine the clean ability of water and chemical circulations, (ii) investigate the influence of flow temperature and velocity on the cleaning time and removal behaviour and (iii) investigate the influence of chocolate solidification process on the cleaning time and removal behaviour. All the experiments in this chapter were performed on the bench scale flow cell cleaning rig as described in section 3.6. Image analysis in conjunction with visual observation was used to determine the cleaning time. Selected images and the area reduction profiles are also presented in this chapter to describe the removal mechanism of the solid chocolate layer. In addition, a comparison was made between the results obtained in this chapter and the micromanipulation measurements reported in Chapter 5.

A preliminary study involving water circulation revealed that the chocolate could not be removed from the polycarbonate surface by water alone even at  $0.5\text{ms}^{-1}$  (the highest velocity for the system) and  $70^{\circ}\text{C}$ . Thus, removal with chemical circulation (0.1% NaOH

solution) was also studied. The experimental conditions investigated for the chemical circulation study are listed in table 6.1.

Table 6.1: The experimental conditions investigated for the removal of solid chocolate layer using the circulation of 0.1% NaOH solution. Each condition was repeated at least twice.

Experiment	Sample	Surface material	Cooling rate (°C/min)	Cooling method	Flow temperature (°C)	Flow velocity (ms <sup>-1</sup> )
1	Tempered	Polycarbonate	1	Peltier stage	25	0.5
	Tempered	Polycarbonate	1	Peltier stage	40	0.5
	Tempered	Polycarbonate	1	Peltier stage	55	0.5
	Tempered	Polycarbonate	1	Peltier stage	70	0.5
2	Tempered	Polycarbonate	1	Peltier stage	70	0.5
	Tempered	Polycarbonate	1	Peltier stage	70	0.37
	Tempered	Polycarbonate	1	Peltier stage	70	0.25
3	Tempered	Polycarbonate	1	Peltier stage	70	0.5
	Tempered	Stainless steel	1	Peltier stage	70	0.5
	Tempered	PTFE	1	Peltier stage	70	0.5
4	Tempered	Polycarbonate	1	Peltier stage	70	0.5
	Tempered	Polycarbonate	10	Peltier stage	70	0.5
	Tempered	Polycarbonate	-	Room (60 minutes)	70	0.5
	Tempered	Polycarbonate	-	Refrigerator (60 minutes)	70	0.5
5	Untempered	Polycarbonate	1	Peltier stage	70	0.5
	Untempered	Polycarbonate	10	Peltier stage	70	0.5
	Untempered	Polycarbonate	-	Room temperature (60 minutes)	70	0.5
	Untempered	Polycarbonate	-	Refrigerator (60 minutes)	70	0.5

## 6.2 Image analysis

Image analysis allows the removal behaviour throughout each experiment to be determined.. As described in section 3.7.3, the area calculated during image analysis was used to identify the cleaning point by which only 1% of the area was still covered with some chocolate. This high area reduction percentage was chosen to define the ‘clean’ state because it is crucial in chocolate manufacturing to ensure a high product quality and hygiene. There is a possibility that chocolate residues remain on the moulds after demoulding which not only affects the appearance of the product, but also can cause the development of microorganisms and subsequently contaminate the upcoming products when brought back in the production cycle.

Figure 6.1 displays an example of the (a) original cropped image and (b) the same image which has undergone the threshold setting in the Image J software giving the calculated area of  $145.56 \text{ mm}^2$  (% reduction from the initial area) . Selected images were analysed to produce the area reduction profile plotted as the area covered versus circulation time. An example of the area reduction profile is given in Figure 6.2. Initially, the area covered remained steady even though the circulation has started and the value was in the range  $388\text{--}405 \text{ mm}^2$ . This variation from the expected initial area of  $400 \text{ mm}^2$  will be discussed in section 6.2.2. Immediate removal after the circulation started only can be seen in a few experiments.

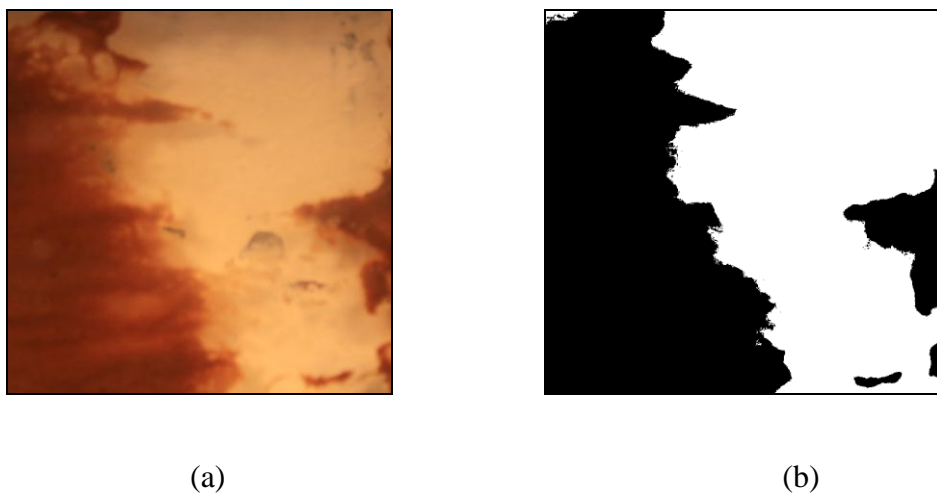


Figure 6.1: Example of the (a) original cropped image and (b) the same image which has undergone the threshold setting in Image J software.

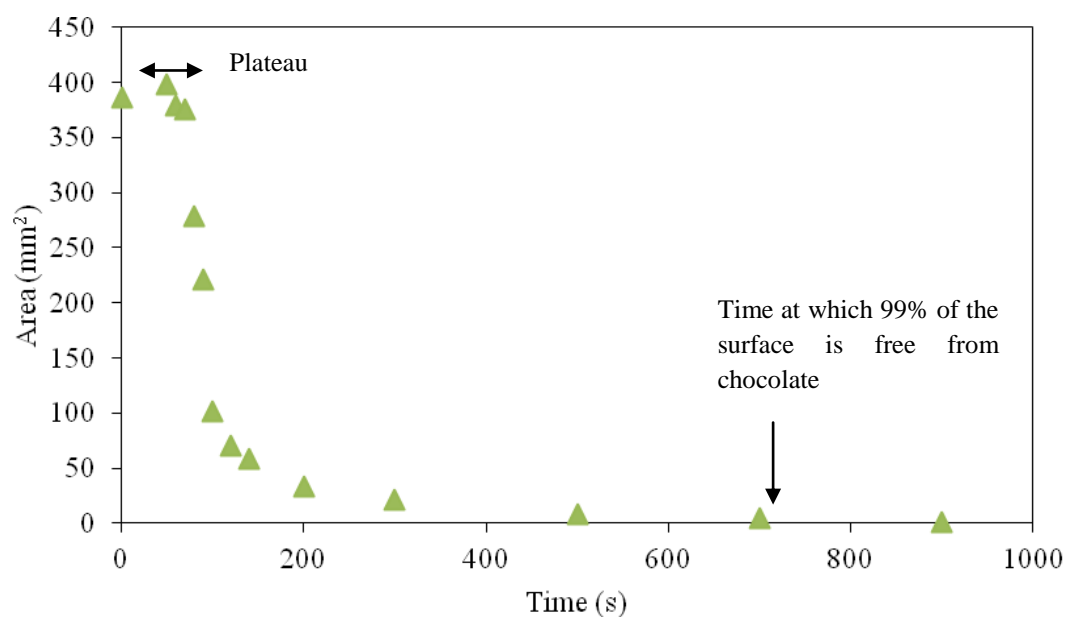


Figure 6.2: Example of the area reduction profile for the circulation of 0.1% NaOH solution at  $0.5\text{ms}^{-1}$  and  $55^{\circ}\text{C}$ .



### 6.2.1 Determination of cleaning time from image analysis

The time to clean was determined when the area covered by the chocolate was less than 4 mm<sup>2</sup> (99% reduction). The time at which the calculated area reached a value less than 4mm<sup>2</sup> was taken as the cleaning time for all the experiments characterised as ‘clean’. For the experiments which were characterised as ‘not clean’, the decision was made when the area covered remained steady for 10 minutes at a value above 4 mm<sup>2</sup>. Figure 6.3 illustrates examples of ‘clean’ and ‘not clean’ images.

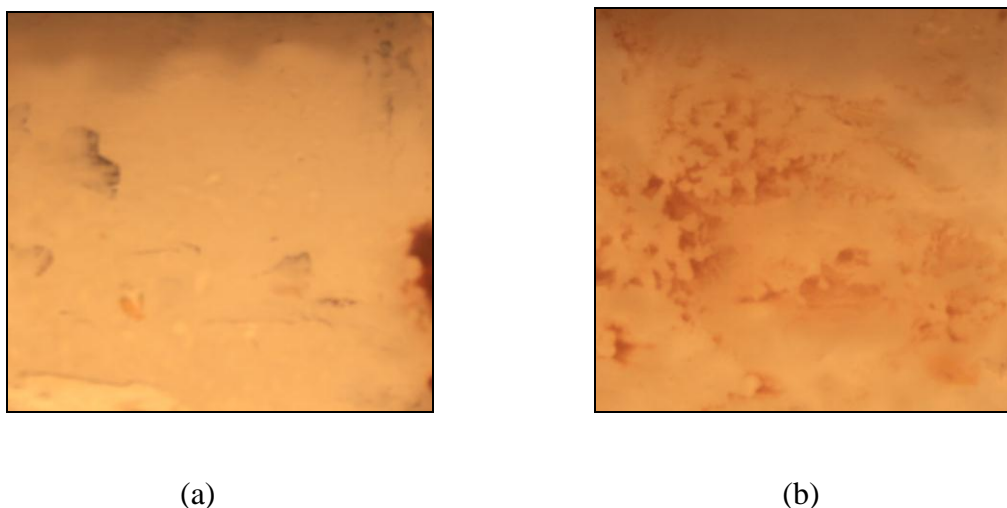


Figure 6.3: Example of the images termed as (a) ‘clean’ and (b) ‘not clean’.

### 6.2.2 Disadvantages of image analysis

Some disadvantages were noticed when performing the image analysis. Although visually some removal was seen to occur at the beginning of the circulation, for example when erosion took place, the area calculated was remained unchanged as there was no area reduction. The time at which the removal started could not be accurately determined. In addition, the experiments involving the chemical circulation underwent a dissolution

process which could not be seen from the images captured. In some cases, the area calculated fluctuates caused by air bubbles passing through the test section which affects the colour intensity and leads to the variation in the values of the area covered.

The light source was also found to influence the image analysis. This happened when there was a thin film left on the PTFE surface for the experiment carried out at 25°C as shown in Figure 6.4. The calculated area reached below 4 mm<sup>2</sup> which can be characterised as 'clean'. However, it can be seen by eye that the surface was not clean. In the presence of the thin film under the light source used in the experiment, the image analysis which measures the area covered by colour measurement could not distinguish between the polycarbonate surface and the chocolate. Consequently, the area measured for that experiment is not reliable and the area reduction profile will not be discussed.

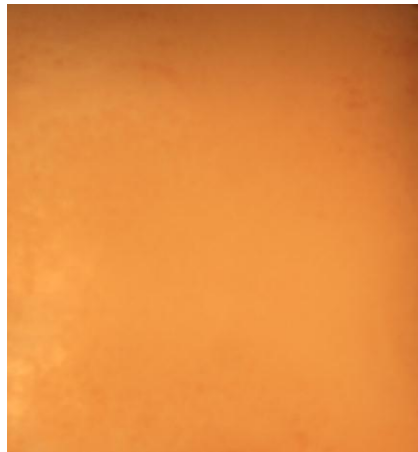


Figure 6.4: PTFE surface covered with a thin film resulted from the water circulation at 25°C.

### **6.3 Determination of clean state**

After considering the problems occurred when performing the image analysis, it was decided to use both visual observation and image analysis to determine the cleaning state. For example, in the case of a thin film present on the PTFE surface (Figure 6.4), it was characterised as ‘not clean’ even though the calculated area covered reached below 4 mm<sup>2</sup>. In all experiments, visual observation was used to confirm that the surface had reached the ‘clean’ state after the image analysis was carried out. The term ‘cleaning time’ will refer to the time for 99% of the surface to be free from chocolate with the confirmation by eye.

### **6.4 Repeatability of the experimental results**

During the preparation of the solid chocolate layer on the surface material, the same procedure was used as described in section 3.3.1 and 3.3.3. Most of the cleaning conditions used are as described in section 3.6. The same amount of liquid chocolate was placed on the coupon as in the experiments in previous chapters. Two possible reasons were found to cause any variation in the experimental results obtained:

- (i) Non-uniform thickness of the chocolate layer, though the liquid chocolate was spread as even as possible to produce a layer with a uniform thickness.
- (ii) Any delay in fitting the coupon to the test section might result in the chocolate melting as the surrounding temperature was quite high during circulation at 70°C.

All experiments in Table 6.1 were repeated at least twice. However, experiments involving water circulation were not repeated because the surface was not clean in the first experiment after circulation was carried out for (i) 3600 seconds for the experiments at

0.25ms<sup>-1</sup> and (ii) 1200 seconds for the experiments conducted at 0.5ms<sup>-1</sup>. This decision was made after considering the practicality. One chemical circulation experiment conducted at 0.5ms<sup>-1</sup> and 25°C was repeated even though the first experiment were characterised as not clean after 2500 seconds because the thin film was present on the polycarbonate surface.

Figure 6.5 compares the area reduction profiles for two experiments conducted at 0.5ms<sup>-1</sup> and 70°C with chemical circulation. It shows that the removal is reproducible with the cleaning time determined for Exp 1 and Exp 2 were 250 seconds and 390 seconds respectively giving 22% variation from the mean value. From the figure, it can be seen that the area reductions were similar at the beginning and slight variation can be seen after 200 seconds due to the slow removal occurred towards the end of the circulation caused by the presence of glue at the coupon edge.

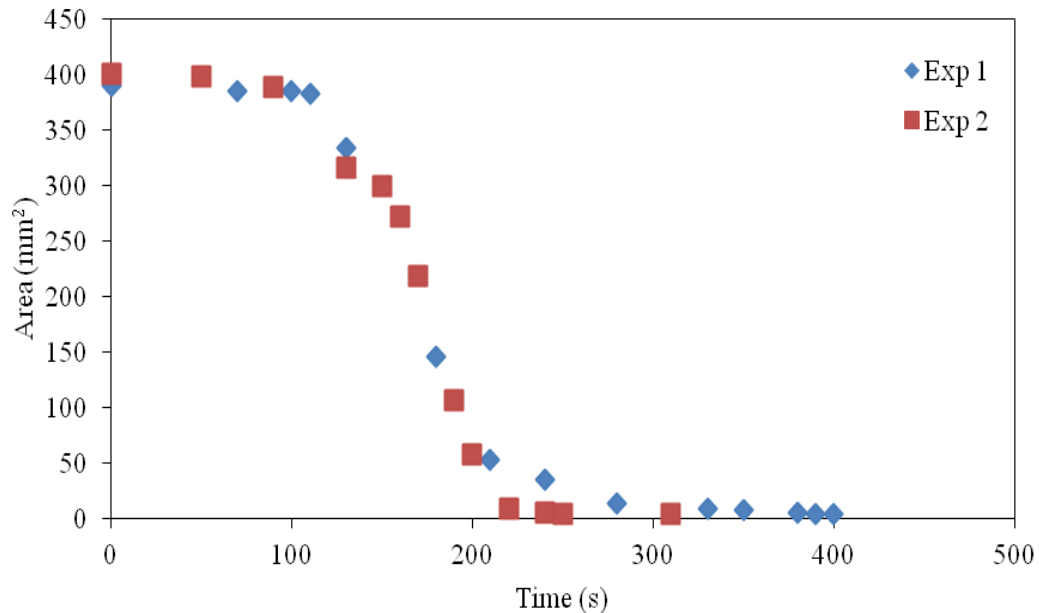


Figure 6.5: Comparison of the area reduction profiles between two experiments carried out at 0.5ms<sup>-1</sup> and 70°C demonstrating the repeatability.

## **6.5 Water circulation**

A preliminary study was carried out using water only to identify the removability of the solid chocolate layer from a polycarbonate surface. Solid tempered chocolate cooled at 1°C/min on the Peltier stage was used for all experiments in this section.

### **6.5.1 Effect of water temperature and velocity**

This study started with the application of water circulation at low velocity of  $0.25\text{ms}^{-1}$  with the water temperature of 50°C. The selected images captured by the camera are shown in Figure 6.6 while the calculated area covered with chocolate is displayed in Figure 6.9. Water circulation was stopped when the area covered by the chocolate remained constant for 600 seconds determined by eye.

From both figures, it can be seen that the removal started with melting of the chocolate for the first 30 seconds resulting in the colour of the chocolate layer becoming lighter. It was followed by some erosion, but all the coupon area was still covered by chocolate even though some chocolate had been removed. For that reason the calculated area remained unchanged at the beginning of the experiment. Small changes noticed were due to the presence of bubbles discussed in section 6.2.2. Melting and erosion continue and after 1650 seconds almost half of the surface was still covered with chocolate. There was no removal observed for the next 800 seconds before further area reduction occurred. Water circulation was stopped when there was no area reduction for 600 seconds determined by eye (after 4520 seconds water circulation). Approximately  $90\text{mm}^2$  of the polycarbonate surface still covered with chocolate and it was specified as ‘unclean’.

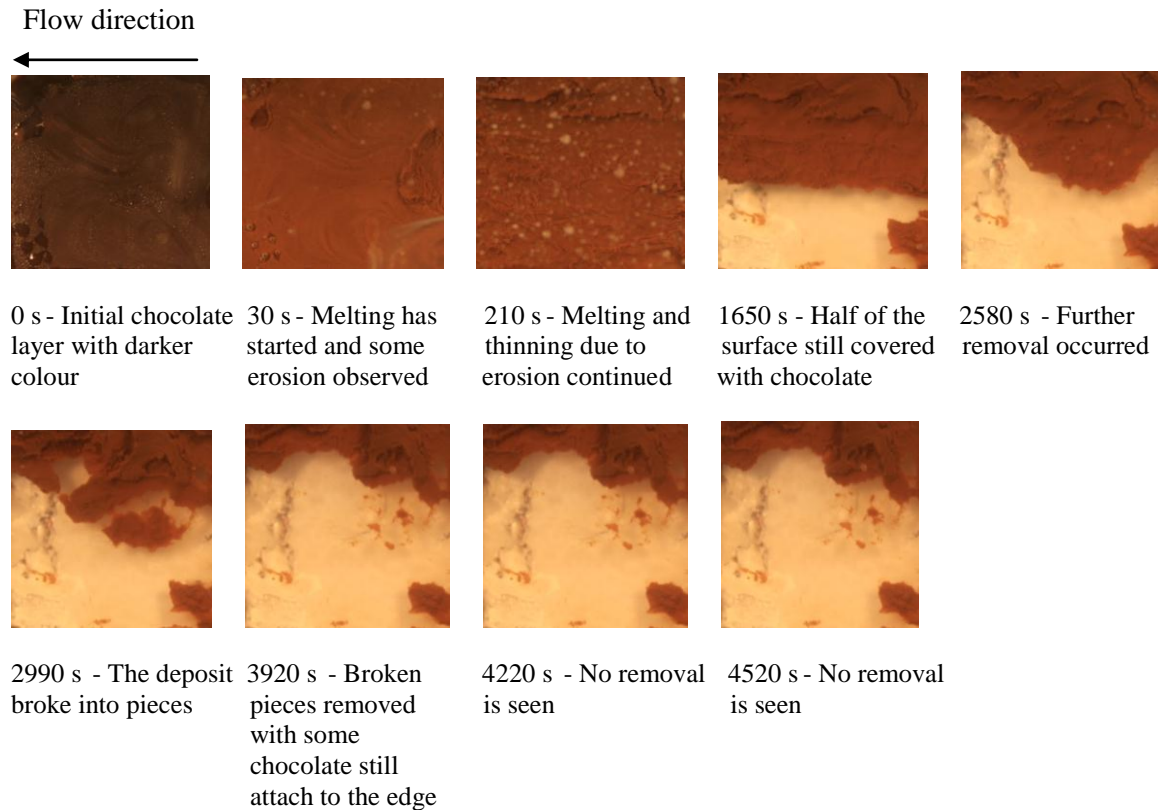


Figure 6.6: Images taken during water circulation at  $0.25\text{ms}^{-1}$  at  $50^{\circ}\text{C}$ .

In the next experiment water temperature was increased to  $70^{\circ}\text{C}$  at the same velocity. The selected images and the area covered throughout the experiment are shown in Figures 6.7 and 6.9 respectively. Different removal behaviour was noticed in that holes developed instead of erosion after the melting step as can be seen at 1590 seconds. The weak parts were then broken and the removal of the small pieces was observed. Slow removal noted from 1830 seconds to 1920 seconds which gave islands of material at 3180 seconds, that were then reduced in size leaving small patches of chocolate on the surface. There was no area reduction from 4280 seconds to 4880 seconds with the area covered was approximately  $11\text{ mm}^2$  which was much lower than the previous experiment. However it was still specified as ‘unclean’. Increasing the temperature did not speed up the removal, but reduce the area covered.

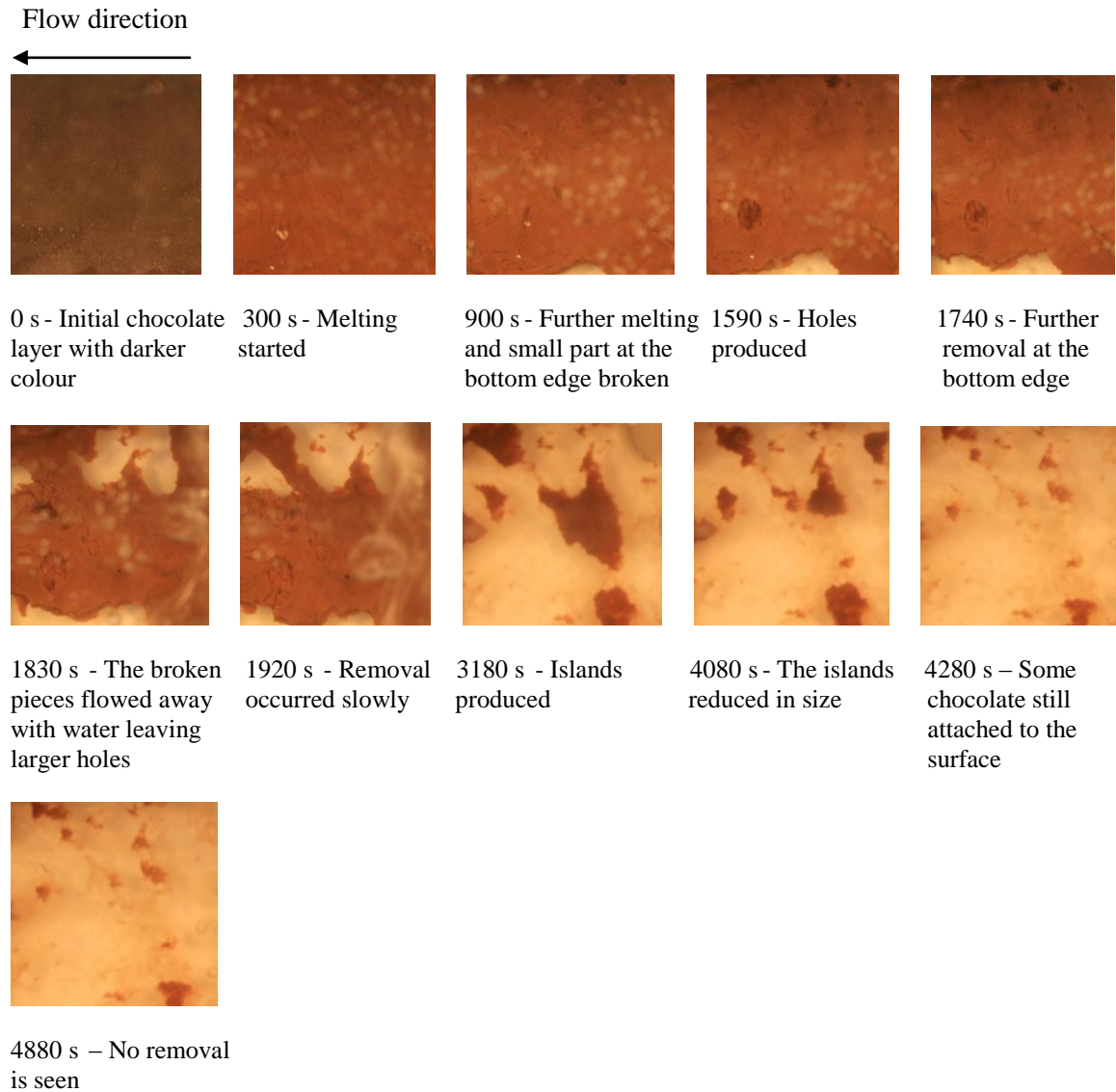


Figure 6.7: Images taken during water circulation at  $0.25\text{ms}^{-1}$  at  $70^\circ\text{C}$ .

The velocity was increased from  $0.25\text{ms}^{-1}$  to  $0.5\text{ms}^{-1}$  and the same temperature of  $70^\circ\text{C}$  was used for the next experiment. The selected images and the area covered are presented in Figures 6.8 and 6.9 respectively. From the images, it can be seen that at high velocity the chocolate removed by sliding from the leading edge of the flow. Once sliding started at 600 seconds, the area covered with chocolate reduced dramatically with less than half of the surface still covered in just about 120 seconds. Then, slow removal was observed and the area covered remained unchanged after 1380 seconds. From the

calculated area and by eye, it was determined that the surface was not clean. Water circulation at high velocity increased the removal even though in this case there was still some chocolate stuck on the polycarbonate surface.

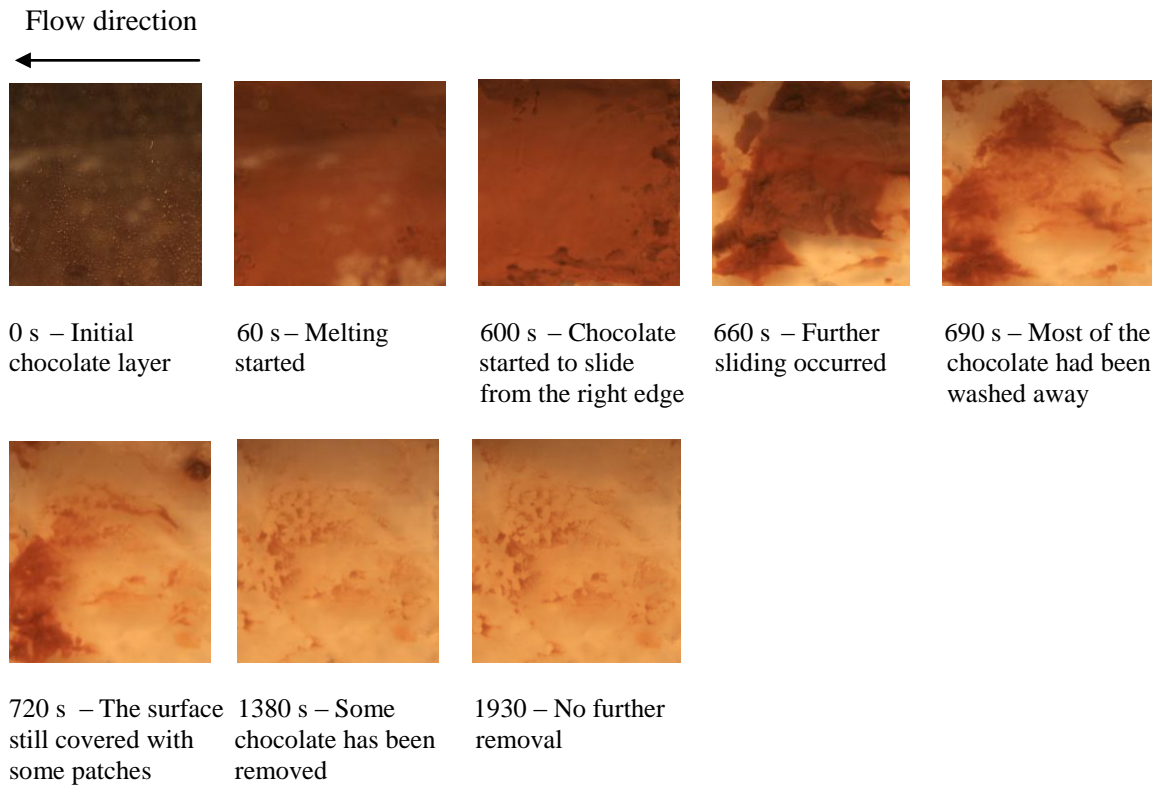


Figure 6.8: Images taken during water circulation at  $0.5\text{ms}^{-1}$  at  $70^{\circ}\text{C}$ .

From Figure 6.9, the experiment conducted at  $0.25\text{ms}^{-1}$  shows a step removal, while continuous removal was observed for the experiment conducted at  $0.5\text{ms}^{-1}$ . From the above description, each experiment was found to show different removal behaviour. This suggests that the flow conditions can influence the removal mechanism.



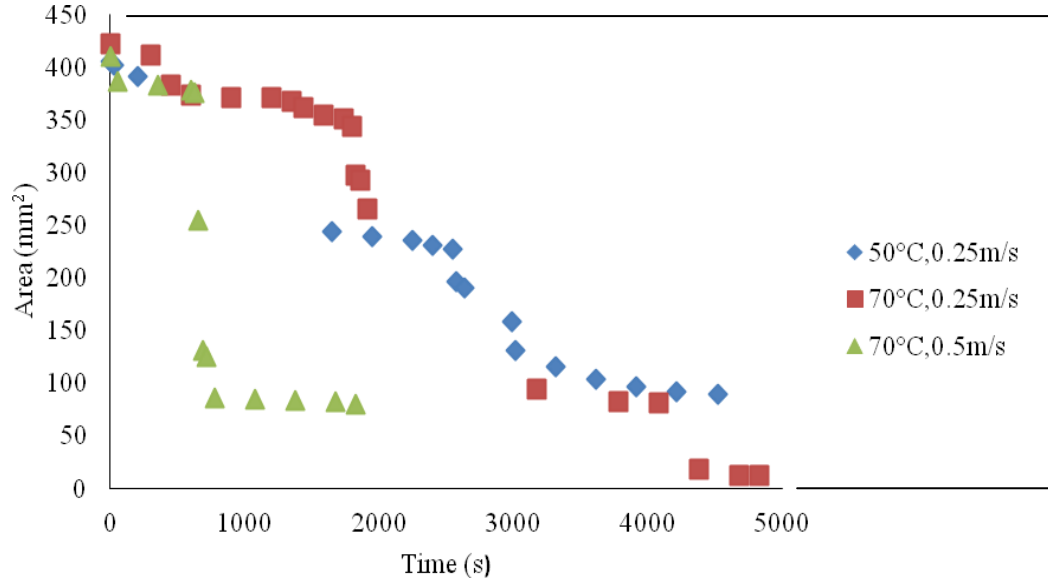


Figure 6.9: Area reduction profiles of chocolate at three different conditions showing different removal mechanism.

In all experiments, the surfaces did not reach the clean state either visually or from the calculated area. However, these results suggest that water circulation at high temperature will result in high reduction of area covered with chocolate, while high velocity will speed up the removal of the chocolate from the polycarbonate surface. Therefore, it was decided to use the temperature of 70°C and velocity of 0.5 ms<sup>-1</sup> as a standard condition for the following experiments.

### 6.5.2 Effect of surface materials

To investigate the influence of surface material on the removal behaviour on the ease of removal of chocolate layer using water circulation, experiments were conducted to remove tempered solidified chocolate from other materials (stainless steel and PTFE). This section will present the results of the experiments carried out using water circulation at 70°C and 0.5 ms<sup>-1</sup>.

Figure 6.10 presents the selected images captured during water circulation to remove chocolate layer from stainless steel, while the area reduction profile is shown in Figure 6.12. From Figure 6.10, the melting can be observed at the beginning before some erosion and sliding from the top edge of the coupon started at about 100 seconds. Sliding started earlier than for the removal from polycarbonate surface in section 6.5.1 at the same condition. Further break up occurred until some chocolate left at the bottom left corner of the coupon after 650 seconds water circulation. At 1050 seconds, only small patches were observed on the stainless steel surface and the area covered remained unchanged until 1650 seconds where the area covered reduced to approximately 20mm<sup>2</sup>. The final surface however was specified as ‘unclean’.

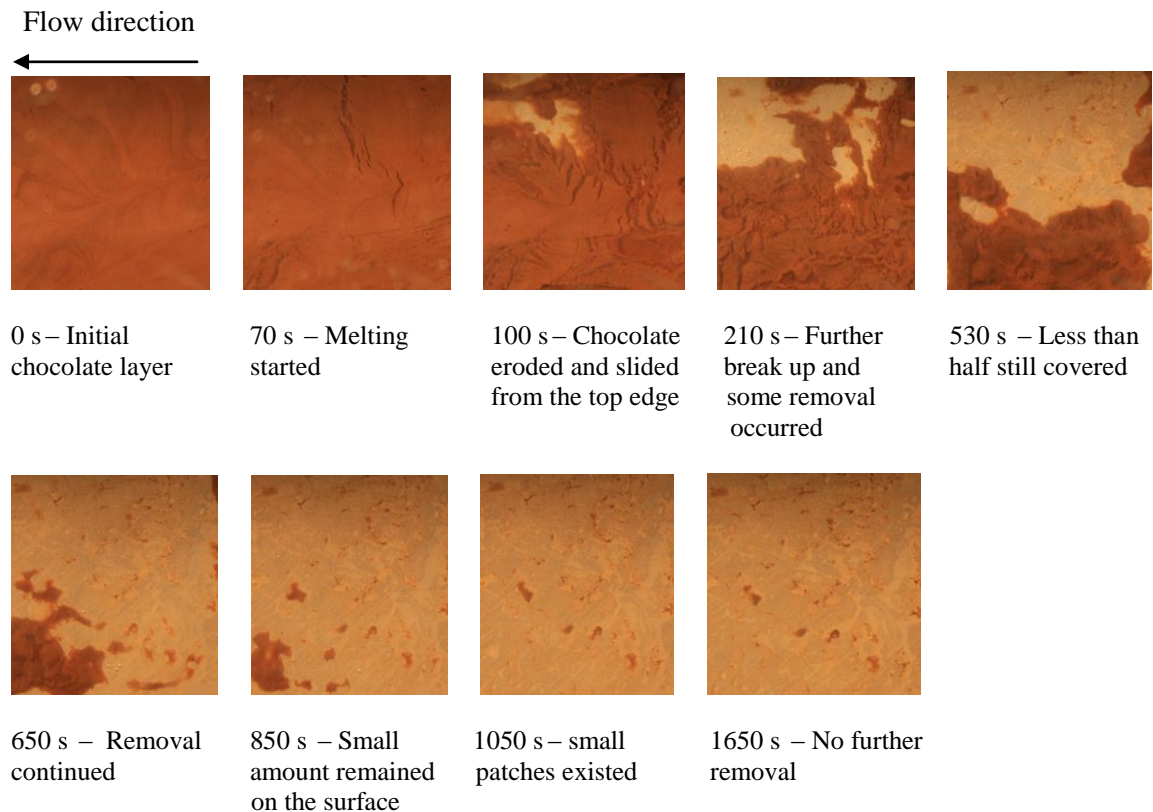


Figure 6.10: Images taken during water circulation to remove chocolate layer from stainless steel surface at  $0.5\text{ms}^{-1}$  and  $70^{\circ}\text{C}$ .

The removal of chocolate layer from PTFE surface is displayed in Figure 6.11 and the area reduction profile is presented in Figure 6.12. Removal started with melting followed by the erosion at the bottom edge of the coupon reducing the thickness of the chocolate layer as can be seen at 70 seconds. Then, sliding started to occur at that part whilst the erosion continued at the other parts. At 470 seconds, half of the surface was still covered with chocolate and further removal occurred leaving some small patches which could not be removed until the water circulation stopped. Approximately  $10\text{mm}^2$  of the PTFE surface covered with chocolate which was specified as ‘unclean’.

It can be seen in Figure 6.12, the area reduction profiles of stainless steel and PTFE were almost similar, but different from the polycarbonate which shows a larger plateau region at the beginning of water circulation followed by sudden reduction of the area covered before it remained unchanged until the circulation stopped. The reason for having a larger plateau region for the polycarbonate surface is still unclear. In general, all the three surfaces show continuous removal with small pieces removed gradually.

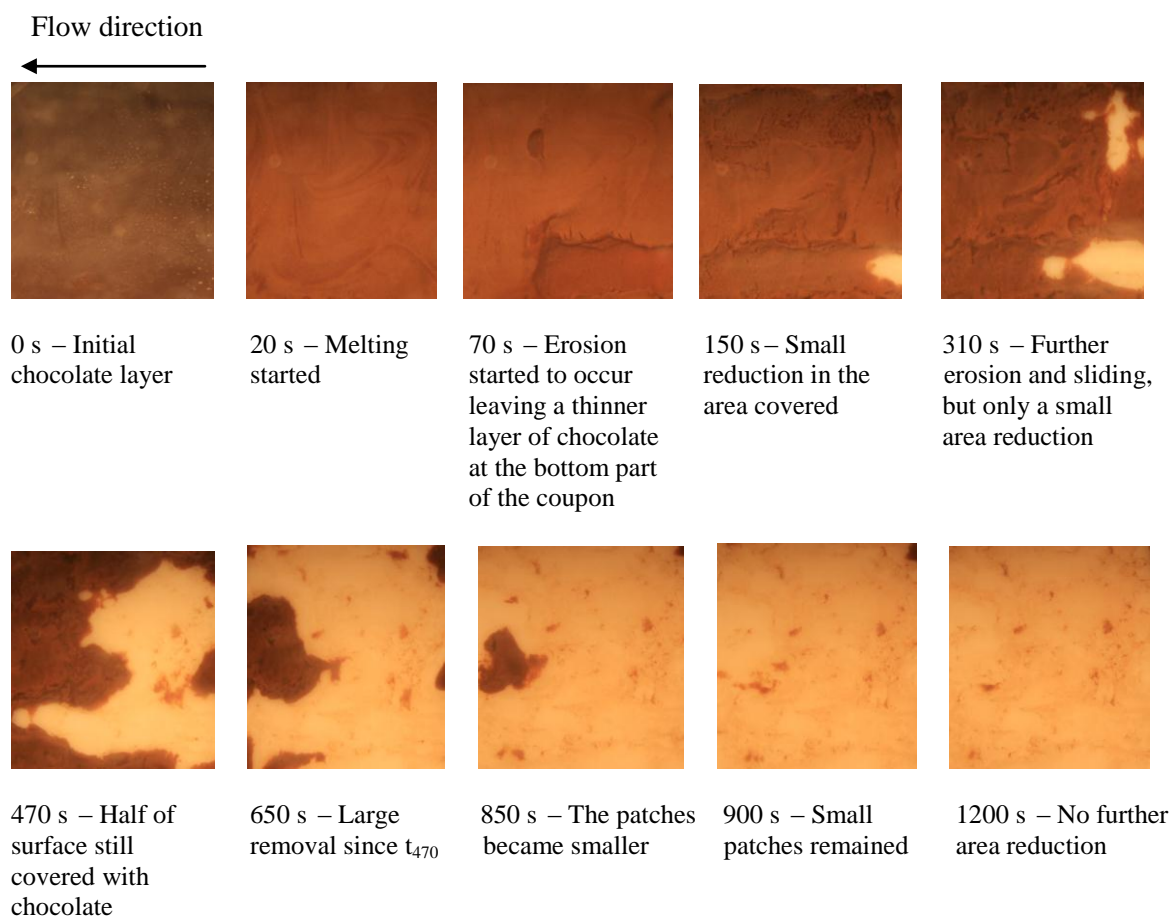


Figure 6.11: Images taken during water circulation to remove chocolate layer from PTFE surface at  $0.5\text{ms}^{-1}$  and  $70^\circ\text{C}$ .

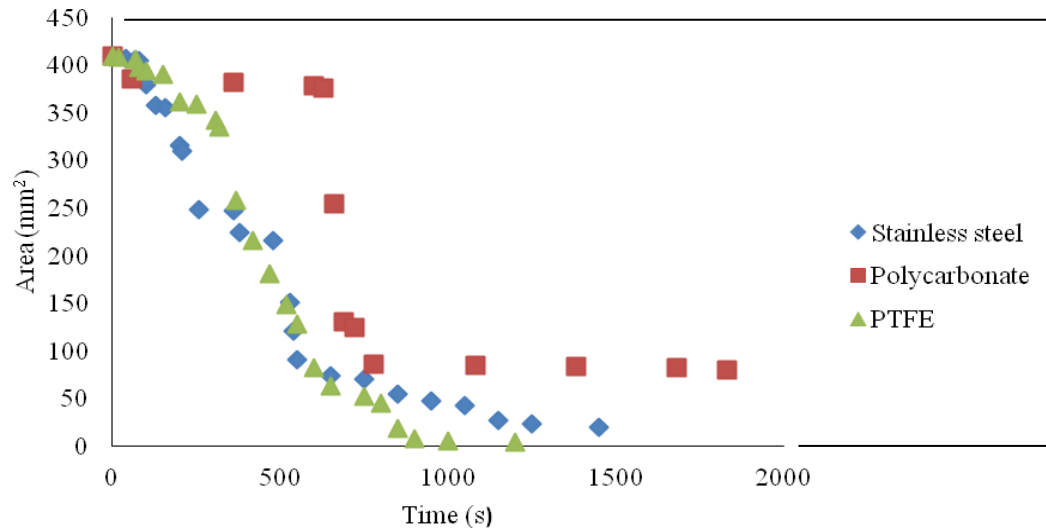


Figure 6.12: Area reduction profiles of chocolate for three different surface materials.

Water alone could not remove all the chocolate from all types or surfaces and conditions investigated in this preliminary study. Small islands or patches often remained even after more than one hour. All images presented in this section are not visually clean and it was also supported by the calculated area covered with the remaining chocolate as defined previously. Goode (2011) in her work also found that the use of water circulation to remove a yeast slurry deposit did not result in a clean surface leaving a film which was identified to be clusters of yeast cells. In different work by Ab.Aziz (2007), egg albumin gel deposit could not also be cleaned by water alone at the flow condition of 2.3 l/min and 70°C. For that reason, it was decided to add chemical with low concentration for the following experiments as it was believed that the chemical would affect the removal behaviour of the chocolate layer.

## 6.6 Chemical circulation

Based on the preliminary in section 6.5, further investigation was carried out involving the circulation of 0.1% NaOH solution to remove the solid chocolate layer which was prepared using the same method as for the water circulation experiments. A very low concentration was chosen to minimise the chemical usage to reduce the environmental impact. This section reports the removal behaviour of the chocolate with respect to various conditions including temperature, velocity, chemical requirement, surface material, tempering and cooling. Before investigating the effect of the parameters mentioned above on the removal behaviour of the chocolate, an experiment was run using the 0.1% NaOH solution at standard condition ( $70^{\circ}\text{C}$  and  $0.5\text{ms}^{-1}$ ) to determine if the polycarbonate surface can reach a clean state.

Figure 6.13 shows the selected images captured during the chemical circulation, while Figure 6.14 presents the area reduction profile which can be divided into three stages (A, B and C) separated by the vertical dashed lines. The following are the descriptions of the stages:

Stage A- Plateau region at the beginning of the chemical circulation. After 400 seconds of circulation, the chocolate has started to melt followed by the erosion and sliding from the leading edge. Dissolution also occurred reducing the thickness of the chocolate layer. This event can be supported by the results obtained in section 5.3.2 whereby the dissolution was found to occur when the chocolate was soaked in 0.1% NaOH even at lower temperature. However, the area covered remained unchanged even though some of the chocolate has been removed

Stage B – At 130 seconds, some area reduction was observed with erosion and sliding. In about 200 seconds, most of the chocolate has been removed and at 240 seconds only small area was still covered with chocolate.

Stage C – The coupon surface was visually clean with no further removal occurred. Cleaning time was also determined based on the procedure given earlier in this chapter.

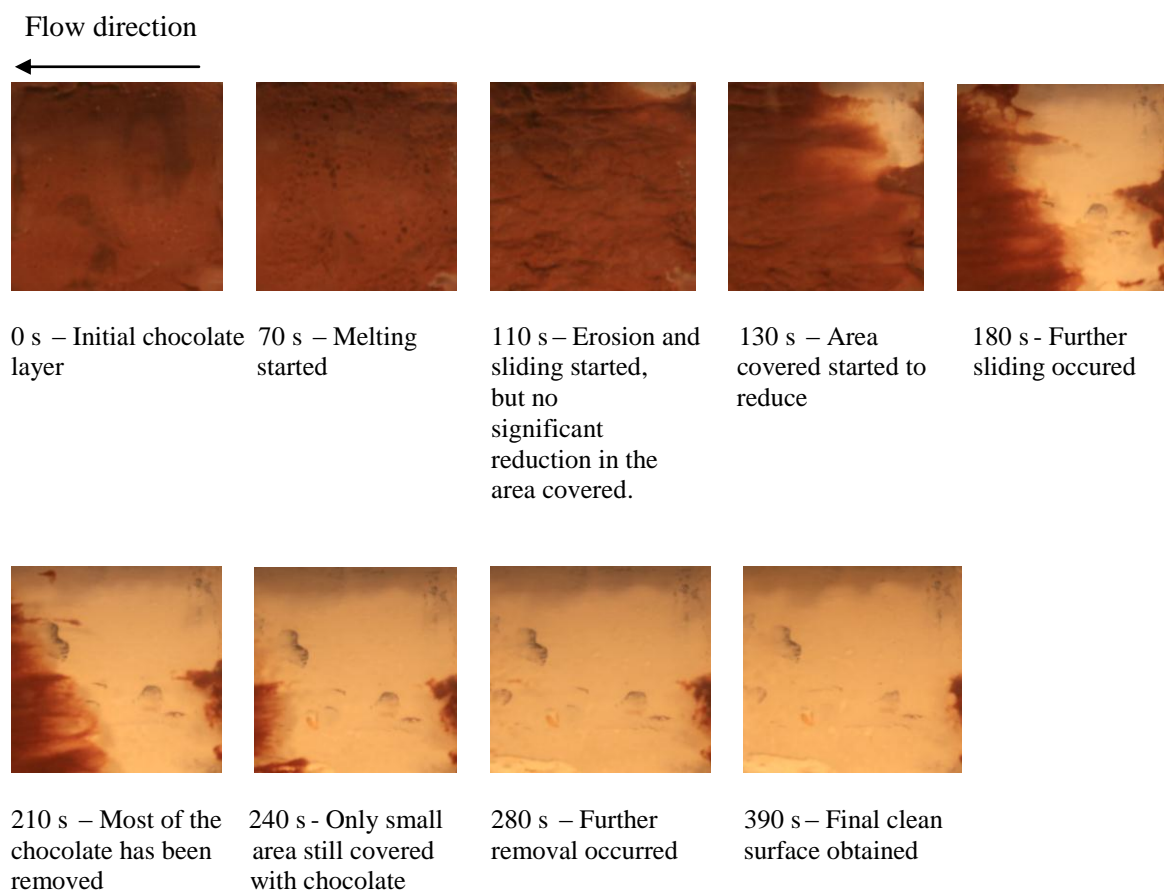


Figure 6.13: Images taken during circulation of 0.1% NaOH solution to remove chocolate layer from polycarbonate surface at  $0.5\text{ms}^{-1}$  and  $70^{\circ}\text{C}$ .

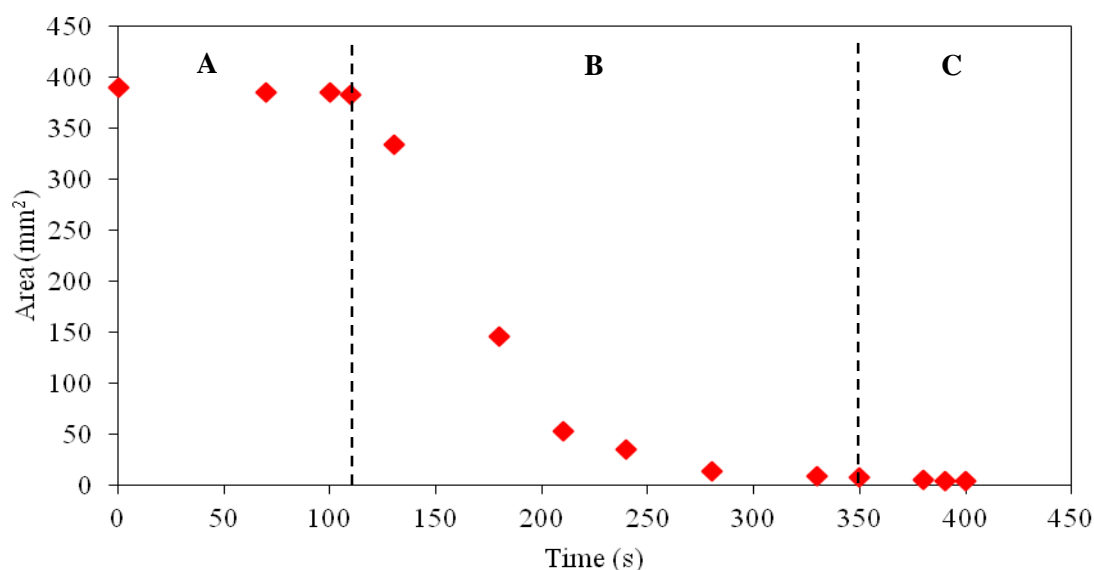


Figure 6.14: Area reduction profiles of chocolate using chemical circulation.

Circulation of NaOH solution even at low concentration can clean 99% of the polycarbonate surface. Thus, further study has been carried out.

### 6.6.1 Effect of temperature and velocity

The effects of temperature and velocity on the cleaning time and removal pattern with the circulation of 0.1% NaOH solution were studied. Figure 6.15 displays the time to clean for the flow temperature ranging between 25°C to 70°C. As expected, an increase in temperature significantly decreased the cleaning time. Experiments run at 40, 55 and 70°C produced a clean polycarbonate surface at the end of each experiment. Approximately a 40% decrease in the cleaning time occurred when increasing the temperature from 40 to 55°C. Increasing the temperature from 55 to 70°C has more effect on the cleaning time as almost 60% reduction was achieved. Removal behaviour at each temperature is discussed below and illustrated in Figures 6.17, 6.18 and 6.19 respectively. However, the experiment



at 25°C did not produce a clean polycarbonate surface, leaving a thin film after about 45 minutes of circulation. The area reduction profiles are shown in Figure 6.20.

This result is comparable with the stress sweep test study discussed in section 4.2.5.1 showing that the yield value decreased with increasing temperature. So, initially it was expected that the removal process at higher temperature would need less time to be completed. The results obtained confirm the hypothesis.

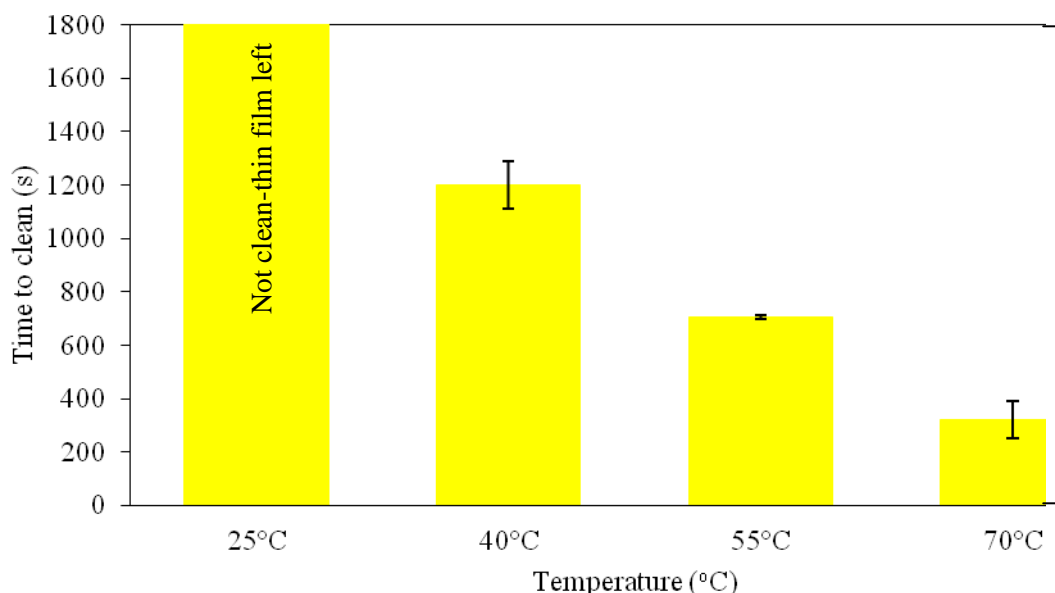
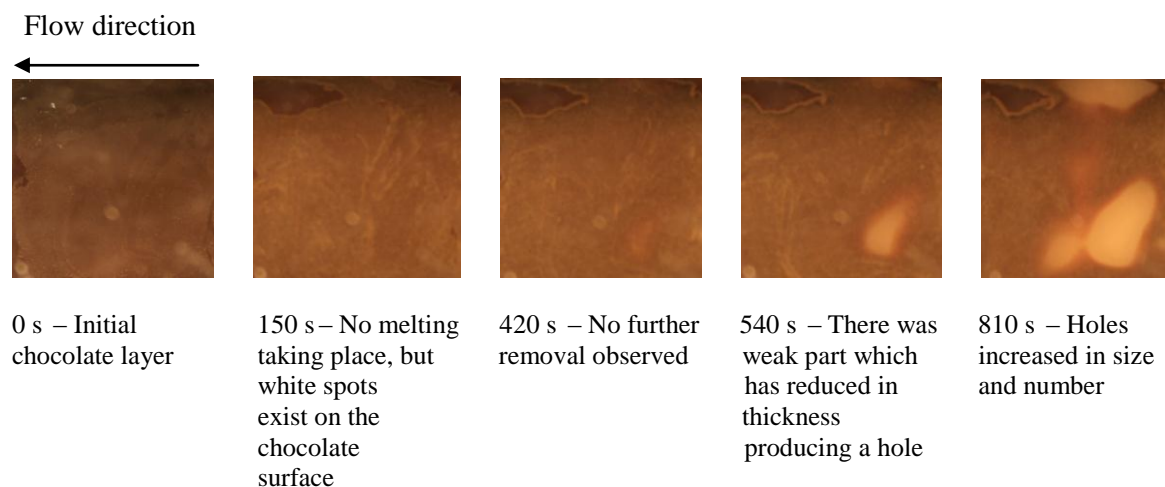


Figure 6.15: The dependence of cleaning time of solid chocolate on the flow temperature at 0.5 ms<sup>-1</sup>. Each data is averaged from two experiments and the standard deviation plotted as error bars.

From Figure 6.16, it was found that there was no melting occurred from the beginning of the circulation of 0.1% NaOH solution. This behaviour can be supported by the DSC melting curve presented in section 4.1.2 with no peak exist at 25°C for tempered chocolate cooled at 1°C/min. Only At 150 seconds, white spots started to form on the

chocolate surface and at 540 seconds a hole was formed and continued to expand and at the same time increased in number. Throughout the experiment, no removal in pieces was seen showing that the removal was controlled by the chemical effect. After 1230 seconds, a few islands were formed at the edges which were then removed gradually. There was no chocolate pieces seen on the polycarbonate surface at 2730 seconds, but it was covered with a thin film which could not be removed by prolonging the circulation time. The area reduction profile shown in Figure 6.20 was found to be unreliable because the calculated area covered with chocolate has reached the clean state based on the definition given earlier in this chapter. The surface was however determined as not clean as the thin film can be visually seen when the coupon was taken out from the test section. This problem with image analysis has been discussed in section 6.2.2.



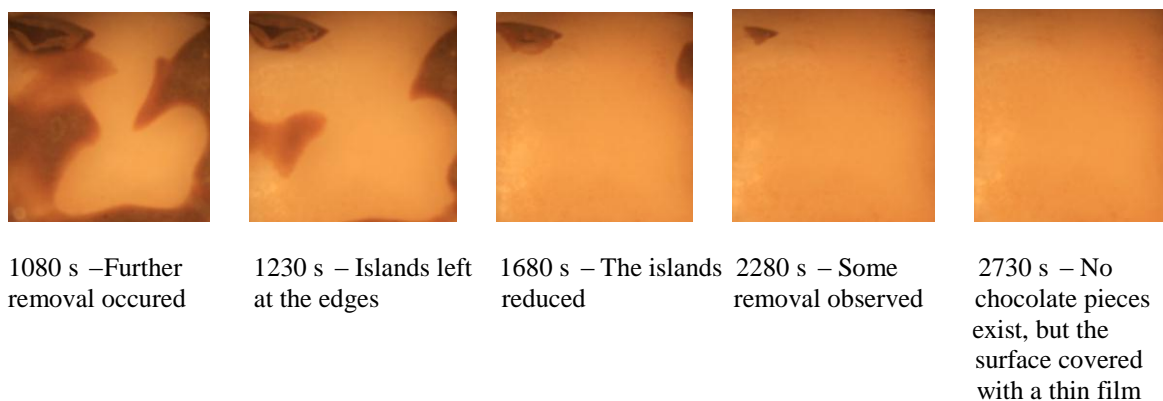


Figure 6.16: Images taken during circulation of 0.1% NaOH solution to remove chocolate layer from polycarbonate surface at  $0.5\text{ms}^{-1}$  and  $25^{\circ}\text{C}$ .

An attempt was made to characterise the thin film using the Confocal Raman Microscope as described in section 3.7.4. In this case, cocoa butter was used as a reference. Figure 6.17 shows the Raman spectra for both cocoa butter and the film. The figure shows peaks at wavenumbers of  $1100$ ,  $1450$ ,  $2900$  and  $3050\text{ cm}^{-1}$  for both spectra indicating that cocoa butter was one of the components of the film. Besides that, the film spectrum shows that there are also some other peaks at wavenumbers of  $400$ ,  $600$ ,  $650$ ,  $700$ ,  $720$ ,  $850$ ,  $1150$ ,  $1200$ ,  $1600$  and  $3000\text{ cm}^{-1}$ . It is expected that cocoa powder and sugar might also contribute to the formation of the film on the polycarbonate surface.

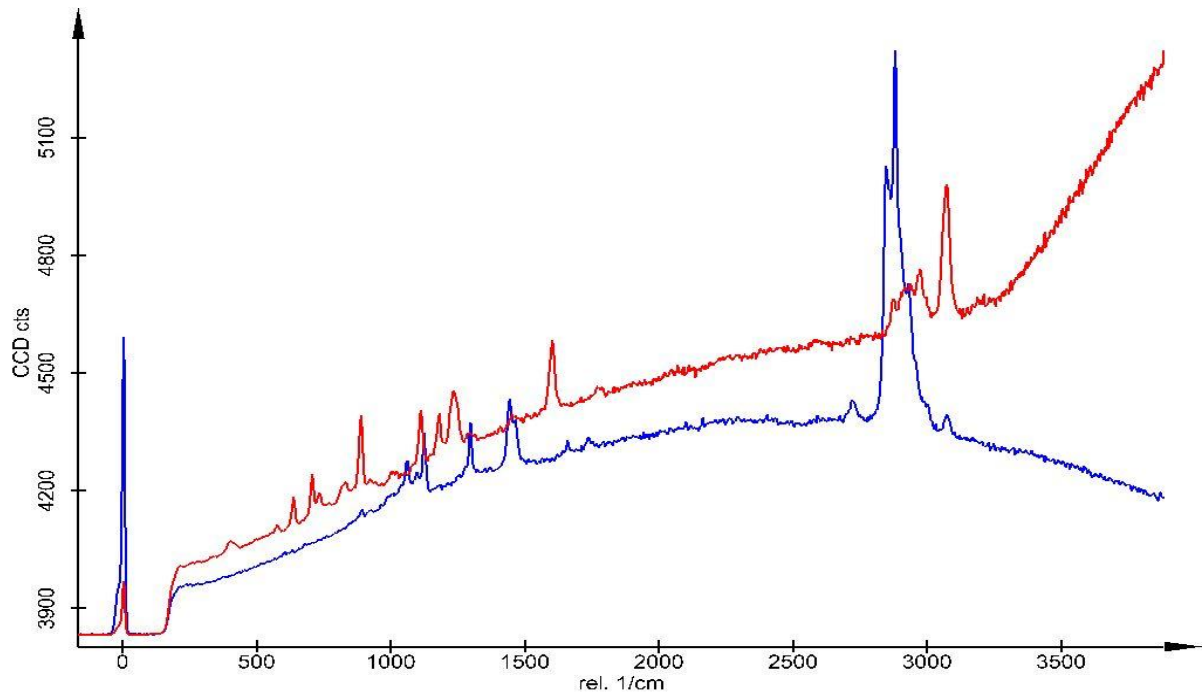


Figure 6.17: Raman spectra for cocoa butter (blue) as a reference and the film (red).

For the experiment run at  $40^{\circ}\text{C}$ , selected images are presented in Figure 6.18 and the area reduction profile is shown in Figure 6.20. Removal started with melting of the solid chocolate as it exceeded the melting temperature followed by the erosion and sliding from the leading edge. Simultaneously, holes started to form at 150 seconds which were then increased in size. Further removal produced islands which finally a small piece of chocolate remained at the edge. A clean surface was observed at 1110 seconds.

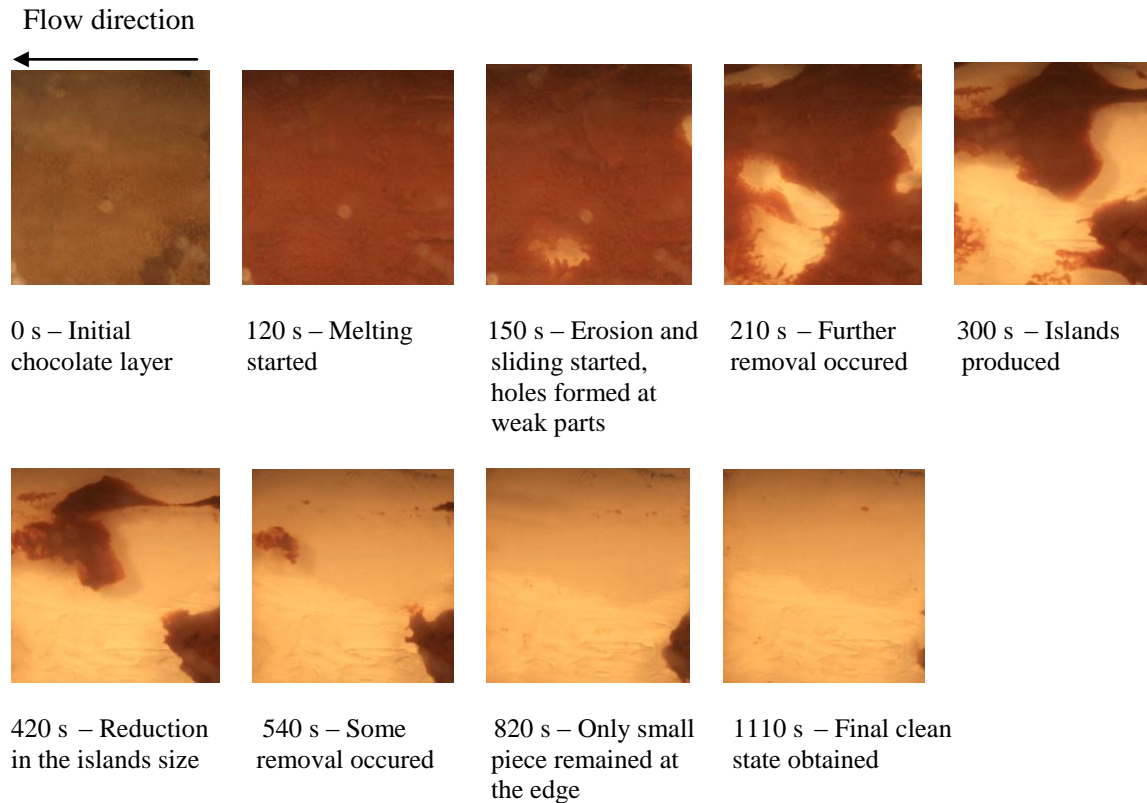


Figure 6.18: Images taken during circulation of 0.1% NaOH solution to remove chocolate layer from polycarbonate surface at  $0.5\text{ms}^{-1}$  and  $40^{\circ}\text{C}$ .

Similar behaviour was observed for the removal of solid chocolate from a polycarbonate surface with the flow temperature of  $55^{\circ}\text{C}$  shown in Figure 6.19 and the area reduction profile is displayed in Figure 6.20. However, a difference was detected in the length of plateau region before the reduction in the area covered with chocolate (named as stage A earlier). Increasing the temperature from  $40$  to  $55^{\circ}\text{C}$  shortened the plateau region by half (50 seconds). Then, erosion, sliding and holes formation occurred simultaneously. However, it was found that at 100 seconds, a large soft piece of chocolate has been pushed to the flow direction. The area reduced drastically leaving some chocolate stuck at the edges. Further removal occurred and finally a clean state was achieved after about 700 seconds of circulation.

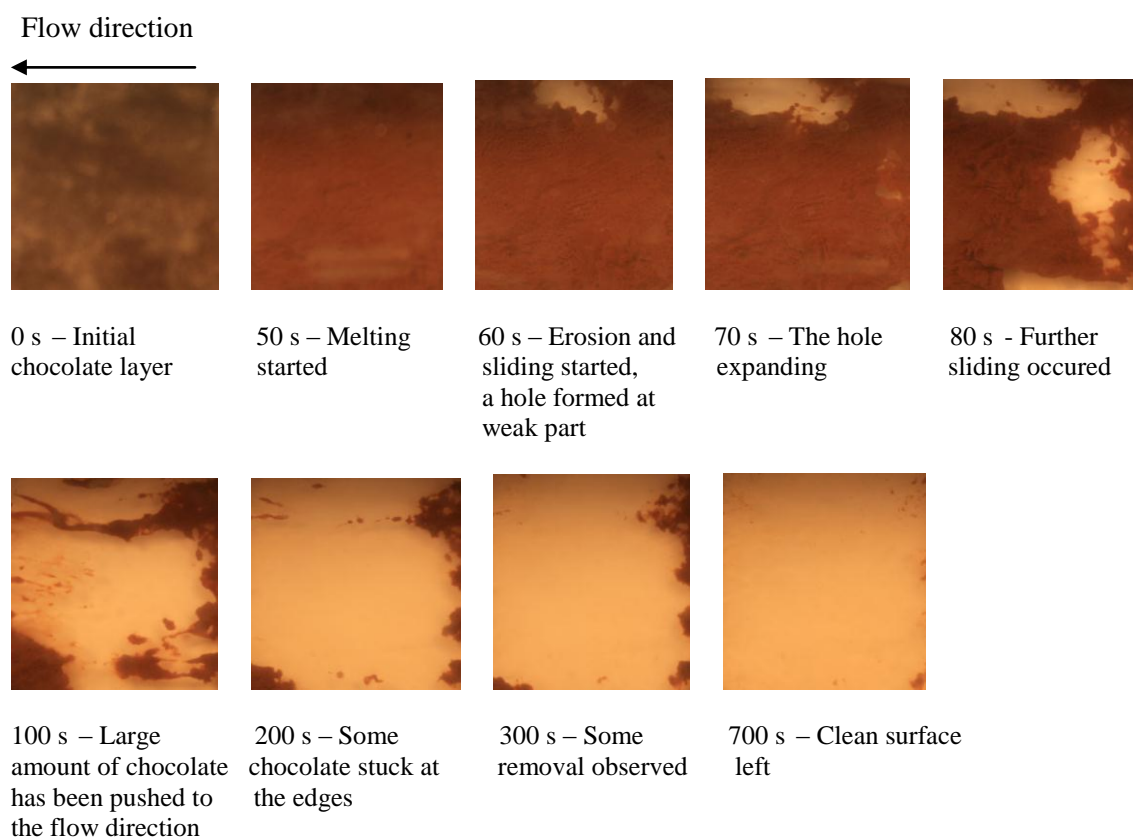


Figure 6.19: Images taken during circulation of 0.1% NaOH solution to remove chocolate layer from polycarbonate surface at  $0.5\text{ms}^{-1}$  and  $55^{\circ}\text{C}$ .

For the removal of solid chocolate at  $70^{\circ}\text{C}$ , the results are similar to Figure 6.13. Removal occurred rapidly with continuous erosion and sliding were observed when stage B started until all the chocolate was removed from the polycarbonate surface.

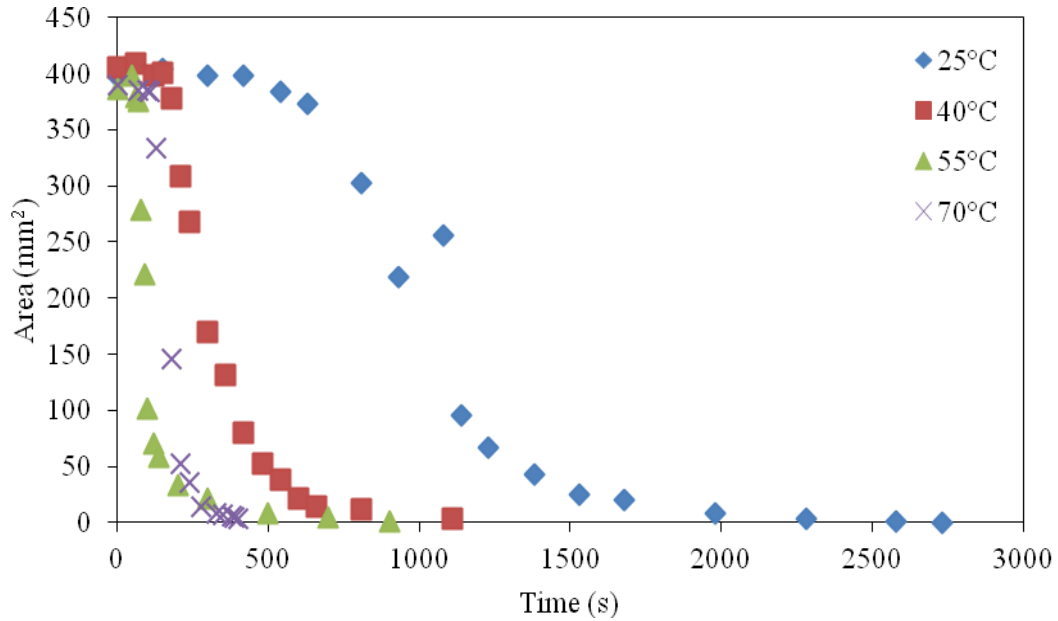


Figure 6.20: Area reduction profiles of chocolate using chemical circulation at different flow temperatures.

Christian (2003) reported that in the process of removing the baked tomato deposit, three major types of removal mechanisms were detected; one step removal, step removal and continuous removal which at high temperature and flow rate, the baked tomato deposit underwent a continuous removal. It is worth to mention that from the images and the changes in the area covered, it was found that the removal mechanism was predominated by the continuous removal for all the flow temperatures investigated (Figures 6.13, 6.16, 6.18, 6.19 and 6.20).

The effect of flow velocity on cleaning time and removal behaviour of solid chocolate from polycarbonate surface was then studied with the circulation of 0.1% NaOH solution at 70°C. Three different velocities were used ; 0.25, 0.37 and 0.5ms<sup>-1</sup>. The influence of the chemical circulation velocity on the cleaning time is shown in figure 6.21. Generally, time to clean decreases with increasing velocity with a reduction of about 20%

when the velocity increased from 0.25 to 0.37ms<sup>-1</sup> and increasing the velocity from 0.37 to 0.5ms<sup>-1</sup> reduced up to 60% of the cleaning time.

According to Ab. Aziz (2007), in removing egg albumin gel deposit, the effect of flow velocity on the cleaning time is also influenced by the temperature and chemical concentration. In current study only one temperature and chemical concentration were studied. At higher chemical concentration, it is expected that the effect of velocity will be less significant as more chemical diffuses and changes the deposit structure aiding the removal. Jennings *et al.* (1957) found that in the removal of milk deposits, the most significant effect was showed by the fluid velocity expressed as Re number followed by the temperature, but the effect of both parameters became less significant when more chemicals were used.

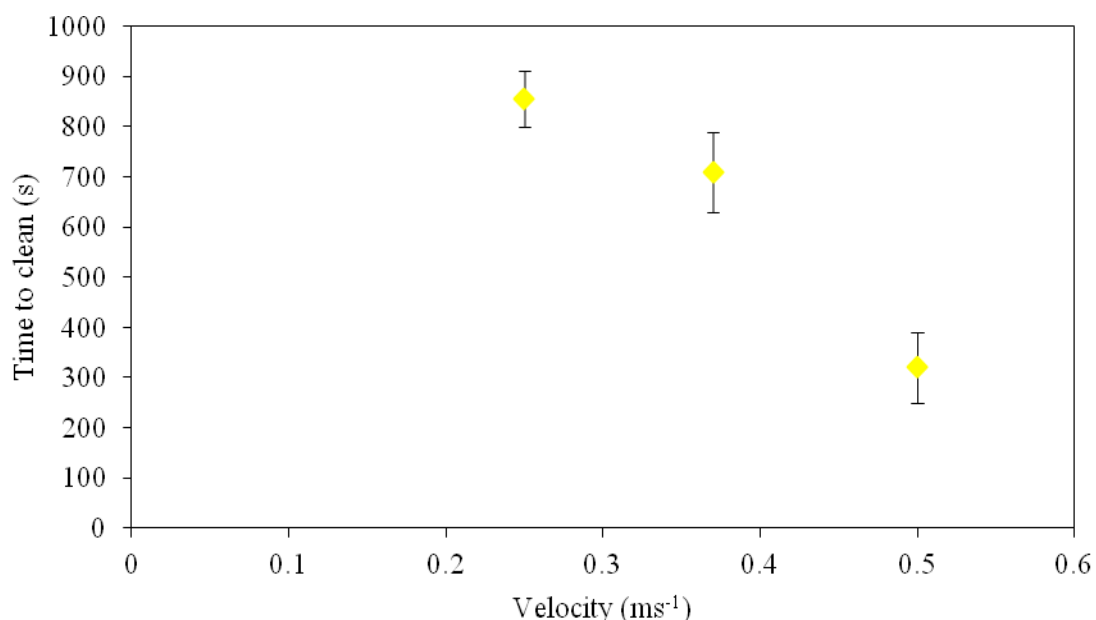


Figure 6.21: The dependence of cleaning time of solid chocolate on the flow velocity at 70°C. Each data is averaged from three experiments and the standard deviation plotted as error bars.



The removal behaviour for all the velocities involved are displayed in figures 6.22, 6.23 and 6.13. It can be seen in figure 6.22, with the velocity of  $0.25\text{ms}^{-1}$  and the temperature of  $70^{\circ}\text{C}$ , the removal of solid chocolate from the polycarbonate surface initiated only after 40 seconds of circulation. Melting started while a thin layer of chocolate was peeled off resulting in a change of colour. Even though some removal has started, the area covered was still unchanged. At 260 seconds, there were some spots with a thinner layer can be seen visually as a result of the erosion and sliding from the leading edge. The area reduction only started at about 310 seconds and simultaneously holes started to form. Sliding continued until small islands left on the surface at 760 seconds and clean surface was noticed at 910 seconds.

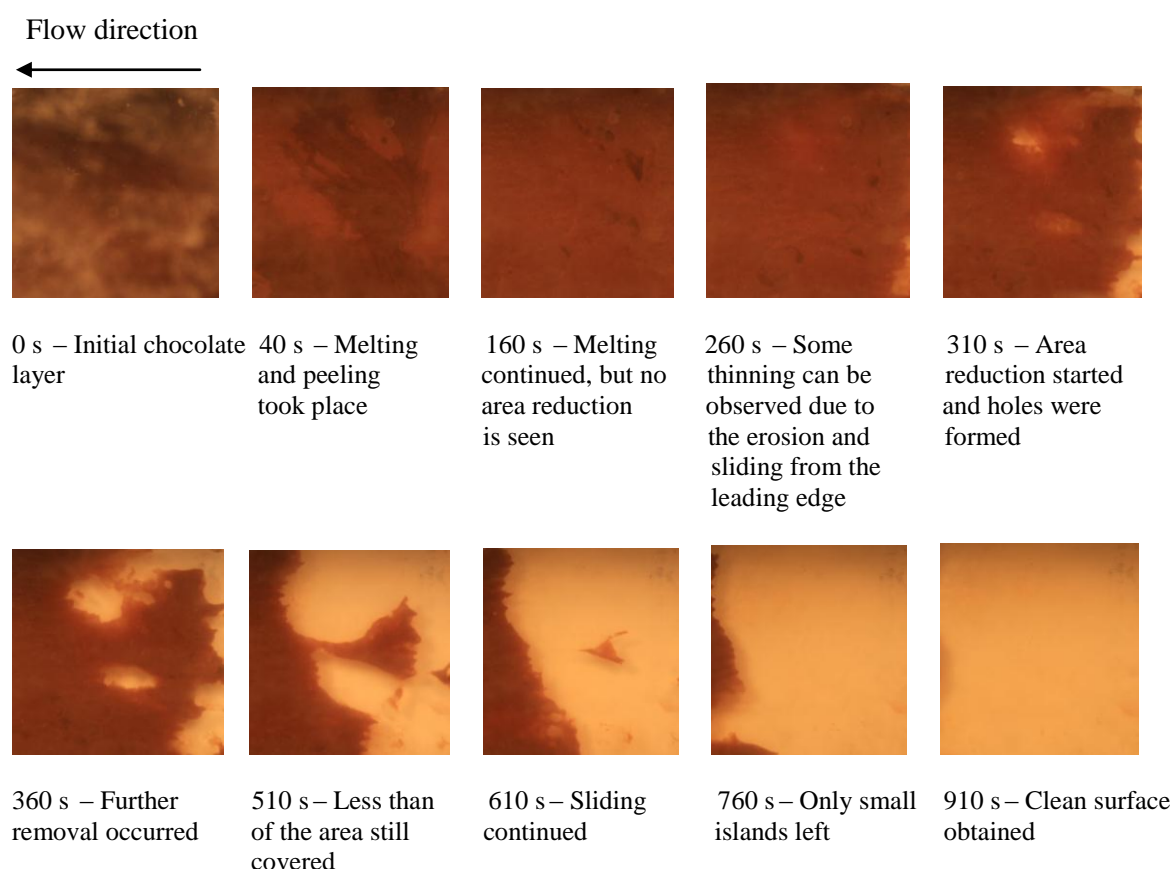
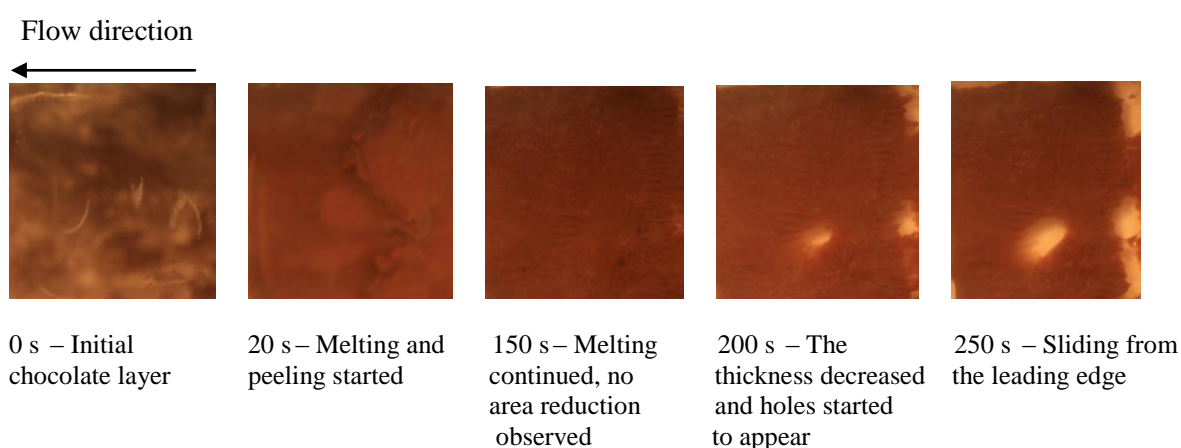


Figure 6.22: Images taken during circulation of 0.1% NaOH solution to remove chocolate layer from polycarbonate surface at  $0.25\text{ms}^{-1}$  and  $70^{\circ}\text{C}$ .

When the flow velocity was increased from  $0.25$  to  $0.37\text{ms}^{-1}$ , similar removal behavior was observed as can be seen in Figure 6.23. However, the melting and peeling process started at 20 seconds of the circulation which is faster than for the experiment conducted at  $0.25\text{ ms}^{-1}$  showing that the increasing in velocity has sped up the initiation of the removal. In addition, higher velocity also shortened the length of stage A whereby the formation of holes and a decrease in thickness occurred faster. It was then followed by the sliding and formation of islands which were then reduced in size. A clean surface was obtained at 790 seconds.

Once again, the selected images for the experiment conducted at  $0.5\text{ms}^{-1}$  and  $70^{\circ}\text{C}$  can be referred at the earlier part of this section that shows a different removal behaviour at high velocity. No holes and islands formation were observed when high velocity was used showing that the shear force provided by the flow is strong enough to sweep away the chocolate in a short time. This indicates that flow velocity affect the removal behaviour of the chocolate layer from the polycarbonate surface.



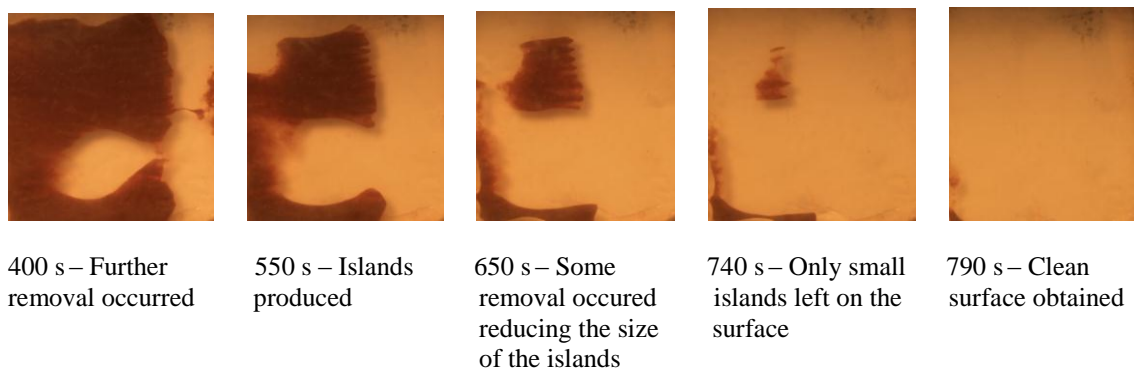


Figure 6.23: Images taken during circulation of 0.1% NaOH solution to remove chocolate layer from polycarbonate surface at  $0.37\text{ms}^{-1}$  and  $70^\circ\text{C}$ .

Figure 6.24 shows the area reduction profiles for the three flow velocities at  $70^\circ\text{C}$ . It has been proven that increasing the velocity from  $0.25$  to  $0.37\text{ms}^{-1}$  shortened the length of stage A and slightly reduced the cleaning time. However, overlapping of the two lines can be seen at some points in stage B. It shows that area reduction occurred almost at the same rate for both velocities used. On the other hand, the area reduction profile for the removal at  $0.5\text{ms}^{-1}$  shows a faster removal with a very short plateau region at the beginning of the chemical circulation.

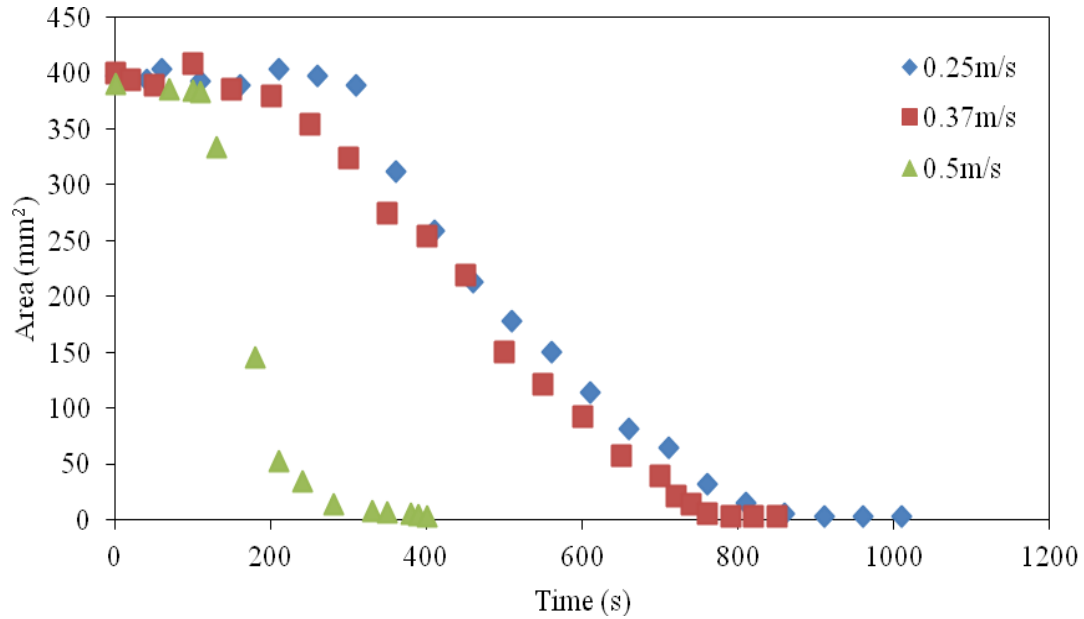


Figure 6.24: Area reduction profiles of chocolate using chemical circulation of 0.1% NaOH at different flow velocities.

The results reported in this section suggest that:

- (i) The removal of solid chocolate from polycarbonate surface is impossible at room temperature.
- (ii) Both flow temperature and velocity affect the cleaning time and removal behaviour of solid chocolate from polycarbonate surface.

### 6.6.2 Effect of surface materials and chemical usage

The previous section noted how temperature and velocity influence both the time taken to remove the chocolate from the polycarbonate surface and the removal behaviour. Here, studies have been carried out to compare the removal of solid chocolate from the stainless steel, polycarbonate and PTFE surfaces. The characteristics of the surfaces have been reported in section 5.2. The same mass of liquid chocolate was placed on the square

coupons which were then solidified at the same cooling rate (1°C/min). Chemical circulation was performed at standard condition. This section will also give a comparison of the cleaning time for the three surface materials which had undergone the circulation of both water (results from section 6.5.2) and 0.1% NaOH solution.

Figure 6.25 presents the time to clean for the three surface materials with a comparison between the circulation of water and 0.1% NaOH solution. It has been reported in section 6.2.3 that water circulation did not clean all the surfaces at the conditions used. However, the circulation of 0.1% NaOH solution in all cases gives a surface free of chocolate suggesting that both intramolecular and intermolecular forces have been broken. All three surfaces managed to reach the clean state even though the time to clean were different as can be seen in figure 6.25. Cleaning time for polycarbonate surface was the fastest followed by stainless steel and PTFE. Approximately 1300 seconds of circulation needed to remove the chocolate from PTFE surface. This could be caused by the surface roughness of PTFE coupon which was the highest among the three surfaces as reported in section 5.2. The crevices present on the surface may prevent a fast removal. The polycarbonate surface only needs 300 seconds to be cleaned which equates to a cleaning time reduction of 73%.

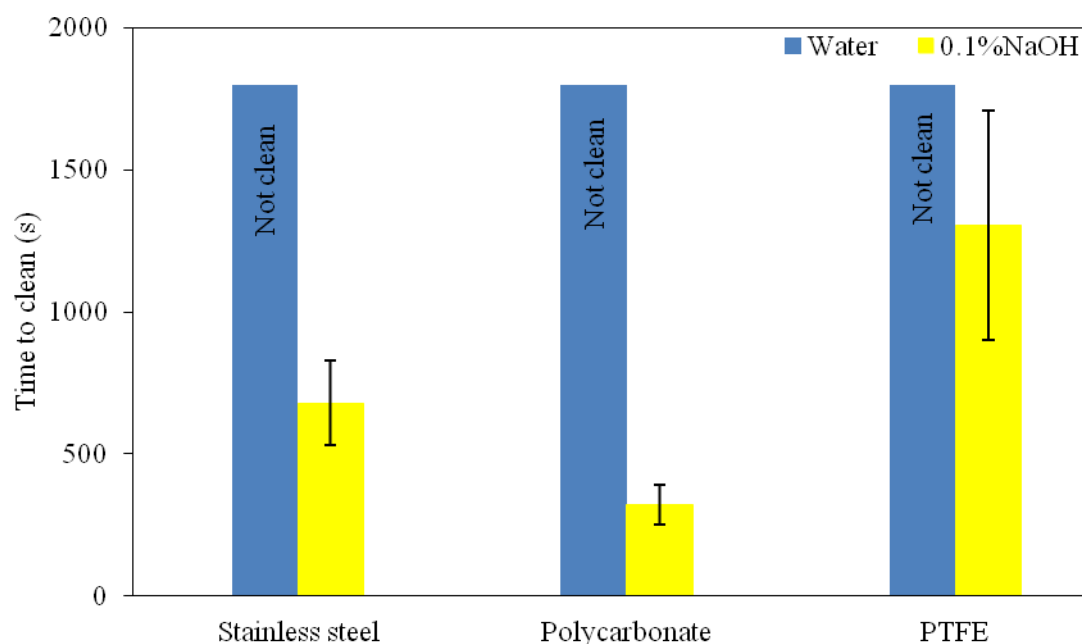


Figure 6.25: Cleaning time as a function of surface material for water and chemical circulations at  $0.5\text{ms}^{-1}$  and  $70^{\circ}\text{C}$ . Each data is averaged from three experiments and the standard deviation plotted as error bars.

Selected images during the removal of chocolate from the stainless steel surface are shown in figure 6.26 while figure 6.28 presents the area reduction profile. Melting and peeling events started as early as 20 seconds of the circulation period followed by sliding from the leading edge 10 seconds after that. The removal occurred gradually until only some chocolate was observed at the edges at 240 seconds. Eventually, a clean surface was obtained at 530 seconds.

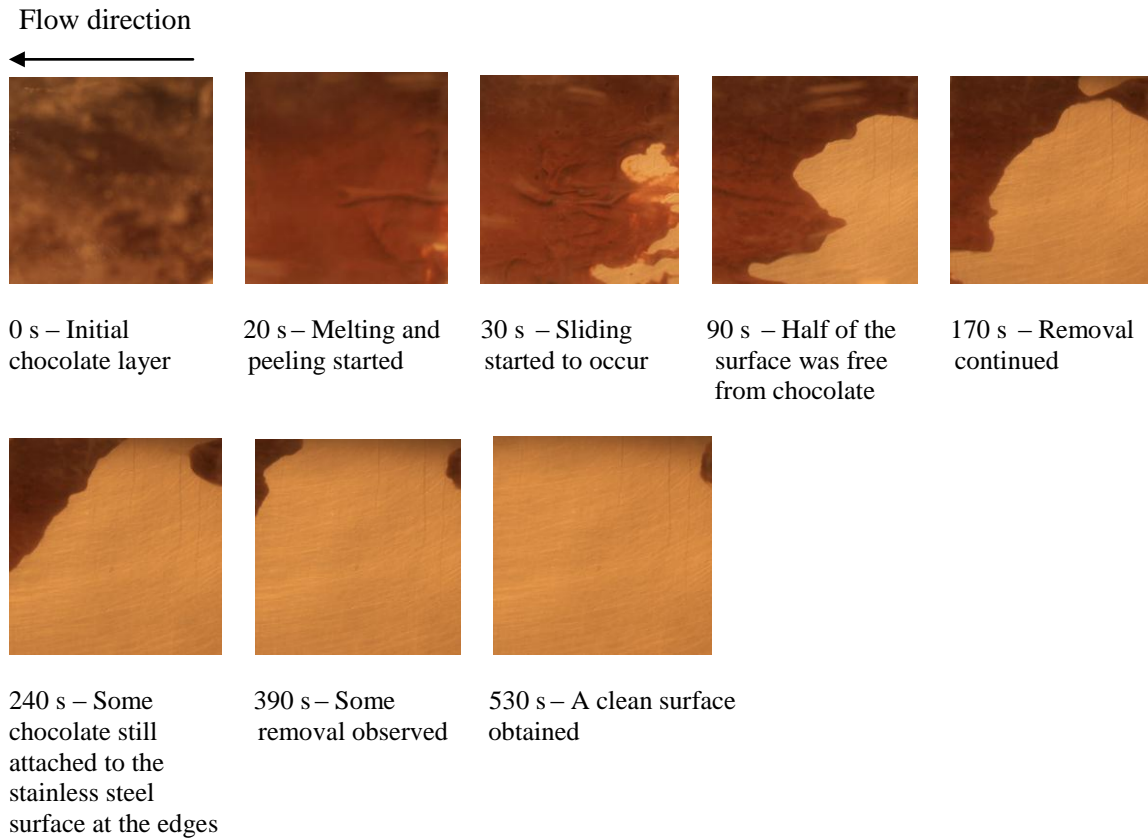


Figure 6.26: Images taken during circulation of 0.1% NaOH solution to remove chocolate layer from stainless steel surface at  $0.5\text{ms}^{-1}$  and  $70^\circ\text{C}$ .

For the removal of chocolate from the PTFE surface, the selected images are displayed in Figure 6.27. Even though the melting event was started at 10 seconds of the circulation period, but stage B was only started at about 110 seconds. Sliding event did not entirely clean the front part of the coupon, but some tails appeared as can be seen at 240 seconds. It is believed that the crevices present on the surface contribute to this event to occur. The measured roughness of the PTFE surface was  $4.3\text{nm}$  which probably larger than the particle size of chocolate could possibly cause the chocolate to get trapped in the crevices. However, it slowly disappeared as the circulation continued. The cleaning time was noted at 900 seconds.

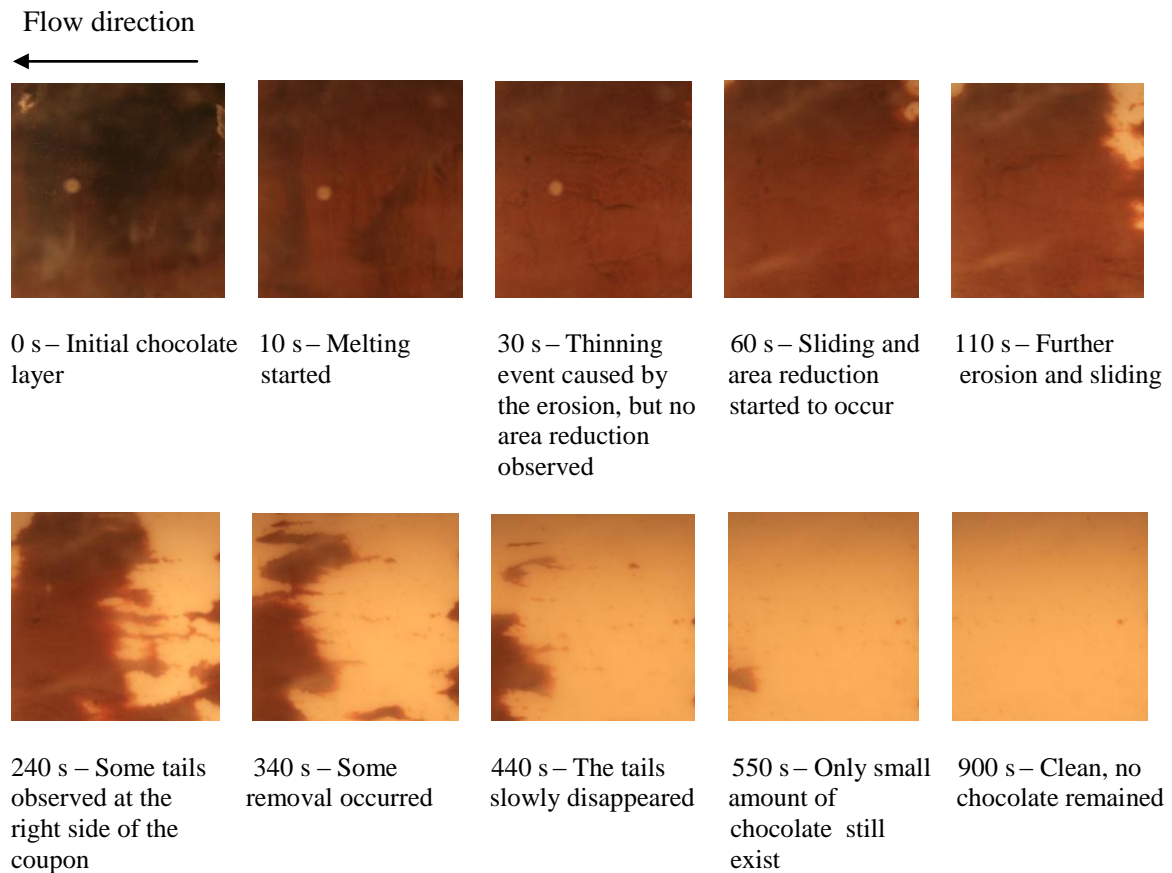


Figure 6.27: Images taken during circulation of 0.1% NaOH solution to remove chocolate layer from PTFE surface at  $0.5\text{ms}^{-1}$  and  $70^\circ\text{C}$ .

From the area reduction profiles presented in figure 6.28, it is observed that the rate of removal of chocolate from polycarbonate was the fastest among the three materials. An overlapping occurs between the area reductions profiles of the stainless steel and polycarbonate. The roughest surface was found to affect the cleaning time and removal behaviour, but not the removal rate and the length of the plateau region. Overall, the removal mechanism for the stainless steel, polycarbonate and PTFE were found to be continuous removal.



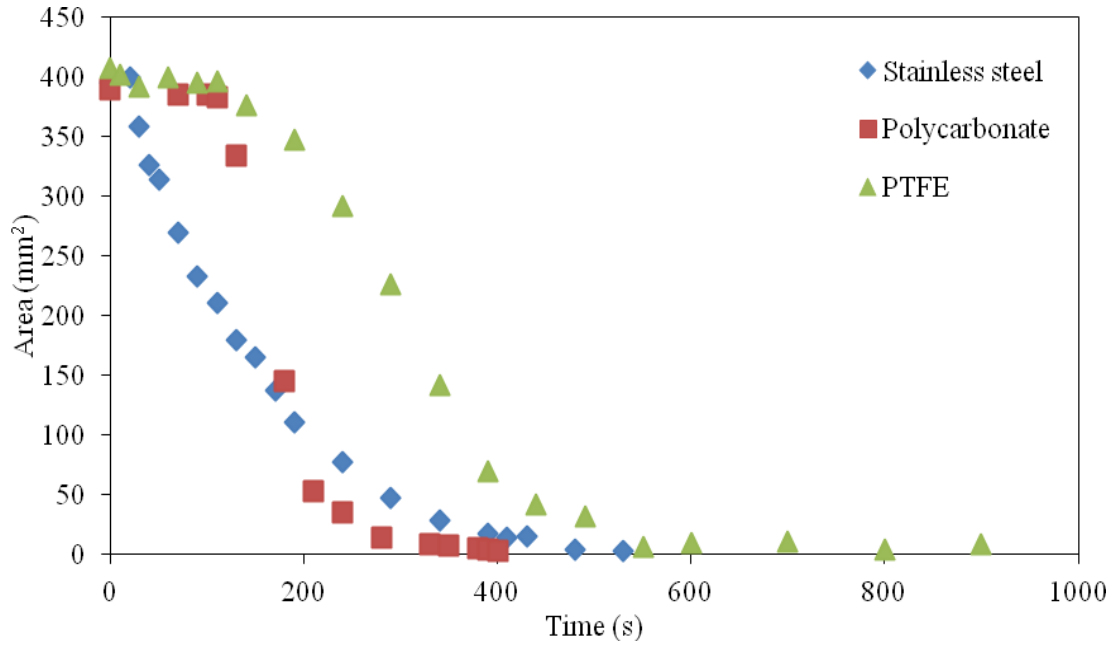


Figure 6.28: Area reduction profiles of chocolate using chemical circulation for removal from different surface materials.

### 6.6.3 Effect of tempering and cooling

The tempered and untempered chocolates have different polymorphs when solidified as discussed in section 4.1.2.1. Different removal behaviour might be expected with an effect on the cleaning time. Thus, in this section the dependency of the cleaning time and removal behaviour to the tempering process were determined. Simultaneously, the influence of cooling on both tempered and untempered chocolate was also studied. In all experiments, only polycarbonate surface and chemical circulation at  $0.5\text{ms}^{-1}$  and  $70^\circ\text{C}$  involved. Figure 6.29 gives a comparison of the cleaning time of tempered and untempered chocolate with different cooling conditions; cooled on the Peltier stage to  $10^\circ\text{C}$  at cooling rates 1 and  $10^\circ\text{C}/\text{min}$ , at room temperature for 60 minutes and in the refrigerator for 60 minutes.

A large variation in the cleaning time was seen for the tempered chocolate compared to the untempered chocolate. The cleaning time for tempered chocolate cooled at 1°C/min was only approximately 350 seconds, but a longer cleaning time of 1100 seconds was found for the sample cooled at 10°C/min. Tempered chocolate cooled at room temperature and in the refrigerator for 60 minutes exhibit a cleaning time of about 900 seconds and 750 seconds respectively. The results show that cleaning time for the chocolate solidified into type V polymorph was significantly shorter than the other polymorphic forms. This finding can also be supported by the results for the untempered chocolate which has been proven in section 4.2.2.1 that it did not crystallise in a correct polymorph for all the cooling conditions applied. The cleaning times for all the untempered chocolates were longer than for the tempered chocolate cooled at 1°C/min with no cooling effect observed. These results suggest that crystallisation process aided by the tempering and application of proper cooling which can produce the desired type V crystals not only results in a good appearance of the chocolate, but also shortens the cleaning time of the surface.

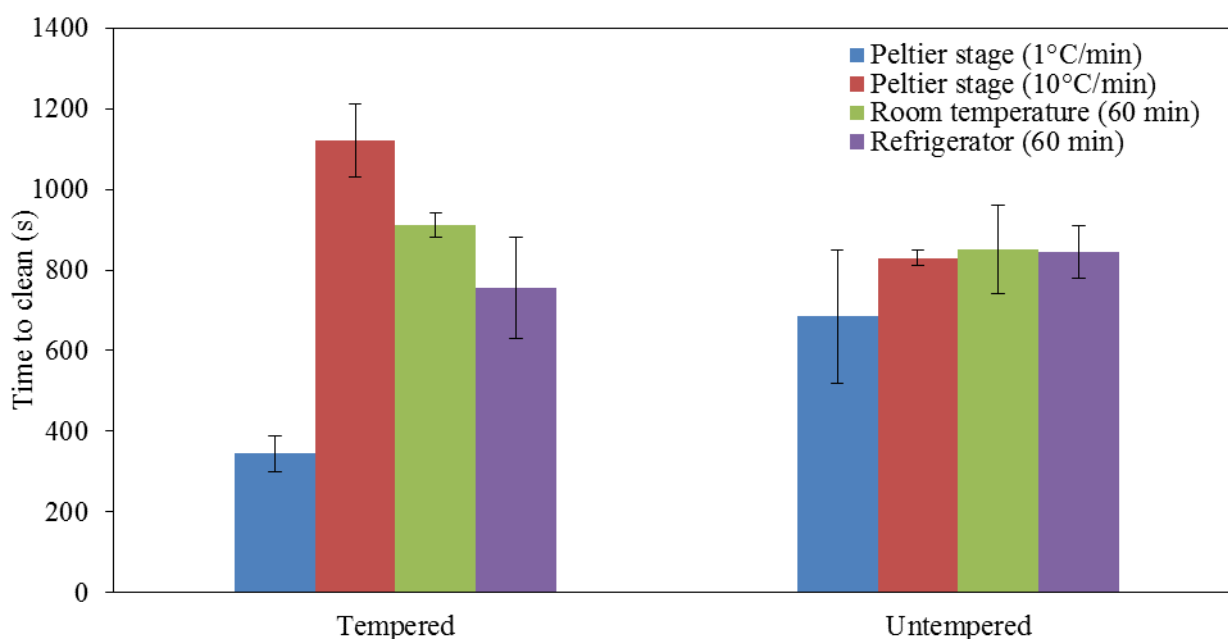


Figure 6.29: Cleaning time for tempered and untempered chocolates cooled at different cooling conditions underwent chemical circulation at  $0.5\text{ms}^{-1}$  and  $70^\circ\text{C}$ . Each data is averaged from three experiments and the standard deviation plotted as error bars.

Figure 6.30 shows selected images for the removal of the untempered solid chocolate cooled on the Peltier stage at  $1^\circ\text{C}/\text{min}$ . The similar behaviour can be seen during stage B removal when compared with the images for the tempered chocolate with the same cooling condition illustrated in Figure 6.13. Both tempered and untempered chocolate was removed in sliding pattern from the leading edge. However, there was a different observed at stage A whereby the melting and peeling events occurred simultaneously for the untempered chocolate as can be seen at 30 seconds of the circulation, but no peeling event observed for the tempered chocolate. In addition, the melting process for the untempered chocolate started 40 seconds earlier than for the tempered chocolate. This is probably because longer time needed to destroy the crystal structure of the tempered chocolate which is in a compact arrangement.

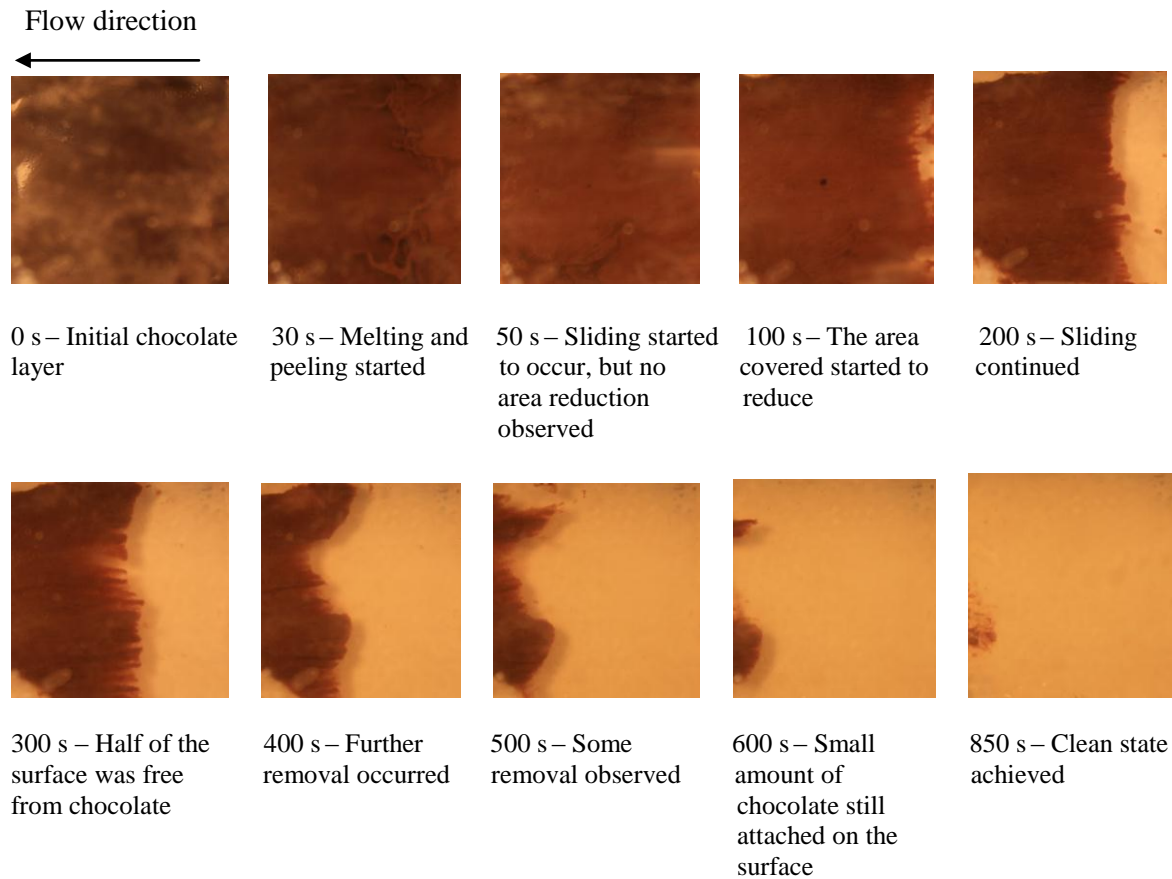


Figure 6.30: Images taken during circulation of 0.1% NaOH solution at  $0.5\text{ms}^{-1}$  and  $70^\circ\text{C}$  to remove the untamped chocolate layer cooled on the Peltier stage at  $10^\circ\text{C}/\text{min}$ .

The area reduction profiles for both the tempered and untamped chocolates are presented in Figure 6.31. It can be seen that the length of stage A for the untamped chocolate is slightly shorter than for the tempered chocolate, but the removal rate (stage B) for the tempered chocolate is higher than for the untamped chocolate.

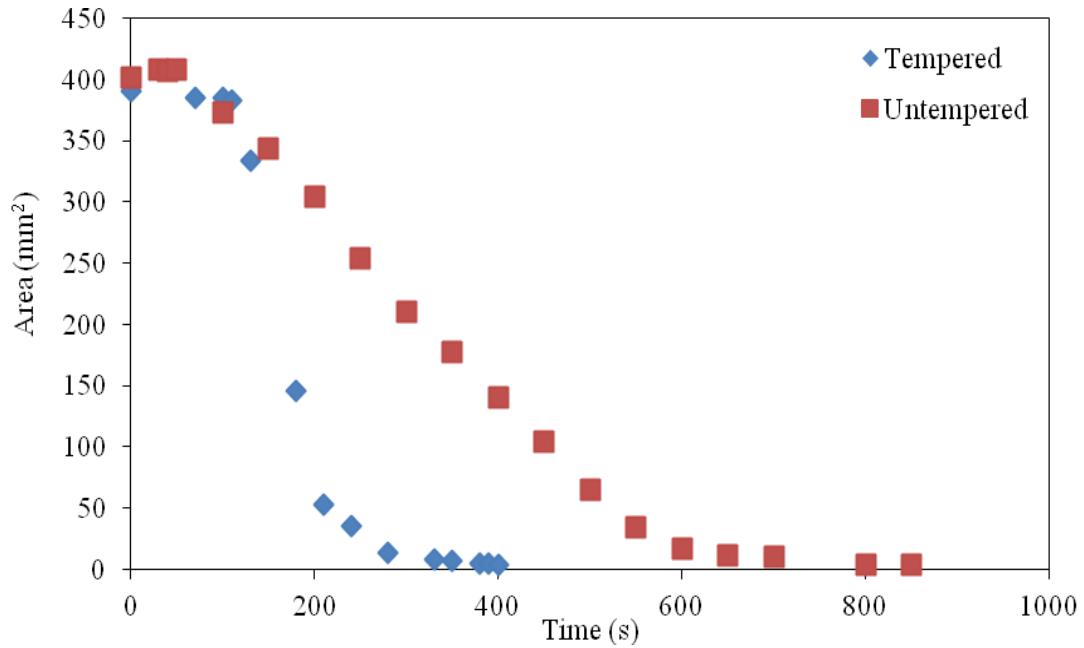


Figure 6.31: Area reduction profiles for the removal of tempered and untempered chocolate cooled on the Peltier stage at 1°C/min.

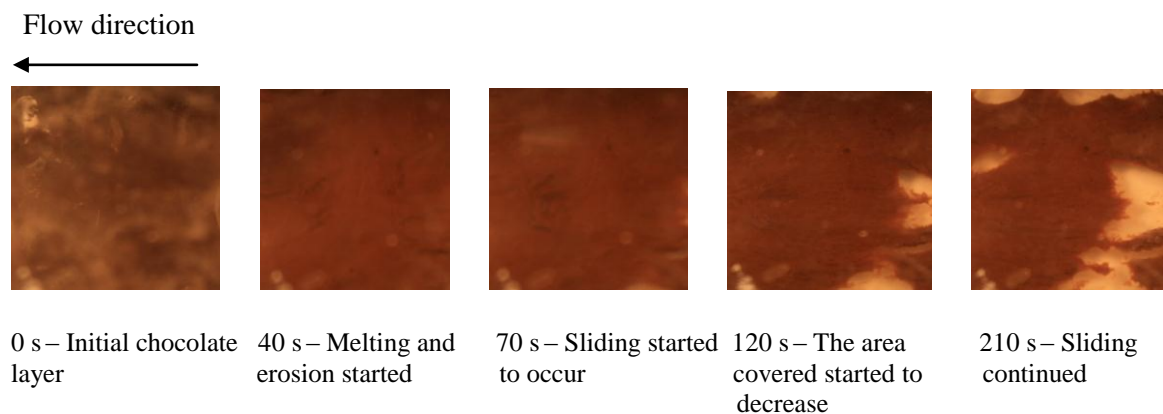
The removal behaviour of different cooling conditions is discussed below. A comparison of the removal of tempered chocolate cooled on the Peltier stage at 1°C/min and 10°C/min, at room temperature for 60 minutes and in the refrigerator for 60 minutes is given in Figures 6.13, 6.32, 6.33 and 6.34 respectively, while the area reduction profiles are presented in Figure 6.35. From all the figures, the following summary can be made:

- Removal of tempered chocolate cooled on the Peltier stage at 1°C/min was initiated by melting process followed by simultaneous erosion and sliding from the leading edge. The sliding occurred until a clean state was achieved. The rate of removal was found to be the fastest.
- Removal of tempered chocolate cooled on the Peltier stage at 10°C/min was initiated by melting process and erosion. Then, sliding event was observed leaving

a few islands on the surface. The islands were then reduced in size whilst sliding continued until a clean surface obtained.

- Removal of tempered chocolate cooled at room temperature for 60 minutes began with the melting process and erosion which occurred simultaneously. Then, the development of holes from any weak points were seen whilst the erosion continued until the surface was entirely clean.
- Removal of tempered chocolate cooled in the refrigerator for 60 minutes started with the simultaneous melting and peeling events followed by sliding event from the leading edge. After some time, holes were developed leaving a few islands on the surface which were then reduced in size and finally a clean surface was obtained.

From Figure 6.35, it can be observed that there was no significant difference in the length of stage A for all the cooling conditions studied. However, the removal rate of tempered chocolate cooled at 1°C/min was found to be the highest, while the other conditions did not show any significant difference, in fact there was a crossover between the area reduction profiles of cooling on the Peltier stage at 10°C/min and in the refrigerator.



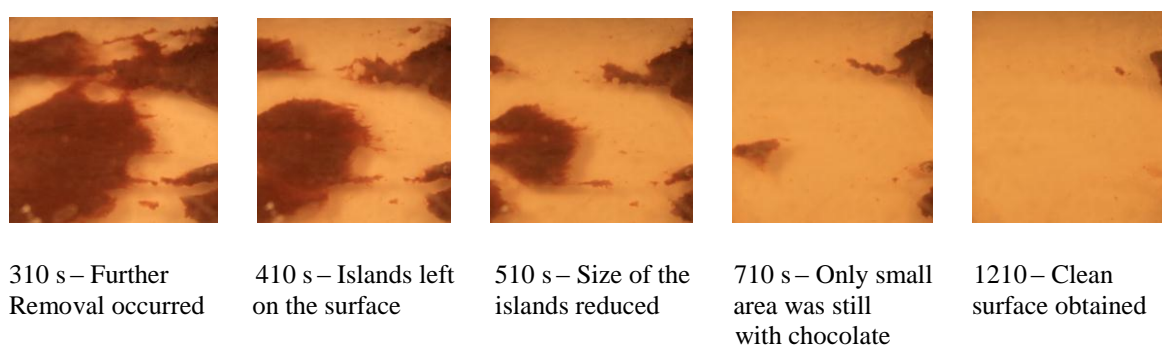


Figure 6.32: Images taken during circulation of 0.1% NaOH solution at  $0.5\text{ms}^{-1}$  and  $70^\circ\text{C}$  to remove the tempered chocolate layer cooled at  $10^\circ\text{C}/\text{min}$  on the Peltier stage.

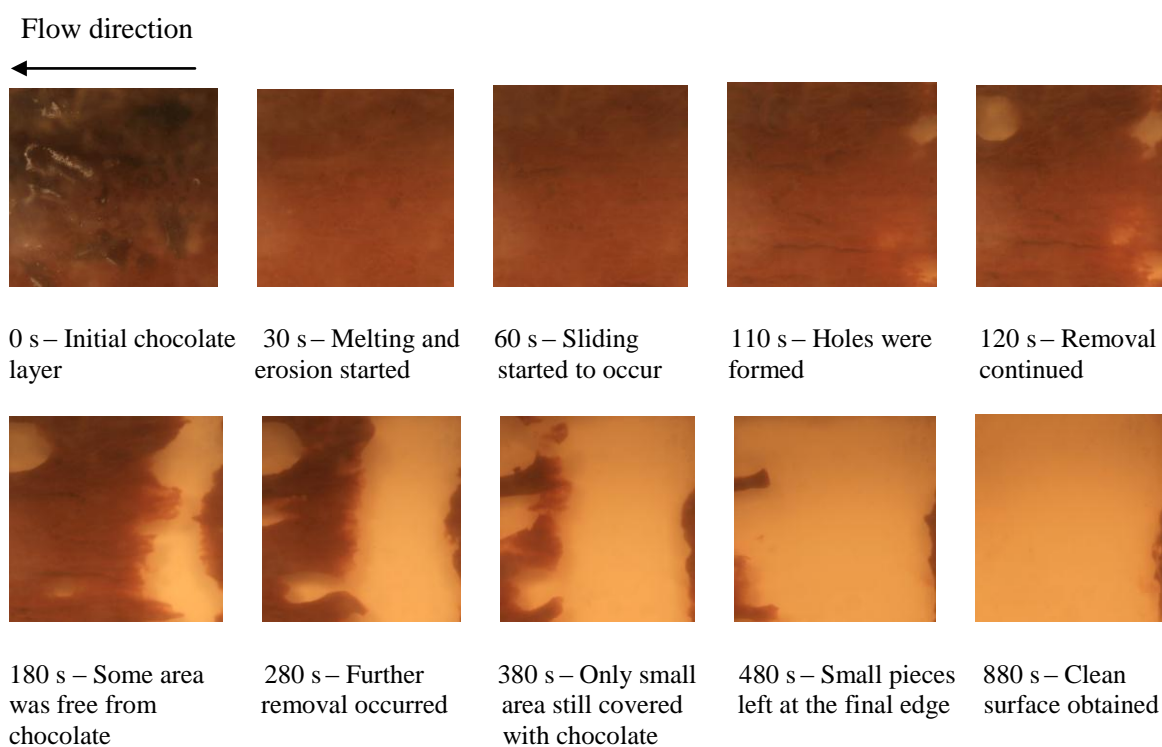


Figure 6.33: Images taken during circulation of 0.1% NaOH solution at  $0.5\text{ms}^{-1}$  and  $70^\circ\text{C}$  to remove the tempered chocolate layer cooled at room temperature for 60 minutes.

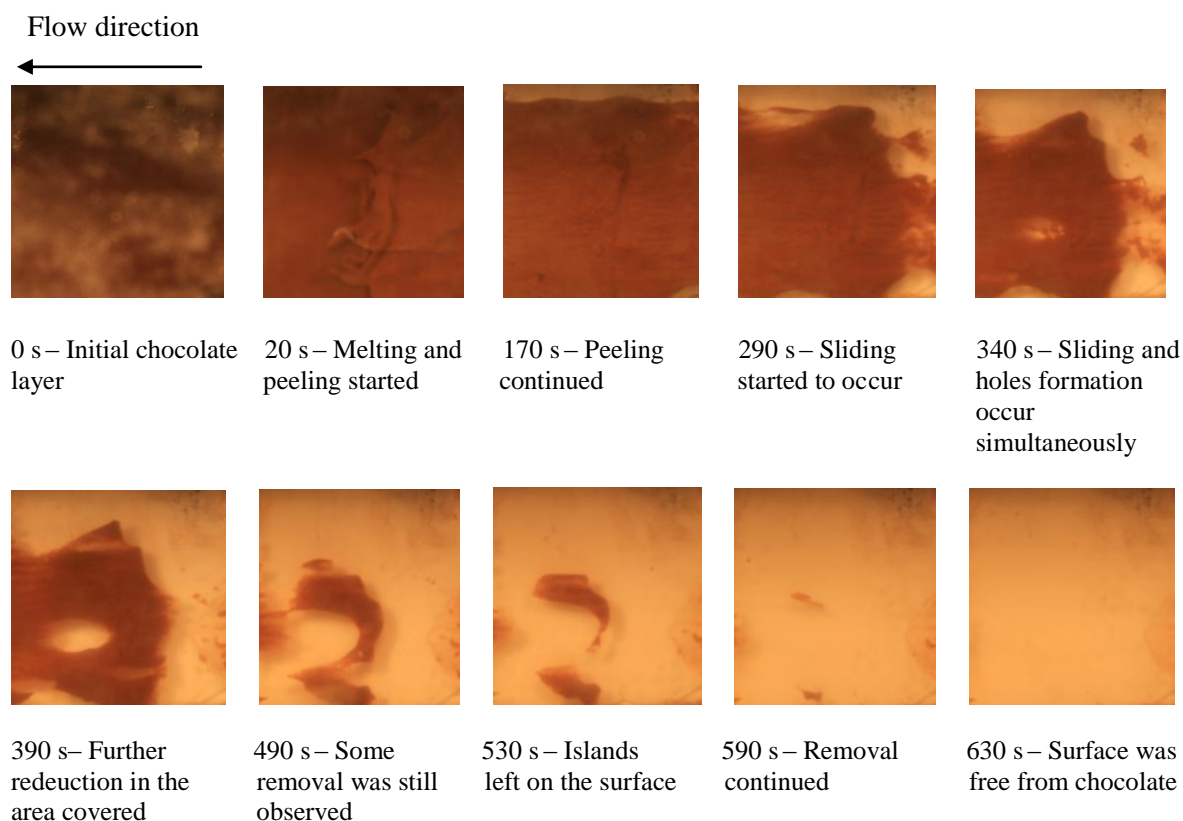


Figure 6.34: Images taken during circulation of 0.1% NaOH solution at  $0.5\text{ms}^{-1}$  and  $70^\circ\text{C}$  to remove the tempered chocolate layer cooled in the refrigerator for 60 minutes.

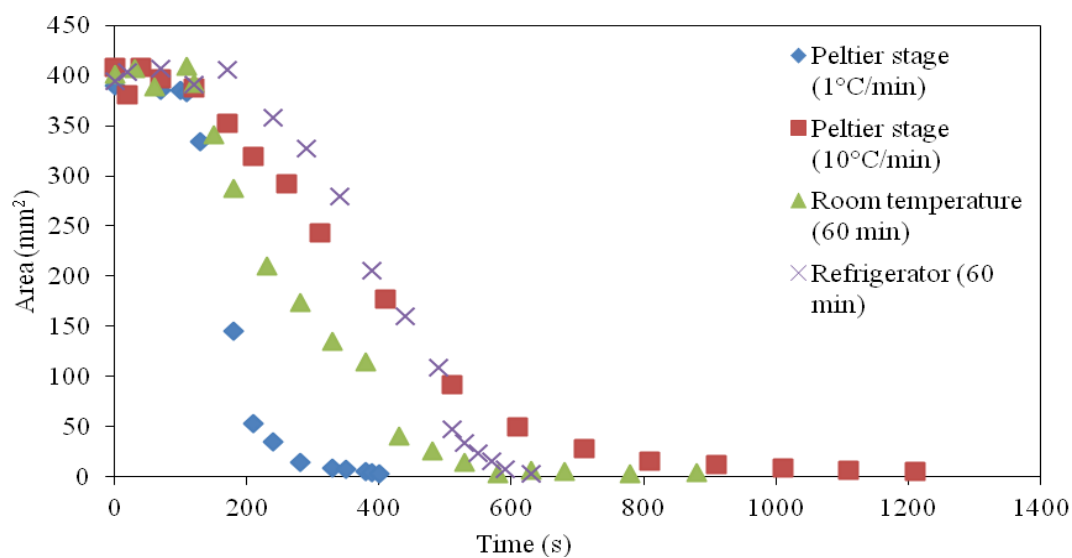


Figure 6.35: Area reduction profiles of chocolate using chemical circulation for removal from different surface materials.



## **6.7 Comparison with micromanipulation and texture analyser measurement**

As discussed in section 5.3, the micromanipulation technique has been used to quantify the amount of energy required to scrap the same amount of chocolate that has been placed on the coupon used in all experiments for this chapter. Generally, the experiment which gave a high amount of pulling energy will also take longer time to be removed and the experiment which gave a low amount of pulling energy will also exhibit a faster cleaning time.

More energy is needed to remove the chocolate which has been soaked in water compared to the amount of energy needed for removal of chocolate soaked in 0.1% NaOH solution. It is comparable with the results in this chapter whereby the water circulation did not clean all the surfaces involved, but the circulation of 0.1% NaOH solution resulting in a clean surface for all experiments. In terms of the temperature, the amount of energy required to remove the solid chocolate layer after soaking in 0.1% NaOH solution was found to decrease with the increasing of the soaking temperature. Here, it was found that the cleaning time was also decreased when the chemical circulation conducted at higher temperature. The pulling energy for removal of solid chocolate layer from a PTFE surface was the highest from the micromanipulation study and during cleaning work conducted using the same surface, it took the longest time to get a surface free of chocolate. The surface roughness of PTFE was reported in section 5.2 as the highest among the three materials which is in line with the pulling energy and the time to clean. The removal of solid chocolate from the surface in horizontal direction was found to be greatly affected by the surface roughness.

Tempered chocolate cooled on the Peltier stage at 1°C/min has lower pulling energy than the one cooled at 10°C/min. The same trend was found in cleaning experiments with the cleaning time for the tempered chocolate cooled on the Peltier stage at 1°C/min was shorter than for the cooling rate of 10°C/min. Pulling energy for the untempered chocolate cooled on the Peltier stage at both rates were also higher than the one cooled at 1°C/min corresponding to the same trend for the cleaning time studied in this chapter. However, the longest cleaning time for the tempered chocolate cooled on the Peltier stage at 10°C/min does not correspond to the amount of pulling energy obtained in the micromanipulation experiment. Cooling in the refrigerator for 60 minutes was found to has the highest pulling energy, but the cleaning time was the second shortest.

The perpendicular separation force measured by the texture analyser gave a different trend whereby the force is least for PTFE, followed by polycarbonate and stainless steel. This measurement was done at room temperature without any temperature control. It is expected that this behaviour is caused by the experimental error as represented by the large error bar in figure 5.31. Besides, the separation of solidified chocolate and hard surface in perpendicular direction is believed to be affected by the contact angle rather than the surface roughness. The ease of perpendicular separation could be achieved by decreasing the surface adhesion or by increasing the cohesion force of chocolate (Keijbet, 2009). The latter solution is not the manufacturer's choice, because it will modify the texture and sensory properties of chocolate. Surface adhesion

Overall, the results from the micromanipulation measurements are comparable with the results obtained from the experiments using the cleaning rig to determine the point of cleaning.

## 6.8 Conclusions

From the results reported in this chapter, it can be concluded that water alone did not clean all the surface materials at the highest temperature (70°C) and velocity (0.5 ms<sup>-1</sup>). Circulation of 0.1% NaOH was then used. Temperatures at 40, 55 and 70°C produced a clean polycarbonate surface at the end of each experiment. However, a thin film was left on the surface for the experiment carried out at 25°C. The area reduction profile can be divided into two stages; A and B. During stage A, melting started followed by some erosion but the area covered was still the same. The area reduction only started to occur in stage B when sliding started. Time to clean decreased when the velocity increased with a reduction of about 20% when the velocity increased from 0.25 to 0.37ms<sup>-1</sup> and increasing the velocity from 0.37 to 0.5ms<sup>-1</sup> reduced up to 60% of the cleaning time. Solid chocolate layer on the PTFE surface was found to be the hardest to be cleaned with the longest cleaning time due to the surface roughness of the surface. No cooling effect observed for the untempered chocolate. Tempered chocolate cooled at 1°C/min took 350 seconds to be cleaned, compared to the sample cooled at 10°C/min which required 1100 seconds of cleaning time. It can also be concluded that the higher the pulling energy needed to remove the chocolate measured by the micromanipulation technique, the longer the cleaning time showing that it is hard to be removed from the surface.

## **7 CONCLUSIONS AND RECOMMENDATIONS**

This chapter will conclude all the work done for this study based on the objectives listed in Chapter 1. In order to meet those objectives, three different investigations were carried out. Some recommendations for further work will also be given.

### **7.1 Conclusions**

#### **7.1.1 Crystallisation and rheological study**

The first objective was to understand the crystallisation behaviour and its relationship with the chocolate rheology. It is very important to identify the polymorphic forms to ensure that the process conditions applied are able to produce a good crystal structure. In this study, liquid chocolate was poured on three different surfaces; stainless steel 316, polycarbonate and PTFE. The crystals formed were examined using the DSC and the information of the type of polymorph was obtained from the melting curve. Tempering using Temperer Revolution 2 was found to be effective and reliable to produce Form V crystals when the tempered liquid chocolate was further cooled at slow cooling rate (1°C/min). Recrystallisation can be observed when fast cooling rate (10°C/min) was applied. There were three peaks existing: 22°C (stable crystals), much larger peak at 15°C (unstable crystals) and a small peak at 40°C (Form VI).

A Peltier stage was used to solidify liquid chocolate (tempered and untempered) with slow and fast cooling rates. The effects of tempering, cooling and material variations have been studied. Properly tempered chocolate produced a single peak for both cooling rates.

However, a slightly higher peak temperature at about 34°C can be observed compared to 33°C with slow cooling. Those are the melting temperatures of Form V crystals showing that the slow and fast cooling rates used produce the desired polymorph. On the other hand, untempered chocolate cooled slowly and rapidly did not crystallise into a correct polymorphic form. The combination of tempering and cooling was found to be one of the controlling factors in crystallisation.

The effect of surface materials was also studied using tempered chocolate cooled on the Peltier stage at 1 and 10°C/min. It was found that the materials used did not affect the crystallisation at both cooling rates applied. The formations of solid chocolate on those three materials were in correct polymorphic form. However, when cooling was carried out without proper control, the stainless steel surface gave one major peak at 40°C (Form VI crystals) while the polycarbonate and PTFE surfaces gave a peak at 34°C. As all the samples were left undisturbed at room temperature for 60 minutes, the variations were probably due to the temperature fluctuation in the room.

From the rheological study conducted using an AR1000 rheometer, it was found that viscosity evolution can provide some information on the crystallisation whereby sudden change in viscosity was approximately similar to the crystallisation temperature from the DSC cooling curve. Effects of cooling, shearing and pre-crystallisation were investigated. The crystallisation rate represented by the rate of change in apparent viscosity was affected by the cooling rate applied. Shearing has been suggested to promote aggregation and speed up the nucleation. The higher the shear rate, the more rapid increase in apparent viscosity was observed for slow cooling rate. Pre-crystallisation process was also found to affect the viscosity evolution whereby there was no sharp increase observed

for tempered chocolate compared to untempered chocolate. Dynamic measurement was also carried out to gain some information on the viscoelastic properties of chocolate. Yield stress decreased as the temperature increased. It can be concluded that it is easier to remove the chocolate at higher temperatures.

### **7.1.2 Force measurement using micromanipulation technique and texture analyser**

In Chapter 5, some experimental data on force measurement was reported. Two techniques were used to investigate the effect of chocolate processing conditions and mould material to the separation force between the chocolate and the mould; micromanipulation rig and texture analyser. The micromanipulation measurements were carried out by considering the effects of chemical usage, soaking time, temperature, probe speed, surface material, tempering and cooling on the pulling energy and removal of solid chocolate layer by scraping off horizontally. Typical profile of force versus sampling time obtained was similar to the removal of other food deposits using the same technique as discussed in section 2.4.2. The data was presented as the amount of energy per unit area and gram combined with the removal percentage. It was observed that complete removal could not be achieved even after soaking the solid chocolate in water at temperature higher than the melting point. For that reason, 0.1% NaOH solution was used as a soaking medium.

Pulling energy decreased when the soaking time and temperature increased. However, the amount of energy required to scrape the chocolate layer from polycarbonate surface was not affected by the increment of probe speed from 0.59 to 2.22mm/s. The pulling energy for removal of chocolate is also dependent on the surface material. PTFE gave the highest pulling energy followed by polycarbonate and stainless steel. In this case

the surface roughness was expected to control the removal. A higher pulling energy of  $400\text{J/m}^2$  was obtained when the tempered chocolate was cooled rapidly, compared to  $250\text{J/m}^2$  for slow cooling. On the other hand, the cooling rate did not affect the pulling energy for untempered chocolate. The removal percentage of untempered chocolate was four times higher than for the tempered chocolate as the untempered chocolate contains less crystal structure.

Force measurement using texture analyser was carried out at room temperature by considering the effects of tempering, probe material, probe-chocolate contact time and the distance between the probe and the chocolate surface (X). Separation between chocolate surface from the probe was carried out horizontally. The data was presented as force per unit area and weight of chocolate residue/mould surface at the end of each experiment. X value did not give any specific trend in both force per unit area and the amount of residue on the surface. However, the contact time was found to affect the separation force. For the first 30 minutes, the separation force was constant at almost  $0\text{ kN/m}^2$ . It then started to increase almost linearly to  $110\text{kN/m}^2$  when the contact time reached 180 minutes. This behaviour is due to the solidification of the liquid chocolate causing the hardness to increase. Separation force was also affected by the tempering and surface material of the probe. Force to separate tempered chocolate from the probe surface was much higher than for the untempered chocolate. The values of force can be ranked as follows: PTFE<polycarbonate<stainless steel. In all cases, the probe surface did not clean at the end of each experiment. This is possibly due to improper cooling was applied as the measurements were carried out at room temperature, with no cooling rate control. Not enough contraction might cause the solidified chocolate to stick to the probe surface.

### **7.1.3 Removal behaviour of solid chocolate layer using flow cell cleaning rig**

The third objective was to study the removal behaviour of solid chocolate from the mould material with and without cleaning chemical. A bench scale flow cell cleaning rig was used to conduct the experiments with respect to a number of parameters; flow temperature, velocity, chemical requirement, surface material, tempering and cooling conditions. Cleaning time was determined using the image analysis.

A preliminary study with water circulation was carried out to identify the flow temperature and velocity which can give a clean surface. For all surface materials, water alone could not remove the solid chocolate layer even at 70°C and 0.5 ms<sup>-1</sup> which was chosen as a standard condition. Thus, chemical was added. Further investigation was then carried out using the circulation of 0.1% NaOH. The cleaning time decreased when the temperature increased and a clean surface was obtained. At 25°C, a thin film was visually seen at the end of the experiment. Characterisation of the film was made using Confocal Raman Microscope. Cocoa butter, cocoa powder and sugar might contribute to the formation of the film. The cleaning time was also found to decrease with the increasing velocity.

Circulation of 0.1% NaOH was able to clean the chocolate from all three surfaces involved. However, removal of chocolate from PTFE surface was found to be the hardest with the cleaning time of 1300 seconds. This could be caused by the surface roughness (highest among the three surfaces). The dependency of the cleaning time to the tempering and cooling processes was then determined. For tempered chocolate, cooling was found to affect the cleaning time, but not for the untempered chocolate. Tempering which aims to



produce a good quality of chocolate that meet the customer requirement can also shorten the cleaning time of the surface. The removal behaviour of tempered chocolate cooled on the Peltier stage at 1°C/min and 10°C/min, at room temperature for 60 minutes and in the refrigerator for 60 minutes have also been compared.

When a comparison was made with the micromanipulation measurement, it can be concluded that longer time is needed to clean the solid chocolate from a surface which gave a higher amount of pulling energy while the cleaning process is faster for the lower amount of pulling energy measured. The removal in horizontal direction was found to be affected by the surface roughness, in this case the PTFE with the roughest surface need the highest amount of energy with longest cleaning time compared to stainless steel and polycarbonate. However, the force measurement in perpendicular direction was not comparable with the cleaning work caused by several factors including the cooling step which was not carried out in a controlled environment and the nature of the measurement.

## **7.2 Recommendations for further work**

Based on the results obtained, it is thought that some future work would be useful to be carried out. More surface materials with variations in surface roughness can be studied as it might give different effect on the pulling energy as well as the removal behaviour of solid chocolate layer. As most of the experiments only involve dark chocolate, a comparison can be made with other type of chocolate, for example, milk and white chocolate or with cocoa butter because the ingredients also affect the crystallisation process. It might also influence the removal behaviour. The variation in cooling temperature is also interesting to be investigated.

As mentioned previously, force measurements using texture analyser were only conducted at room temperature. For future work, a better experimental set up can be used to provide a controlled cooling. This can be carried out using a jacketed vessel. The effect of cooling on the separation force which is carried out vertically can be studied. This study only involves two force measurement techniques. Development of other methods to measure force would be useful and a comparison can be made between all the methods used.

As for the cleaning work, it is recommended to study the effect of fat content and particle size distribution on the cleanability of hard surfaces. The pH of polycarbonate should be reduced below 9 and the temperature of the cleaning solution should be reduced to 60°C.

## REFERENCES

- Ab. Aziz, N. (2007). Factors that affect cleaning process efficiency. School of Chemical Engineering: University of Birmingham.
- Adhikari, B., Howes, T., Bhandari, B.R. and Truong, V. (2001). Stickiness in foods: A review of mechanisms and test methods. *International Journal of Food Properties* 1(4), 1-33.
- Adhikari, B., Howes, T., Shrestha, A. & Bhandari, B.R. (2007). Effect of surface tension and viscosity on the surface stickiness of carbohydrate and protein solutions. *Journal of Food Engineering* 79, 1136-1143.
- Afoakwa, E.O. (2011). *Chocolate Science and Technology*. John Wiley & Sons.
- Afoakwa, E.O., Paterson, A. & Fowler, M. (2007). Factors influencing rheological and textural qualities in chocolate - a review. *Trends in Food Science & Technology* 18, 290-298.
- Afoakwa, E.O., Paterson, A., Fowler, M. & Vieira, J. (2008a). Effects of tempering and fat crystallisation behaviour on microstructure, mechanical properties and appearance in dark chocolate systems. *Journal of Food Engineering* 89(2), 128-136.
- Afoakwa, E.O., Paterson, A., Fowler, M. & Vieira, J. (2008b). Particle size distribution and compositional effects on textural properties and appearance of dark chocolates. *Journal of Food Engineering* 87, 181-190.
- Afoakwa, E.O., Paterson, A., Fowler, M. & Vieira, J. (2009). Microstructure and mechanical properties related to particle size distribution and composition in dark chocolate. *International Journal of Food Science and Technology* 44, 111-119.

- Akhtar, N.R. (2010). The fundamental interactions between deposits and surfaces at nanoscale using atomic force microscopy. School of Chemical Engineering, University of Birmingham.
- Asteriadou, K., Othman, A.M., Goode, K. & Fryer, P.J. (2009). Improving cleaning of industrial heat induced food and beverages deposits: A scientific approach to practice. In International Conference on Heat Exchanger Fouling and Cleaning VIII. Edited by H. Muller-Steinhagen, M.R. Malayeri & A.P. Watkinson. Schlading, Austria. 159-164.
- Baichoo, N. (2007). The effect of rapid cooling on the fat phase of chocolate. University of Nottingham.
- Baldino, N., Gabriele, D. & Migliori, M. (2010). The influence of formulation and cooling rate on the rheological properties of chocolate. European Food Research and Technology 231, 821-828.
- Becket, S.T. (2001). Milling, mixing and tempering - an engineering view of chocolate. Journal of Process Mechanical Engineering 215, 1-8.
- Beckett, S.T. (2008). The Science of Chocolate. York, UK: The Royal Society of Chemistry.
- Beckett, S.T. (2009). Traditional Chocolate Making. In Industrial Chocolate Manufacture and Use. Edited by S.T. Becket. York, UK: Wiley-Blackwell.
- Bhandari, B.R. (2007). Stickiness and Caking in Food Preservation. In Handbook of Food Preservation. Edited by M.S. Rahman. New York: CRC Press.
- Bird, M. R. and Fryer, P.J. (1991). An experimental study of the cleaning of surfaces fouled by whey proteins. Trans IChemE 69(C), 13-21.

- Bolliger, S., Breitschuh, B., Stranzinger, M., Wagner, T. & Windhab, E.J. (1998). Comparison of precrystallization of chocolate. *Journal of Food Engineering* 35, 281-297.
- Boudreau, A. and Saint-Amant, L. (1985). Butter. In *Dairy Science and Technology; Principles and Applications*. Edited by Julien, J.P., Nadeau, R. Dumais, R. La Fondation de Technologie Laitiere du Quebec, Inc. Quebec, Canada.
- Briggs, J.L. & Wang, T. (2004). Influence of shearing and time on the rheological properties of milk chocolate during tempering. *Journal of the American Oil Chemists Society* 81(2), 117-121.
- Campos, R., Narine, S.S. & Marangoni, A.G. (2002). Effect of cooling rate on the structure and mechanical properties of milk fat and lard. *Food Research International* 35, 971-981.
- Chen, M. J. (2000). Mechanical Strength and Destruction of Biofilms in Pipes. School of Chemical Engineering, University of Birmingham.
- Chen, M. J., Zhang, Z., and Bott, T. R. (2005). Effects of operating conditions on the adhesive strength of *Pseudomonas fluorescens* biofilms in tubes. *Colloids and Surfaces B: Biointerfaces* 43, 61–71.
- Cho, K., Nabi Saheb, D., Yang, H., Kang, B., Kim, J. and Lee, S. (2003). Memory effect of locally ordered  $\alpha$ -phase in the melting and phase transformation behavior of  $\beta$ -isotactic polypropylene. *Polymer* 44, 4053-4059.
- Christian, G.K. (2003). Cleaning of carbohydrate and dairy protein deposits. School of Chemical Engineering, University of Birmingham.
- Cole, P.A. (2011). Cleaning of toothpaste from process equipment by fluid flow at laboratory and pilot scales. School of Chemical Engineering, University of Birmingham.

- Davis, T.R. and Dimick, P.S. (1986). Solidification of cocoa butter. Proc. PMCA Prod. Conf., 40: 104-108.
- De Graef, V., Depypere, F., Minnaert, M. & Dewettinck, K. (2011). Chocolate yield stress as measured by oscillatory rheology. Food Research International 44, 2660-2665.
- De Graef, V., Goderis, B., Puyvelde, P.V., Foubert, I. & Dewettinck, K. (2008). Development of a rheological method to characterize palm oil crystallizing under shear. European Journal of Lipid Science Technology 110(6), 521-529.
- Dhonsi, D., & Stapley, A. G. F. (2006). The effect of shear rate, temperature, sugar and emulsifier on the tempering of cocoa butter. Journal of Food Engineering, 77, 936-942.
- Duck, W. (1964). The measurement of unstable fat in finished chocolate. The Manufacturing Confectioner, 35 (6): 67-72.
- Evans, I. D. (1992). On the nature of the yield stress. Journal of Rheology 36(7), 1313-1316.
- Fessas, D., Signorelli, M. & Schiraldi, A. (2005). Polymorphous transitions in cocoa butter - A quantitative DSC study. Journal of Thermal Analysis and Calorimetry 82, 691-702.
- Fryer, P.J. & Asteriadou, K. (2009). A prototype cleaning map: A classification of industrial cleaning processes. Trends in Food Science & Technology 20(6-7), 255-262.
- Gaikwad, V. (2012). Oral processing of dark and milk chocolate. The Riddet Institute, Massey University.
- Goncalves, E.V. and Lannes, S.C.D.S. (2010). Chocolate rheology. Cienc. Tecnol. Aliment., Campinas 30 (4), 845-851.

- Goode, K.R. (2011). Characterising the cleaning behaviour of brewery foulants. In School Chemical Engineering: University of Birmingham.
- Gray, M.P. (2009). Moulding, Enrobing and Cooling Chocolate Products. In Industrial Chocolate Manufacture and Use. Edited by S.T. Beckett. John Wiley & Sons.
- Hartel, R.W. (2001). Crystallization in Foods. Madison, Wisconsin. Aspen Publishers, Inc.
- Hodge, S.M. and Rousseau, D. (2002). Fat bloom formation and characterization in milk chocolate observed by atomic force microscopy. *Journal of the American Oil Chemists Society* 79, 1115-1121.
- Hooper, R.J., Liu, W., Fryer, P.J., Paterson, W.R., Wilson, D.I. & Zhang, Z. (2006). Comparative studies of fluid dynamic gauging and a micromanipulation probe for strength measurements. *Food and Bioprocess Processing* 84(C4), 353-358.
- Jennings, W. G., McKillop, A. A. and Luick, J. R. (1957). Circulation cleaning. *Journal of Dairy Science* 40, 1471-1479.
- Keijbets, E.L., Chen, J.S., Dickinson, E. & Vieira, J. (2009). Surface energy investigation of chocolate adhesion to solid mould materials. *Journal of Food Engineering* 92(2), 217-225.
- Keijbets, E.L., Chen, J.S. & Vieira, J. (2010). Chocolate demoulding and effects of processing conditions. *Journal of Food Engineering* 98(1), 133-140.
- Kinta, Y. & Hartel, R.W. (2010). Bloom Formation on Poorly-Tempered Chocolate and Effects of Seed Addition. *Journal of the American Oil Chemists Society* 87(1), 19-27.
- Kloek, W., Vliet, T.V. and Walstra, P. (2005). Mechanical properties of fat dispersions prepared in a mechanical crystallizer. *Journal of Texture Studies* 36, 544-568.

- Le Reverend, B.J.D. (2009). Modelling of the phase change kinetics of cocoa butter in chocolate and application to confectionery manufacturing. School of Chemical Engineering, University of Birmingham.
- Le Reverend, B.J.D., Bakalis, S. & Fryer, P.J. (2008). Structured Chocolate Products. In Food Materials Science. Edited by Aguilera J.M. & Lillford, P.J. New York. Springer Science.
- Le Reverend, B.J.D., Fryer, P.J., Coles, S. & Bakalis, S. (2009). A Method to Qualify and Quantify the Crystalline State of Cocoa Butter in Industrial Chocolate. Journal of the American Oil Chemists Society 87(3), 239-246.
- Le Reverend, B.J.D., Smart, I., Fryer, P.J. and Bakalis, S. (2011). Modelling the rapid cooling and casting of chocolate to predict phase behaviour. Chemical Engineering Science 66 (6): 1077-1086.
- Liang, B. and Hartel, R.W. (2004). Effects of milk powders in milk chocolate. Journal Dairy Science 87, 20-31.
- Liu, W., Ab. Aziz, N., Zhang, Z. & Fryer, P.J. (2007). Quantification of the cleaning of egg albumin deposits using micromanipulation and direct observation technique. Journal of Food Engineering 78, 217-224.
- Liu, W., Christian, G.K., Zhang, Z. & Fryer, P.J. (2002). Development and use of a micromanipulation technique for measuring the force required to disrupt and remove fouling deposits. Trans IChemE 80, 286-291.
- Liu, W., Christian, G.K., Zhang, Z. & Fryer, P.J. (2006a). Direct measurement of the force required to disrupt and remove fouling deposits of whey protein concentrate. International Dairy Journal 16, 164-172.
- Liu, W., Fryer, P.J., Zhang, Z., Zhao, Q. & Liu, Y. (2006b). Identification of cohesive and adhesive effects in the cleaning of food fouling deposits. Innovative Food Science and Emerging Technologies 7, 263-269.



- Liu, W., Zhang, Z. & Fryer, P.J. (2006c). Identification and modelling of different removal modes in the cleaning of a model food deposit. *Chemical Engineering Science* 61(22), 7528-7534.
- Lonchampt, P. and Hartel, R.W. (2004). Fat bloom in chocolate and compound coatings. *European Journal of Lipid Science and Technology*, 106: 241-274.
- Lonchampt, P. and Hartel, R.W. (2006). Surface bloom on improperly tempered chocolate. *European Journal of Lipid Science and Technology*, 108 (2): 159-168.
- Lovegren, N., Gray, M. and Feuge, R. (1976). Polymorphic changes in mixtures of confectionery fats. *Journal of the American Oil Chemists' Society*, 53 (2): 83-88
- MacMillan, S.D., Peacock, C.A., Roberts, K., Rossi, A., Wells, M.A., Polgreen, M.C. and Smith, I.H. (2005). In-situ XRD studies of cocoa butter fat under thermal processing and shearing conditions.  
<http://www1.food.leeds.ac.uk//mp/LipidConference/AbstractRoberts.html>
- MacMillan, S. D., Roberts, K. J., Rossi, A., Wells, M. A., Polgreen M. C. and Smith I. H. (2002). In situ small angle X-ray scattering (saxs) studies of polymorphism with the associated crystallization of cocoa butter fat using shearing conditions. *Crystal Growth & Design* 2(3), 221-226.
- Merken, G.V. and Vaeck, S.V. (1980). A study of the polymorphism of cacao butter by means of DSC calorimetry. *Lebensmittel-Wissenschaft & Technologie*, 13 (6): 314-317.
- Metin, S. and Hartel, R.W. (2005). Crystallization of Fats and Oils. In *Bailey's Industrial Oil and Fat Products*. John Wiley and Sons. 45-76.
- Michalski, M.C., Desobry, S., Babak, V. & Hardy, J. (1999). Adhesion of food emulsions to packaging and equipment surfaces. *Colloids and Surfaces a-Physicochemical and Engineering Aspects* 149(1-3), 107-121.

- Minifie, B.W. (Ed.) (1989). *Chocolate, Cocoa, and Confectionery: Science and Technology*. New York: Van Nostrand Reinhold.
- Nor Aini, I. & Sabariah, S. (1995). Development of specialty fats for selected food. In *National Seminar on Food Technology '95 "Food Ingredients"* Kuala Lumpur.
- Othman, A.M., Asteriadou, K. & Fryer, P.J. (2009). Removal force measurement and rheological characterization of sweetened condensed milk deposits: A preliminary study. In *International Conference on Heat Exchanger Fouling and Cleaning VIII*, pp. 168-174. Edited by H. Muller-Steinhagen, M.R. Malayeri & A.P. Watkinson. Schlading, Austria.
- Palabiyik, I. (2013). Investigation of fluid mechanical removal in the cleaning process. School of Chemical Engineering, University of Birmingham.
- Pinschower, K. (2003). Direct measurement of the contraction of chocolate during solidification. School of Chemical Engineering, University of Birmingham.
- Rao, M.A. (2006). Introduction: Food Rheology and Structure. In *Rheology of Fluid and Semisolid Foods: Principles and Applications*. Second Edition. Springer Link.
- Reddy, S.Y., Full, N.A., Dimick, P.S. and Ziegler, G.R. (1996). Tempering method for chocolate containing milk fat fractions. *Journal of American Oil Chemists Society* 73, 723-727.
- Roos, Y.H. (1995). *Phase transitions in Foods*. New York. Academic Press.
- Sato, K. (2001). Crystallization behaviour of fats and lipids - a review. *Chemical Engineering Science* 56, 2255-2265.
- Sato, K., Arishima, T., Wang, Z.H., Ojima, K., Sagi, N., and Mori, H. (1989). Polymorphism of POP and SOS. I. Occurrence and Polymorphic Transformation. *Journal of the American Oil Chemists' Society* 66(5), 664-674.

- Stapley, A.G.F., Tewkesbury, H. & Fryer, P.J. (1999). The effects of shear and temperature history on the crystallization of chocolate. *Journal of the American Oil Chemists' Society* 76(6), 677-685.
- Svanberg, L., Ahrne, L., Loren, N. & Windhab, E. (2011). Effect of sugar, cocoa particles and lecithin on cocoa butter crystallization in seeded and non-seeded chocolate model systems. *Journal of Food Engineering* 104, 70-80.
- Tarabukina, E., Jegu, F., Haudin, J.M., Navard, P. & Peuvrel-Disdier, E. (2009). Effect of shear on the rheology and crystallisation of palm oil. *Journal of Food Science* 74 (8), 405-416.
- Tewkesbury, H., Stapley, A.G.F. & Fryer, P.J. (2000). Modelling temperature distributions in cooling chocolate moulds. *Chemical Engineering Science* 55, 3123-3132.
- Toro-Vazquez, J.F., Perez-Martinez, D., Dibildox-Alvarado, E., Charo-Alonso, M.A. & Reyes-Hernandez, J. (2004). Rheometry and polymorphism of cocoa butter during crystallization under static and stirring conditions. *Journal of the American Oil Chemists' Society* 81, 195-202.
- Tuladhar, T.R., Paterson, W.R., Macleod, N. & Wilson, D.I. (2000). Development of a novel non-contact proximity gauge for thickness measurement of soft deposits and its application in fouling studies. *Canadian Journal of Chemical Engineering* 78.
- Vaeck, S. V. (1960). Cacao butter and fat bloom. *Manufacturing Confectioner* 40, 35-73.
- Walewijk, A., Cooper-White, J.J. and Dunstan, D.E. (2008). Adhesion measurements between alginate gel surfaces via texture analysis. *Food Hydrocolloids* 22, 91-96.
- Walls, H. J., Caines, S. B., Sanchez, A. M., & Khan, S. A. (2003). Yield stress and wall slip phenomena in colloidal silica gels. *Journal of Rheology*, 47(4), 847–868.
- Wells, M.A. (2009). Chocolate Crumb. In *Industrial Chocolate Manufacture and Use* Edited by S.T. Beckett. John Wiley & Sons.

Whetstone, H. (1996). Moulds and moulding: examples and techniques. *The Manufacturing Confectioner* 6, 93-99.

Wille, R. and Lutton, E. (1966). Polymorphism of cocoa butter. *Journal of the American Oil Chemists' Society* 43 (8): 491-496.

World Cocoa Foundation. (2012). Cocoa Market Update. [www.worldcocoa.org](http://www.worldcocoa.org).